AN ABSTRACT OF THE DISSERTATION OF

Hang Thi Le for the degree of Doctor of Philosophy in Pharmacy presented on June 13, 2008

Title:
(1) Hydrocortisone Permeation Study using a Synthetic Membrane, a Mouse Skin, and an Epiderm™ Cultured Skin.
(2) Preparation of Orally Disintegrating Tablets of Melatonin and Acetaminophen.
(3) Pharmacokinetics of Terbinafine in Penguins.

Abstract approved

John Mark Christensen James W. Ayres

The first project of this thesis is an *in vitro* study. This study was performed with 8 hydrocortisone topical products on the market for the purpose of comparing one Tec Lab product, a Corticool gel, to the other seven common products on the market. The permeation of these products was tested with three types of membranes: a synthetic membrane, a mouse skin, and an Epiderm™ using a Franz Cell apparatus. The synthetic membrane seemed to over-estimate the hydrocortisone permeation through the skin. Mouse skin has a higher permeation compared to human cultured skin, Epiderm™. Corticool gel (1% hydrocortisone), which has a higher hydrocortisone solubility compared to other creams and lotions, showed a significantly higher drug diffusion rate through all of the three membranes. The Corticool gel exhibited better hydrocortisone permeation than the Prescription hydrocortisone cream 2.5%. Cortizone-10 ointment (1% hydrocortisone) showed a very low hydrocortisone

permeation through all of the three membranes. It is predicted that the same comparative behavior would be observed *in vivo* on applying these formulations. Corticool gel is suggested to be used for fast action treatment.

The second project related to a preparation of orally disintegrating tablets of melatonin and orally disintegrating tablets containing sustained-release beads of acetaminophen. A combination of superdisintegrants, amino acids, effervescent materials, and sweeteners was placed into a melatonin tablet and then compressed into a normal-shaped tablet. The melatonin tablet exhibited a short disintegration time in water, had adequate hardness, and passed the friability test. This tablet also tasted good and could be used for children and vulnerable subjects having difficulty in swallowing.

The acetaminophen tablet combines two desirable properties: fast disintegration and sustained release of the drug. Acetaminophen sustained-release beads were added inside the tablet. The tablet disintegrated very quickly in water to release the sustained-release beads. By using hydrophilic polymers (HPMC and polyethylene oxide), the sustained release beads were protected and the sustained-release properties maintained. Similar excipients to those used in the melatonin tablet were used as excipients in the acetaminophen tablet to obtain fast tablet disintegration. A higher pressure was needed to combine beads and other excipients surrounding the beads into tablets. The tablets also had longer disintegration times but were still considered fast disintegrating tablets.

The third project is a pharmacokinetic study of terbinafine in penguins aiming at treatment aspergillosis. Terbinafine was administered orally by single dosing and

multiple dosing to African penguins (*Spheniscus demersus*). The pharmacokinetics parameters were calculated. The best-fitted model, a two-compartment open model with a deep-tissue elimination phase, was selected. A recommended dose also was calculated to treat fungal infections in penguins.

(1) Hydrocortisone Permeation Study using a Synthetic Membrane, a Mouse Skin and an Epiderm™ Cultured Skin, (2) Preparation of Orally Disintegrating Tablet of Melatonin and Acetaminophen, (3) Pharmacokinetics of Terbinafine in Penguins

by
Hang Thi Le

A DISERTATION

submitted to

Oregon State University

in partial fulfillment of
the requirement for the
degree of

Doctor of Philosophy

Presented June 13, 2008
Commencement June 2009

Doctor of Philosophy thesis of Hang Thi Le presented on June 13, 2008

APPROVED:

Major Professor, representing Pharmacy

Dean of the College of Pharmacy

Dean of the Graduate School

I understand that my thesis will become part of the permanent collection of Oregon State University libraries. My signature below authorizes release of my thesis to any reader upon request.

Hang Thi Le, Author

ACKNOWLEDGEMENTS

I owe enormous thanks to Dr. James W. Ayres, for his philosophy, kindness, and understanding. Dr. Ayres is a brilliant scientist. His new ideas and inventions are wonderful asserts to pharmaceutics. He is a wonderful advisor with whom every student enjoys working. I would like to pay my heartfelt gratitude to my advisor, Dr. John Mark Christensen, for his support throughout the several years of my Ph.D. program. His profound knowledge in topical formulation and pharmacokinetics, his tireless efforts in doing research and his discoveries new aspects of science have impressed me deeply. Both of these professors in the College of Pharmacy have taught me not only knowledge, methods of studying, but also they have instilled a burning desire in me to be a conscientious scientist.

My special thanks go to Dr. Rosita R. Proteau, Dr. Zhenrong Cui, two other professors in the Pharmaceutics division who were excellent mentors and were always available to give me advice, comments and encouragement.

I would like to express my acknowledgement to my friends in the Pharmaceutics department who have supported and boosted my spirit.

My family is always in my heart, especially my parents, who have been there sharing, enjoying, helping, listening and supporting me through any successes and failures in my life.

CONTRIBUTION OF AUTHORS

Dr. Monica Chuong assisted with guidance and doing experiments of Chapter 1.

TABLE OF CONTENTS

		Page
CHAPTER 1:	HYDROCORTISONE PERMEATION STUDY USING SYNTHETIC MEMBRANE, MOUSE SKIN AND EPIDERM™ CULTURED SKIN……..	1
	ABSTRACT…….	2
	INTRODUCTION……	4
	MATERIALS AND METHODS…….	31
	RESULTS AND DISSCUSSION……	42
	CONCLUSIONS……..	91
	REFERENCES…….	94
CHAPTER 2:	PREPARING ORALLY DISINTEGRATING TABLETS OF MELATONIN AND PARACETAMOL……	96
	ABSTRACT…….	97
	INTRODUCTION……	98
	MATERIALS AND METHODS…….	119
	RESULTS AND DISSCUSSION……	146
	CONCLUSIONS……..	199
	REFERENCES…….	200
CHAPTER 3:	PHARMACOKINETICS OF TERBINAFINE IN PENGUINS……..	206
	ABSTRACT……..	207

TABLE OF CONTENTS (Continued)

	Page
INTRODUCTION……	208
RESULTS AND DISSCUSSION……....	230
CONCLUSIONS……...	308
REFERENCES……..	309
BIBLIOGRAPHY…….	312

LIST OF FIGURES

Figure		Page
1.1	The structure of skin with two main layers: The Epiderm™ and Dermis…….....	4
1.2	Epidermal differentiation in the epidermis……..	7
1.3	The structure of the stratum corneum……..	11
1.4	The hair follicle structure and capability of particle-size penetration through the follicle……..	12
1.5	Lacunae formed by degrading desmosomes provided on an obvious site for water pooling, and during prolonged exposure to water, the lateral expansion of lacunae occuring through the polar-head regions of the intercellular lipids …….	14
1.6	Schematic depiction of Fick's-law and a substance illustrating the diffusion……...	16
1.7	Drug diffusions from a matrix…….	18
1.8	Depection of an acute-response allergic mechanism to a foreign substance……..	22
1.9	Synthetic filter membrane 0.45µm……..	26
1.10	Mouse skin without hair……..	27
1.11	Histology of an an EpiDerm™ 200 (a), and an EpiDermFT™ 200 (b)……	28
1.12	A transmission electron micrograph of Epiderm™ –Intercellular-Lamellar-Lipid Sheets-broad-narrow-Broad Spacing (Magnification 150,000x)…….	28
1.13	A Comparison of a Lipid profile for an Epiderm™ and Normal Human abdominal Skin……..	29

LIST OF FIGURES (Continued)

Figure		Page
1.14	An depiction of an Epiderm™ unit in a kit shipped from Mattek….	29
1.15	EpiDerm™-cultured human skin models……	36
1.16	The HPLC machine, LC Module I, from Waters used to assay hydrocortisone…….	37
1.17	The Fanz-cell diffusion apparatus……..	38
1.18	The standard curve plot for hydrocortisone concentration versus the area ratio of hydrocortisone over the internal standard, propyl paraben…….....	44
1.19	A box plot of the thickness of 10 mouse skin patches showing the variation of thickness observed within each skin patch (mm)…….....	46
1.20	Percutanous absorption of water compared to cadaver samples……	47
1.21	Release profiles of HC permeation over time through a nylon membrane (non-prewashed), using Fick's-law (cumulative-percentage hydrocortisone release vs. time in hours)…….....	53
1.22	The 95% Confidence interval band and prediction band of a Corticool diffusion profile through a synthetic membrane…….	54
1.23	Quantity of drug diffused through a synthetic membrane over 24 hours……	55
1.24	Diffusion profiles of hydrocortisone versus square roots of time for eight formulations through a synthetic membrane……..	58
1.25	A cut off graph of showing an enlarged dissolution profile showing creams and lotions having a high rate of hydrocortisone diffusion over the first hours……	59
1.26	A hydrocortisone release profile from an ointment that has two separate diffusion phases. A permeation study performed with a mouse skin……...	60

LIST OF FIGURES (Continued)

Figure		Page
1.27	The percentage of hydrocortisone permeation through a non-pre-washed mouse skin over 24 hours…….	64
1.28	The 95% confidence interval and 95% prediction band hydrocortisone permeation from a Corticool gel through a mouse skin using Fick's-law model…….	64
1.29	Amount of hydrocortisone diffusing through a non-pre-wahsed mouse skin using Fick's law model over 24 hours……	65
1.30	A cut off graph showing hydrocortisone release behavior for the first few hours from creams, lotions, and an ointment formulation through a mouse skin…….	65
1.31	The diffusion profile of hydrocortisone from Cortizone-10 ointment through a mouse skin showing two phases of release…….……...	66
1.32	The diffusion profiles of eight formulations through a mouse skin using the Higuchi model……	69
1.33	A hydrocortisone diffusion profile over 24 hours through a pre-washed mouse skin using Fick's law model……..	72
1.34	The amount of hydrocortisone permeation profiles through a mouse skin over 24 hours from hydrocortisone topical products…..	73
1.35	The 95% confidence-interval band and a 95% prediction-band showing Corticool gel hydrocortisone diffusion rate though prewashed mouse skin……...	74
1.36	A cut off graph the initial diffusion profiles for the first few hours of all hydrocortisone formulations through a pre-washed mouse skin showing the depletion phases for Aveeno cream and Cortaid cream……...	74

LIST OF FIGURES (Continued)

Figure		Page
1.37	The square root of time-diffusion profiles of hydrocortisone from eight formulations over 24 hours using the Higuchi model through the prewashed mouse skin……..	75
1.38	Hydrocortisone diffusion profiles from eight formulations through Epiderm™ over 24 hours using the Fick's law model……...	80
1.39	The square root of time of hydrocortisone diffusion profiles from seven formulations through Epiderm™ over 24 hours using Higuchi model…….……...	81
1.40	The 95% confidence interval and a 95% prediction band of hydrocortisone diffusion from Corticool gel though a non-pre-washed Epiderm™ over 24 hours……...	82
1.41	The 95% confidence interval and a 95% prediction band of hydrocortisone diffusion from Corticool gel though a pre-washed Epiderm™ over 24 hours……	82
1.42	The 95% confidence interval and 95% prediction band of hydrocortisone diffusion from Corticool gel though non-prewashed Epiderm™ and prewashed Epiderm™ over 24 hours……	83
1.43	The diffusion profile of the amount of hydrocortisone release from eight topical formulations through an Epiderm™ over 24 hours…..	85
1.44	The hydrocortisone-diffusion profile of Cortizone-10 ointment through an Epiderm™ over 24 hours……..	85
1.45	A depiction of the initial depletion phase for seven formulations that lasted for half hour……...	86
2.1	The metabolism pathway of acetaminophen in human body……..	102
2.2	The relationship of incidence of toxicity and plasma concentration..	109

LIST OF FIGURES (Continued)

Figure		Page
2.3	Bottom-fluid bed spray coater……	113
2.4	Acetaminophen mingled with other excipients of the core beads and water……...	128
2.5	Spheronizing beads……..	129
2.6	The resultant uncoated beads loaded with the drug …….	129
2.7	The process of dissolving polymer in water…….	130
2.8	Coated beads scheme……	131
2.9	Spray coater used in the coating process, a fluid bed spray coater...	132
2.10	Melatonin tablets……..	133
2.11	A simple tablet compressor used to make tablets…….	134
2.12	Acetaminophen tablets…….	135
2.13	A basket rack assembly for tablet disintegration testing…..…….	136
2.14	A disintegration test of ODTs using a 25ml cylinder……...	137
2.15	A friability tester……...	138
2.16	A tablet hardness tester…….	139
2.17	A dissolution machine, apparatus 2, to conduct dissolution studies on melatonin and acetaminophen tablets……..	141
2.18	A spectrophotometer- Model Backman DU 640……..	142
2.19	Biopharmaceutic drug \-classification system……..	144
2.20	The effects of disintegrants on disintegration times of the tablets...	149

LIST OF FIGURES (Continued)

Figure		Page
2.21	The hardness of tablets containing different disintegrants…..…….	150
2.22	The effect of the concentration of Amberlite IRP 88 on the disintegration times of tablets……..	152
2.23	The correlation between compression forces and hardnesses of a 400mg-maltose tablet (♦), granular mannitol (▲) and 100% microcrystalline cellulose (■)…….	154
2.24	The surface-free energy of dispersive component and polar component of the low- and high-compressibility saccharides. The-surface-free energy of dispersive component (▒) and polar component (▓)…….	156
2.25	The disintegration times of formulations granuated with sorbitol 15%, maltose 15% and maltose 5%.....	158
2.26	The hardnesses of formulations granulated with sorbitol 15%, maltose 15% and maltose 5%.....	158
2.27	The taste locations on the tongue…….	160
2.28	The disintegration times of formulations containing amino acids…..	164
2.29	The disintegration times of formulation containing low-melting-point waxes…..……	166
2.30	The hardnesses of tablets containing low-melting point wax……..	167
2.31	The disintegration times of formulations containing effervescent materials versus not containing effervescent materials……	170
2.32	The standard curve of acetaminophen within the linear range……	172
2.33	The dissolution profiles of acetaminophen from three core beads…..	174
2.34	The dissolution profiles of acetaminophen from coated beads with different levels of the coating with Surelease……..	177

LIST OF FIGURES (Continued)

Figure		Page
2.35	Hydrophilic gel polymers create gel to protect compressed beads….....	179
2.36	The sealing effect of some coating agents on acetaminophen-loaded beads…….	181
2.37	The effects of compression pressure on ability of the sealing sub-coat to reseal beads and maintain the sustained action of the coated beads in releasing acetaminophen……	182
2.38	The dissolution profiles of acetaminophen release from stearic acid containing and non-stearic acid coating beads…….	186
2.39	The tablets containing sustained release beads and without sustained release beads…….	188
2.40	The dissolution profile of melatonin tablets…….	193
2.41	Theoretical plasma concentration after an IV administration for the convolution process of acetaminophen tablets..……..……...	195
2.42	The dissolution profile of tested formulations and an IR tablet of acetaminophen…….	196
2.43	Predicted plasma concentrations of acetaminophen with different pressures……	197
3.1	An african penguin……..	210
3.2	The chemical structure of terbinafine……..	212
3.3	The mechanism of action of terbinafine……..	213
3.4	The individual plasma concentration time curves of individual subjects (a) treatment 1, 3mg/kg, (b) treatment 2, 7mg/kg, (c) treatment 3, 15mg/kg……	246

LIST OF FIGURES (Continued)

Figure		Page
3.5	Spaghetti-scatter plots of the three dosing regimes (a) 3mg/kg, (b) 7mg/kg, 15mg/kg for Terbinafine given as a single oral dose to penguins …….	247
3.6	Mean Terbinafine plasma concentrations and SE error bars of the three single oral doses given in penguins: 3mg/kg, 7mg/kg, and 15mg/kg……...	249
3.7	Dose and AUC proportional evaluation of AUC calculated using non-compartmental analysis by linear regression. (a) uniform weight, (b) weight 1/Y, (c) weight 1/YY……..	261
3.8	Non compartmental analysis of average plasma concentration versus time for the three single oral Terbinafine doses given to penguins (3, 7, and 15mg/kg) with three different weighting functions: uniform, 1/Y and 1/YY……..	262
3.9	Model 3, one-compartment open model, 1st-order absorption, no lag time, 1st-order elimination ……..	269
3.10	Model 13, two-compartment open model, 1st-order absorption, no lag time, 1st-order elimination ……	280
3.11	Terbinafine-plasma-concentration-time curve in penguins fitted to a one-compartment open model, weight 1/YY……..	293
3.12	The individual penguin Terbinafine plasma-concentration-time curves of treatment 4, multiple dosings 15mg/kg per day for four days…….	301
3.13	Terbinafine plasma-concentration-time curves for each penguin presented as Spaghetti plots of all subjects for multiple dosing regimens of 15mg/kg per day for four days…….	301
3.14	The mean Terbinafine plasma-concentration-time curve of multiple dosing of 15mg/kg/day for four days in penguins……	302
3.15	One-compartmental analysis with initial pharmacokinetic estimates	302

LIST OF TABLES

Table		Page
1.1	The studied formulations: 1 gel, 1 ointment, 2 lotions and 4 creams	42
1.2	The standard curve of the area ratios of hydrocortisone over the internal standard propyl paraben, and the drug's concentration …..	43
1.3	Thickness of a synthetic membrane filter, 0.45μm pore size……	45
1.4	The mouse skin thickness of 10 samples, each mouse skin patch was measured 10 different positions (mm)……	45
1.5	Measured Epiderm^{TM} thickness after experiment completion……..	48
1.6	The percentage release of hydrocortisone from eight topical formulations through a synthetic nylon membrane over 24 hours…	49
1.7	The amount of hydrocortisone release from 8 topical formulations through synthetic nylon membrane over 24 hours…….	50
1.8	The permeability coefficients of hydrocortisone from all formulations through the synthetic membrane 0.45 μm……	50
1.9	Lower and upper confidence interval and prediction band of hydrocortisone release from Corticool gel using Fick's-law of diffusion…….	53
1.10	The diffusion coefficients calculated by Higuchi model for synthetic-membrane diffusion……...	56
1.11	The percentage of hydrocortisone drug diffused through a non-pre-washed-mouse skin over 24 hours…….	61
1.12	Amount of hydrocortisone (mg) diffused through a non-pre-washed mouse skin over 24 hours…….	61
1.13	The hydrocortisone permeability coefficient and the R^2 for linear fitting of all formulations permeating through non-prewashed mouse skin ……	62

LIST OF TABLES (Continued)

Table		Page
1.14	The diffusion coefficients following the Higuchi model for hydrocortisone from eight formulations for hydrocortisone diffusing through the non-pre-washed mouse skin ……	68
1.15	The percentage of hydrocortisone (%) diffusion through prewashed mouse skin over 24 hours……	70
1.16	The amount of hydrocortisone (mg) diffusion through a pre-washed mouse skin over 24 hours……	70
1.17	The permeability coefficient of hydrocortisone from eight formulations permeating through pre-washing a mouse skin by water……	71
1.18	The diffusion coefficients of hydrocortisone through a pre-washed mouse skin for the topical hydrocortisone formulations…….	75
1.19	The percentage release of hydrocortisone from seven formulations over 24 hours through an Epiderm^{TM}……..	76
1.20	The amount of hydrocortisone (mg) released from seven formulations over 24 hours through Epiderm^{TM}…….	77
1.21	The permeability coefficients of hydrocortisone from seven topical formulations through Epiderm^{TM}…….	78
1.22	The diffusion coefficients of hydrocortisone from seven formulations using Higuchi model ..……...	80
1.23	The flux and hydrocortisone-release rates of study samples through three different membranes, in the Franz cells derived from the Fick's law of diffusion model……..	88
1.24	The flux and hydrocortisone release rates of study samples through three different membranes in the Franz cell, derived from the Higuchi model……	90

LIST OF TABLES (Continued)

Table		Page
2.1	The spray-coating conditions in fluid bed chamber……....	131
2.2	The effect of disintegrants on the disintegration time……...	147
2.3	The disintegration time and the percentage of Amberlite IRP 88….	152
2.4	Test showing the combination of disintegrants…….	153
2.5	Formulations used to test the combination of high compressible polysaccharides and low-copressible polysaccharides in combination with mannitol…….....	156
2.6	The disintegration time and hardness of sorbitol 15%, maltose 15%, and maltose 5% solution for mannitol granulation……...	157
2.7	The effect of sweeteners on disintegration time and hardness of the tablet…….....	161
2.8	The effects of simple amino acids on disintegration time of tablets..	163
2.9	The effects of low melting-point waxes on the disintegration times of the tablets……...	165
2.10	The effect of cocoa butter on tablet-disintegration time and hardness with and without one-week curing…….	168
2.11	The effects of effervescent materials on disintegration time and hardness of tablet……...	170
2.12	Acetaminophen concentration and respective absorbance of the standard solutions……..	172
2.13	The ingredients used for three different core beads……..	174
2.14	The dissolution of acetaminophen from three different core beads...	175

LIST OF TABLES (Continued)

Table		Page
2.15	The percentage drug released from surelease coated beads……..	176
2.16	Power-law fitting with different surelease weight gain…….	178
2.17	Polymer tested as sealing agents for coated beads…….	180
2.18	Power-law fitting for beads under different pressures……...	183
2.19	The percentage of acetaminophen dissolved versus time from beads containing stearic acid and beads not containing stearic acid.	185
2.20	Power-law fitting acetaminophen-dissolution parameters of stearic acid containing beads and non stearic acid containing beads……	187
2.21	Trial polymers and sweeteners for the taste-masking layer……...	188
2.22	The disintegration times, hardnesses, and friability of tablets containing beads and not containing beads……	190
2.23	Melatonin release from an orally disintegrating tablet……..	193
2.24	Theoretical data generated for acetaminophen-plasma concentration after IV administration.....	195
2.25	Pharmacokinetic parameters from non-compartmental analysis of acetaminophen from IR tablet and tablet produced under 3500lbs...	196
3.1	MIC and MFC of terbinafine on Aspegillus spp. …….	214
3.2	MIC_{95} of terbinafine on fungi……	214
3.3	Plasma concentrations versus time of Terbinafine in each penguin (3, 7 and 15mg/kg single oral dose)……...	230
3.4	Mean plasma concentration of three single dosing treatments 3mg/kg, 7mg/kg, 15mg/kg…….	248

LIST OF TABLES (Continued)

Table		Page
3.5	Pharmacokinetic parameters for Terbinafine in penguins after fitting single-dosing of mean plasma concentration versus time data fitting with uniform weight, 1/Y, 1/YY…….	263
3.6	Pharmacokinetic parameters for Terbinafine in each individual penguin by non-compartmental analysis, and uniform weighting …	263
3.7	Pharmacokinetic parameters for Terbinafine in each individual penguin by non-compartmental analysis, and weight 1/Y…….	264
3.8	Pharmacokinetic parameters for Terbinafine in each individual penguin by non-compartmental analysis, and weight 1/YY……..	265
3.9	Pharmacokinetic parameters for a one compartment open model fitted with no initial parameter estimates, and uniform weight ……	272
3.10	Pharmacokinetic parameters for a one compartment open model fitted with no initial parameter estimates, and weight 1/Y……...	273
3.11	Pharmacokinetic parameters for a one compartment open model fitted with no initial parameter estimates, and weight 1/$\sqrt{Y}$ ……...	273
3.12	Pharmacokinetic parameters for a one compartment open model fitted with no initial parameter estimates, and weight 1/YY…….	274
3.13	Pharmacokinetic parameters for a one compartment open model fitted with no initial parameter estimates, and weight 1/$\sqrt{YY}$	275
3.14	Pharmacokinetic parameters for a one compartment open model fitted with initial parameter estimates, and uniform weight …….	275
3.15	Pharmacokinetic parameters for a one compartment open model fitted with initial parameter estimates, and weight 1/Y…….	276
3.16	Pharmacokinetic parameters for a one compartment open model fitted with initial parameter estimates, and weight 1/$\sqrt{Y}$ ……	277

LIST OF TABLES (Continued)

Table		Page
3.17	Pharmacokinetic parameters for a one compartment open model fitted with initial parameter estimates, and weight 1/YY……..	277
3.18	Pharmacokinetic parameters for a one compartment open model fitted with initial parameter estimates, and weight 1/ $\hat{Y}\hat{Y}$ …….	278
3.19	Pharmacokinetic parameters for a two compartment open model fitted using no initial parameter estimates, and uniform weight …..	282
3.20	Pharmacokinetic parameters for a two compartment open model fitted using no initial parameter estimates, and weight 1/Y……..	282
3.21	Pharmacokinetic parameters for a two compartment open model fitted using no initial parameter estimates, and weight 1/ $\hat{Y}$ …….	283
3.22	Pharmacokinetic parameters for a two compartment open model fitted using no initial parameter estimates, and weight 1/YY……	284
3.23	Pharmacokinetic parameters for a two compartment open model fitted using no initial parameter estimates, and weight 1/ $\hat{Y}\hat{Y}$ …….	285
3.24	Pharmacokinetic parameters for a two compartment open model fitted using initial parameter estimates, and weight uniform……	285
3.25	Pharmacokinetic parameters for a two compartment open model fitted using initial parameter estimates, and weight 1/Y……..	286
3.26	Pharmacokinetic parameters for a two compartment open model fitted using initial parameter estimates, and weight 1/ $\hat{Y}$ …….	287
3.27	Pharmacokinetic parameters for a two compartment open model fitted using initial parameter estimates, and weight 1/YY……	287
3.28	Pharmacokinetic parameters for a two compartment open model fitted using initial parameter estimates, and weight 1/ $\hat{Y}\hat{Y}$ …….	288

LIST OF TABLES (Continued)

Table		Page
3.29	AIC and SBC values for comparison after fitting the data to a one-compartment open model using no initial parameter estimates, weight 1/ YY …….	289
3.30	Pharmacokinetic parameters for the Terbinafine concentration time data that fitted the model for a one compartment open model best, weight 1/YY……..	290
3.31	Pharmacokinetic parameters from best fitted one-compartment open model, weight 1/YY, for mean Terbinafine plasma-concentration-time curve……..	293
3.32	Terbinafine plasma concentration versus time in penguins after dosing of 15mg/kg/day for four days……	294
3.33	The mean plasma-concentration time curve values of Terbinafine after 15mg//kg/day oral multiple dosing in penguins for four days	302
3.34	Pharmacokinetic parameters for Terbinafine in penguins determined by non-compartmental analysis of multiple dosing of 15mg/kg/day for four days in penguins…….	303
3.35	Pharmacokinetic parameters of Terbinafine in penguins after 15mg/kg/day for four days of multiple dosings after being fitted with unique initial pharmacokinetic parameter estimates……..	303
3.36	The mean trough-penguin-Terbinafine concentrations of the multiple-dose study……	306
3.37	The deep-tissue-elimination constant of the mean plasma-concentration-time curve……...	306
3.38	Pharmacokinetic parameters of Terbinafine after multiple dosings in penguins accounting for the deep tissue elimination phase……...	307
3.39	The individual pharmacokinetic parameters of Terbinafine in penguins after the manual fitting of the data to the one compartment open model……..	307

3.40 The final pharmacokinetic parameters of terbinafine in penguins with 15mg/kg/day multiple dosing…… 308

CHAPTER 1

HYDROCORTISONE PERMEATION STUDY USING A SYNTHETIC MEMBRANE, MOUSE SKIN AND AN EPIDERM™ CULTURED SKIN

Hang Le, Monica Chuong, John Mark Christensen

ABSTRACT

Purposes: Several permeable membranes have been used to evaluate topical medicaments formulated in different vehicles, such as synthetic membranes, animal, and human skin obtained from either a cadaver or plastic surgery. The synthetic membrane reflects dissolution properties of the drug, but not permeation behavior; whereas, animal and human skin have limited availability. EpiDerm™ is human-derived epidermal keratinocytes cultured to form a multilayered, highly differentiated human epidermis. This study was set to compare the release of hydrocortisone from six topical over-the-counter products along with one prescription cream using a Nylaflo membrane, a mouse skin and an Epiderm™, human cultured skin. In addition, the effect of pre-washing the skin with an exfoliating cleanser prior to applying a hydrocortisone topical gel product was evaluated. **Methods:** A Franz upright dissolution apparatus was used to study six over-the-counter 1% hydrocortisone products: 1 gel, 2 creams, 2 lotions, 1 ointment, and one prescription cream, USP, 2.5%. Nylaflo membranes were obtained from Pall Life Sciences, while 24 Epiderm™ -cultured human skins were purchased from MatTek. EpiDerm™ cultured in a 2.2-cm-cell insert was mounted directly on to a Franz cell with a 2.0-cm orifice. Collected samples from the Franz cells were assayed by HPLC to quantify the hydrocortisone. **Results:** Similar rank order was observed for hydrocortisone release from the topical products with each permeable membrane (the synthetic membrane, mouse skin, and EpiDerm™). Topical hydrocortisone-gel formulation ranked the highest in permeation through both the mouse skin and the EpiDerm™ (2.24±0.38% vs. 0.68 ± 0.20% in 24 h with EpiDerm™) among the seven products evaluated. The hydrocortisone

penetration through the synthetic membrane was significantly higher than through the mouse skin or the EpiDerm™. **Conclusions:** Similar release patterns for hydrocortisone patterns were observed among three barriers. Hydrocortisone formulation in a topical gel facilitated greater drug permeation through membranes exceeding the other topical products after 10 h. Skin pre-washed with an exfoliating cleanser increased the hydrocortisone penetration through the EpiDerm™.

INTRODUCTION

STRUCTURE AND FUNCTION OF SKIN

The skin is the largest organ of the body making up 10% of the body mass. It performs many vital roles and provides a barrier for the inner body from outside environment.

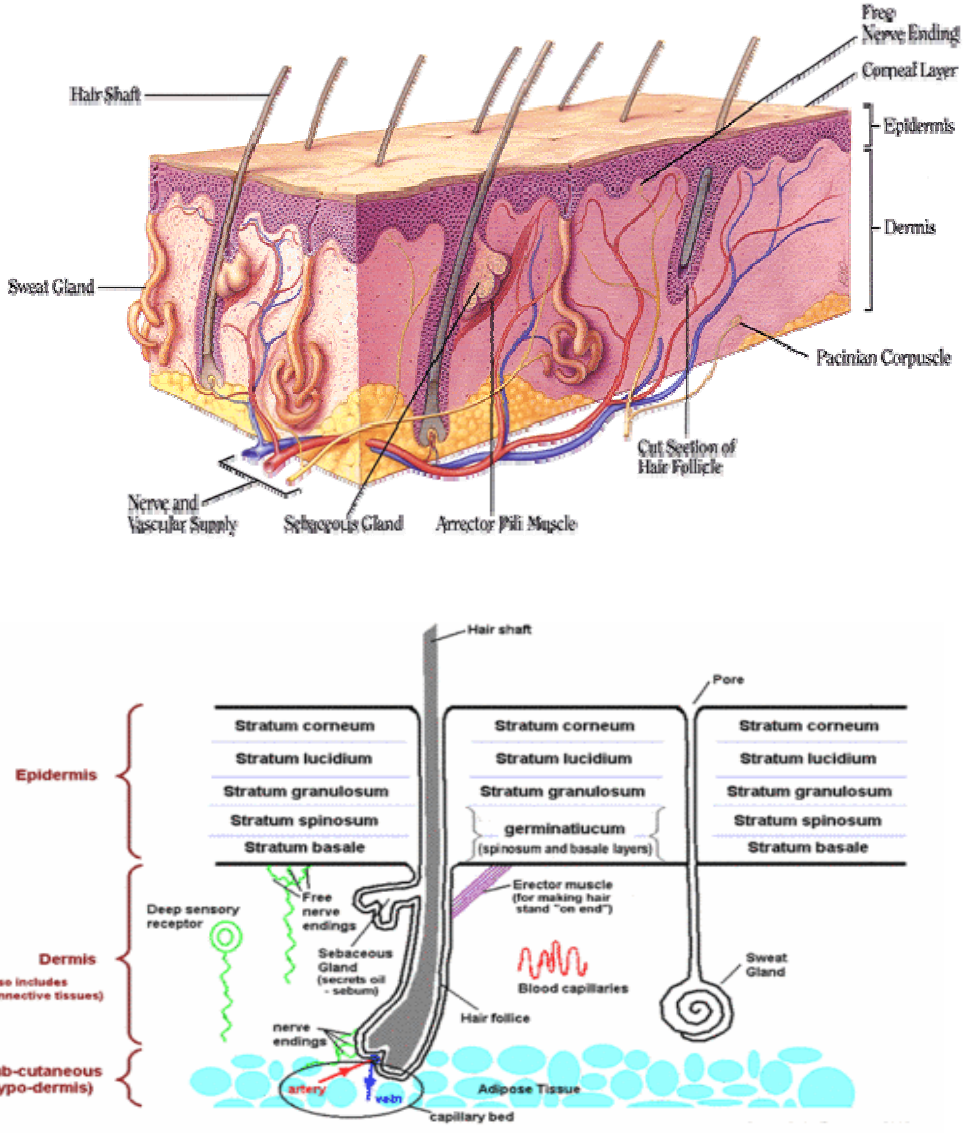

Figure 1.1. The structure of skin with its two main layers: The Epiderm and Dermis

The skin participates in internal-heat regulation, and protects the body from dangerous agents (bacteria, virus, chemicals, radiation, allergens…). It is also the major sensory organ. There are two main layers of the skin: the epidermis and dermis [1].

Epidemis

The epidermis generates stratum corneum composing the outmost layer of the skin. The stratum corneum is heterogenous consisting of 15-20 layers of flattened, stacked, hexagonal, and cornified cells about 10-20μm thick. These non-viable cells originate in the viable epidermis and undergo morphological differentiation to desquamation. The thickness varies with the inner layer being more thick and flattened toward the outside. The thickness of the stratum coneum varies according to its position on the body, palms and soles being the thickest parts. The stratum corneum also provides an insulation layer to prevent fluid loss from inside the body. Stratum corneum has a very high density with low hydration 15-20%. The stratum corneum contains insoluble bundled keratins (70%) and lipid (20%). The intercellular region contains mainly lipids and desmosomes for corneocyte cohesion. Desquamation of the horny layer allows the protection function to be more enhanced and reduces remarkably the evaporation of water. Usually, it takes 2-3 weeks for a complete turn over of the stratum corneum. Basal lamina are the original cells of the epidermis which have melanocytes, Langerhans cells, and Merkel cells, and two keratinic cell types: stem cells, which differentiate to other new cells types and the other cell type which connects the epidermis to the basement membrane.

The connection between cell lines of the desmosomal junction and the basal lamina to the basement membrane is made up of hemi-desmosomes.

The cells of Langerhans are intimately involved in the facilitation of the interaction of antigen within the skin's immune system. On the activation of the skin's immunity, these cells facilitate migration of agents of the body's immune system from the epidermis on to the dermis and onto regional lymph nodes where they contact to T-cells.

Melatonocytes produce melanins, high molecular weight polymers of indole quinone that cause pigmentation of the skin.

Merkel cells are thought to have a role as sensors because they are closely associated with nerve endings [1].

Dermis

The thickness of the dermis is 0.1-0.5cm. The Dermis provides nutrition and immune support to the epidermis. The dermis also plays a role in temperature, pressure, and pain regulation. The typical cells are fibroblasts, mast cells, and melanocytes. 70% of the dermis is collagenous fibers. An abundant blood or vascular system is present providing nutrition to the skin, and facilitating repair, immune response, and heat regulation.

Arteriovenous anastomoses provide direct shunting of up to 60% of the skin's blood flow, approximately 0.05ml/(min*cm^{-3}). The lymphatic system is an essential part of the skin acting as a regulator of its interstitial pressure, and playing a role in defense mechanisms and waste removal.

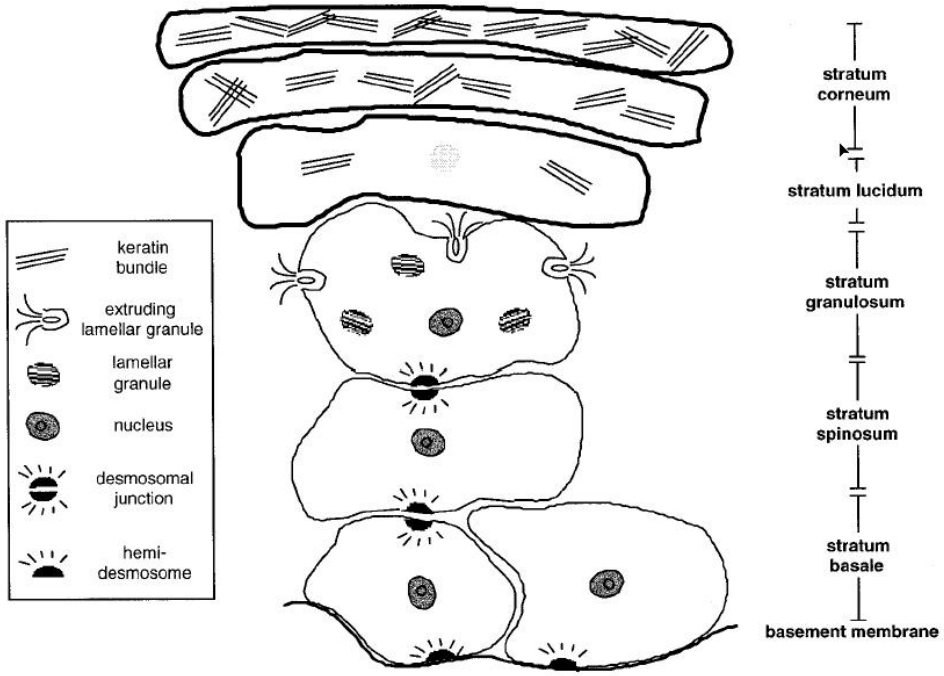

Figure 1.2. Epidermal differentiation in the epidermis [1]

Subcutis

The subcutis is the deepest layer of the skin. It is also called the hypodermis, serving as a heat isolator and shock absorber. It consists mainly of fat cells lying within lobules and connects to the dermis by inter-connecting collagen and elastin fibers. Besides fat cells, fibroblasts and macrophases are also observed.

Skin Appendages

Hair follicles are distributed across the entire skin's surface. Erector pilorum, a type of smooth muscle, appends to the dermal tissue and allows the hair to stand up in response to fear and cold. Each hair follicle is associated with a sebaceous gland, which secretes sebum (triglycerides, free fatty acids, protects, lubricates, etc….), for the skin. The pH value of sebum is maintained around 5. Eccrine glands are distributed over most of the whole body; whereas, Apocrine glands are seen in

Axillae, nipples, and anogenital areas. The nail can be considered as a vestigial in human's but it still provides some protective functions. The nail consists of keratinized cells fused into dense, elastic unity. The nail-basement membrane is very similar to the epidermal-basement membrane in structure.

SKIN TRANSPORT

The stratum corneum is recognized as the major rate-limiting barrier for drug permeation through the skin. The brick and mortar of the stratum corneum vary with the hydration and pathological condition of the skin. Transport through the epidermis is mostly a passive process. This is why permeability through the skin is dependent largely on drug characteristics.

Another important barrier to skin transport is the sebum. As a vital organ, the skin is always covered by a secreted sebum, sweat, bacteria, and dead cells. The presence of these substances also adds to some extent to the resistance of drug transportation. Under normal conditions, these components on the human skin are considered to have negligible influence [2].

Transport pathways through the stratum corneum

Trans-cellular, Inter-cellular and trans-appendeal pathways are three major routes that many authors mention for a drug to cross through the skin.

Trans-cellular

The trans-cellular pathway is not considered a major route for most APIs to cross the skin. Drugs would have to transport through a lipophilic membrane, then a hydrophilic compartment, the cytoplasm, and finally through the other lipophilic

membrane. The process is repeated for the entire thickness of the skin. Solutes of drug in vehicle are preferred for drug transportation through the skin [3]. It is suggested that polar and non-polar solutes pass through stratum corneum by different mechanisms. Polar molecules are thought to diffuse through high-energy pathways relating to water in the outer surface of keratin filaments. Lipophilic substances prefer to go through membranes. However, now there is abundant evidence that the main pathway for a drug to cross the skin is the inter-cellular route.

Inter-cellular

Although the intercellular component occupies a small volume in the whole stratum corneum, the physical distribution of lipids and the void area of it is considered to facilitate drug permeation [4]. Intercellular pathway is the most attractive for researchers to modify to get desirable drug permeability. Many studies confirm that the inter-cellular lipid, not the corneocyte protein, was the main permeability barrier. Other studies report that the diffusion of solutes through the tortuous inter-cellular pathway is much more dominant than through the keratinized cell membranes (trans-cellular route) [5, 6].

Histo-chemical studies show that the intra-cellular spaces of the stratum corneum are devoid of lipids and the inter-cellular fraction is much larger than estimated. Other studies indicate that the permeability of soluble substances like urea, manitol, tetraethylammonium, corticosteroids is controlled by the porous inter-cellular permeation pathway. The thickness, number of cell layers, the drug concentration, and the structure of inter-cellular lipids make the percutanous absorption of a dug different when applied to leg versus abdominal skin [7].

Lipid lamellae in the cell gaps within the stratum corneum are the rate-controlling barrier for drug transportation where the major lipid molecules are ceramides, cholesterol, or free fatty acids (Figure 1.5) [8]. An individual lamella is about 10nm thick and consists of two or three lipid bi-layers. A lamella of 13.4 nm is predominant and sometimes a 6.4nm lamella was observed scattering. An X-ray-image capture revealed that the lamella is a parallel structure in inter-cellular domains.

Lipid and polar pathways through the intercellular lipids are the two main mechanisms through which a solute diffuses.

Trans-appendal pathway

A trans-appendal pathway is not a major pathway but can not be a negligible drug transportation route either. The earliest evidence supports the existence of a follicular route of drug penetration. Drug absorption through hair follicles involves the hair fiber, outer-root sheath, air-filled canal, and the sebaceous gland [9].

The route of drug penetration through the sweat duct involves diffusion either through the lumen or wall to below the epidermis and through the ring of keratinized cells.

It is estimated that there are approximately 500-1000 pilosebaceous units/cm^2 on either the face or scalp. The diameter of each unit is 50-100 μm. The orifices take up 0.1% of the surface area in low-density areas of hair and 10% in high-density areas of hairs. Therefore, the role of hair-follicle and sweat-duct drug penetration can be remarkable [10].

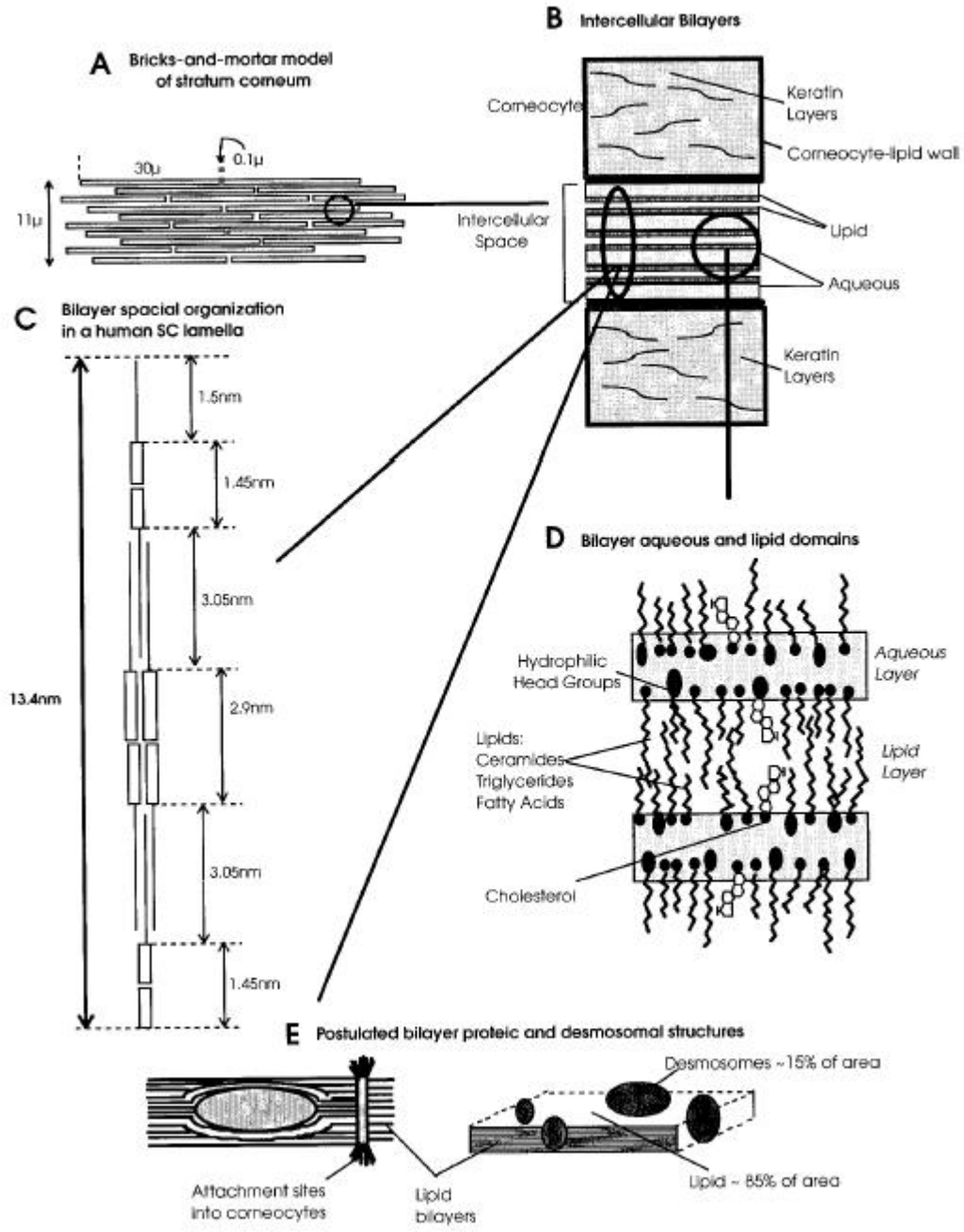

Figure 1.3. Structure of the stratum corneum [2]

A. "Brick and mortar" model
B. Intercellular bilayers
C. The spatial organization of lipids within the bilayers
D. The location of polar and lipid domains
E. Proteic and desmosomal structures within the lipid bilayers

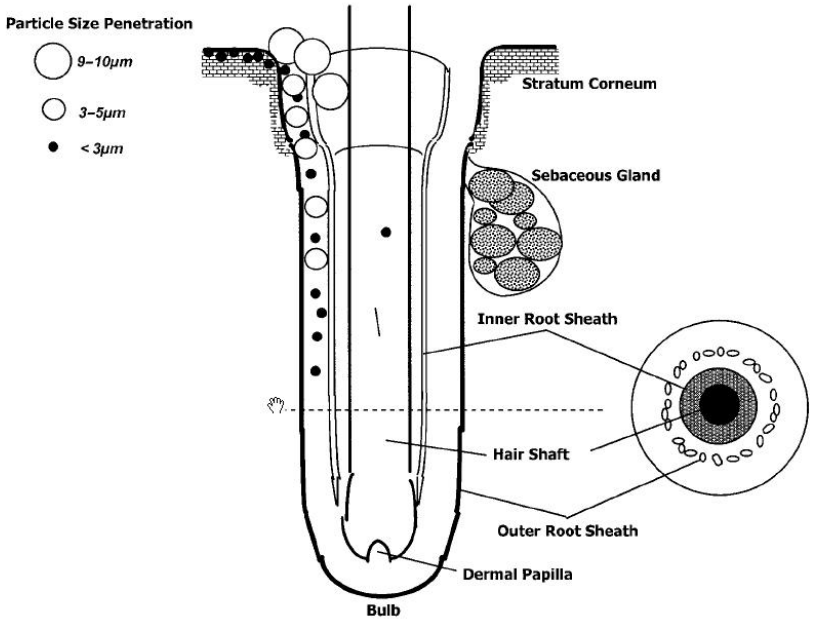

Figure 1.4. Hair follicle structure and the capability of particle size penetration through the follicle

Polymers and colloidal particles can be targeted to the follicle pathway [11]. The size of the applied particles determines the extent of follicular drug transportation due to the limit of the follicle's diameter. The optimal size at which penetration reaches maximum absorption is 3-10μm. Either smaller or larger size particles are rejected. The beads smaller than 1μm are kept on the surface due to surface energy. Beads larger than 10 μm are too big for the follicles.

Effect of hydration

Hydration of the stratum corneum can lead to profound changes to its barrier properties. Water effects on the skin are due to the combination of the swelling of hydrated corneocytes and the water-induced expansion of the intercellular lipid lamellae. The dead cells that make up the stratum corneum are dry and desquamated.

The insulated layer prevents water loss to the environment and aids in heat preservation. Under normal conditions, the stratum corneum maintains a 15-20% level of water. Under excessive soaking, the stratum corneum weight can increase by 400% compared to dry weight [12]. By interacting with water, α-helix keratin filaments become loosely packed and more flexible. Nevertheless, wide-angle X-ray diffraction studies indicated that no bilayer swelling occurs with hydration. This suggests that water molecules are not absorbed between the lamellar regions. Besides that, other studies reveal that fully-hydrated stratum corneum contains swollen corneocytes with pools of water apparently displacing and separating keratin filaments [13].

Water also causes an extraction of lipid and creates vesicle-like lipid structures. These lacunae are discontinuous microdomains located in the middle to outer layers of the stratum corneum. It has been suggested that the lacunae are the result of desmosomal degradation. The lacunae's expansion occurs through polar-head regions of the intercellular lipids, and the lacunae facilitate the replacement of water and create pools of water. The whole process of hydration leads to a dramatic change of permeability of the human skin to the drug.

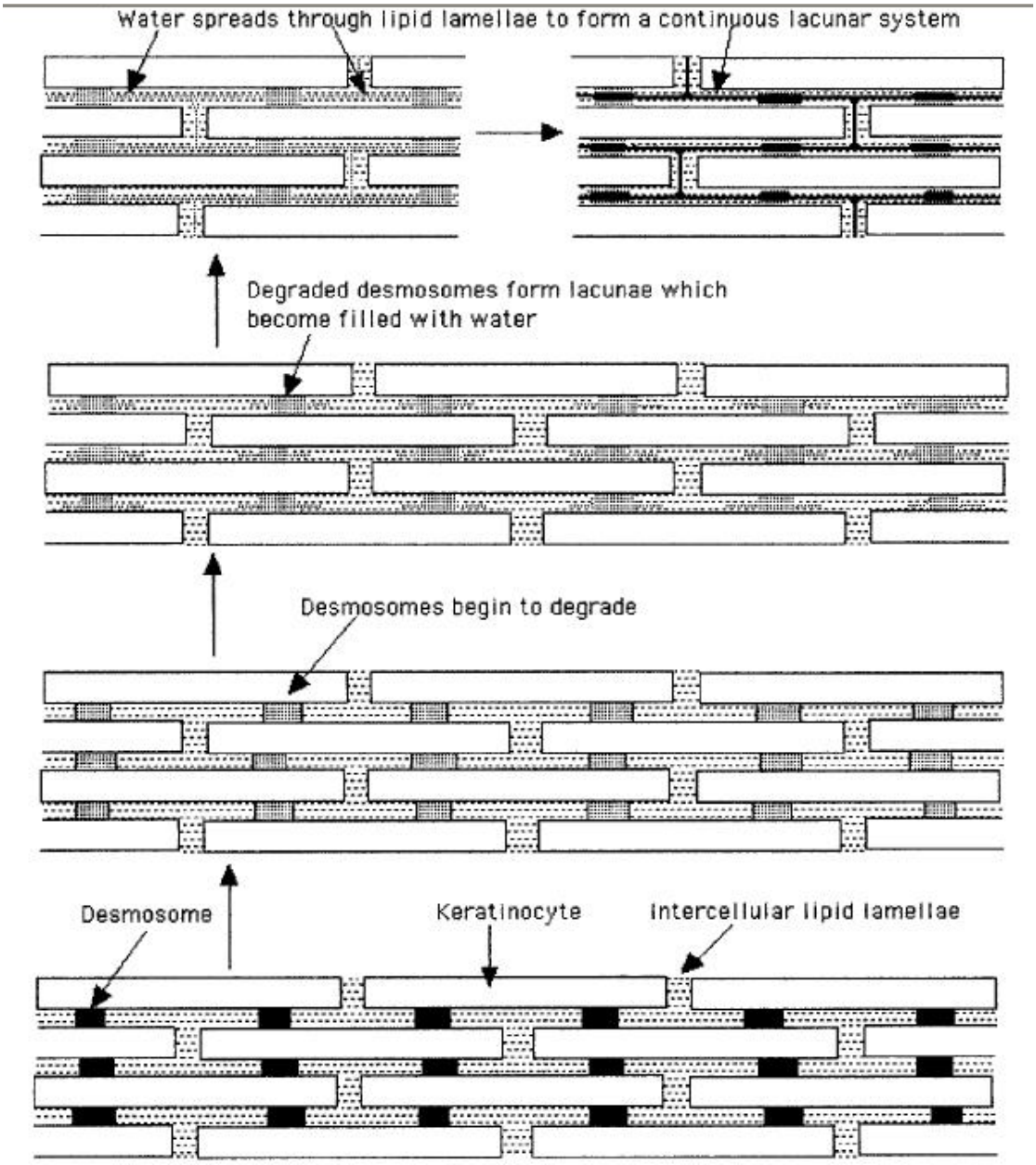

Figure 1.5. Lacunae formed by degrading desmosomes provide an obvious site for water pooling, and during prolonged exposure to water, lateral expansion of the lacunae occurs through the polar head regions of the intercellular lipids [2].

MATHEMATICAL MODELS FOR DRUG TRANSPORT THROUGH SKIN

Fick's-first-law of diffusion

The flux J is related to velocity and the concentration of molecules in motion [14]:

$$J_i = C_i \upsilon \quad \text{(equa. 1)}$$

For one dimension x

$$J = -D\frac{\partial C}{\partial x} = \frac{dM}{Sdt} \quad \text{(equa. 2)}$$

Fick's second law

$$\frac{dC}{dt} = D\frac{\partial^2 C}{\partial^2 x} \quad \text{(equa. 3)}$$

$$J = -D*(\frac{\partial C}{\partial x}) = D(\frac{C_1 - C_2}{h}) \quad \text{(equa. 4)}$$

J: flux
D: Diffusion Coeficient
C: Concentration
x: Pathway direction

$\frac{C_1 - C_2}{h}$ approximates dC/dx

$$K = \frac{C_1}{C_d} = \frac{C_2}{C_r} \text{(equa. 5)}$$

C_d, C_r is concentration in donor side and receiver side respectively
K: partition coefficient

$$\frac{dM}{dt} = \frac{DSK(C_d - C_r)}{h} \quad \text{(equa. 6)}$$

If $C_r = 0$. The equation become

$$\frac{dM}{dt} = \frac{DSKC_d}{h} \quad \text{(equa. 7)}$$

$$P = \frac{DK}{h} \quad \text{(equa. 8)}$$

The amount of drug release is proportional with time.

$$M = PSC_d t \quad \text{(equa. 9)}$$

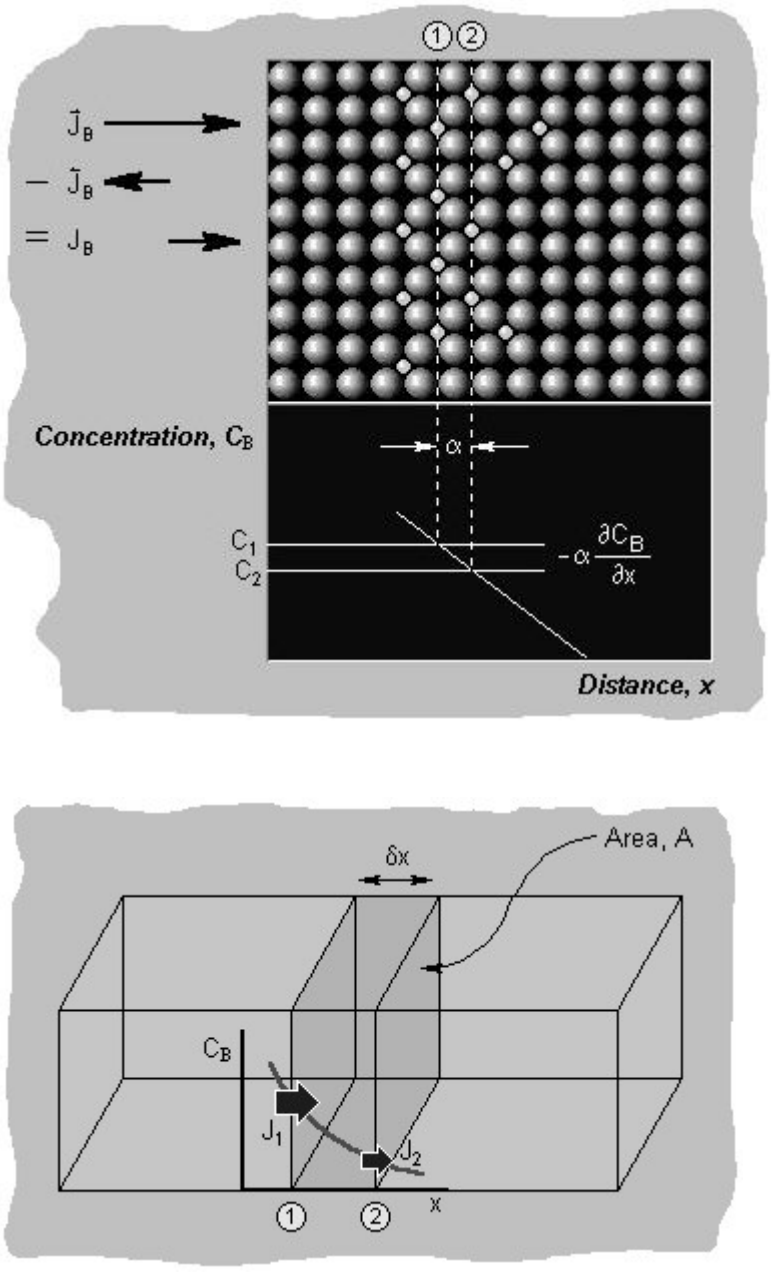

Figure 1.6. Schematic depiction of Fick's-law and a substance illustrating the diffusion

Higuchi model

When a drug is deposited inside a matrix, the drug undergoes two processes. First, the matrix absorbs solvent from the surrounding medium into the deep parts of the matrix. The drug dissolves and becomes a solute. The solute transits through a

tortuous path from far inside the matrix to the surface of the matrix. Second, from the surrounding medium, the drug travels through the membrane (usually the skin).

Higuchi developed an equation for the release of a drug from an ointment base and solid drugs dispersed in a homogenous and granular matrix dosage form [15].

Fick's first law:

$$\frac{dM}{Sdt} = \frac{dQ}{dt} = \frac{DC_d}{h} \text{ (equa. 10)}$$

$$dQ = Adh - \frac{1}{2}C_d dh \text{ (equa. 11)}$$

The derivation given:

$$(A - \frac{1}{2}C_d)dh = \frac{DC_d}{h} \text{ (equa. 12)}$$

$$\frac{2A - C_d}{2DC_d}\int hdh = \int dt \text{ (equa. 13)}$$

$$t = \frac{(2A - C_d)}{4DC_d}h^2 + C \text{ (equa. 14)}$$

at t = 0, h = 0

Thus, it gives:

$$t = \frac{(2A - C_d)h^2}{4DC_d} \text{ (equa. 15)}$$

$$h = \left(\frac{4DC_d th^2}{2A - C_d}\right) \text{ (equa. 16)}$$

The quantity of drug completely diffuses

$$Q = hA - \frac{1}{2}hC_d \text{ (equa. 17)}$$

$$Q = \left(\frac{DC_d t}{2A - C_d} \right)^{1/2} (2A - C_d) \quad \text{(equa. 18)}$$

$$Q = [D(2A - C_d)C_d t]^{1/2} \quad \text{(equa. 19)}$$

The equation if differentiate to yield the rate of drug release at time t

$$\frac{dQ}{dt} = \frac{1}{2}\left(\frac{D(2A - C_d)C_d}{t} \right)^{1/2} \quad \text{(equa. 20)}$$

if A is much greater than C_s. It means the sink condition is maintained

$$Q = (2ADC_d t)^{1/2} \quad \text{(equa. 21)}$$

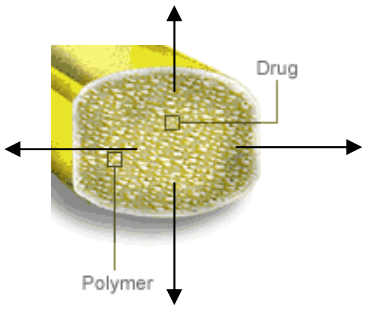

Figure 1.7. The drug diffuses from a matrix

TOPICAL DOSAGE FORM

A topical dermatological product is designed to deliver the drug into the skin for treating dermal disorders. According to traditional classification, the topical dosage forms are divided by their physical properties and the dispersion phases in the dosage form. The two major phases are oil and water. Gels, creams, lotions and ointments are semisolid preparations intended for external application to the skin or mucous membranes.

Ointments

USP defines “ointments” as semisolid preparations intended for external application to the skin or mucous membranes. Ointment bases recognized for use as

vehicles fall into four general classes: The hydrocarbon bases, absorption bases, water-removable bases, and water-soluble bases". Each therapeutic ointment possesses as its base a representative of one of these four general classes.

Hydrocarbon bases:

These bases, which are known also as oleaginous ointment bases, typically contain hydrocarbons or paraffins and are represented by white petrolatum and white ointment. Only small amounts of an aqueous component can be incorporated into them. These bases are hydrophobic and are difficult to remove.

Absorption bases:

This class is comprised of bases divided into smaller groups:

1. This group is bases that permit the incorporation of a limited amount of aqueous solutions with the formation of a water-in-oil emulsion (hydrophilic Petrolatum and Lanolin).
2. This group permits the incorporation of additional quantities of aqueous solutions (Lanolin).

An ointment classically is considered "occlusive dressings" since it retains drug for an extensive period of time on the surface of the skin causing the drug to be difficult to remove. Water-removable bases and water-soluble bases are related to "cream" and gel forms.

Creams

Creams are semi-solid dosage forms containing one or more drug substances dissolved or dispersed in a suitable base. This term recently refers to the products

consisting of oil-in-water emulsions or aqueous microcystalline dispersions of long-chain fatty acids or alcohols that are water washable. However, many authors consider creams as both water-in-oil and oil-in-water systems. Creams are semisolid emulsion systems with opaque appearances.

In most pharmaceutical emulsions, the system consists of water, oil and surfactants (ionic or nonionic) to stabilize the systems. The common surfactants are sodium alkyl sulfates (anionic), alkylammonium halides (cationic) and polyoxyethylene alkyl ethers or polysorbates (anionic).

Lotions

Like creams, a lotion is a fluid suspension or emulsion; whereas, most ointments are based on mineral oil and petrolatum. Lotions, on the other hand, usually contain a larger amount of water than creams, are softer, and closer to liquid in texture than other semi-solids such as creams. Sometimes, however, there is no mark or point in texture to distinguish between a cream and lotion.

Gels

Gels are semisolid systems consisting of either suspensions made up of small inorganic particles or large organic molecules interpenetrated by a liquid. Gels contain a continuous structure that provides solid-like properties. Depending on constituents, gels may be clear or opaque, polar or non-polar. Natural gums were the early known agent to provide gels from such gums as tragacanth, guar, xanthan. Semi-synthetic and synthetic materials including methyl cellulose (MC), carboxymethylcellulose (CMC), hydroxyethylcellulose (HEC), hydroxypropylcellulose (HPC), and hydroxypropyl

methylcellulose (HPMC) are available. Gels have now become popular as a topical dosage form.

Single-phase gels are usually clear transparent semisolids consisting of dispersions of small or large molecules in an aqueous-liquid-vehicle-rendered-jelly-like substance by the addition of gelling agents. Their consistency and rheologic character depend on whether the emulsion is a water-in-oil or oil-in-water type and on the nature of the solids in the internal phase. Ninety percent of these systems' composition (e.g., water, ethanol, propylene glycol) are appreciably volatile. Evaporation of these ingredients begins immediately upon application of the dosage form and continues until all of the volatile substances are exhausted. The rate of evaporation of a given ingredient depends on its momentary vapor pressure, which changes as the formula is evaporative concentrated.

The two-phase system contains gel and small discrete particles. If the particle size is relatively large, the gel mass is referred to as magma. Both gels and magmas are thixotropic, forming semisolids on standing and becoming liquid on agitation.

HYDROCORTISONE

Hydrocortisone is a naturally occurring glucocorticoid with well-known effects to the immune system. Glucocorticoids also have profound effects on metabolism, and they are used in to treat many disorders such as endocrine disorders, rheumatic disorders, allergic states, ophtalmic disease, respiratory disease, and hematologic disorders. Hydrocortisone (HC) has anti-pruritic and anti-inflammatory effects that benefit many skin conditions, and dermatologic diseases like pemphigus, bullous

dermatitis herpetifomis, erythema multiforme, exfoliative dermatitis, mycosis fungoides, psoriasis, and seborrehic dermatitis. These skin conditions can be treated by hydrocortisone in a topical dosage form. Various nonprescription topical products are available in different dosage forms, such as a gel, cream, lotion and an ointment.

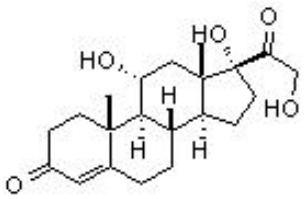

Hydrocortisone

UPAC: (11β)-11,17,21-Trihydroxypregn-4-ene-3,20-dione

The hydrocortisone solubility (mg/ml) in water is 0.28. ethanol 15; methanol 6.2; acetone 9.3; chloroform 1.6; propylene glycol 12.7; ether 0.35.

Itchy reaction and the mechanism of hydrocortisone to reduce the itchy

Itch (Latin: pruritus) is defined as an unpleasant sensation that evokes the desire or reflex to scratch. Itch has many similarities to pain and both are unpleasant sensory experiences but their behavioral response patterns are different. Pain creates a reflex withdrawal, while an itch leads to a scratch reflex [16]. An itch is a reaction to an allergy. Allergy is classified into two types: acute response and late-phase response.

Acute response

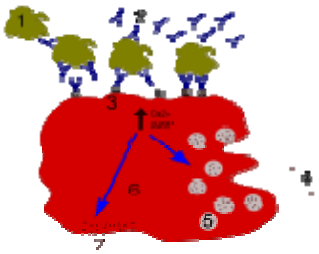

Figure 1.8. Depiction of an acute-response allergic mechanism to a foreign substance

The degranulation process in an allergy.**1** - antigen; **2** - IgE antibody; **3** - FcεRI receptor; **4** - preformed mediators (histamine, proteases, chemokines, heparine); **5** - granules; **6** - mast cell; **7** - newly formed mediators (prostaglandins, leukotrienes, thromboxanes, PAF)

In the early stages of an allergy, a type I hypersensitivity reaction against an allergen encountered for the first time causes a response in a type of immune cell called a T_H2 lymphocyte, which belongs to a subset of T-cells that produce a cytokine called interleukin-4 (IL-4). These T_H2 cells interact with other lymphocytes called B-cells, whose role is the production of antibodies. Coupled with signals provided by IL-4, this interaction stimulates the B cell to begin production of a large amount of a particular type of antibody known as IgE. Secreted IgE circulates in the blood and binds to an IgE-specific receptor (a kind of Fc receptor called FcεRI) on the surface of other kinds of immune cells called mast cells and basophils, which are both involved in the acute inflammatory response. The IgE-coated cells at this stage are sensitized to the allergen [17].

If later exposure to the same allergen occurs, the allergen can bind to the IgE molecules held on the surface of the mast cells or basophils. Cross-linking of the IgE and Fc receptors occurs when more than one IgE-receptor complex interacts with the same allergenic molecule, and activates the sensitized cell. Activated mast cells and basophils undergo a process called degranulation, during which histamine and other inflammatory chemical mediators (cytokines, interleukins, leukotrienes, and prostaglandins) are released from their granules into the surrounding tissue causing

several systemic effects, such as vasodilatation, mucous secretion, nerve stimulation and smooth muscle contraction. This results in rhinorrhea, itchiness, dyspnea, and anaphylaxis. Depending on the individual, allergen, and mode of introduction, the symptoms can be system-wide (classical anaphylaxis) or localized to particular body systems; for example, asthma is localized to the respiratory system and eczema is localized to the dermis [17].

Late-phase response

After the chemical mediators of the acute response subside, late phase responses can often occur. This is due to the migration of other leukocytes such as neutrophils, lymphocytes, eosinophils and macrophages to the initial site. The reaction is usually seen 2-24 hours after the original reaction [18]. Cytokines from mast cells may also play a role in the persistence of long-term effects. Late-phase responses seen in asthma are slightly different from those seen in other allergic responses although they are still caused by the release of mediators from eosinophils and are still dependent on activity of T_H2 cells [19].

Mechanism action of hydrocortisone

Glucocorticoids have well-known genomic effects. Glucocorticoids bind to various receptors including the glucocorticoid receptor (GR or hGRα), mineralocorticoid receptor (MR), progesterone receptor (PR), androgen receptor (AR), and estrogen receptor (ER). All of these receptors have a close relationship with the thyroid hormone, retinoids, vitamin D, and the peroxisome proliferators-activated receptors.

Conversely, a range of isoforms of these receptors are known. Glucocorticoids receptors consist of an N-terminal domain activating gene expression, a central DNA-binding moiety and a C-terminal ligand-binding domain. In the nucleus, GR binds to glucocorticoid response elements (GREs). Glucocoticoids may also inhibit the gene expression by binding monomers of GR to a promoter containing negative GREs (nGREs). In epidermal layer, the synthesis of basal-cell-specific (K5, K14) and disease-associated keratins (K6, K16, K17) is under the control of four nGREs [19-21].

Besides the genomic activity, glucocorticoids inhibit the formation of inflammatory cytokines, and glucocorticoids interfere with the activation of a variety of immunologic cells such as dendritic cells. Glucocorticoids also enhance eosinophil and T cell apotosis. These *in situ* activities on the skin can explain the immediate activity of hydrocortisone; whereas, the genomic effects are related to long-term drug action [22, 23].

MEMBRANES FOR THE HYDROCORTISONE PERMEATION STUDY

The most common method for evaluation of skin permeation is drug diffusion through a membrane. Permeation barriers that have been studied include synthetic membranes, animal skin and human skin donated from either a cadaver or from plastic surgery. The advantages of an *in vitro* study are the experimental conditions can be controlled precisely with simple equipment. However, the method has limits since it lacks some *in vivo* conditions like blood flow, and viable cells.

Synthetic membrane

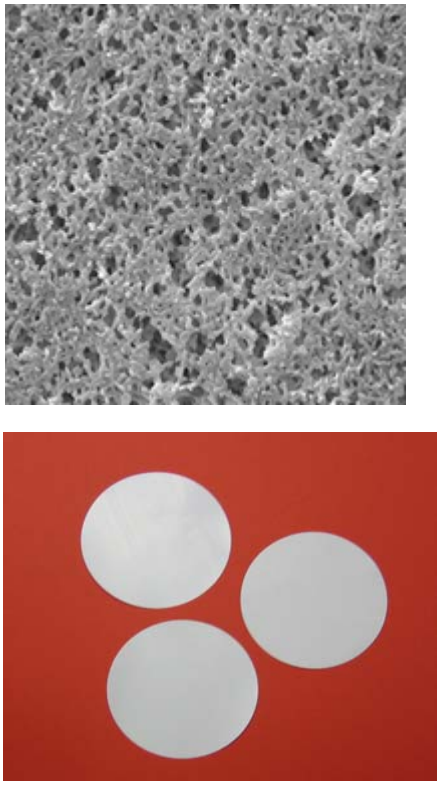

Figure 1.9. Synthetic filter membrane 0.45µm

The nylon filter membrane is a plastic that is porous. The pore size is 0.45 µm. This kind of membrane is compatible with many solvents and pH ranges [24]. As a result, concern for its physical stability during the diffusion study is null. The thin membrane and large pore size offer an expectation of a high drug-diffusion rate.

Mouse skin

Among laboratory experimental animals, the expected skin permeability to exogenous substances is ranked in the following order: mouse > rat > guinea pig > rabbit > monkey > dog > goat > sheep > pig > cattle > human [25]. Mouse skin is a convienient and common source that can be obtained in the laboratory scale. The water permeability coefficient of a hairless mouse skin is 350.7 cm^2/hr and an intact mouse skin's is 143.75 cm^2/hr, compared to human skin, which has a water permeability coefficient of is 92.97. A mouse skin has a 3.77 times higher

permeability [26]. The thickness of the stratum corneum of a mouse skin is half that of a human's. As regard to surface lipid deposits in skin, a hairless mouse skin contains 212 μg/cm^2 compared to a human's 60.5 μg/cm^2 [27]. This resulted in a high permeability through the mouse skin for hydrophobic solutes compared to hydrophilic compounds.

Figure 1.10. Mouse skin without hair

Human culture skin

MatTek markets two skin models: EpiDerm™ and EpiDermFT™ (FT stands for full thickness). The EpiDerm™ consists of normal human-derived epidermal keratinocytes (NHEK) cultured to form a multi-layered, highly-differentiated model of the human epidermis. The EpiDermFT™ is a NHEK with human-derived dermal fibroblasts (NHDF) based 3-dimensional, highly-differentiated human-skin-like structure having both epidermis and dermis that exhibits *in vivo* like morphological and growth characteristics which are uniform and highly reproducible. The EpiDerm™ consists of organized basal, spinous, granular, and cornified layers analogous to those found *in vivo*. It has well a developed basement membrane, *in vivo* like a lipid profile and has been used as an *in vitro* means to assess dermalirritancy and toxicology. The EpiDerm™ is mitotically and metabolically active [28]. Markers of mature epidermis-

specific differentiation such as profilaggrin, the K1/K10 cytokeratin pair, involucrin, and type I epidermal transglutaminase have been localized in the model. Unfortunately, it was discovered that for the EpiDermFT™ the hydrocortisone used in the final stages of culturing was still present in the skin samples obtained from Mattek. Thus, the EpiDerm™ was chosen for the present study.

This study sets out to address the following issues: (1) The evaluation of the *in vitro* percutaneous penetration of corticosteroids from seven over-the-counter products as well as one prescription cream, USP, using a commercially available static-diffusion-cell system, (2) the comparison of the permeation differences among three reproducible membranes: a synthetic membrane, a mouse skin, and an EpiDerm™-human cultured skin.

(a) 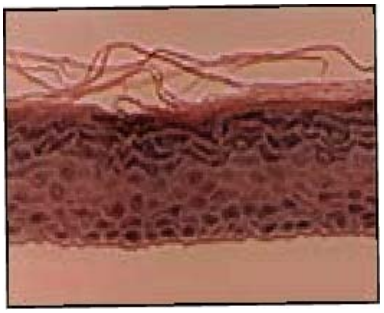 (b) 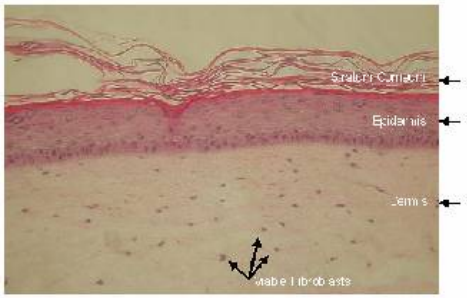

Figure 1.11. Histology of an an EpiDerm™ 200 (a), and an EpiDermFT™ 200 (b) [28].

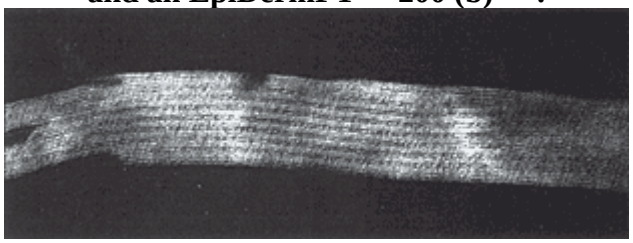

Figure 1.12.Transmission Electron Micrograph of Epiderm™ Intercellular Lamellar Lipid Sheets with Broad-Narrow-Broad Spacing (Magnification 150,000x) [28].

	EpiDerm EPI-100	EpiDerm EPI-812	Human Abdominal
Phospholipids	58.8 ± 3.4	46.0 ± 1.2	41.0
Glucosylceramides (GLB-D)	4.4 ± 0.1	1.8 ± 0.4	4.0
Acylglucosylceramides (GLA)	0.9 ± 0.0	0.7 ± 0.1	1.2
Ceramides (2-6)	8.9 ± 0.5	16.4 ± 1.9	9.7
Acylceramides (CER-1)	0.7 ± 0.1	1.0 ± 0.1	0.9
Cholesterol	13.1 ± 1.4	16.2 ± 2.0	15.7
Fatty Acids	2.9 ± 1.0	8.8 ± 1.3	21.4
Triglycerides	8.3 ± 2.9	6.3 ± 2.9	-----
Cholesterol esters	2.0 ± 0.2	2.8 ± 0.2	4.7
Other			1.4

Figure 1.13. Comparison of a Lipid profile for an Epiderm™ and a Normal Human abdominal Skin [28]

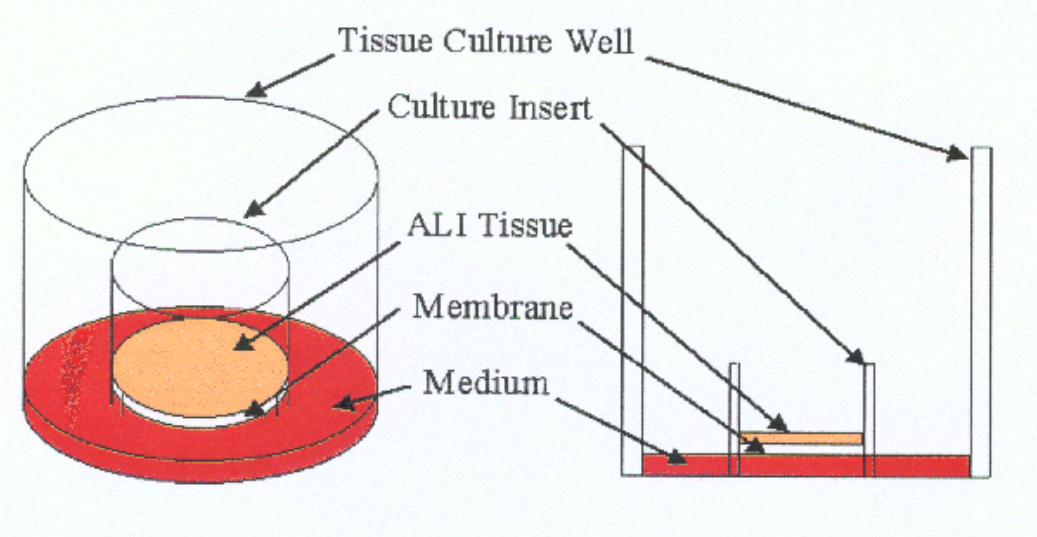

Figure 1.14. An depiction of an Epiderm™ unit in a kit shipped from Mattek [28].

A typical EpiDerm shipment (1 kit, EPI-200) contains 24 tissues, each tissue is 9 mm in diameter and in its own culture plate insert, plus a small amount of medium. For shipment, each insert is placed in one well of a standard 24-well plate.

Epiderm histology

Mattek dictates the histology of Epiderm™ membrane that consists of 8-12 cell layers (basal, spinous, and granular layers) in which the stratum corneum consists of 10-15 layers (based on Transmission Electron Microscopy (TEM)[28].

An initial evaluation of an EpiDerm™'s permeability characteristics was made using a side-by-side diffusion chamber. A permeability coefficient, kp, for tritiated water flux was determined for standard EpiDerm™ (EPI-100) and somewhat more for a mature EpiDerm™ (EPI-612). Kp's of 5.0 x 10-3 and 3.6 x 10-3 cm/hr were calculated for EPI-100 and EPI-612 respectively, compared with 2.5 x 10-3 cm/hr for the cadaver skin using the same diffusion apparatus. From these initial tests, an EpiDerm™ appears more reproducible than cadaver skin, possibly due to EpiDerm™'s highly regular structure. Also, permeability studies were facilitated since a steady state is reached more quickly due to the EpiDerm™'s uniform thickness. Finally, similar to a living epidermis, an EpiDerm™ is metabolically and mitotically active, and, hence, studies using an EpiDerm™ should be more accurate than those obtained using a non-viable cadaver or animal skin.

MATERIALS AND METHODS

REAGENTS AND STANDARDS

Hydrocortisone USP reference standard, Lot 2001, was from PCCA.

Propylparaben USP reference standard, Lot 130011, was obtained from USP (Rockville, MD).

Absolute – 200 Proof Ethyl alcohol USP was obtained from AAPER Alcohol and Chemical Co. (Shelbyville, KY).

HPLC-grade acetonitrile, and methanol were from EMD Chemicals, Inc. (Gibbstown, NJ).

FD&C Blue was from Allied Chemical & Dye Co. (New York, NY).

TOPICAL HYDROCORTISONE PRODUCTS STUDIED

Eight over-the-counter 1% HC products, one gel, one ointment, two lotions and four creams, were evaluated. In addition, a prescription hydrocortisone cream USP, 2.5% (E. Fougera & Co.) was included in the study.

Gel: The HC gel studied was **Corticool** (with/without pretreatment using an exfoliant cleanser; Tec Laboratories, Inc.)

Ingredients: Hydrocortisone, Benzethonium Chloride, Benzophenone 4, Hypromellose, Menthol, Peppermint Oil, Polysorbate 20, Propylene Glycol, Water (Purified), SD Alcohol 40B (20% by weight), Sodium Gluconate, Sodium Metabisulfite.

Ointments: Cotizone-10 ointment

Ingredients: Hydrocortisone,white petrolatum

Lotions: Corticool Lotion (TEC Laboratories, Inc.)

Unknown Ingredients

Cortaid lotion (Johnson & Johnson)

Ingredients: Hydrocortisone 1.0%, Benzalkonium Chloride, Butylparaben, Carbomer, Ceteareth-6, Cetyl Alcohol, Citric Acid, Dimethicone, Ethylparaben, Glycerin, Isobutylparaben, Methylparaben, Mineral Oil, Petrolatum, Propylparaben, Sodium Citrate, Sodium Hydroxide, Stearyl Alcohol, Tetrasodium EDTA, Tocopheryl Acetate, Water.

Creams: Hydrocortisone cream (Aveeno)

Ingredients: Hydrocortisone (1.0%), aloe Barbadensis Leaf Juice, Avena Sativa Kernel Flour (oat), Bees Wax, Cetyl Alcohol, Citric Acid, Glyceryl Stearate, Isopropyl Myristate, Methylparaben, PEG 40 Stearate, Polysorbate 60, Propylene Glycol, Propylparaben, Sodium Citrate, Sorbic Acid, Sorbitan Stearate, Stearyl Alcohol, Tocopheryl Acetate, Water.

Cortizone-10 plus (Pfizer)

Ingredients: Hydrocortisone (1%), Aloe Barbadensis Leaf Juice, Aluminum Sulfate, Beeswax, Calcium Acetate, Cetearyl Alcohol, Cetyl Alcohol, Cholecalciferol, Dextrin, Glycerin, Isopropyl Palmitate, Maltodextrin, Methylparaben, Mineral Oil, Petrolatum, Propylene Glycol, Propylparaben, Retinyl Palmitate, Sodium Cetearyl Stearate, Sodium Lauryl Sulfate, Tocopheryl Acetate, Water, Zea Mays Oil (Corn)

Cortaid cream (Johnson & Johnson)

Ingredients: Hydrocortisone (1.0%), Aloe Barbadensis Leaf Juice, Avena Sativa (Oat) Kernel Extract, Benzyl Alcohol, Cetearyl Alcohol, Cetyl Palmitate, Chrysanthemum Parthenium (Feverfew) Extract, Citric Acid, CyclopentaSiloxane, Dimethicone/Vinyl Dimethicone Crosspolymer, Dimethyl MEA, Glycerin, Isopropyl

Myristate, Isostearyl Neopentanoate, Methylparaben, PEG 40 Stearate, Potassium Lactate, Sodium Hydroxide, Water.

Hydrocortisone USP 2.5%

Ingredients: Hydrocortisone**,** glyceryl monosterate, polyoxyl 40 stearate, glycerin, paraffin stearyl alcohol, isopropyl palmitate, sorbitan monostearate, benzyl alcohol, potassium sorbate, lactic acid, water.

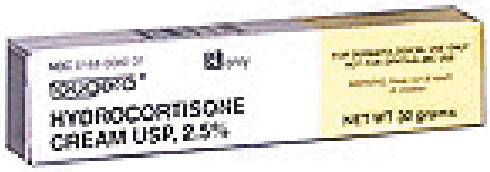

A synthetic Membrane, Mouse Skin and an EpiDerm™ Cultured Human Skin

Forty-seven mm diameter, 0.45-μm porosity Nylaflo nylon membrane filters, were purchased from Pall Life Science in Ann Arbor, MI. (Nylaflo is known for its stable property). The mouse skin was obtained from Balb/C mice (Charles River Laboratories, Wilmington, MA), the mice were 6 to 8-week-old females. The hair was removed with a shaver, and the skin was excised and cut into approximately 37-mm-diameter pieces. Twelve EpiDerm™-cultured human skin models were ordered twice from MatTek (Ashland, MA). The tissues were stored at 4°C upon arrival via overnight shipping and used within three days.

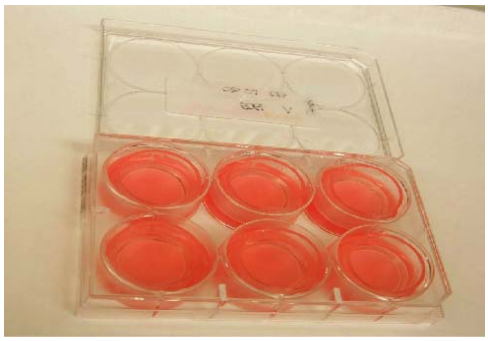

Figure 1.15. EpiDerm™-cultured human skin models

HPLC ASSAY DEVELOPMENT AND VALIATION

The HPLC assay was adopted from a hydrocortisone cream monograph, USP 28/NF23 (Rockville, MD), excepts that an equal amount of acetonitrile was added to the assay samples to precipitate protein prior to the addition of the internal standard, propyl paraben. An filtered solution of water, methanol, and acetonitrile (61:19.5:19.5) was used as the mobile phase, instead of 50:25:25 as listed in the USP 28/NF 23, to ensure separation among the analyte, internal standard, and unidentified peaks for all tested HC products. Thus, the hydrocortisone retention time was about 22 minutes. The HPLC system with an auto-injector consisted of a C_{18} column (3.9 x 150 mm, 5 μ, Waters, Milford, MA) with a precolumn (Model 590, Waters, Milford, MA), a UV-VIS wavelength detector set at 254 nm and an integrator recorder (Model 740 Data Module, Waters, Milford, MA). The injection loop volume was 50 μL. The flow rate of the pump was 1 ml/min. The HPLC method for hydrocortisone exhibited linearity in the working range from 0.5 to 120 μg/ml with reproducibility under the reported conditions of the analytical curve. The accuracy, precision, robustness, and stability of this analytical procedure were inherited as it had been recognized by the USP.

Figure 1.16. The HPLC machine, LC Module I, from Waters used to assay hydrocortisone

IN VITRO PERMEATION STUDY

Three different membranes were studied. The synthetic Nylaflo membrane reflects the diffusion properties of the drug, while the animal and EpiDerm™ cultured skin were the representative membranes used to study the skin barrier to study drug permeation. The effect of pre-washing the skin with an exfoliating cleanser for 30 sec prior to applying the Corticool gel was also evaluated as exfoliating cleanser is included in the topical gel commercial product.

The Franz Cell (Crown Glass, Somerville, NJ) and water bath (Forma Scientific, Marietta, OH) consist of 6 vertical cells (each with a 2.2 cm orifice and a 15-mL internal volume and a sampling port). A 25 mm section with 0.45-µm porosity of Nylaflo membrane filter (Pall Gelman, Ann Arbor, MI) was pre-wetted before use in the receptor medium of 25 % ethyl alcohol for 15 minutes.

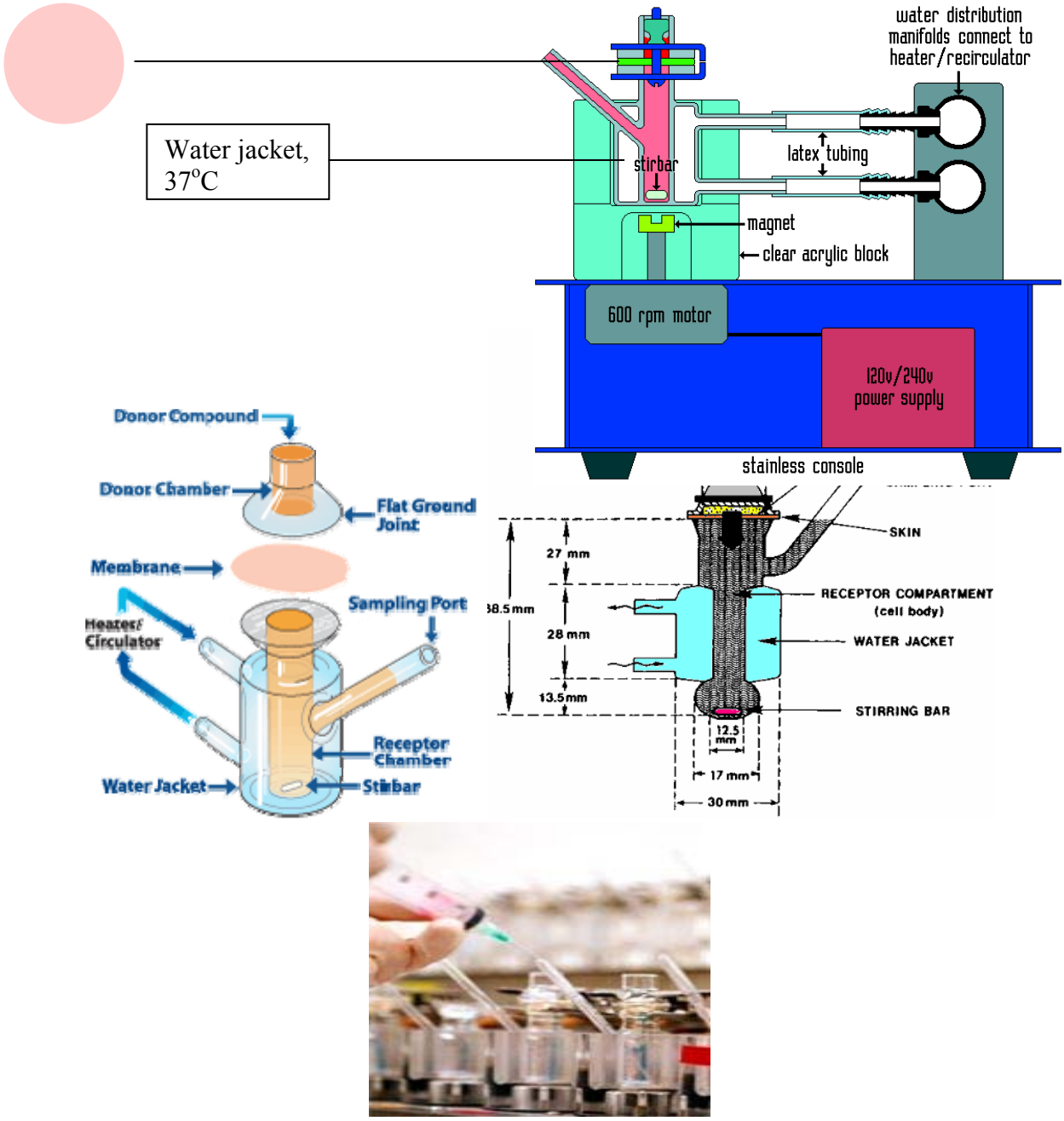

Figure1.17. The Franz-cell diffusion apparatus

Seven over-the-counter 1% HC topical dosage forms were tested. A sample from each product was loaded onto weighing paper and the approximately 1 gram of weight was measured. After transferring a topical product into the center of the pre-

wetted filter membrane, the weighing paper and the permeate left on the weighing paper were measured again. By doing so, the exact amount of permeate loaded on the membrane was known. A glass cap was then place over permeate and was clamped to the top of the Franz cell. The Franz cell was maintained at 32^{o}C by a circulating water bath running across the water jacket. The dissolution medium was stirred at 300 rpm using a mini magnetic stirring rod. During the dissolution, 150 μL samples were taken from the sampling port at 0.5, 1.5, 3, 6, 10, 20 and 24 h. After each withdrawal, the receptor media was replenished with the same amount of volume of fresh medium (25 % ethyl alcohol). 50 μL of the collected sample was mixed with the same volume of 15 μg/mL propyl paraben, the internal standard, for the HPLC assay.

DATA MANAGEMENT

After obtaining the hydrocortisone concentration from the HPLC assay, the cumulative amount of HC per contact area (μg/cm^2) at each time point was determined. The percentage of hydrocortisone release at each time point was calculated by taking the ratio of the released amount of HC to the amount of HC loaded. The amount of HC loaded occupied 1% or 2.5% (OTC or prescription product respectively) of the weight of the topical product loaded. The two mathematical models were used to construct hydrocortisone-release profiles were Fick's law of diffusion and the Higuchi equation [7]. For Fick's law:

$$P = \frac{DK}{h} \quad \text{(equa. 8)}$$

$$M = PSC_d t \quad \text{(equa.9)}$$

$$P = \frac{Slope}{SC_d} \quad \text{(equa. 22)}$$

Where M is the amount of drug (mg), K is the distribution or partition coefficient, S is the unit cross section (cm^2), and P is the permeability coefficient (cm/hr).

Based on the Higuchi equation, the percentage of drug release was plotted against the square root of time ($hour^{1/2}$) to compile a release profile for hydrocortisone from each product. From the built profile the release-rate constant for hydrocortisone can be determined. This equation, grounded on principles of diffusion as expressed by Fick's fist law of diffusion, describes the release of a drug from topical dosage forms such as gels, creams, and ointments. The drug at the surface of the system, in close contact with the medium cream, is released first and sets up a front. As drug passes out of the system, the front moves inward, and when this layer becomes exhausted of the drug, the next layer begins to deplete. In this manner, the boundary of the drug forms. The amount of drug depleted per unit area of the system, Q, at time t, is given by the Higuchi equation:

$$Q = [2ADC_d]^{1/2} t^{1/2} \quad \text{(equa. 21)}$$

$$D = \frac{[Slope]^2}{2AC_d} \quad \text{(equa. 23)}$$

Where Q is the amount of drug depleted per unit area of the matrix at time t (mg/cm^2),

D is the diffusion coefficient of the drug in the matrix ($mg \cdot ml/cm^4/hr$),

C_s is the solubility of the drug (mg/cm^3),

A is the total concentration dissolved and undissolved of the drug in the matrix (mg/cm^3),

S is the unit's cross section (cm^2).

After the hydrocortisone release rate was obtained from the slope of the dissolution profile, the diffusivity or diffusion coefficient, D, was calculated. The total quantity for each topical formulation placed on the membrane was measured and was around 1g for each Franz cell well. The drug penetrates through the membranes to the receiver chamber analyzed by the HPLC assay. The amount and the percentage release over 24 hours is calculated with the assumption that the theoretical maximum amount that can diffuse into the donor chamber is 25mg for the prescription hydrocortisone cream 2.5% and 10 mg for the 1% hydrocortisone topical formulations.

RESULTS AND DISSCUSION

THE COMPOSITIONS AND PACKING OF THE STUDIED HYDROCORTISONE PRODUCTS

Among eight pharmaceutical products investigated, six were packaged in plastic tubes, with one in a pump plastic bottle and one in a metal tube (Table 1). Cortizone-10 Plus cream has the highest number of excipients (ten). Cortizon-10 ointment only has one excipient, which is white petrolatum. Some products also incorporated a thickening agent and an ultraviolet light absorber.

Table 1.1. The studied formulations: 1 gel, 1 ointment, 2 lotions and 4 creams

Product Name	Dosage Form	Strength	Packaging	OTC or Prescription	Manufacturer
Cortaid	Lotion	1 %	Pump Bottle	OTC	Johnson & Johnson
Cortaid	Cream	1%	Plastic Tube	OTC	Johnson & Johnson
Aveeno	Cream	1%	Plastic Tube	OTC	Johnson & Johnson
Cortizone-10 Plus	Cream	1%	Plastic Tube	OTC	Pfizer
Cortizon-10	Ointment	1%	Plastic Tube	OTC	Pfizer
Hydrocortisone	Cream	2.5%	Metal Tube	Prescription	E. Fougera & Co
Corticool	Gel	1%	Plastic Tube	OTC	Tec Lab
Cortilotion	Lotion	1%	Plastic Tube	OTC	Tec Lab

Each formulation contains different ingredients. They are enhancers, surfactants, emollients, and thickening agents. The amount of each component is unknown. It is hard to predict the permeation profiles of hydrocortisone based on the information of ingredients only since the penetration depends on drug solubility and the number of phases in the formulations (creams, ointment). The viscosity of the

formulations also affects the diffusion of the drug from the inside matrix to the surface of the skin.

THE STANDARD CURVE OF HYDROCORTISONE

Hydrosortisone is slightly soluble in water (0.28mg/ml). It is freely soluble in methanol (6.2mg/ml). Therefore a hydrocortisone stock solution of 200μg/ml in methanol was prepared. From the stock solution, a range of hydrocortisone solution is prepared in 25% ethyl alcohol/water medium and then assayed by HPLC. The area of hydrocortisone HPLC peak is compared to the area of the internal standard peak, propyl paraben. The standard curve is drawn based on the correlation between the hydrocortisone concentration assayed by the HPLC method and the ratio of the area of hydrocortisone to the area of the peak, propyl paraben.

Table 1.2. The standard curve of the area ratios of hydrocortisone over the internal standard propyl paraben, and the drug's concentration

Conc. (μg/ml)	Hydrocortisone Area	Propyl paraben Area	Area Ratio	Predicted Conc (μg/ml)	% Theory
0.6	59706	1614043	0.037	0.674	112.27
1.2	147676	1659391	0.089	1.286	107.18
3	353763	1656031	0.214	2.754	91.80
6	778329	1641627	0.474	5.822	97.04
12	1631195	1630485	1.000	12.022	100.18
30	4336543	1677190	2.586	30.693	102.31
60	8640489	1736164	4.977	58.857	98.10
120	17004360	1667343	10.198	120.361	100.30
				std	40.071
				Average	117.812
				CV%	34.01303

The linear range of the HPLC assay for hydrocortisone concentration is up to 120 μg/ml with R^2 is 0.9998. The standard curve of hydrocortisone shows that there is good correlation between hydrocortisone's concentration and its area peak analyzed

by HPLC. Since the method was modified slightly from the USP method, validation for the method is not necessary.

The internal standard, propyl paraben, was used to adjust for the variability of volume injection, and it was used to check the resolution of the mobile phase, as well.

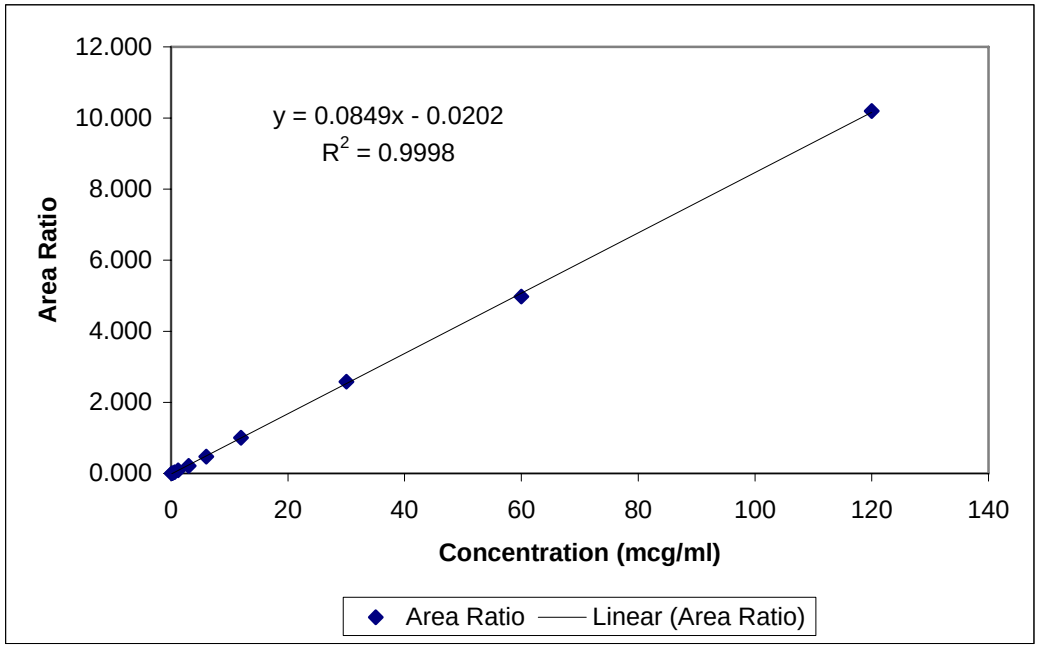

Figure 1.18. Standard curve plot for hydrocortisone concentration versus the area ratio of hydrocortisone over the internal standard, propyl paraben

THE THICKNESS OF THE STUDIED MEMBRANE

The membrane's thickness was measured by a vernier caliper. The precision of the measuring scale for the vernier caliper is 0.01mm.

The Thickness of the synthetic membrane

The synthetic nylon membrane patches were prepared with highly precise replication and the precision thickness was probably smaller than 0.01mm. Therefore, the vernier caliper could not detect any variability in membrane thickness. All of the tested nylon filter membranes had a thickness of 0.1mm with a standard deviation of

zero. The homogenous property of the synthetic membrane suggests its effects in drug diffusion through the membrane will be similar in all cases and any variation seen can be minimally attributed to the membrane and more to the product formulation.

Table 1.3. Thickness of the synthetic membrane filter, 0.45µm pore size

Number	Thickness (mm)
1	0.1
2	0.1
3	0.1
4	0.1
5	0.1
6	0.1
7	0.1
8	0.1
9	0.1
10	0.1
Average	**0.1**
SD	**0**

Mouse-skin thickness

Thickness plays a role in percutanous penetration of the drug. The thickness reflects the number of cell layers lying in the epidermis. Each mouse skin patch was measured at ten random different positions.

Table 1.4. Mouse-skin thickness of 10 samples, each mouse-skin patch was measured at 10 different positions (mm)

Sample skin	Site 1	Site 2	Site 3	Site 4	Site 5	Site 6	Site 7	Site 8	Site 9	Site 10	Mean	SE
1	0.31	0.39	0.3	0.23	0.27	0.25	0.33	0.39	0.4	0.38	**0.325**	**0.0629**
2	0.48	0.42	0.49	0.51	0.48	0.43	0.6	0.45	0.46	0.38	**0.470**	**0.0594**
3	0.36	0.59	0.35	0.44	0.38	0.45	0.57	0.42	0.36	0.41	**0.433**	**0.0848**
4	0.28	0.58	0.37	0.26	0.3	0.47	0.26	0.38	0.41	0.42	**0.373**	**0.1029**
5	0.41	0.37	0.4	0.62	0.54	0.43	0.36	0.48	0.38	0.45	**0.444**	**0.0826**
6	0.36	0.49	0.46	0.37	0.44	0.24	0.37	0.36	0.41	0.35	**0.385**	**0.0701**
7	0.31	0.36	0.49	0.46	0.53	0.35	0.43	0.27	0.34	0.3	**0.384**	**0.0879**
8	0.41	0.50	0.42	0.36	0.38	0.55	0.37	0.41	0.33	0.36	**0.409**	**0.0680**
9	0.28	0.54	0.46	0.42	0.39	0.48	0.36	0.42	0.26	0.31	**0.392**	**0.0904**
10	0.50	0.59	0.48	0.47	0.38	0.47	0.52	0.45	0.42	0.37	**0.465**	**0.0655**

Two main extreme positions are abdominal and dorsal skin. The average value and variability within one sample and among other samples are calculated. The F test demonstrated that there is a significant inter-subject variation in skin thickness (p=0.015) and within each skin patch. Significant intra-subject variation was also observed. The mean value of mouse skin thickness is 0.408mm. The CI 95% confidence interval of the mouse-skin thickness is 0.408 ± 0.1433*1.96 = 0.1271↔0.6889.

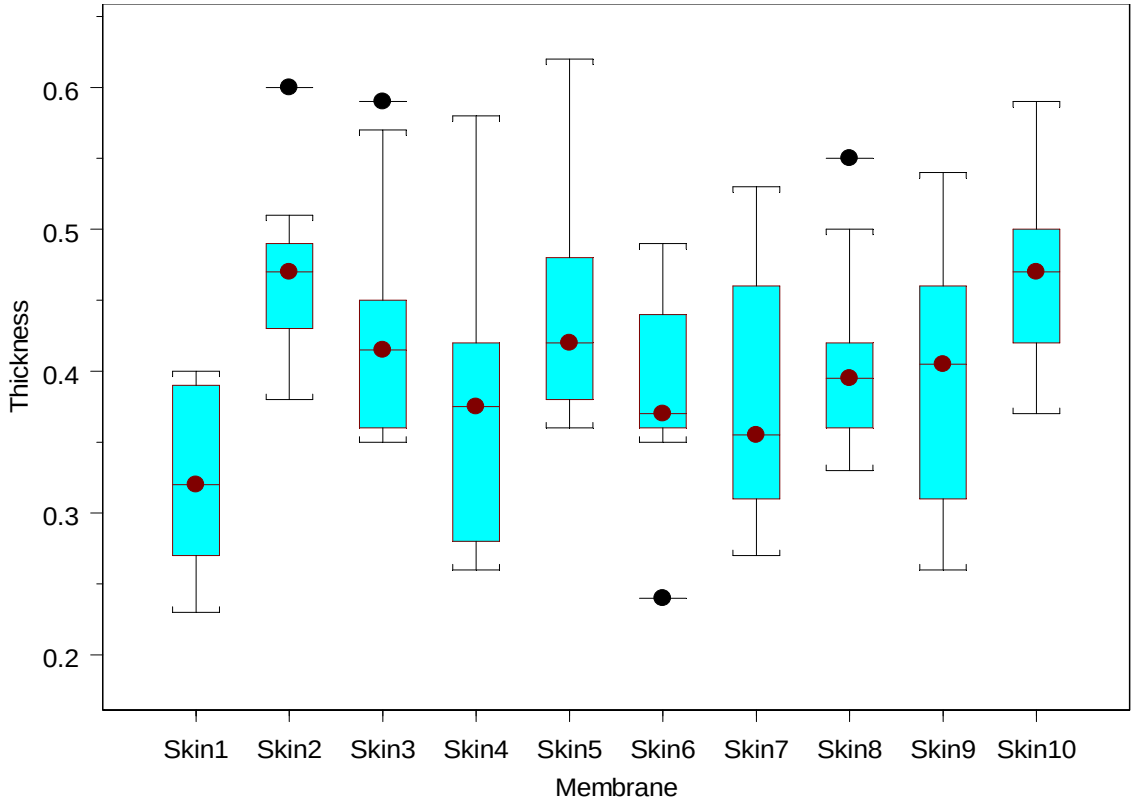

Figure 1.19. A box plot of the thickness of 10 mouse skin patches showing the variation of thickness observed within each skin patch (mm)

Due to the observed variation, a high variability of percutanous penetration is expected. Other components also have influence in drug penetration through the skin

such as skin structure and the lipid composition. A high variation in drug transport through the mouse skin was observed.

The box plot shows a distribution of ten mouse-skin patches, some outliners lying outside the range of the 75% of the quantile value and 50%, 75% of quantile value also reveal a high intra-subject variability in the skin thickness. The median value of each patch also demonstrates a high intervariability.

The Thickness of an Epiderm^{TM}

The technical reference of an Epiderm^{TM} did not report the thickness of the epidermis layer. The company technician states that the stratum corneum consists of 10-15 layers (based on Transmission Electron Microscopy (TEM)) and there are 8-12 cell layers (basal, spinous, and granular layers). The water flux through an Epiderm^{TM} is more rapid than through acadaver skin's epiderm layers. An Epiderm^{TM} is more uniform in structure and has less variability compared to a cadaver-donor's skin (Figure 1.20).

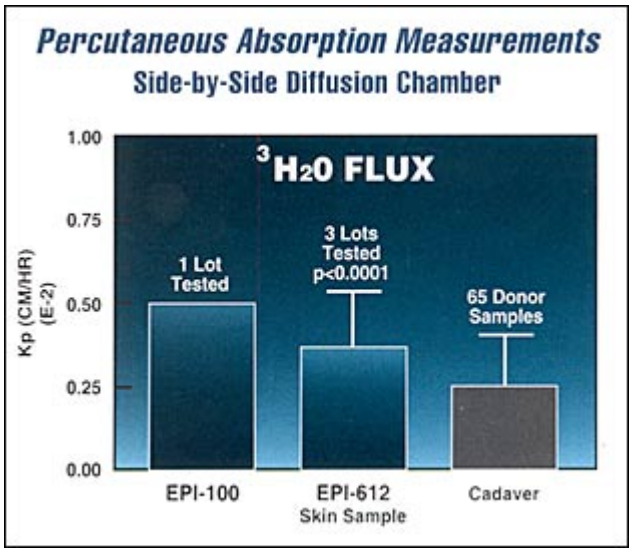

Figure 1.20. Percutanous absorption of water compared to cadaver samples [28]

The thickness of the Epiderm™ could not be measured as the membrane is fixed to a round holder. The thickness of the Epiderm™ was measured after the experiment was completed and presented in the Table 1.5.

The thickness of the Epiderm™ after the experiment may not indicate the precise true thickness of the Epiderm™ at the start of the experiment because after 24 hours, the membrane thickness may change. Nevertheless, the Epiderm™ seems to be thicker than the mouse skin, the p value of the t test is <0.01.

Table 1.5. Measured Epiderm™ thickness after experiment completion

Number of sample	Epiderm thickness after experiment (mm)
1	0.48 0.52 0.47 0.49 0.49
Average **SD**	**0.49** **0.0187**

DIFFUSION PROFILES WITH NYFLO SYNTHETIC MEMBRANE FILTERS

Hydrocortisone needs to reach deep into the skin layer to exhibit it's inhibition activity on allergy reaction. The hydrocortisone non-genomic targets and genomic targets occur in the viable layer. The stratum corneum is the main barrier for hydrocortisone permeation. The experimental design for the hydrocortisone release from it to topical-dosage form penetrates through the synthetic membrane, mouse skin, and Epiderm™, is appropriate to reflect the *in vivo* comparative behaviors of all formulations.

The cumulative amount (mg) and the percentage of drug release from the 8 topical hydrocortisone products against time and the square root of time ($h^{1/2}$) were

compiled, see Table 1.8. The shapes of the hydrocortisone dissolution profiles were linear for the 24 h of the study. The percentage release of HC in 24 hours was at 59.12% from gel formulation (Table 1.6). Cortizone-10 ointment at 24 hours released only 0.17%. The creams and lotions have a cumulative percentage release from 4.56% (Cortizone Plus cream) to over 14.8% (Corticool Lotion).

Based on the slope of the diffusion profile, the equation for Fick's law for diffusion was used to calculate the permeability coefficients (Table 1.8).

Table 1.6. The Percentage release of hydrocortisone from eight topical formulations through the synthetic nylon membrane over 24 hours

Time (hr)	Percentage release (%)							
	Corticool gel	**Cortizone-10 Plus cream**	**Cortaid cream**	**Cortizone-10 ointment**	**Cortaid lotion**	**Corticool lotion**	**Aveeno cream**	**Prescription cream 2.5%**
0	0	0	0	0	0	0	0	0
0.5	6.51 ± 1.37	0.757 ± 0.118	1.04 ± 0.411	0.096 ± 0.004	1.19 ± 0.304	0.783 ± 0.486	2.71 ± 0.671	0.960 ± 0.308
1.5	9.43 ± 2.42	1.78 ± 0.378	1.67 ± 0.370	0.139 ± 0.007	2.55 ± 0.994	0.814 ± 0.460	4.50 ± 0.732	1.289 ± 0.447
3	9.75 ± 3.73	2.51 ± 0.243	2.89 ± 0.694	0.137 ± 0.008	4.58 ± 0.929	1.99 ± 1.66	6.42 ± 0.440	3.21 ± 1.06
6	12.54 ± 5.83	3.34 ± 0.306	3.77 ± 0.820	0.141 ± 0.009	6.39 ± 1.60	3.46 ± 2.66	6.52 ± 0.206	3.97 ± 1.32
10	16.02 ± 6.64	3.50 ± 0.917	3.90 ± 1.06	0.146 ± 0.014	7.28 ± 1.51	5.26 ± 3.14	7.28 ± 0.275	4.48 ± 1.36
20	38.3 ± 5.19	3.87 ± 0.244	5.81 ± 1.69	0.156 ± 0.020	10.4 ± 2.61	11.7 ± 3.16	7.83 ± 0.341	7.54 ± 0.690
24	59.1 ± 3.92	4.56 ± 0.136	6.23 ± 0.804	0.174 ± 0.014	14.8 ± 2.19	14.19 ± 3.44	9.14 ± 0.646	12.0 ± 0.732

In the Fick's law formula

$$Slope = PSC_d$$

C_d is the concentration of hydrocortisone in the donor compartment. Solubility of hydrocortisone in water is 0.28mg/ml. 1% HC formulation contains 1mg/ml.

Table1.7. The amount of release of hydrocortisone from 8 topical formulations through the synthetic nylon membrane over 24 hours

Time (hr)	Amount release (mg)							
	Corticool gel	**Cortizone-10 Plus cream**	**Cortaid cream**	**Cortizone-10 ointment**	**Cortaid lotion**	**Corticool lotion**	**Aveeno cream**	**Prescription HC cream 2.5%**
0	0	0	0	0	0	0	0	0
0.5	0.651 ± 0.137	0.0757 ± 0.0118	0.104 ± 0.0411	0.0096 ± 0.0004	0.119 ± 0.0304	0.0783 ± 0.0486	0.271± 0.0671	0.204 ± 0.077
1.5	0.943 ± 0.242	0.178 ± 0.0378	0.167 ± 0.370	0.0139 ± 0.0007	0.255 ± 0.0994	0.0814 ± 0.0460	0.450 0.0732	0.322 ± 0.112
3	0.975 ± 0.373	0.251 ± 0.0243	0.289 ± 0.0694	0.0137 ± 0.0008	0.458 ± 0.0929	0.199 ± 0.166	0.642± 0.0440	0.801 ± 0.264
6	1.25 ± 0.583	0.334 ± 0.0306	0.377 ± 0.0820	0.0141 ± 0.0009	0.639 ± 0.160	0.346 ± 0.266	0.652± 0.0206	0.993 ± 0.331
10	1.60 ± 0.664	0.350 ± 0.0917	0.390 ± 0.106	0.0146 ± 0.0014	0.728 ± 0.151	0.526± 0.314	0.728 ± 0.0275	1.12 ± 0.341
20	3.82 ± 0.519	0.387 ± 0.0244	0.581 ± 0.169	0.0156 ± 0.0020	1.04 ± 0.261	1.170 0.316	0.783 ± 0.0341	1.88 ± 0.173
24	5.91 ± 0.392	0.456 ± 0.0136	0.623 ± 0.0804	0.0174 ± 0.0014	1.48 ± 0.219	1.42± 0.344	0.914 ± 0.0646	3.01 ± 0.183

Table 1.8. The Permeability coefficients of hydrocortisone from all formulations through the synthetic membrane 0.45 µm

Formulation	**n**	**Permeability coefficient (cm/hr)**	**R^2**
Corticool gel*	10	$2.356*10^{-2}$	0.939
Corticool gel**	10	$7.8*10^{-3}$	0.939
Cortizone-10 plus cream	5	$2.555*10^{-3}$	0.728
Cortaid Cream	6	$2.547*10^{-3}$	0.875
Cortaid Lotion	4	$5.582*10^{-3}$	0.944
Cortizone-10 ointment**	4	$2.313*10^{-5}$	0.399
Corticool lotion	4	$6.589*10^{-3}$	0.997
Aveeno cream	4	$2.253*10^{-3}$	0.740
Prescription HC cream 2.5%	7	$4.713*10^{-3}$	0.939

* The permeability with solubility 0.28mg/ml

**The permeability with solubility 1mg/ml

If the formulation is water-based, hydrocortisone exists mostly in suspension with a small amount dissolved in water, but the majority of the amount is in solid form. Thus, without solubility enhancer, C_d is 0.28 mg/ml. If C_d changes, the slope of the rate of drug diffusion would change proportionally to the C_d value. In Corticool gel, the presence of propylene glycol and ethanol increase the solubility of hydrocortisone (solubility is 12.7mg/ml and 15mg/ml, respectively) and in these solvents all of hydrocortisone is in solution. The value C_d of hydrocortisone is in the Corticool gel 1mg/ml and causes an increase of the rate of diffusion according to Fick's law of diffusion.

The permeability coefficient of hydrocortisone from the Corticool gel after the high solubility was accounted for is $7.8^{*}10^{-3}$ cm/hour which is not much higher than the permeability coefficient of hydrocortisone from the Corticool lotion and the Cortaid lotion. Solubility accounts for most of the high diffusion rate. X-ray diffraction has shown that ethyl alcohol and other alcohols increase drug penetration by physically altering the stratum corneum's lipids. The order of the corneocyte-bound lipid fraction is lost and the lateral-packing distance of the hexagonally-arranged lipid fraction decreases. This coincides with an increase of lipid fluidity [29]. This effect is not expected with a synthetic membrane since there is no expected lipid component inside the membrane.

Ethyl alcohol and propylene glycol also increase skin penetration of the drug by causing swelling of the skin. This addition increased the solubility of hydrocortisone in the gel formulation and caused the permeability coefficient of

hydrocortisone from gel to be larger than in creams. Besides that, the gel form is a single phase with a high percentage of water. Hydrocortisone inside the gel moves toward the membrane according to its concentration gradient, and the C_d is maintained on the surface of the membrane to keep the drug-release rate high.

With regard to the hydrocortisone's diffusing through the synthetic membrane, the Corticool gel had a statistically significant higher diffusion rate compared to other formulations. The 95% CI of the drug percentage released over 24 hours is $59.12 \pm 3.924 * t_{(0..975,\ 9)} = 59.12 \pm 2.262 * 3.924 = 50.243\text{-}67.997$. The 95% confidence interval band and predicted band of linear regression drug release from Corticool gel was constructed. Both of these bands separated from any values from other formulations (Figure 1.22). This is strong evidence that the drug diffusion from the Corticool gel is superior to the drug diffusion from other tested formulations.

The ointment containing hydrocortisone produced the lowest drug release rate through the synthetic membrane. Hydrocortisone in the single oiled-based phase of the ointment formulation is mostly in solution since the hydrocortisone dissolves well in organic solvents. The C_d value for the hydrocortisone in the ointment is 1mg/L. White paraffin petrolatum, the major hydrophobic oil-base of the hydrocortisone ointment, does not act as a deep-drug-penetration enhancer as it is hydrophobic, highly viscous, and insoluble in water. As mentioned previously, the transportation of the drug through the skin is mainly through the pores. The hydration of the skin has an effect and facilitates the drug's transportation through the skin. The overall net effect of the water is a higher partition coefficient for the hydrocortisone in the ointment compared to the gel, cream or lotions, trapping the drug in the ointment vehicle decreasing the

hydrocortisone release from the formulation. Thus, hydrocortisone could not deeply penetrate inter-cellularly within the lamellae layer. Although hydrocortisone is present as the solute in the ointment, the permeability would become small as a consequence of the partition coefficient (equation 8). Therefore, the whole process allowing hydrocortisone to dissolve in water and penetrate through the membrane is less. Even the C_d value is much higher compared to the water-based formulations.

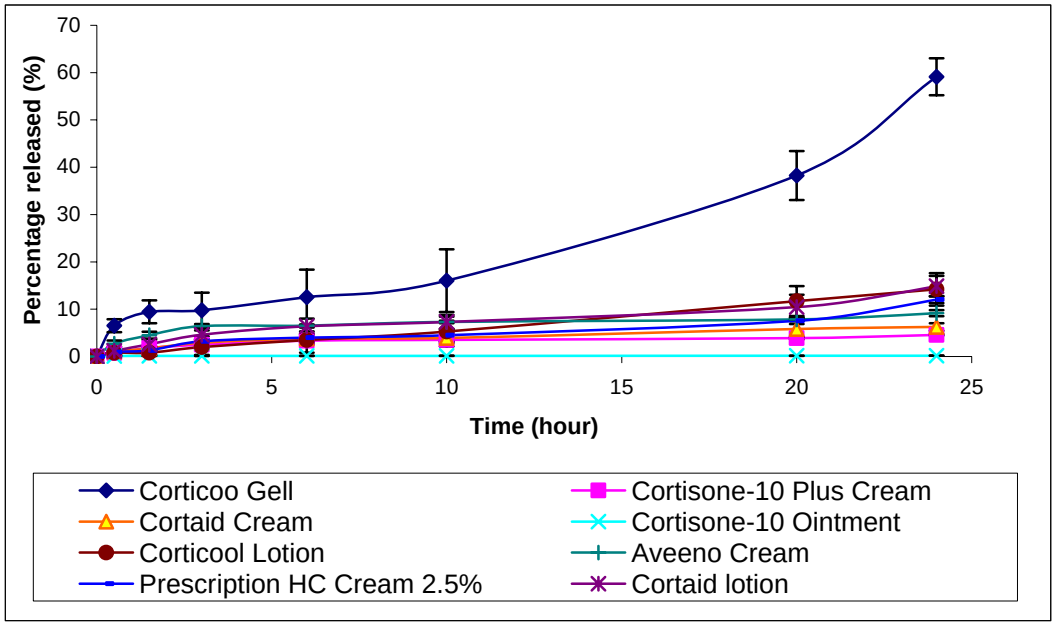

Figure 1.21. Release profiles of HC permeation over time through a nylon membrane (non-prewashed), using Fick's-law (cumulative-percentage hydrocortisone release vs. time in hours)

Table 1.9. Lower and upper confidence intervals and prediction bands of hydrocortisone release from Corticool gel by Fick's-law of diffusion

Time (hr)	Corticool gel	CI 95% L	CI 95% U	Pred 95% L	Pred 95% U
0	0	-4.16	8.38	-12.24	16.47
0.5	6.51	-2.95	9.24	-11.13	17.43
1.5	9.43	-0.536	10.98	-8.92	19.36
3	9.75	3.02	13.64	-5.63	22.29
6	12.54	9.85	19.25	0.804	28.29
10	16.02	18.17	27.51	9.10	36.58
20	38.25	35.80	51.33	28.49	58.64
24	59.12	42.29	61.42	35.79	67.92

In addition, ointment is a semi-solid condensed base with a very high viscosity. The diffusion of the drug inside the excipients' base is very slow, decreasing the availability of the drug on the surface of the membrane for release. It results in a reduction of the drug's release rate compared to other formulations.

Other formulations in the form of cream or lotion, which are water-based products, produced quite similar drug-release profiles. The total amount of hydrocortisone released from the cream or lotion was higher than that from the ointment. None of the hydrocortisone creams or lotions exhibited a drug-release pattern superior to another.

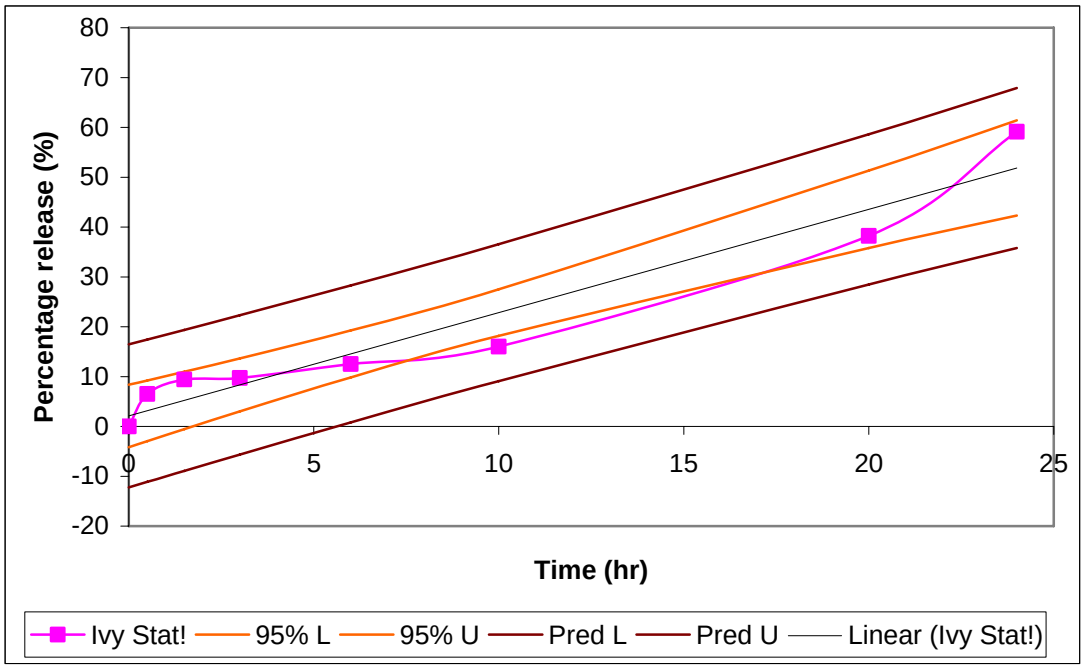

Figure 1.22. The 95% Confidence interval band and prediction band of the Corticool diffusion profile through the synthetic membrane

These products contain more water than base ointment. All formulations contain surfactants which are the emulsifying agents and permeation enhancers. The presence of these substances also affects the partition coefficient values.

The hydrocortisone cream 2.5% has high quantities of the drug for diffusion since there is a higher amount of the drug in the donor chamber facilitating a more rapid transfer of solid hydrocortisone to the dissolved drug as the drug is released from the formulations. This allows more rapid dissolution of solute from the inner matrix to the contact the surface of membrane (Figure 1.23).

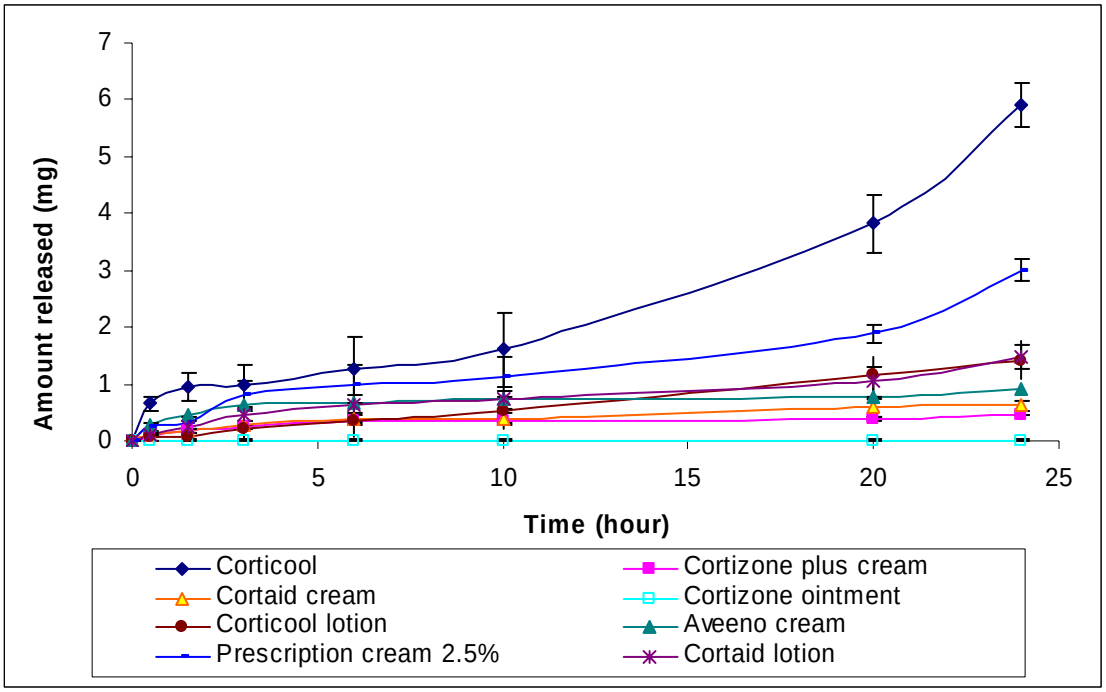

Figure 1.23. Quantity of the drug diffused through the synthetic membrane over 24 hours

The Higuchi equation does not describe well the hydrocortisone release data from the gel. However, the Higuchi model described the data of the hydrocortisone release from the creams, lotions and ointment. The diffusion coefficient can be calculated according to the equation 23. The Diffusion coefficient, D, also is equal to the square of the fitted slope of the drug release versus the square root of the time data divided by C_d (concentration in the donor compartment) and A.

$$D = \frac{[Slope]^2}{2AC_d} \quad \text{(equa. 23)}$$

Similar to the argument for Fick's law of the diffusion model for formulation of lotions, and creams, the assumption is that the drug diffuses along a concentration gradient from a high concentration, with C_d being 0.28mg/ml, to a low concentration, $C_r \approx 0$. Also assumed is the solubility of the hydrocortisone in the ointment and the C_d value of the Corticool gel as 1mg/ml with a assumption that all of the hydrocortisone present in the formulation is the solute.

Table 1.10. The diffusion coefficients calculated by the Higuchi model for the synthetic membrane diffusion

Formulation	**n**	**Diffusion Coefficient (cm^2/hr)**	**R^2**
Corticool gel*	10	$2.672*10^{-3}$	0.839
Corticool gel	10	$9.29*10^{-4}$	0.839
Cortizone-10 plus cream	5	$7.267*10^{-5}$	0.912
Cortaid cream	6	$7.111*10^{-4}$	0.981
Cortaid lotion	4	$7.495*10^{-4}$	0.961
Cortizone-10 ointment**	4	$4.458*10^{-7}$	0.617
Corticool lotion	4	$8.381*10^{-4}$	0.916
Aveeno cream	4	$2.404*10^{-4}$	0.849
Prescription HC cream 2.5%	7	$4.497*10^{-4}$	0.904

* The diffusion coefficient with solubility 0.28mg/ml
** The diffusion coefficient with solubility 1mg/ml

If the C_d for hydrocortisone solubility is 1mg/ml instead of the 0.28 mg/ml in equation 23, the hydrocortisone diffusion coefficient from Corticool gel is close to other formulations: Corticool lotion, Cortizone Plus cream, Cortaid lotion, and Cortaid cream. Therefore, the high rate of hydrocortisone diffusion from the gel can be

explained by the difference in the hydrocortisone concentration on the two sides of the membrane. The ointment's topical-dosage form could not provide hydrocortisone concentration on the surface of the membrane, thus the diffusion coefficient of that formulation is low.

The R^2 values show the linearity for the drug release for both the Fick's law and the Higuchi model. The R^2 indicated that the Corticool-gel hydrocortisone permeation followed the Fick's law of diffusion model ($R^2 = 0.939$) better than the Higuchi model ($R^2 = 0.839$). The Corticool gel shows an overlap of the three phases. The first phase is called the "depletion phase" which lasted for about a half hour. In this phase, the hydrocortisone lying on or close to the surface of the membrane diffuses rapidly though the membrane. After that, the dissolved hydrocortisone needs to move towards the membrane across the distance created during the depletion phase in the base-matrix formulation. This process creates the second slower-rate phase of the drug diffusion. When the equilibrium is set up between the diffusion of the drug through the matrix of the formulation base and the diffusion of the drug through the membrane, a saturated concentration of the hydrocortisone can be maintained on the surface of the membrane and the drug diffusion rate increases and reaches a constant rate. The first and second phases proceeded to produce a lag time phase of about three hours.

The Ointment-diffusion profile showed two separate phases. A short initial phase lasting the first half hour shows a high rate of the drug's diffusion since the hydrocortisone in the layers close to the membrane dissolves quickly by water and diffuses through the membrane. The hydrocortisone lying deeper inside the ointment

matrix needs to diffuse towards the membrane's surface. However, the low partition coefficient and high viscosity of the ointment's base prevent hydrocortisone from diffusing rapidly along its concentration gradient. The whole process is slower and the hydrocortisone's release rate drops many times. The second phase with the small drug release rate is the dominant phase for hydrocortisone release from the ointment.

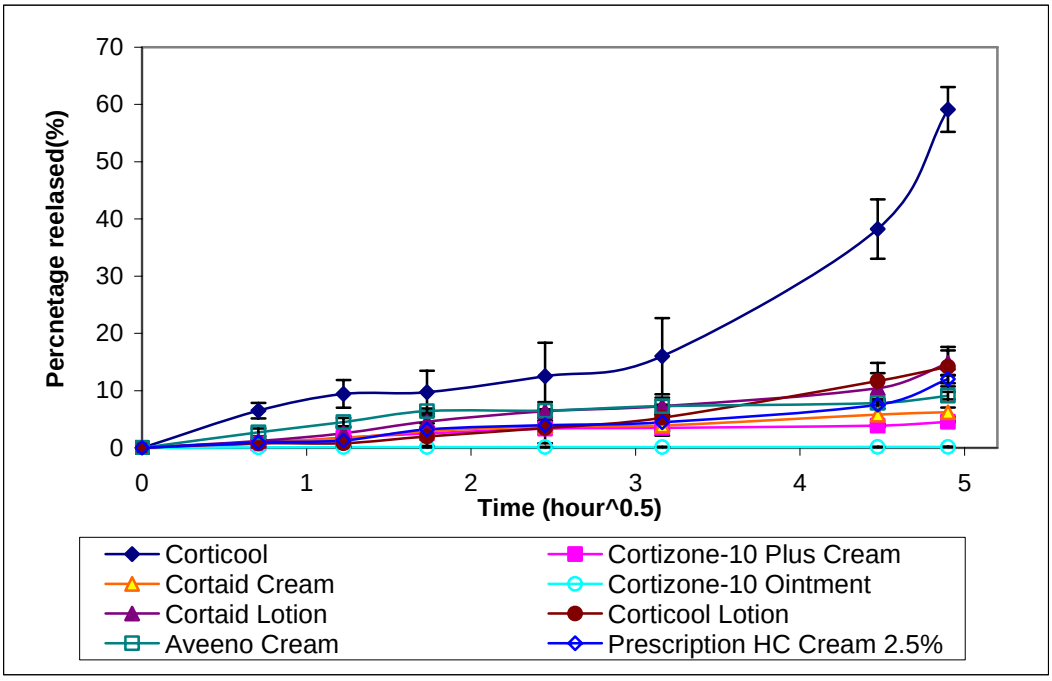

Figure 1.24. Diffusion profiles of hydrocortisone versus the square root of time for the eight formulations through the synthetic membrane

Two phases of hydrocortisone diffusion were observed for the other formulations such as the Cortaid cream, Cortaid lotion, Aveeno cream, prescription HC 2.5%, and the Cortaid Plus cream (Figure 1.24). The diffusion of the hydrocortisone through the matrix was significantly slower than through the membrane. Thus, the creams and lotions fitted the Higuchi model better with the higher R^2 values compared to the Fick's law of diffusion model. In other words, drug

diffusion within the matrix of the ointment, creams, and lotions was slower than the diffusion of the hydrocortisone between the two sides of the membrane for the first few hours until it reached a steady state rate; whereas, the Corticool gel had a diffusion rate from the beginning that was slower through the membrane than the hydrocortisone-diffusion rate within the gel entity (Figure 1.24, 1.25).

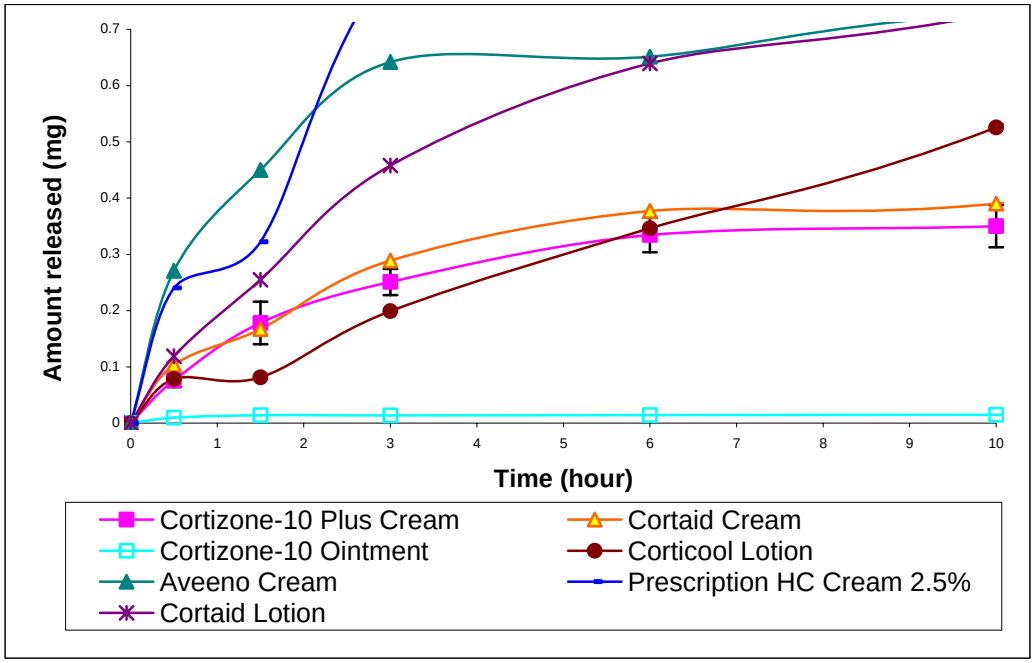

Figure 1.25. A cut-off graph showing an enlarged dissolution profile of creams and lotions with a high rate of hydrocortisone diffusion over the first hours

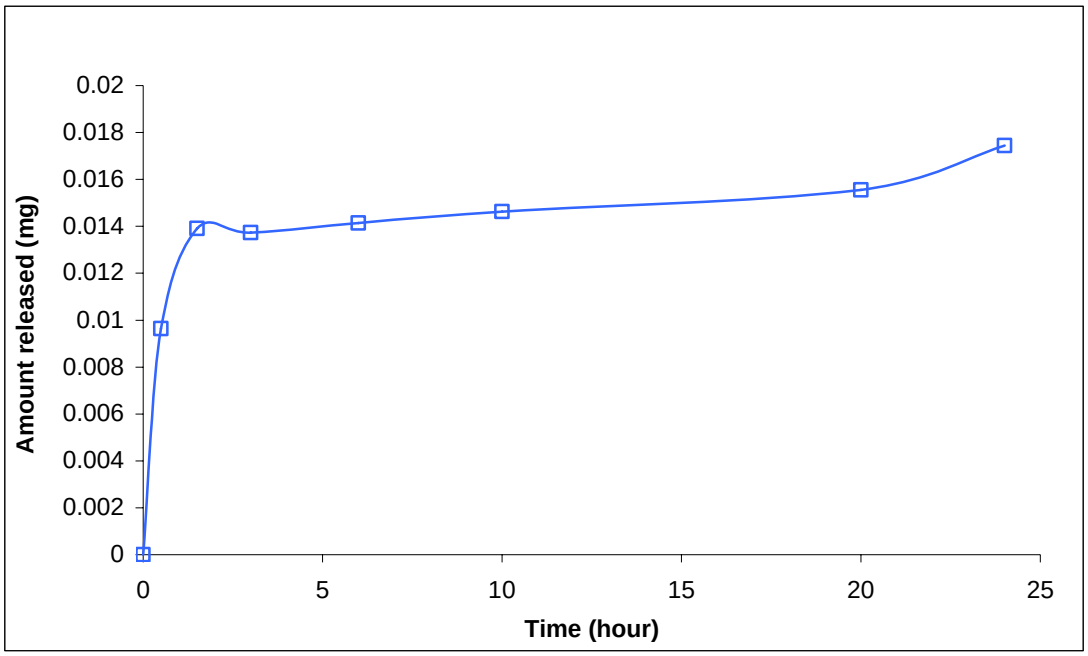

Figure 1.26. A hydrocortisone release profile from the Cortizone-10 ointment that has two separate diffusion phases. A permeation study performed with a mouse skin

PERMEATION OF HYDROCORTISONE FROM THE TOPICAL PRODUCT THROUGH MOUSE SKIN

The diffusion through the mouse skin was performed both with pre-exfoliating wash and without pre-exfoliating wash conditions.

Hydrocortisone permeation through the non-pre-washed mouse skin

The cumulative amount of hydrocortisone release (mg/cm^2) from topical hydrocortisone products against the square root of time ($h^{1/2}$) was compiled. The shapes of the dissolution profiles for hydrocortisone from the topical products were a linear release over 24 hours. Over all, the diffusion hydrocortisone rates through the mouse skin, compared to the synthetic membrane, was slower. After twenty four hours, the percentage of hydrocortisone penetrating through the mouse skin was over 20% for the Corticool gel and 3 to 4.9% for other formulations. The hydrocortisone

diffusion rate through the mouse skin for all formulations was slower than through the synthetic membrane. The profile for the percentage of hydrocortisone diffusion from the Corticool gel was concaved.

Table 1.11. Percentage of hydrocortisone drug diffused through a non-pre-washed mouse skin over 24 hours

Time (hr)	Corticool gel	Cortizone -10 ointment	Aveeno cream	Cortizone-10 plus cream	Cortaid cream	Cortaid lotion	Corticool lotion	Prescription cream 2.5%
0	0	0	0	0	0	0	0	0
0.5	0.085 ± 0.013	0.015 ± 0.015	0.066 ± 0.013	0.097 ± 0.041	0.077 ± 0.029	0.176 ± 0.103	0.030 ± 0.002	0.035 ± 0.013
1.5	0.200 ± 0.020	0.042 ± 0.010	0.157 ±0.045	0.180 ± 0.126	0.087 ± 0.031	0.298 ± 0.197	0.046 ± 0.004	0.056 ± 0.013
3	0.784 ± 0.055	0.049 ± 0.012	0.278 ± 0.076	0.268 ± 0.312	0.159 ± 0.012	0.543 ± 0.225	0.195 ± 0.071	0.136 ± 0.029
6	2.649 ± 0.420	0.120 ± 0.068	0.435 ± 0.125	0.610 ± 1.159	0.408 ± 0.085	0.805 ± 0.418	0.445 ± 0.231	0.322 ± 0.091
10	5.511 ± 1.029	0.154 ± 0.071	0.551 ± 0.185	0.706 ± 1.421	0.951± 0.383	1.266 ± 0.563	1.554 ± 1.038	0.732 ± 0.177
20	13.472 ± 1.873	0.217 ± 0.089	1.542 ± 0.507	1.032 ± 2.233	3.490 ± 2.300	1.993 ± 0.416	3.306 ± 1.563	1.556 ± 0.413
24	20.517 ± 1.901	0.223 ± 0.092	2.413 ± 0.433	1.912 ±2.125	4.510 ± 3.210	3.226 ± 0.235	4.897 ± 0.978	3.048 ± 0.877

Table 1.12. Amount of hydrocortisone (mg) diffused through a non-pre-washed mouse skin over 24 hours

Time (hr)	Corticool gel	Cortizone -10 ointment	Aveeno cream	Cortizone-10 plus cream	Cortaid cream	Cortaid lotion	Corticool lotion	Prescription HC cream 2.5%
0	0	0	0	0	0	0	0	0
0.5	0.0085 ± 0.0013	0.0015 ± 0.0015	0.0066 ± 0.0013	0.0097 ± 0.0041	0.0077 ± 0.0029	0.0176 ± 0.0103	0.030 ± 0.002	0.00776 ± 0.0032
1.5	0.0200 ± 0.00200	0.0042 ± 0.0010	0.0157 ± 0.0045	0.0180 ± 0.0126	0.0087 ± 0.0031	0.0298 ± 0.0197	0.046 ± 0.004	0.0139 ± 0.0033
3	0.0784 ± 0.0055	0.0049 ± 0.0012	0.0278 ± 0.0076	0.0268 ± 0.0312	0.0159 ± 0.0012	0.0543 ± 0.0225	0.195 ± 0.071	0.0339 ± 0.0073
6	0.265 ± 0.0420	0.0120 ± 0.0.068	0.0435 ± 0.0125	0.0610 ± 0.1159	0.0408 ± 0.0085	0.081 ± 0.0418	0.0445 ± 0.0231	0.806 ± 0.0227
10	0.551 ± 0.103	0.0154 ± 0.0071	0.0551 ± 0.0185	0.0706 ± 0.142	0.0951± 00383	0.127 ± 0.0563	0.1554 ± 0.1038	0.1831 ± 0.0443
20	1.35 ± 0.187	0.0217 ± 0.0089	0.1542 ± 0.0507	0.1032 ± 0.223	0.349 ± 0.230	0.199 ± 0.0416	0.331 ± 0.156	0.389 ± 0.103
24	2.05 ±	0.0223 ±	0.2413 ±	0.191 ±	0.451 ±	0.3226 ±	0.490 ±	0.762 ±

	0.190	0.0092	0.0433	0.2125	0.321	0.0235	0.0978	0.219

Table 1.13. Hydrocortisone Permeability coefficient and the R^2 for linear fitting of all formulations permeating through non-prewashed mouse skin

Formulation	**n**	**Permeability coefficient (cm/hr)**	**R^2**
Corticool gel*	3	$8.572*10^{-3}$	0.998
Corticool gel **	3	$2.400*10^{-3}$	0.998
Cortizone-10 plus cream	4	$2.366*10^{-3}$	0.862
Cortaid cream	5	$2.138*10^{-3}$	0.961
Cortaid lotion	3	$1.326*10^{-3}$	0.987
Cortizone-10 ointment**	3	$2.419*10^{-5}$	0.904
Corticool lotion	3	$2.681*10^{-3}$	0.976
Aveeno cream	6	$1.026*10^{3}$	0.952
Prescription HC 2.5%	6	$1.264*10^{-3}$	0.916

* The permeability with solubility 0.28mg/ml
**The permeability with solubility 1mg/ml

Similar results for hydrocortisone permeation to those observed in the synthetic membrane could be seen in the experiments with the mouse skin. The Corticool gel had a significantly higher hydrocortisone diffusion through the mouse skin compared to the rest of the other formulations, cream, lotion, or ointment (Figure 1.26). Similar to the results for the hydrocortisone release rate through the synthetic membrane, the 95% confidence interval and 95% prediction band from the drug release rate for Corticool gel are distinctly different from the drug diffusion profiles of other formulations after 5 hours (Figure 1.28).

Corticool gel has three diffusion phases similar to the phases seen for the synthetic membrane. The early stage of diffusion is the surface depletion of hydrocortisone that produces an initial high diffusion rate; the second phase is slower than the first with the second phase being considered a lag time for hydrocortisone to diffuse through the vehicle to the mouse skin membrane. After the first three hours, the drug's diffusion rate increases and follows the Fick's law of diffusion model. The Corticool gel's hydrocortisone release profile suggests that it takes time for the hydrocortisone to reach and maintain a saturated concentration of hydrocortisone on the surface of the membrane. Since all of the hydrocortisone is in solution, and there must be a rapid transfer of hydrocortisone within the formulation matrix toward the diffusion membrane.

The hydrocortisone ointment formulation permeation file differs with the depletion of the surface hydrocortisone occurring in two hours producing an initial rapid drug release rate. Following the initial higher hydrocortisone diffusion rate, the diffusion rate slows down notably. Nevertheless, the two phases for hydrocortisone release in the mouse skin were not as significantly separated or observable as with that of the synthetic membrane. It is speculated that the deletion of the penetrant occurs more quickly with the synthetic membrane.

The topical prescription product still ranked second in the amount of hydrocortisone diffusing through the mouse skin (Figure 1.29). As observed with the hydrocortisone diffusion through the synthetic membrane, a higher drug percentage in the product facilitates greater diffusion of the drug as the concentration gradient is better maintained.

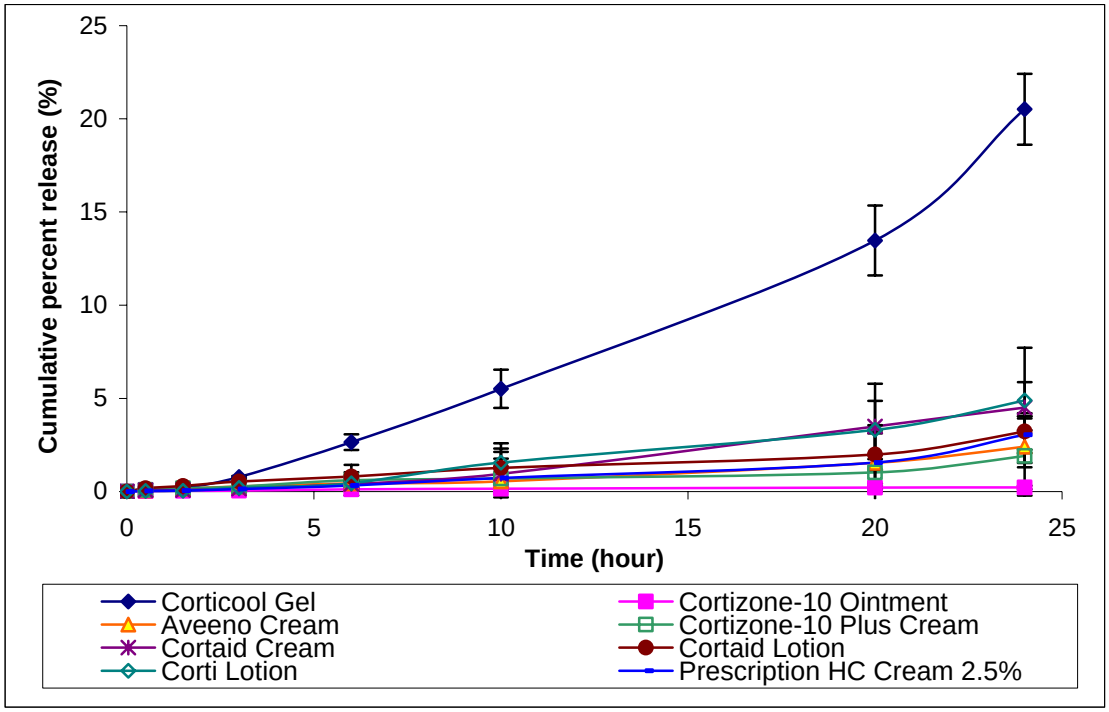

Figure 1.27. Percentage of hydrocortisone permeation through non-pre-washed mouse skin over 24 hours

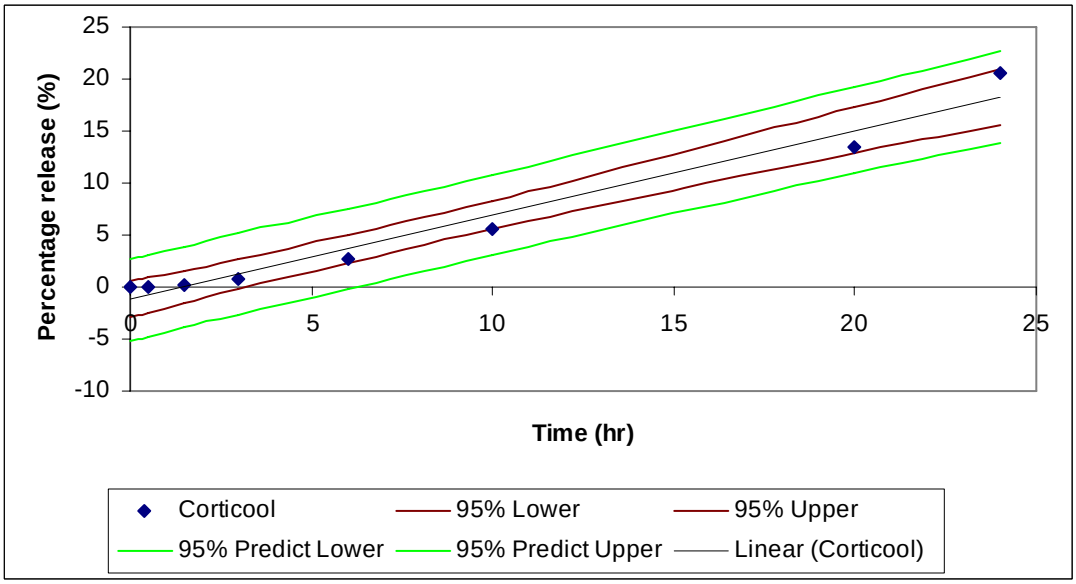

Figure 1.28. The 95% confidence interval and 95% prediction band hydrocortisone permeation from Corticool gel through a mouse skin using Fick's-law model

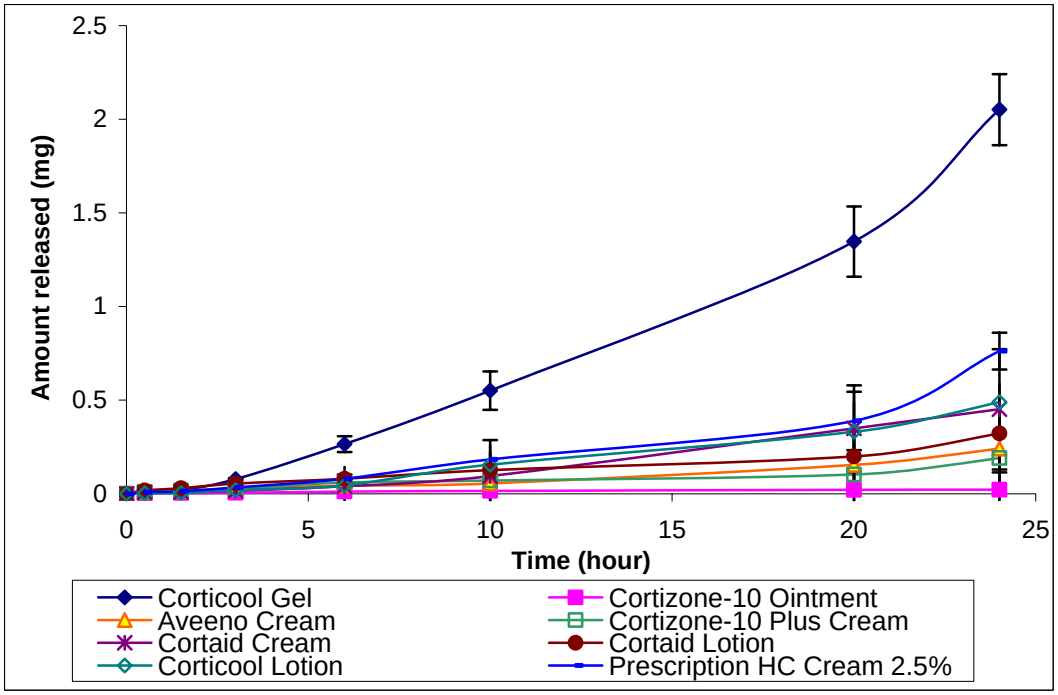

Figure 1.29. Amount of hydrocortisone diffusing through a non-prewashed mouse skin using the Fick's law model over 24 hours

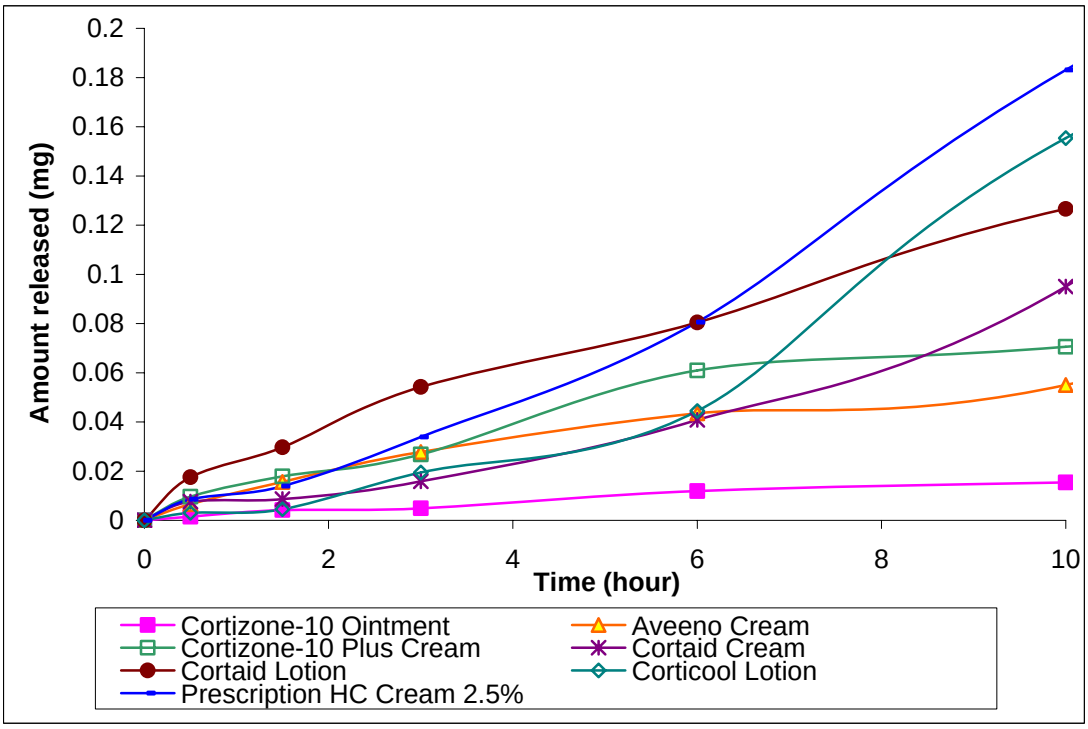

Figure 1.30. A cut off graph showing hydrocortisone release behavior for the first few hours from creams, lotions and an ointment formulation through a mouse skin

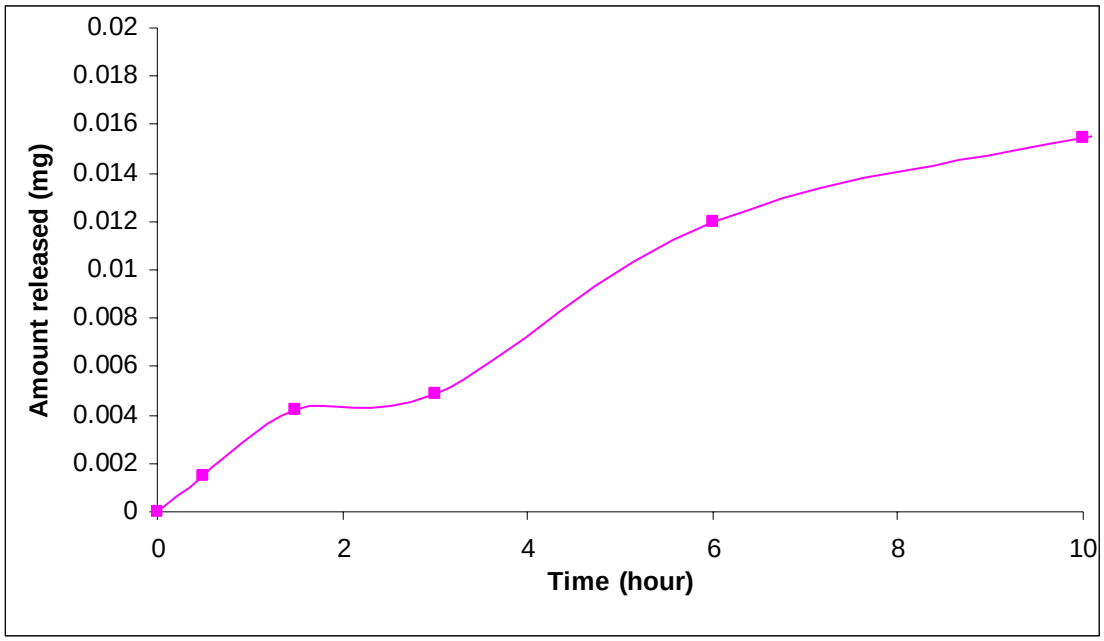

Figure 1.31. The diffusion profile of hydrocortisone from Cortizone-10 ointment through a mouse skin showing two phases of release

The calculation of hydrocortisone permeability from the Corticool Gel was similarly calculated for mouse skin as a synthetic membrane with C_d = 0.28mg/ml and C_d = 1mg/ml, while C_d = 1mg/ml for the Cortizone ointment and C_d = 0.28mg/ml for the other formulations. The permeability coefficient of hydrocortisone from the Corticool gel is close to the permeability coefficients observed for the hydrocortisone in the Cortaid cream, the Corticool lotion, and the Cortizone Plus cream using hydrocortisone solubility of 1mg/ml. It is noted that the presence of ethyl alcohol and Propylene Glycol also increase hydrocortisone permeability through skin. Previous studies show that alcoholic vehicles are among those increasing drug permeation both by transcellular and transfollicular pathways [30]. Ethanol is primarily a lipid solvent that not only increases lipid fluidity within the intracellular space, but also it extends the hydrophobic domain between the polar head groups in the stratum corneum. As the result of the ethanol and other enhancers, the permeability may change. However,

for hydrocortisone permeation from Corticool gel, the effect of enhancers appears to be negligible in comparison to the higher effect that high hydrocortisone solubility produces.

The high rate of drug release can mostly be explained by the high solubility of the hydrocortisone in the gel form. The solubility of the hydrocortisone in the ointment dosage form of 1mg/ml was used to calculate the permeability coefficient and diffusion coefficient of the hydrocortisone in Cortizone ointment. Both of these two coefficients are low due to the low-partition coefficient. The initial high rate of hydrocortisone diffusion is not clear even though it is still observed in the ointment formulation (Figure 1.30). With the existing depletion phase for the hydrocortisone in the Cortizone-10 ointment's permeation profile, and the release data of this formulation fitted better to the Higuchi model; whereas the other formulations fitted Fick's law model of diffusion better.

The diffusion coefficients of the hydrocortisone from the formulations are listed in Table 14. The diffusion coefficient of the hydrocortisone from the gel formulation is calculated with the solubility C_d = 0.28mg/ml and C_d = 1mg/ml. The Cortizone ointment displayed the smallest hydrocortisone diffusion coefficient due to its very low diffusion rate (Figure 1.32).

Fitting the hydrocortisone release data with the Higuchi model using the adjustment of the C_d value of 1mg/ml reduces the diffusion coefficient of hydrocortisone in the Corticool gel, but the value is still higher than hydrocortisone diffusion out from other formulations. Thus, the high rate of diffusion of the Corticool

gel is mostly due to the high solubility of the hydrocortisone in the gel matrix (Table 14).

Table 1.14. The diffusion coefficients following the Higuchi model for hydrocortisone from eight formulations for hydrocortisone diffusing through the non-pre-washed mouse skin

Formulation	n	Diffusion coefficient (cm^2/hr)	R^2
Corticool gel *	3	$3.465*10^{-3}$	0.969
Corticool gel **	3	$1.203*10^{-3}$	0.969
Cortizone-10 plus cream	4	$1.478*10^{-5}$	0.868
Cortaid cream	5	$1.112*10^{-5}$	0.949
Cortaid lotion	3	$3.415*10^{-5}$	0.977
Cortizone-10 ointment**	3	$8.477*10^{-7}$	0.979
Corticool lotion	3	$2.790*10^{-5}$	0.966
Aveeno cream	6	$9.685*10^{-5}$	0.832
Prescription HC 2.5%	6	$9.336*10^{-5}$	0.953

* The diffusion coefficient with solubility 0.28mg/ml
** The diffusion coefficient with solubility 1mg/ml

The Hydrocortisone permeation profile from the Cortizone-10 ointment can be described well by the Higuchi model due to the dual-phase permeation of the hydrocortisone in the Cortizone-10 ointment. The diffusion coefficient of the hydrocortisone in this formulation is many times lower than the other formulations since the diffusion coefficient also depends on the partition coefficient.

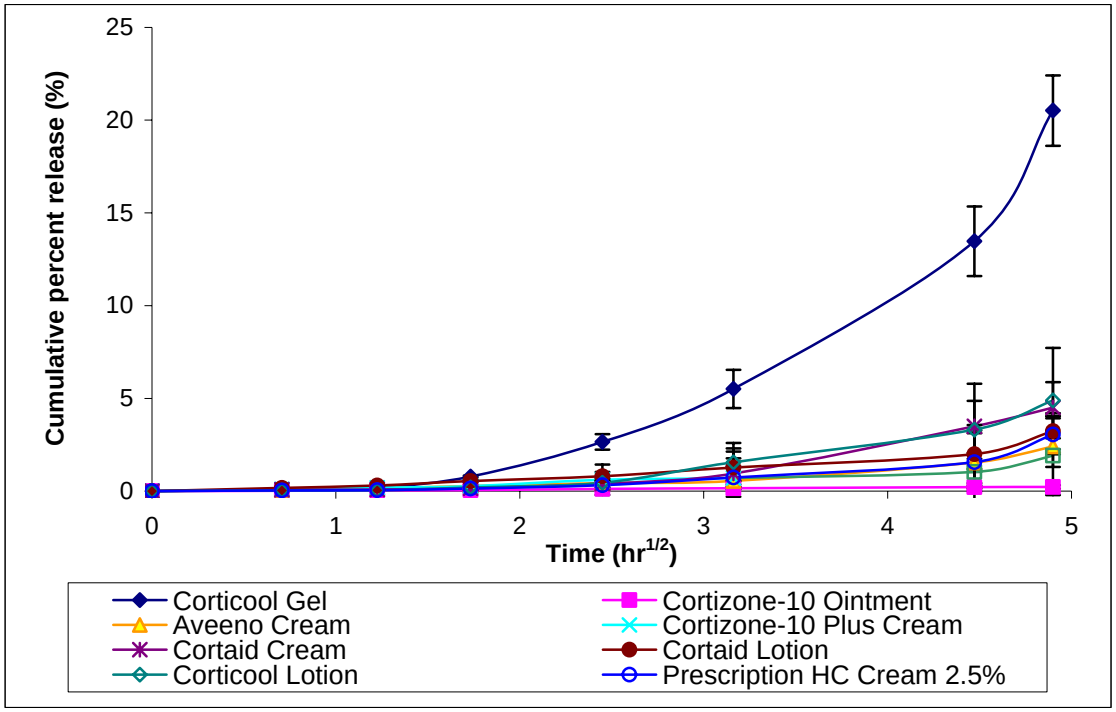

Figure 1.32. The diffusion profiles of eight formulations through non-prewashed mouse skin using Higuchi model

Prewashed mouse skin permeation

As mentioned previously in the literature review, hydration of the skin usually results in an increase in the drug diffusion rate through the skin and the water acts as a natural penetration enhancer. An expected higher permeation of the hydrocortisone occurs with the hydrated mouse skin. The mouse skin was flushed for 30 seconds with exfoliating cleanser. Repeat experiments were performed using the same procedures that were done with the dry mouse skin.

The hydrocortisone diffusion profiles (percentage permeation and amount permeation) for the topical hydrocortisone products are displayed in Table 15 and Table 16. The hydrocortisone permeability coefficient values from each topical product are presented in Table 17.

Table 1.15. The percentage of hydrocortisone (%) diffusion through pre-washed-mouse skin over 24 hours

Time (hr)	Corticool gel	Cortizone-10 ointment	Aveeno cream	Cortizone-10 plus cream	Cortaid cream	Cortaid lotion	Corticool lotion	Prescription HC cream 2.5%
0	0	0	0	0	0	0	0	0
0.5	0.217 ± 0.474	0.037 ± 0.012	0.212 ± 0.041	0.055 ± 0.010	0.170 ± 0.068	0.135 ± 0.055	0.049 ± 0.014	0.0106 ± 0.00033
1.5	0.493 ± 0.942	0.173 ± 0.098	0.170 ± 0.126	0.164 ± 0.088	0.175 ± 0.068	0.288 ± 0.063	0.189 ± 0.002	0.0174 ± 0.0071
3	1.32 ± 3.08	0.223 ± 0.115	0.423 ± 0.312	0.227 ± 0.078	0.467 ± 0.154	0.555 ± 0.166	0.558 ± 0.292	0.0268 ± 0.0109
6	4.99 ± 1.333	0.337 ± 0.203	1.16 ± 0.820	0.625 ± 0.289	0.884 ± 0.155	0.961 ± 0.327	1.626 ± 0.110	0.0267 ± 0.0109
10	11.3 ± 0.087	0.341 ± 0.179	2.08 ± 1.421	1.13 ± 0.510	1.75 ± 0.308	1.47 ± 0.561	2.971 ± 1.64	0.114 ± 0.0464
20	18.8 ± 1.13	0.448 ± 0.207	4.16 ± 2.23	2.00 ± 0.762	3.37 ± 0.944	3.27 ± 0.344	4.20 ± 2.26	0.4116 ± 0.168
24	23.4 ± 0.828	0.451 ± 0.227	4.99 ± 2.13	2.78 ± 0.657	5.24 ± 1.030	3.98 ± 0.436	5.34 ± 1.38	0.468 ± 0.191

Table 1.16. The amount of hydrocortisone (mg) diffusion through pre-washed skin over 24 hours

Time (hr)	Corticool gel	Cortizone-10 ointment	Aveeno cream	Cortizone-10 plus cream	Cortaid cream	Cortaid lotion	Corticool lotion	Prescription HC cream 2.5%
0	0	0	0	0	0	0	0	0
0.5	0.0217 ± 0.0474	0.0037 ± 0.0012	0.0212 ± 0.0041	0.0055 ± 0.0010	0.0170 ± 0.0068	0.0135 ± 0.0055	0.0049 ± 0.0014	0.043 ± 0.0013
1.5	0.0493 ± 0.0942	0.0173 ± 0.0098	0.0170 ± 0.0126	0.0164 ± 0.0088	0.0175 ± 0.0068	0.0288 ± 0.0063	0.0189 ± 0.0002	0.0881 ± 0.028
3	0.132 ± 0.308	0.0223 ± 0.0115	0.0423 ± 0.0312	0.0227 ± 0.0078	0.0467 ± 0.0154	0.0555 ± 0.0166	0.0558 ± 0.0292	0.178 ± 0.107
6	0.499 ± 0.1333	0.0337 ± 0.0203	0.116 ± 0.0820	0.0625 ± 0.0289	0.0884 ± 0.0155	0.0961 ± 0.0327	0.163 ± 0.0110	0.406 ± 0.044
10	1.13 ± 0.0087	0.0341 ± 0.0179	0.208 ± 0.142	0.113 ± 0.0510	0.175 ± 0.0308	0.147 ± 0.0561	0.297 ± 0.164	1.06 ± 0.186
20	1.88 ± 0.113	0.0448 ± 0.0207	0.416 ± 0.223	0.200 ± 0.0762	0.337 ± 0.0944	0.327 ± 0.0344	0.420 ± 0.226	2.67 ± 0.672
24	2.34 ± 0.0828	0.0451 ± 0.0227	0.499 ± 0.213	0.278 ± 0.0657	0.524 ± 0.103	0.398 ± 0.0436	0.534 ± 0.138	3.40 ± 0.764

All the formulations exhibited a higher hydrocortisone diffusion rate through the pre-washed mouse skin compared to the non-wash mouse skin. The permeability

and diffusion coefficients were calculated using C_d = 0.28mg/ml or C_d =1mg/ml for the Corticool gel. The higher hydrocortisone-permeability and diffusion-rate values were observed for the Corticool gel in comparison with the non-prewashed mouse skin (Table 1.16 and Table 1.17).

Very similar to the hydrocortisone diffusion profiles through the dry mouse skin, the Corticool gel had the highest hydrocortisone diffusion rate compared to the rest of the other formulations with a distinguished 95% confidence interval for the linear regression band and a 95% prediction band (Figure 1.35). The hydrocortisone diffusion profile from the Cortisool gel had two phases with a lag time. An initial with a slow diffusion rate follows by a second high diffusion rate. The system required one hour before reaching the steady-state diffusion rate.

Table 1.17. The permeability coefficients of the hydrocortisone from eight formulations permeating through pre-washed mouse skin by water

Formulation	n	Permeability coefficient (cm/hr)	R^2
Corticool gel*	3	$1.152*10^{-2}$	0.985
Corticool gel	3	$3.22*10^{-3}$	0.985
Cortizone-10 plus cream	4	$1.261*10^{-3}$	0.998
Cortaid cream	5	$2.425*10^{-3}$	0.964
Cortaid lotion	3	$1.851*10^{-3}$	0.998
Cortizone-10 ointment**	3	$3.194*10^{-5}$	0.904
Corticool lotion	3	$2.527*10^{-3}$	0.976
Aveeno cream	6	$2.479*10^{3}$	0.998
Prescription HC 2.5%	6	$1.877*10^{-3}$	0.999

* The diffusion coefficient with solubility 0.28mg/ml
** The diffusion coefficient with solubility 1mg/ml

Hydrocortisone-10 ointment also showed two phases, a fairly rapid depletion phase of hydrocortisone near the surface membrane followed by a slow diffusion-rate phase. Other formulations showed one short phase of depletion but the dominant phase occured when the system reached equilibrium (Figure 1.35).

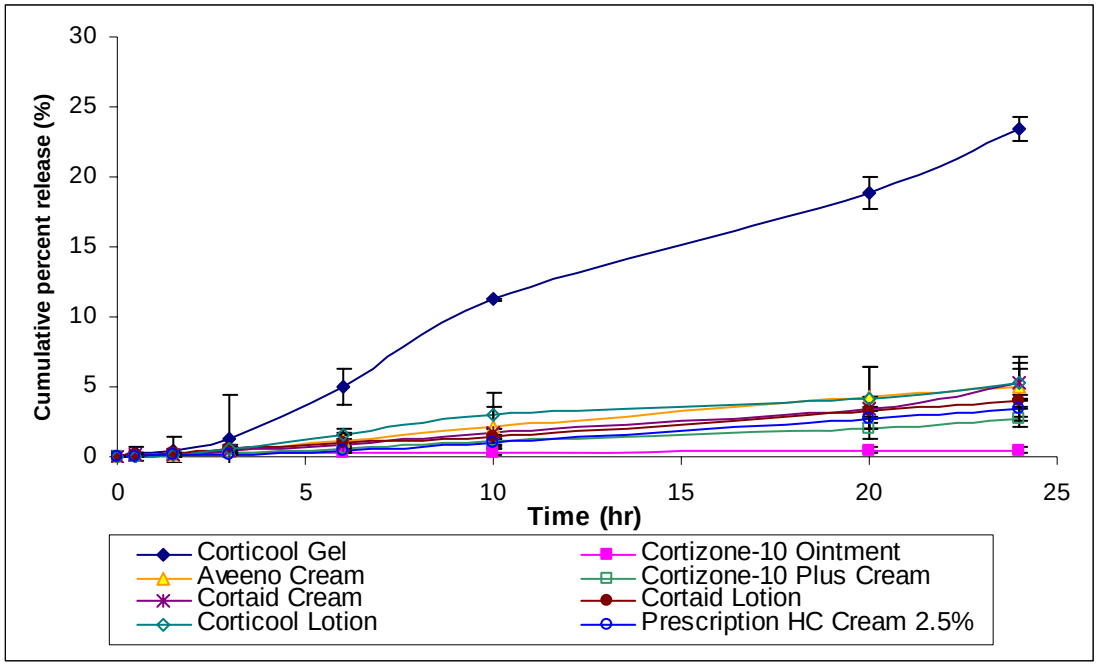

Figure 1.33. A hydrocortisone diffusion profile over 24 hours through the pre-washed mouse skin using the Fick's-law model

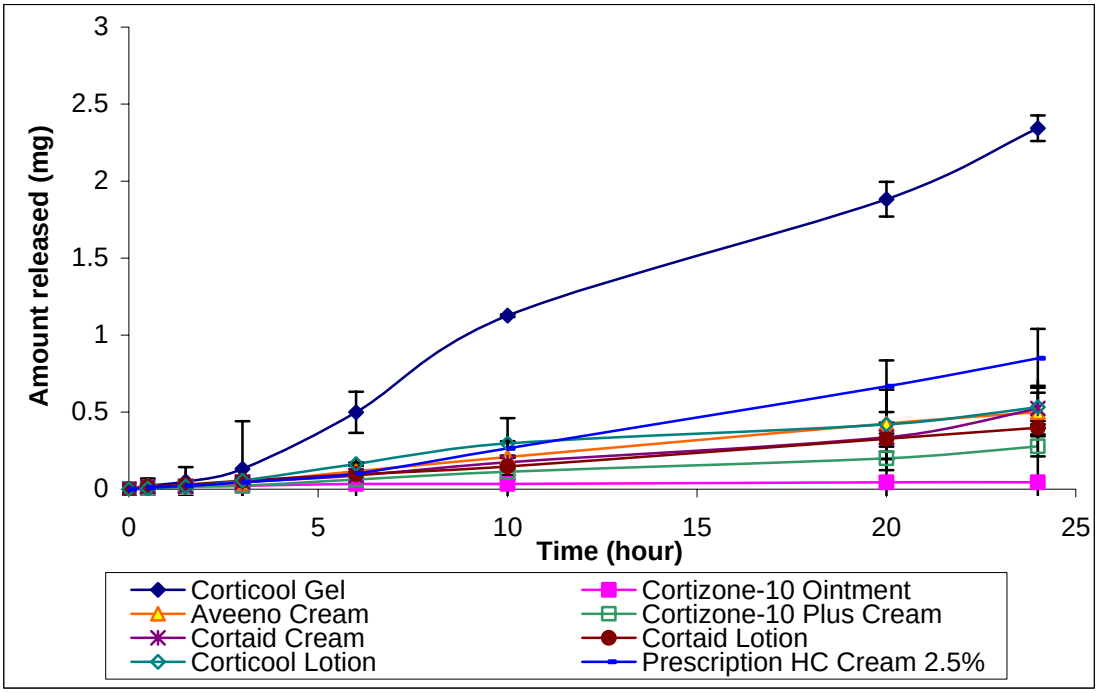

Figure 1.34. The amount of hydrocortisone permeation profiles through mouse skin over 24 hours from hydrocortisone topical products

The solubility of the hydrocortisone in the Cortizone 10 ointment was 1mg/ml. With this high solubility, the permeability and diffusion values of hydrocortisone in ointment were still much lower than those of other formulations. The partition coefficient of the hydrocortisone in the ointment formulation was much lower than the partition coefficients of the other formulation on the pre-washed mouse skin.

Prescription hydrocortisone 2.5% cream had a higher amount of the drug diffusion through the pre-washed mouse skin than the other creams and lotions dosage forms (Figure 1.34). However, the hydrocortisone permeation rate through the mouse skin of this formulation was still much lower than that of the Corticool gel. The high concentration of hydrocortisone in the prescription formulation better facilitates the hydrocortisone dissolution from solid hydrocortisone to a solute in the water-based phase maintaining a saturated concentration compared to the other creams and lotion.

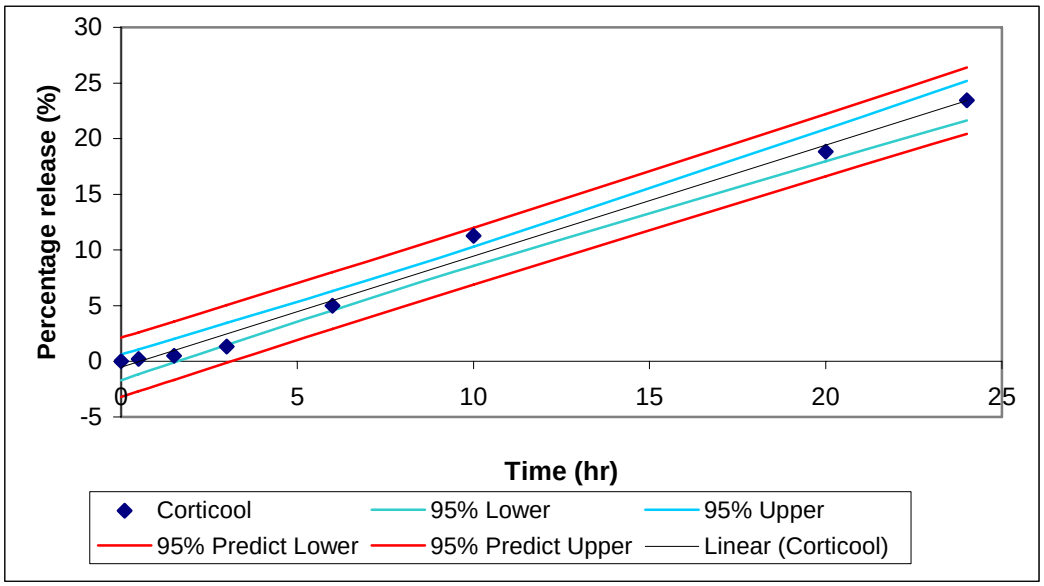

Figure 1.35. The 95% confidence interval band and the 95% prediction band showing Corticool gel hydrocortisone-diffusion rate though the pre-washed mouse skin

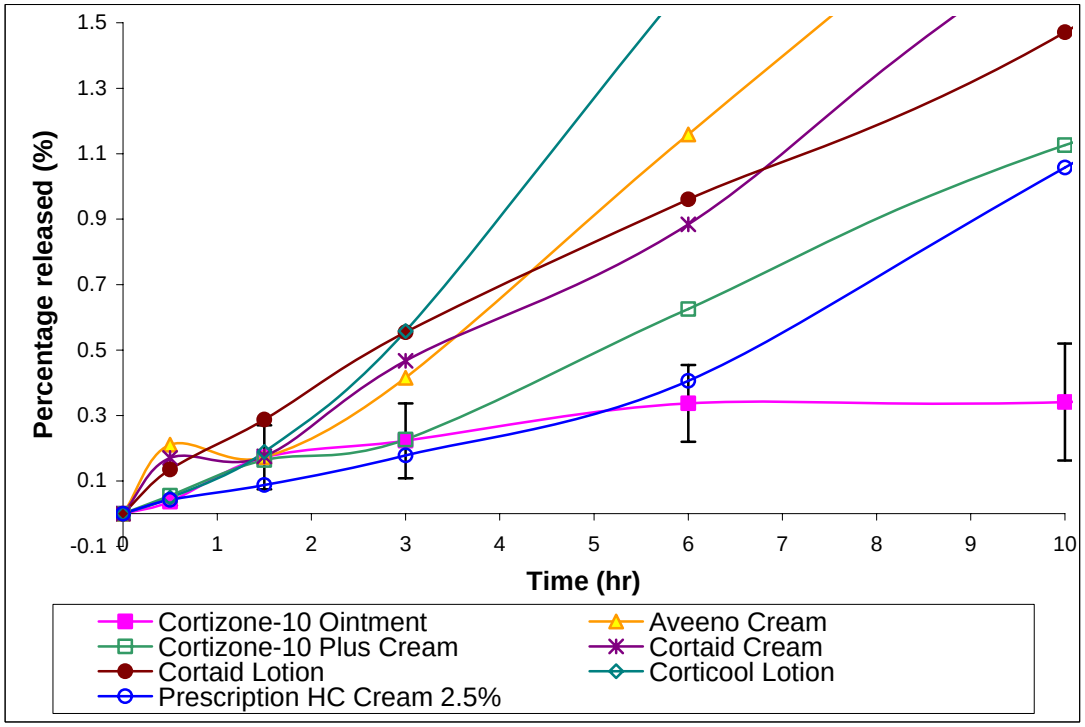

Figure 1.36. A cut-off graph depicting the initial diffusion profiles for the first few hours of all the hydrocortisone formulations through the pre-washed mouse skin showing the depletion phases for Aveeno cream and Cortaid cream.

Table 1.18. The diffusion coefficients of hydrocortisone through the pre-washed mouse skin for the topical hydrocortisone formulations

Formulation	n	Diffusion coefficient (cm^2/hr)	R^2
Corticool gel*	3	$1.534*10^{-3}$	0.982
Corticool gel**	3	$5.352*10^{-4}$	0.982
Cortizone-10 plus cream	4	$6.590*10^{-5}$	0.909
Cortaid cream	5	$9.669*10^{-5}$	0.865
Cortaid lotion	3	$6.558*10^{-5}$	0.918
Cortizone-10 ointment**	3	$2.850*10^{-7}$	0.934
Corticool lotion	3	$1.284*10^{-4}$	0.944
Aveeno cream	6	$2.111*10^{-4}$	0.992
Prescription HC 2.5%	6	$1.439*10^{-4}$	0.982

* The diffusion coefficient with solubility 0.28mg/ml
**The diffusion coefficient with solubility 1mg/ml

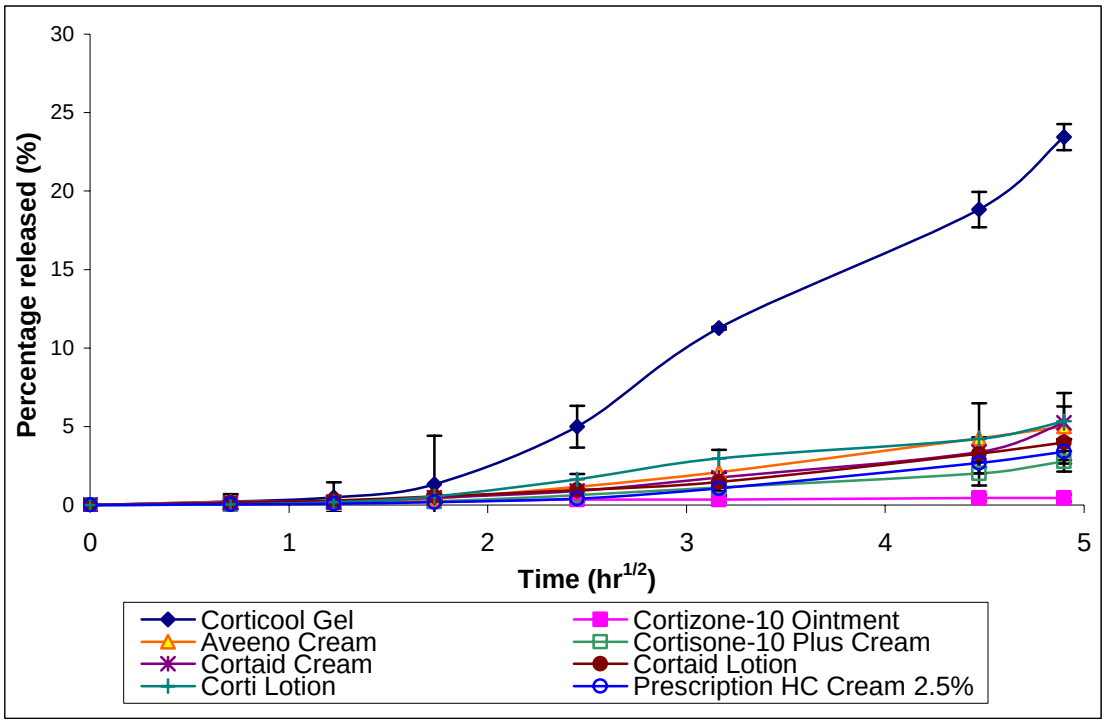

Figure 1.37. The square root of time-diffusion profiles of hydrocortisone from eight formulations over 24 hours using the Higuchi model through the prewashed mouse skin

PERMEATION OF HYDROCORTISONE FROM TOPCAL PRODUCTS THROUGH EPIDERM™

The cumulative amount of the drug release (mg/cm^2) from the topical hydrocortisone products, three creams (Cortizone-10 Plus, Cortaid and HC Cream USP, 2.5%) two lotions (Cortaid and Corticool lotion), one ointment (Cortizone-10) and one gel (Corticool with and without pretreatment with exfoliating cleanser) against the square root of time ($h^{1/2}$) were compiled. The shapes of the hydrocortisone dissolution profiles for all of the topical products were linear with the total percentage of the hydrocortisone release over 24 h ranging from 0.163 to 0.643%, except for the Corticool gel. Both the hydrocortisone-release profiles of Corticool gel with and without pretreatment with an exfoliating cleanser produced at 10 h a steep change in the release rate. The 24h drug release of the Corticool gel was 2.24% without pretreatment with the exfoliating cleanser and 6.21% with pretreatment with exfoliating cleanser (Table 1.19).

Table 1.19. The percentage release of hydrocortisone from seven formulations over 24 hours through an Epiderm™

Time (hr)	Corticool gel w/o	Corticool gel w/w	Cortaid lotion	Cortaid cream	Corticool Lotion	Cortizone-10 Plus cream	Cortizone-10 ointment	HC cream 2.5%
0	0	0	0	0	0	0	0	0
0.5	0.148 ± 0.003	0.143 ± 0	0.157 ± 0.006	0.141 ± 0.007	0.144 ± 0.014	0.148 ± 0.004	0.142 ± 0 0017	0.056 ± 0.002
1.5	0.153 ± 0.004	0.184 ± 0	0.173 ± 0.015	0.171 ± 0.037	0.147 ± 0.012	0.151 ± 0.002	0.143 ± 0.0013	0.073 ± 0.017
3	0.153 ± 0.0021	0.143 ± 0	0.219 ± 0.043	0.204 ± 0.061	0.173 ± 0.026	0.166 ± 0.007	0.145 ± 0.0012	0.068 ± 0.007
6	0.318 ± 0.003	0.646 ± 0	0.277 ± 0.073	0.173 ± 0.007	0.209 ± 0.039	0.180 ± 0.004	0.148 ± 0.0024	0.074 ± 0.010
10	0.510 ± 0.044	1.378 ± 0	0.398 ± 0.117	0.187 ± 0.028	0.206 ± 0.058	0.194 ± 0.011	0.149 ± 0.0018	0.112 ± 0.027
20	1.63 ± 0.053	4.516 ± 0	0.410 ± 0.107	0.575 ± 0.180	0.494 ± 0.066	0.259 ± 0.012	0.155 ± 0.0021	0.363 ± 0.185
24	2.24 ± 0.132	6.207 ± 0	0.467 ± 0.127	0.643 ± 0.207	0.684 ± 0.114	0.280 ± 0.013	0.163 ± 0.0069	0.424 ± 0.177

Table 1.20. The amount of hydrocortisone (mg) released from seven formulations over 24 hours through an Epiderm™

Time (hr)	Corticool gel w/o	Corticool gel w/w	Cortaid lotion	Cortaid cream	Corticool Lotion	Cortizone -10 Plus cream	Cortizone-10 ointment	HC cream 2.5%
0	0	0	0	0	0	0	0	0
0.5	0.0148 ± 0.0003	0.0143 ± 0	0.0157 ± 0.0006	0.0141 ± 0.0007	0.0144 ± 0.0014	0.0148 ± 0.0004	0.0142 ± 0.0002	0.0152 ± 0.0002
1.5	0.0153 ± 0.0004	0.0184 ± 0	0.0173 ± 0.0015	0.0171 ± 0.0037	0.0147 ± 0.0012	0.0151 ± 0.0002	0.0143 ± 0.00013	0.0198 ± 0.0008
3	0.0153 ± 0.0002	0.0143 ± 0	0.0219 ± 0.0043	0.0204 ± 0.0061	0.0173 ± 0.0026	0.0166 ± 0.0007	0.0145 ± 0.0001	0.0183 ± 0.0002
6	0.0318 ± 0.0003	0.0646 ± 0	0.0277 ± 0.0073	0.0173 ± 0.0007	0.0209 ± 0.0039	0.0180 ± 0.0004	0.0148 ± 0.0002	0.0201 ± 0.0004
10	0.0510 ± 0.0044	0.1378 ± 0	0.0398 ± 0.0117	0.0187 ± 0.028	0.0206 ± 0.0058	0.0194 ± 0.0011	0.0149 ± 0.0002	0.0299 ± 0.0012
20	0.1625 ± 0.0053	0.4516 ± 0	0.0410 ± 0.0107	0.575 ± 0.180	0.0494 ± 0.0066	0.0259 ± 0.0012	0.0155 ± 0.0002	0.0493 ± 0.0029
24	0.2242 ± 0.0132	0.6207 ± 0	0.0467 ± 0.0127	0.643 ± 0.207	0.0684 ± 0.0114	0.0280 ± 0.0013	0.0163 ± 0.0007	0.0709 ± 0.0053

An Epiderm™ is a strong barrier. Consequently, the diffusion process of hydrocortisone through it is much slower than what was observed in the synthetic membrane (smaller than 20 times) and the mouse skin (smaller than 6-8 times). The hydrocortisone from the Corticool gel permeated 5-8 times faster through the Epiderm™ than from the other creams and lotions and 15 times faster through Epiderm™ than the Cortizone 10 ointment.

The effect of pre-washing with an exfoliating cleanser seems to have had a greater effect on the Epiderm™ than the mouse skin. After 24 hours, the total amount of hydrocortisone in the receiver compartment of the Franz cell using the Epiderm™-pre-washed membrane was 2.7 times higher than when a non-prewashed Epiderm™ was used; whereas, the prewashed mouse skin produced only a 13% increases in hydrocortisone permeation compared to the non-prewashed skin. This may be due to

the fact that the structure of human skin is more sensitive to water than a mouse skin. However, the lack of replicate experiments with a prewashed Epiderm™, the greater the effect of water on the hydrocortisone permeation through the Epiderm™ can not exclude the explanation it may just be due to the normal variability or an actual higher sensitivity of human skin to water.

Table 1.21. The permeability coefficients of hydrocortisone from seven topical formulations through an Epiderm™

Formulation	n	Permeability coefficient (cm/hr)	R^2
Corticool gel w/o*	3	$1.012*10^{-3}$	0.955
Corticool gel w/o**	3	$2.832*10^{-4}$	0.955
Corticool gel w/w*	1	$2.951*10^{-3}$	0.964
Corticool gel w/w**	1	$8.263*10^{-4}$	0.964
Cortizone-10 plus cream	3	$6.366*10^{-4}$	0.995
Cortaid cream	2	$2.478*10^{-4}$	0.904
Cortaid lotion	3	$1.432*10^{-4}$	0.880
Cortizone-10 ointment**	3	$2.546*10^{-6}$	0.952
Corticool lotion	3	$3.023*10^{-4}$	0.928
Prescription HC cream 2.5%	3	$2.531*10^{-4}$	0.939

* The diffusion coefficient with solubility 0.28mg/ml
**The diffusion coefficient with solubility 1mg/ml

The permeability coefficient values listed in Table 24 indicate the hydrocortisone permeability coefficient from the Corticool gel before accounting for its solubility (0.28mg/ml) are much higher than those of the other formulations. After utilizing the higher hydrocortisone solubility (1mg/ml), the hydrocortisone permeability from the Corticool gel was close to other creams and lotions. This means

that the concentration gradient, the difference between C_d and C_s, acts as the main reason for the higher drug diffusion rate through the Epiderm™ membrane. Other factors like surfactants and enhancers appear to have a negligible effect if drug solubility is the main driving force.

Corticool gel's hydrocortisone diffusion profiles, the 95%-confidence interval band and the 95% prediction band of both the non-prewashed and the prewashed Epiderm™ are considerably different from the other creams, lotions, and ointment formulation. The Cortiool gel is superior to all of the tested formulations. (Figure 1.38, 1.39, 1.40).

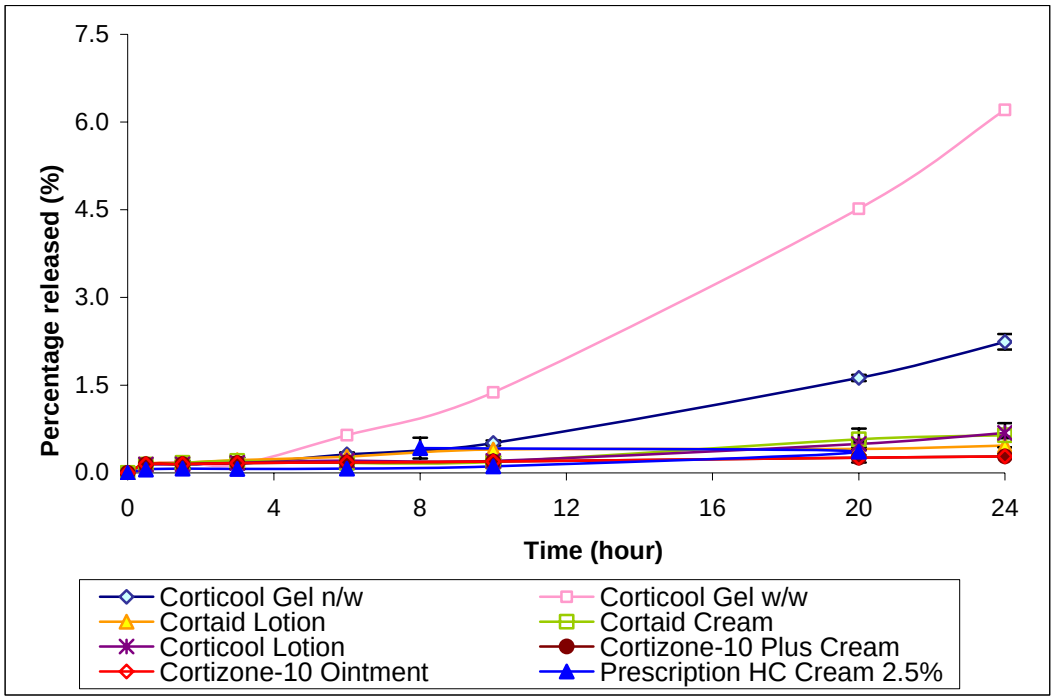

Figure 1.38. Hydrocortisone diffusion profiles from eight formulations through an Epiderm™ over 24 hours using the Fick's-law model

Table 1.22. The diffusion coefficients of hydrocortisone from seven formulations using the Higuchi model

Formulation	n	Diffusion coefficients (cm^2/hr)	R^2
Corticool gel w/o*	2	$2.318*10^{-5}$	0.848
Corticool gel w/o**	2	$8.049*10^{-6}$	0.848
Corticool gel w/w*	1	$1.987*10^{-4}$	0.861
Corticool gel w/w**	1	$6.899*10^{-5}$	0.861
Cortizone-10 plus cream	3	$5.057*10^{-7}$	0.885
Cortaid cream	2	$1.373*10^{-6}$	0.791
Cortaid lotion	3	$5.603*10^{-7}$	0.947
Cortizone-10 ointment	3	$1.969*10^{-9}$	0.914
Corticool lotion	3	$1.380*10^{-6}$	0.918
Prescription HC 2.5%	6	$6.833*10^{-6}$	0.658

* The diffusion coefficient with solubility 0.28mg/ml
**The diffusion coefficient with solubility 1mg/ml

Although the hydrocortisone 2.5% prescription cream has a lower percentage release rate diffusion compared to the Cortaid lotion, Corticool lotion, and the Cortaid cream, the total amount of hydrocortisone in the cream is higher and its total diffusion rate is higher than all of the other formulations except the Corticool gel.

As noted previously, the hydrocortisone 2.5% prescription cream has a higher amount of drug diffusing through the Epiderm™ since the saturated drug concentration on the membrane's surface is maintained as the drug dissolution rate from the suspended solid form to a soluble form in the solution and it is facilitated by the high concentration of hydrocortisone in the dosage form (Figure 1.41). Hydrocortisone 2.5% cream by FDA standards is prescription strength even though the amount of the drug absorbed is lower than that from the Corticool gel.

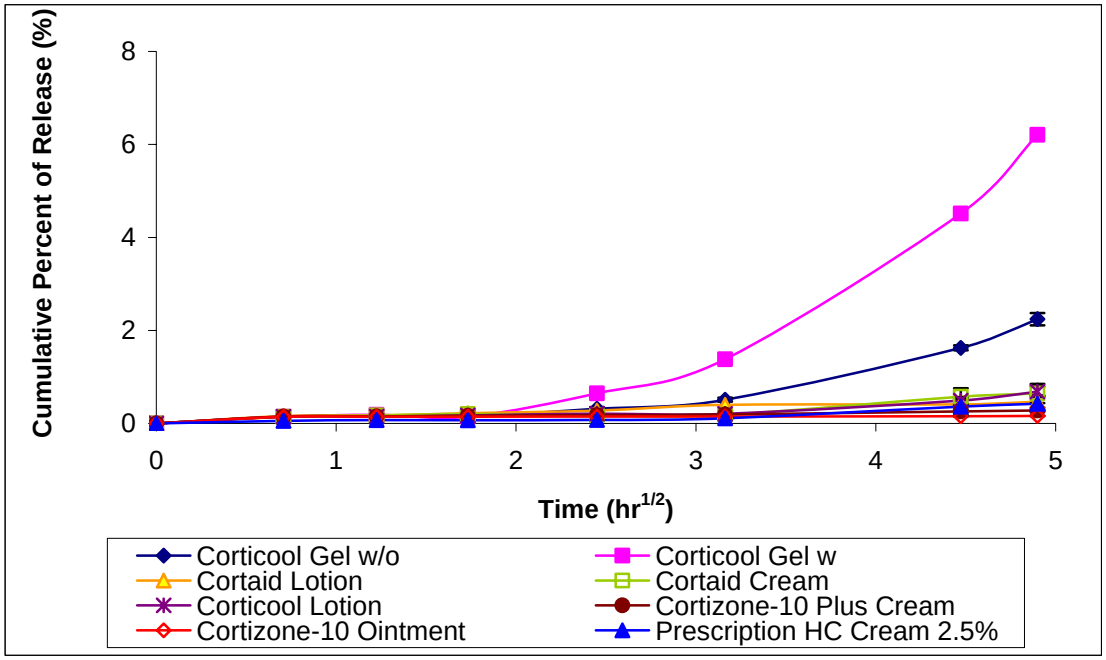

Figure 1.39. The square root of time hydrocortisone-diffusion profiles from seven formulations through an Epiderm™ over 24 hours using the Higuchi model

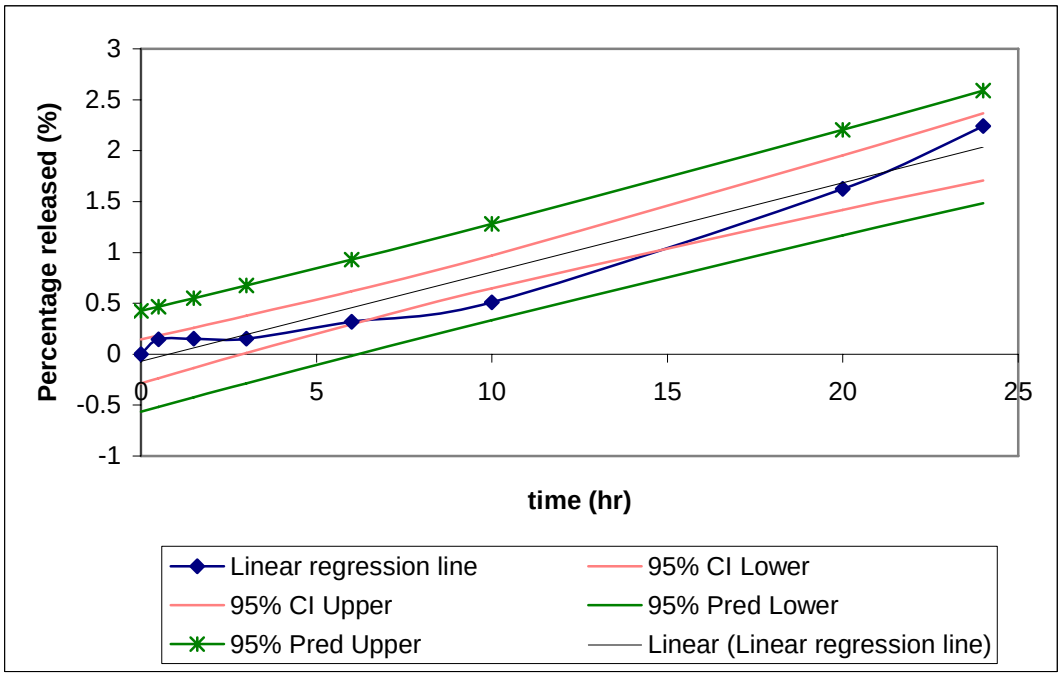

Figure 1.40. The 95% confidence interval and 95% prediction band of hydrocortisone diffusion from Corticool gel though a non-pre-washed Epiderm™ over 24 hours

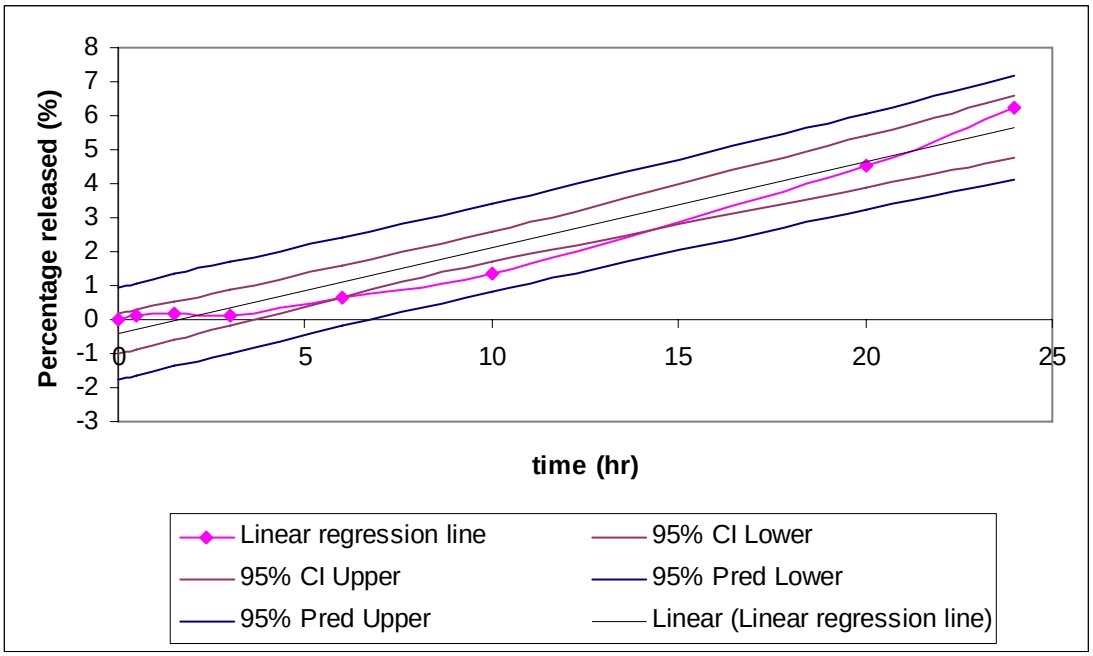

Figure 1.41. The 95% confidence interval and 95% prediction band of hydrocortisone diffusion from Corticool gel though a pre-washed Epiderm™ over 24 hours

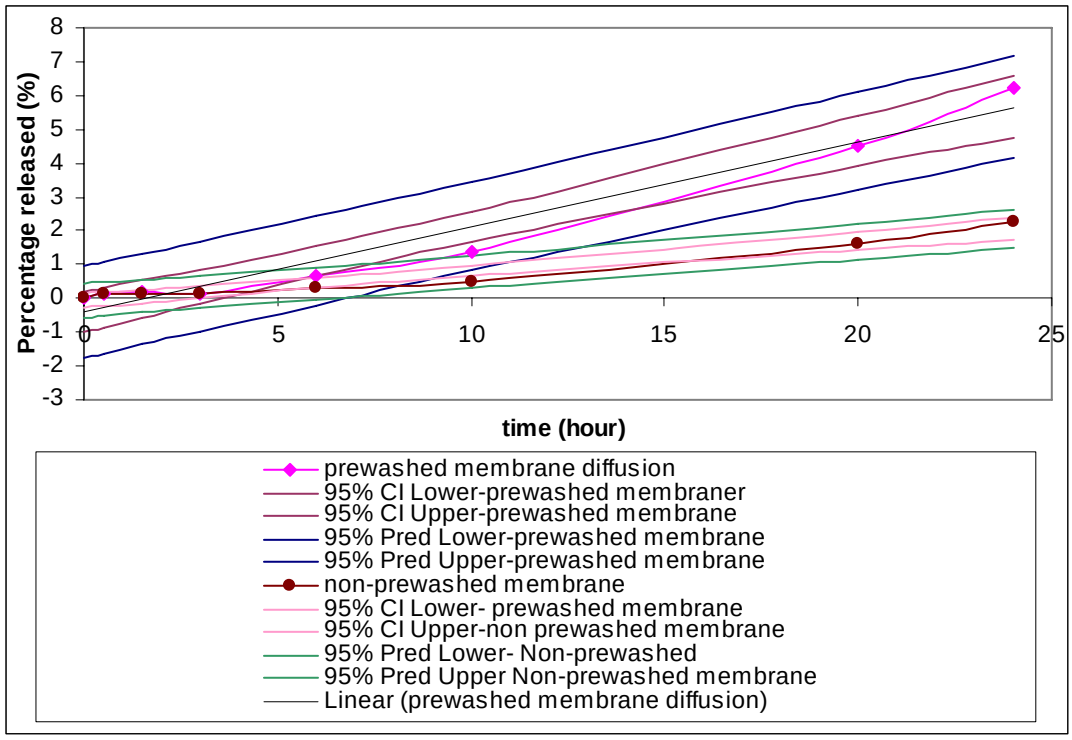

Figure 1.42. The 95% confidence interval and 95% prediction band of hydrocortisone diffusion from Corticool gel though a non-prewashed Epiderm™ and a prewashed Epiderm™ over 24 hours

Hydrocortisone permeation from Corticool gel was described well using the Fick's-law of diffusion model with R^2 = 0.955. Similar to the observation with the synthetic membrane and the mouse skin, the hydrocortisone diffusion profile exhibited three drug-release phases. The first phase is a surface-depletion phase lasting about 0.5 hour. When the hydrocortisone available on the surface of the membrane is depleted, the following diffusion phase is slow since the hydrocortisone inside the gel matrix must diffuse toward the membrane's surface and establish equilibrium for the drug being released and the drug arriving from the gel matrix (Figure 1.45). Once the equilibrium is established, the third phase begins where a higher steady drug release rate exists. The first and second phases are considered the lag phase for hydrocortisone release from Corticool gel. It takes the first hour for the applied formulation to set up a

saturated concentration of hydrocortisone at the membrane's surface and reach a steady-state diffusion of hydrocortisone. The saturated concentration was maintained up to 24 hours.

The hydrocortisone diffusion profile from the Cortizone-10 ointment shows two distinct diffusion phases as observed in the synthetic membrane and the mouse skin (Figure 1.42). The first phase relates to the depletion of hydrocortisone near the membrane's surface. This phase has a high hydrocortisone diffusion rate and lasts for only a half hour. The second phase exhibited a low rate of drug diffusion lasting the rest of the 24 hour period. The second phase reached a steady state and the drug diffusion resembled a straight line. Dissolved hydrocortisone being transported within the matrix toward the membrane's surface is the controlling rate for drug release, and the amount of the drug as a solute that is available on the membranes surface is much less than for gel, creams, or lotions due to the low-partition coefficient of ointment base on Epiderm^{TM} surface. Other formulations, the creams and lotions, also had two phases of diffusion: a depletion phase and a steady-state phase. However, the hydrocortisone-diffusion rates were much higher than observed in the ointment-dosage form. This implies that hydrocortisone diffuses rapidly though the creams' and lotions' formulation matrices. To explain more clearly, there is an abundant amount of water in a cream or lotion to obtain a high-partition coefficient. In addition, the viscosity of creams or lotions is much lower than an ointment-based formulation.

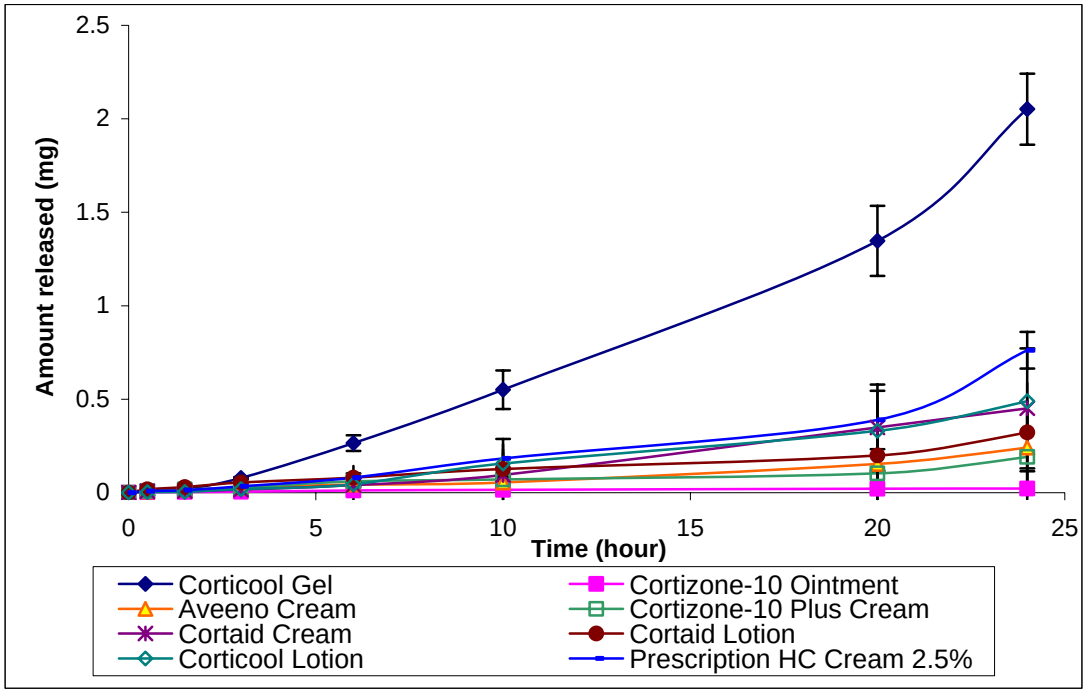

Figure 1.43. Diffusion profile of the amount of hydrocortisone released from eight topical formulations through an Epiderm™ over 24 hours

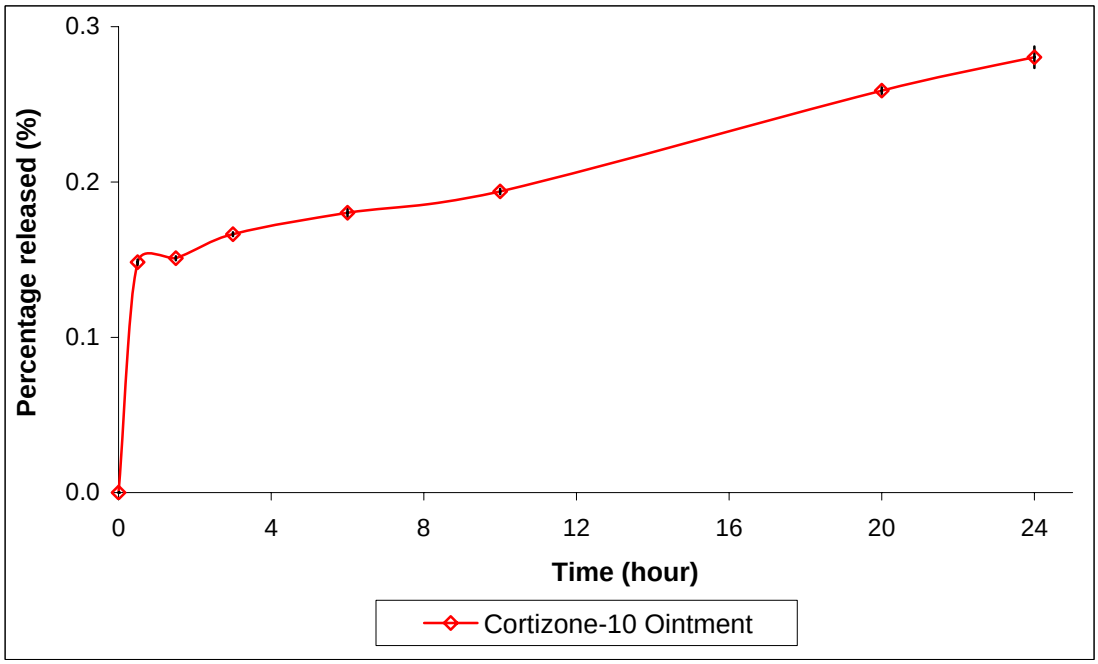

Figure 1.44. The hydrocortisone-diffusion profile of Cortizone-10 ointment through an Epiderm™ over 24 hours

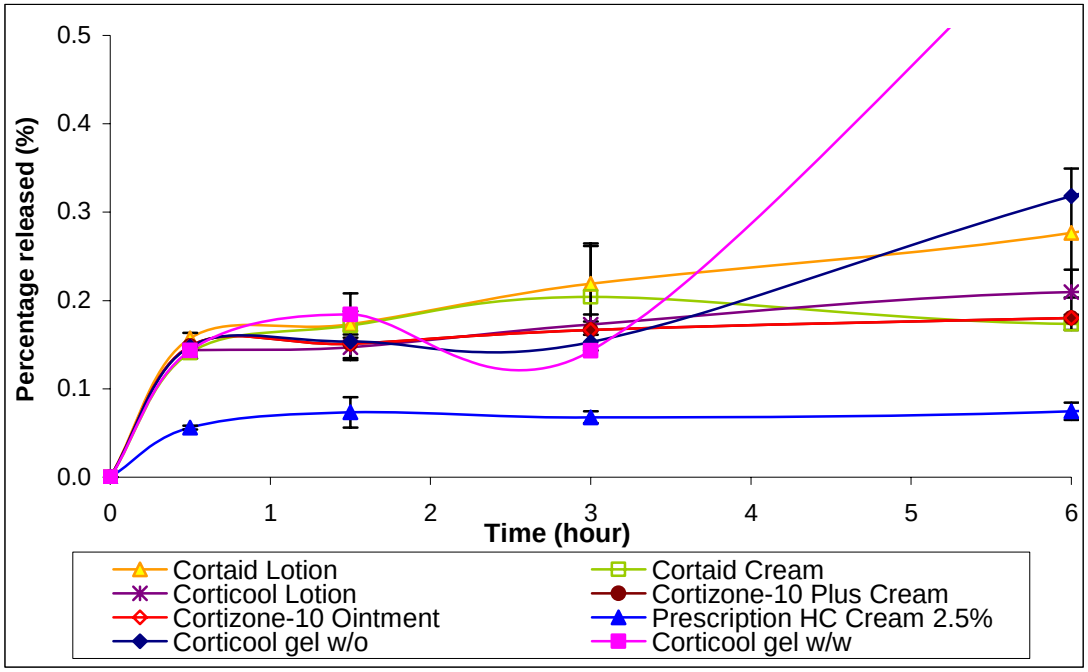

Figure 1.45: A depiction of the initial depletion phase for seven formulations that lasted for half hour

Overall diffusion rates though the synthetic membrane, mouse skin and the Epiderm™

The flux is calculated according to the amount (mg) of hydrocortisone that passes through a surface area (the square of unit measured) over a specific time period. The flux exhibits exactly the drug rate (amount/time) getting through the membrane's surface. Hydrocortisone's overall flux can be calculated by both the Fick's-law-of-diffusion model (Table 24) and the Higuchi-of-diffusion model (Table 25).

A similar rank order and pattern was observed for the extent and release rate of hydrocortisone through the three membranes: the synthetic membrane, mouse skin, and the Epiderm™. The Corticool gel (1% hydrocortisone) exhibited the highest diffusion rate through all of the membranes. The prescription hydrocortisone 2.5% cream had a higher hydrocortisone diffusion rate than the other creams and lotions, but

it was still lower than Corticool gel. The Corticool lotion did not exhibit a significant difference in its diffusion rate compared to the other formulations on the market: Cortaid cream, Cortaid lotion, Aveeno cream, and Cortizone 10 cream.

The hydrocortisone diffusion rate from the Cortizone-10 ointment and the total amount of the hydrocortisone penetration through all of the membranes were considerably less than the other topical hydrocortisone products.

Table 1.23. The flux and hydrocortisone release rates of the study samples through the three different membranes in the Franz cells derived from the Fick's-law-of-diffusion model

Formulation	Number of replication	Synthetic Membrane ($mg/cm^2/h$)	Number of replication	Mouse Skin $mg/cm^2/h$	Number of replication	EpiDerm Cultured Human Skin $mg/cm^2/h$
Cortaid Lotion	4	0.0491	3	w/o w 0.0117	3	0.00126
			5	w/w w 0.0163		
Corticool Lotion	4	0.0580	3	w/o w 0.0200	3	0.00228
			3	w/w w 0.0280		
Cortaid Cream	2	0.0224	4	w/o w 0.0304	2	0.00218
			4	w/w w 0.0213		
Cortizone-10 Plus Cream	6	0.0147	4	w/o w 0.00642	3	0.00056
			4	w/w w 0.0111		
HC Cream USP, 2.5%	7	0.0635	6	w/o w 0.0031	3	0.0066
			6	w/w w 0.0039		

Cortiszone-10 Ointment	4	0.0016	3	w/o w 0.00076	3	0.00008
			3	w/w 0.00121		
Aveeno Cream	4	0.0118	3	w/o w 0.00903		
			3	w/w 0.0021		
Corticool Gel w/o Exfoliate	10	0.2073	3	0.0744	2	0.0084
Corticool Gel w Exfoliate		-	3	0.1013	2	0.0260

Table 1.24. The flux and hydrocortisone-release rates of study samples through the three different membranes in the Franz cell, derived from Higuchi model

Formulation	Number of replication	Synthetic Membrane ($mg/cm^2/h^{1/2}$)	Number of replication	Mouse Skin $mg/cm^2/h^{1/2}$	Number of replication	EpiDerm Cultured Human Skin $mg/cm^2/h^{1/2}$
Cortaid Lotion	4	0.0884	3	w/o w 0.0019	3	0.0019
			5	w/w w 0.0026		
Corticool Lotion	4	0.093	3	w/o w 0.0054	3	0.0031
			3	w/w w 0.0037		
Cortaid Cream	2	0.0397	4	w/o w 0.00034	2	0.0032
			4	w/w w 0.0032		
Cortizone-10 Plus Cream	6	0.0275	4	w/o w 0.0011	3	0.00087
			4	w/w w 0.0026		
HC Cream USP, 2.5%	7	0.0473	6	w/o w 0.0031	3	0.0012

			6	w/w w 0.0039		
Cortiszone-10 Ointment	4	0.000279	3	w/o w 0.000159	3	0.0004
			3	w/w 0.0003		
Aveeno Cream	4	0.050	3	w/o w 0.0968		
			3	w/w 0.034		
Corticool Gel w/o Exfoliate	10	0.328 (10-20h)	3	0.127 (10-24 h)	2	0.004
Corticool Gel w Exfoliate		-	3	0.203	2	0.009

CONCLUSIONS

Several commercial pharmaceutical topical-dosage forms of HC were studied and compared. There were no significant differences in the extent and rate of drug release among the creams or lotions. However, the hydrocortisone gel released the highest percentage of the drug of all of the formulations compared. The ointment showed the smallest rate of drug diffusion.

The release profiles of the hydrocortisone from the creams, lotions, ointment and the gel through synthetic membrane, mouse skin and Epiderm^{TM} (cultured human skin cell models) were similar. The drug's diffusion rate through the synthetic membrane was rapid. In addition, the synthetic membrane does not have similar structures to that of human skin since it lacks lipids, keratin and other components that are usually seen in skin. Therefore, the synthetic membrane did not accurately predict drug diffusion through skin. The membrane can still be used for a relative comparison of drug diffusion from topical formulations. Furthermore, the calculation of permeability through adjusting the hydrocortisone solubility proved that drug-penetration enhancement is mostly affected by higher drug solubility, and the concentration gradient in the Fick's-law-of-diffusion model was the largest influence in increased hydrocortisone permeation.

Mouse skin is an abundant membrane source even though it is thinner and its physio-biological structure is not very close to human skin. For common topical formulations of hydrocortisone, the mouse skin appears to be suitable as it reflects the same pattern (not actual magnitude) of drug diffusion as does human skin.

The Epiderm™ appears to be a excellent choice for a membrane to conduct drug permeability studies in as expected *in vivo* results through human skin would have results similar to those observed *in vitro* with this model is membrane.

REFERENCES

1. Walters, K.A., *Dermatological and Transdermal Formulations*. The structure and Function of Skin, ed. M.S.R. Kenneth A. Walters. Vol. 1. 2002, New York, Basel: Marcel Dekker, Inc.
2. Kenneth A. Walters, M.S.R., *Dermatological and Transdermal Formulation*. Skin transport, ed. S.E.C. Michael Roberts, Mark A. Pellet. Vol. 4. 2002.
3. Scheuplein, R.J., *Mechanism of percutaneous adsorption. I. Routes of penetration and the influence of solubility.* J Invest Dermatol, 1965. **45**(5): p. 334-46.
4. Sweeney, T.M. and D.T. Downing, *The role of lipids in the epidermal barrier to water diffusion.* J Invest Dermatol, 1970. **55**(2): p. 135-40.
5. Elias, P.M. and D.S. Friend, *The permeability barrier in mammalian epidermis.* J Cell Biol, 1975. **65**(1): p. 180-91.
6. Albery, W.J. and J. Hadgraft, *Percutaneous absorption: theoretical description.* J Pharm Pharmacol, 1979. **31**(3): p. 129-39.
7. Elias, P.M., et al., *Percutaneous transport in relation to stratum corneum structure and lipid composition.* J Invest Dermatol, 1981. **76**(4): p. 297-301.
8. Bouwstra, J.A., et al., *The role of ceramide composition in the lipid organisation of the skin barrier.* Biochim Biophys Acta, 1999. **1419**(2): p. 127-36.
9. Ebling F.J. G., R.V.A., *Physiology, biochemistry, and molecular biology of the skin*. Hormones and hair growth, ed. R.V.A. Ebling F.J. G. Vol. 1. 1991, New York: Oxford University Press. 660-698.
10. Hueber, F., J. Wepierre, and H. Schaefer, *Role of transepidermal and transfollicular routes in percutaneous absorption of hydrocortisone and testosterone: in vivo study in the hairless rat.* Skin Pharmacol, 1992. **5**(2): p. 99-107.
11. Barry, B.W., *Penetration enhancer classification*. Percutaneous Penetration Enhancers, ed. H.I.M. Eric Wane Smith. Vol. 1. 2006: Taylor and Francis Group. 14.
12. Walters K. A., H.J., *Pharmaceutical Skin Penetration Enhancement*. Water-The most natural penetration enhancer, ed. W.M. Roberts M.S. 1993, New York: marcel Dekker. 1-30.
13. Van Hal, D.A., et al., *Structure of fully hydrated human stratum corneum: a freeze-fracture electron microscopy study.* J Invest Dermatol, 1996. **106**(1): p. 89-95.
14. Richard H. Guy, J.H., *Transdermal drug delivery*. Feasibility assessment in topical and transdermal delivery: mathematical models and *In vitro* studies, ed. J. Hadgraft. Vol. 1. 2003, New York: Marcel Dekker.
15. Martin, *Physical Pharmacy and Pharmaceutical Sciences*. 5 ed. transport pathway, ed. P.J. Sinko. Vol. 12. 2006: Lippincott Williams & Wilkins. 319-327.
16. koma A., S.M., Stander S., Yosipovitch G., Schmelz M., *The Neurobiology of Itch.* Nature Reviews Neuroscience, 2006. **7**(7): p. 535-547.

17. Janeway, C., Paul Travers, Mark Walport, Mark Shlomchik, *Immunobiology*. 2001, New York and London: Garland Science.
18. Grimbaldeston, M.A., et al., *Effect and potential immunoregulatory roles of mast cells in IgE-associated acquired immune responses.* Curr Opin Immunol, 2006. **18**(6): p. 751-60.
19. Holt, P.G. and P.D. Sly, *Th2 cytokines in the asthma late-phase response.* Lancet, 2007. **370**(9596): p. 1396-8.
20. Bledsoe, R.K., et al., *Crystal structure of the glucocorticoid receptor ligand binding domain reveals a novel mode of receptor dimerization and coactivator recognition.* Cell, 2002. **110**(1): p. 93-105.
21. Radoja, N., et al., *Novel mechanism of steroid action in skin through glucocorticoid receptor monomers.* Mol Cell Biol, 2000. **20**(12): p. 4328-39.
22. Shahin, V., et al., *Glucocorticoids remodel nuclear envelope structure and permeability.* J Cell Sci, 2005. **118**(Pt 13): p. 2881-9.
23. Schafer-Korting, M., et al., *Glucocorticoids for human skin: new aspects of the mechanism of action.* Skin Pharmacol Physiol, 2005. **18**(3): p. 103-14.
24. products, M., *Nylon membrane and net filter-specification*. 2007.
25. Wester R.C., N.P.K., *Relevance of animal models for percutanous absorption.* International Journal of Pharmaceutics, 1980. **7**: p. 99-110.
26. Scott R. C., W.M., Dugard P.H., *A comparison of the in vitro permeability properties of human and some laboratory animal skins.* International Journal of Cosmetics Sciences, 1986. **8**: p. 189-194.
27. Sato, K., K. Sugibayashi, and Y. Morimoto, *Species differences in percutaneous absorption of nicorandil.* J Pharm Sci, 1991. **80**(2): p. 104-7.
28. Mattek corp., *Epiderm™ skin model.* http://www.mattek.com/pages/products/epiderm.
29. Brinkmann, I. and C.C. Muller-Goymann, *Role of isopropyl myristate, isopropyl alcohol and a combination of both in hydrocortisone permeation across the human stratum corneum.* Skin Pharmacol Appl Skin Physiol, 2003. **16**(6): p. 393-404.
30. Bamba, F.L. and J. Wepierre, *Role of the appendageal pathway in the percutaneous absorption of pyridostigmine bromide in various vehicles.* Eur J Drug Metab Pharmacokinet, 1993. **18**(4): p. 339-48.

CHAPTER 2

PREPARING ORALLY DISINTEGRATING TABLETS OF MELATONIN AND ACETAMINOPHEN

Hang Le, James W. Ayres, John Mark Christensen

ABSTRACT

Orally disintegrating tablets are a dosage form that has a promising market thanks to its ease of patient use and modern technology for production that reduces the price.

The study aimed at preparing oral disintegrating tablets of melatonin and fast - disintegrating tablets containing sustained release beads of acetaminophen. A range of excipients: superdisintegrants, amino acids, sweeteners, flavors, low-temperature melting fats… were investigated. A combination of excipients that reduce the disintegrating time of a tablet can produce an oral disintegrating tablet with acceptable hardness and friability. The small amount of melatonin in each tablet does not affect the physical properties of the tablet.

Therefore the orally disintegrating tablet of acetaminophen is very promising in pediatrics. A pressure of 3500 lbs is needed to obtain an adequate friability, and hardness when putting sustained release beads of acetaminophen into the tablet.

Acetaminophen is a common medicine for children. The beads in the tablet with a hydrophilic polymer in them as the sealing agent sin subcoat can protect the beads and maintain the sustained drug release characteristics of the beads. The addition of sweeteners, flavors, and modification of the taste masking layer of the sustained release beads improved the taste sensation of the tablet.

INTRODUCTION

MELATONIN

Chemical structure

Systematic (IUPAC) name *N*-dic
ethanamide

Melatonin, 5-methoxy-*N*-acetyltryptamine, formula $\mathbf{C_{13}H_{16}N_2O_2}$ Mol. mass 232.278 g/mol, is a ubiquitous hormone found in all living creatures from algae [1] to humans, at levels that vary in a daily cycle. It plays a role in the regulation of the circadian rhythm of several biological functions [2]. Many biological effects of melatonin are produced through activation of melatonin receptors [3] while others are due to its role as a pervasive and extremely powerful antioxidant [4] with a particular role in the protection of nuclear and mitochondrial DNA [5, 6]. In mammals and humans, melatonin is produced from pinealocytes in the pineal glands, retina lens, and GI tract.

Melatonin is used as a supplement for blind children, autism, and epilepsy patients [7, 8]. Products containing either or both of isolated or synthesized melatonin have been available as a health supplement in the United States since 1993.

Physicochemical properties

Melatonin comes in a crystal form and it is freely soluble in water. A solution of melatonin should be sterile as it is consumed by microorganisms. A solution of melatonin is stable at 4^0C for 6 months [9].

Pharmacokinetics

Pharmacokinetics of melatonin in children is significantly different from adults. Pre-pubertal children have a higher elimination-rate constant (1.08 h^{-1}) compared to adults' elimination-rate constant (0.89 hr^{-1}) with half lives of 0.67 hours and 0.79 hours, respectively [10]. Melatonin's half life is longer in cirrhotic patients [11]. Melatonin is considered an endogenous hormone in the body and in many mammalian animals and is metabolized as such in the body.

Roles in humans

Circadian rhythm

Melatonin is known as one of the regulators involved in drowsiness.
The secretion of melatonin by the pineal gland is "light dependent". Light inhibits melatonin production and conversely, darkness stimulates melatonin's secretion affecting a daily rhythm of melatonin levels.

Immune system

The presence of melatonin increases the tumor necrosis factor-alpha (TNF-alpha) and some interleukins (IL2, IL4, IL5) providing support for the theory of a putative immune-pineal axis [12, 13].

ACETAMINOPHEN

Chemical structure

Paracetamol (/pærə'sitəmɒl, -□sɛtə-/) or **acetaminophen**, is the active metabolite of phenacetin, a so-called coal tar analgesic. Unlike phenacetin, paracetamol has not been shown to be a carcinogenic in any way. It has analgesic and antipyretic properties. Paracetamol, unlike other common analgesics such as aspirin and ibuprofen, has relatively little anti-inflammatory activity, and it is not a very effective anti-inflammatory agent. As a result, it is *not* considered to be a non-steroidal anti-inflammatory drug (NSAID).

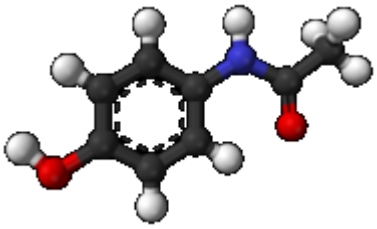

Systematic (IUPAC) name *N*-(4-hydroxyphenyl)acetamide

Physicochemical properties

Paracetamol consists of a benzene ring core, substituted by one hydroxyl group and the nitrogen atom of an amide group in the *para* (1,4) position. The amide group is an acetamide (ethanamide). It is an extensively conjugated system; as the electron of the hydroxyl oxygen, the benzene pi-cloud electrons, the nitrogen ione-electron pair, the p orbital on the carbonyl carbon, and the lone pair on the carbonyl oxygen are all conjugated. The presence of two activating groups also makes the benzene ring highly reactive toward electrophilic aromatic substitution. As the substituents are ortho, para-directing and para with respect to each other, all positions on the ring are more or less equally activated. The conjugation also greatly reduces the basicity of the oxygens and

the nitrogen, while making the hydroxyl acidic through the delocalization of the charge developed on the phenoxide anion.

Some other important chsracteristics about acetaminophen are the following:

Melting point: 169^{o}C

Solubility in water: 0.1-0.5 g/100 mL (20 °C)

Acetaminophen is stable in water.

Mechanism of action

Paracetamol reduces the production of prostaglandins. It has been shown that paracetamol reduces the oxidized form of the COX enzyme, preventing it from forming pro-inflammatory chemicals.[14-16]

Another possible mechanism of acetaminophen is that paracetamol also modulates the endogenous cannabinoid system[17]. Paracetamol is metabolized to AM404, a compound with several actions: the most important thing is that it inhibits the uptake of the endogenous cannabinoid/vanilloid anandamide by neurons. Anandamide uptake would result in the activation of the main pain receptor (nociceptor) of the body, the TRPV1 (older name: vanilloid receptor). Furthermore, AM404 inhibits the sodium channels in a manner similar to that of anesthetics such as lidocaine and procaine[18].

Metabolism

Paracetamol is metabolized primarily in the liver by conjugation resulting in glucuronides and sulfate conjugates, which are excreted by the kidneys. Only a small portion is metabolized via the hepatic cytochrome P450 enzyme system (its CYP2E1

and CYP1A2 isoenzymes), which is responsible for the toxic effects of paracetamol due to a minor alkylating metabolite (*N*-acetyl-*p*-benzo-quinone imine, abbreviated as NAPQI)[19] .

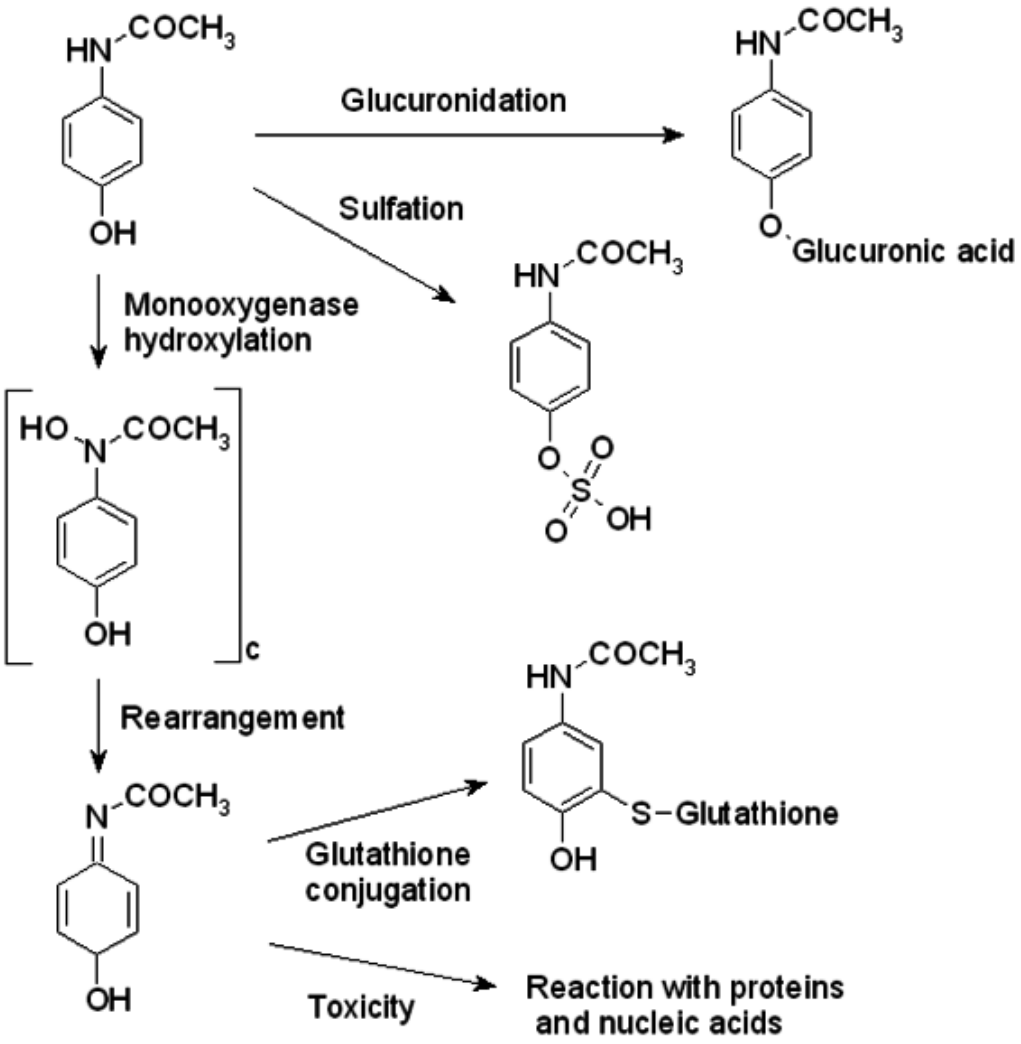

Figure 2.1. Metabolism pathway of acetaminophen in human body
(http://en.wikipedia.org/wiki/Paracetamol)

The toxicity of acetaminophen is dose-dependent and is related to glutathione depletion in the liver at high doses of acetaminophen [20].

Pharmacokinetics and metabolism of acetaminophen also are age-dependent. In children the major pathway for acetaminophen metabolism is sulfation. This pathway proceeds faster compared to glucuronidation that is the dominant metabolic pathway in adults. Sulfation conjugation is fast, and the drug residue for oxidation by cytochrome systems is small. Thus, it reduces the toxicity in children compared to adults [21] .

Pharmacokinetics

Paracetamol is a popular medicine, and there are many studies that have investigated the pharmacokinetics of acetaminophen in adults, children, patients and normal subjects. After oral and intravenous administration of acetaminophen, the drug appears to follow a two-compartmental open model. Acetaminophen's half-life is 2-3 hour when the plasma concentration resides in the treatment-dose range with a volume of distribution of about 0.8-1L/kg [22]. An IV bolus of acetaminophen can be described by a two-compartmental open model; whereas, the plasma concentrations after oral administration may follow a one-compartmental open model [22, 23].

There is no difference in pharmacokinetics in children, adults, and febrile children [24-26]. Another study of acetaminophen in Japanese persons shows that sulfation and glucuronidation occur at the same rate and extent as in Caucasian populations, and the acetaminophen metabolism is similar in both populations [27].

Acetaminophen is considered safe and when given at the standard treatment dose, it can be used with many drugs without any interaction. Concurrent use of acetaminophen with a common vaccine, influenza for example, is not a concern [28] . Pentazocine and diclofenac also do not interact with acetaminophen[29, 30] .

Roger H. Rumble et al. found that acetaminophen is absorbed faster in ambulatory subjects than in supine subjects, but the volume of distribution does not change [31]. No significant differences in half-life were observed between obese, exercise, anephric patients, and normal subjects [32-34]. Bowel irrigation reduced acetaminophen concentrations, but the reduction was not statistically significant [35].

Rectal administration is a common route of acetaminophen administration in children. The bioavailability of rectal dosage forms ranges from 0.24 to 0.98 with the average value being 0.52 [36]. Water-based (PEG) excipients will facilitate better rectal acetaminophen absorption [37]. The absorption process by rectal route is slow and follows a one-compartmental open model [38]. By investigating rectally-administered acetaminophen in neonates, Richard A. et al. reported that acetaminophen absorption varied and drug plasma concentrations were higher in boys than in girls [39].

FITTING A SUSTAINED RELEASED PROFILE

If the drug releases from an immediate-release dosage form, the amount of the drug available for absorption at time zero, is large, it will reduce according to time. The appropriate model fitting this process is first-order kinetics:

$$\frac{M_t}{M_\infty} = ke^{-\alpha t} + L$$

M_t is the amount of drug releases at time t

M_∞ is the amount of drug release to infinity

k is the coefficient constant

α is the release constant rate

For coated pellets, if the coating layer is complete, the drug should follow Fick's -law of diffusion, and the drug release may follow zero order kinetics [40, 41].

If during the drug release a sink condition exists ($C_r << C_d$), the diffusion-boundary layer (h) is constant, the surface areas of the beads remain constant, and C_d is the saturated solubility of the drug, then we have:

$$J = \frac{dM}{Sdt} = D\left(\frac{C_1 - C_2}{h}\right)$$

$$J = -D\frac{dC}{dx}$$

$$\frac{dM}{dt} = \frac{DSK(C_d - C_r)}{h}$$

$$P = \frac{DK}{h}$$

$$J = PSC_d$$

J: Flux
M: Amount of drug
S: Area unit cross section
t: Time
D: Diffusion coefficient
P: Permeability
K: Partition Coefficient

The equation for zero-order kinetics is:

$$\frac{M_t}{M_\infty} = kt + L$$

M_t is the amount of drug releases at time t

M_∞ is the amount of drug release to infinity

k is the coefficient constant

If the drug is deposited in a granular matrix, Higuchi divided the drug release process from a matrix to surrounding environment into two separate processes: The Drug diffuses from the inner matrix to the surface of the matrix and then from the surface of matrix through the membrane [41].

The equation to describe that process is:

$$\frac{M_t}{M_\infty} = kt^{1/2}$$

M_t is the amount of drug releases at time t

M_∞ is the amount of drug release to infinity

k is the coefficient constant

When the coating process is not complete, the dissolution and release of drug is a complicated process, which is a multi-mechanistic combination [40, 42].

Korsmeyer et al. recommended the use of the power law as the general model for drug release [43]:

$$\frac{M_t}{M_\infty} = kt^n$$

$0 < n < 1$

M_t is the amount of drug releases at time t

M_∞ is the amount of drug release to infinity

k is the coefficient constant

n=1/2, we have Higuchi model

E. Rinaki simulated the drug release from the matrix tablets and found that the power law can be used to describe the entire drug release curve [44].

Peppas, N.A., Sahlin used a dual model to describe drug dissolution profiles [45]:

$$\frac{M_t}{M_\infty} = k_1 t^m + k_2 t^{2m}$$

M_t is the amount of drug releases at time t

M_∞ is the amount of drug release to infinity

k is the coefficient constant

m is the exponential integer

Hixson-Crowell model [46]:

The Hixson-Crowell cube root model is used when the dosage-form dimension diminishes proportionally in such a manner that the geometric shape of the dosage form stays constant as dissolution is occurring; then dissolution occurs in planes that are parallel to the dosage form surface. While the diameter of dosage form (particles, tablets) reduces gradually with a constant rate, the ratio of the amount of drug releases follows a cubic exponential.

$$\frac{M_t}{M_\infty} = 1 - (1 - kt)^3$$

M_t is the amount of drug releases at time t

M_∞ is the amount of drug release to infinity

k is the coefficient constant

The Akaike information criterion and the Bayesian information criterion for the best fitted model

The Akaike information criterion (AIC) or Bayesian information criterion (BIC) are used to select the best fitted model and avoid an over-fitting procedure [47]. In this study, AIC and BIC is used to find the best fitted model for dissolution profiles.

AIC definition: $AIC = 2k - 2\ln(L)$

Where k is the number of parameters in the statistical model and L is the likelihood function.

As regard to residual sums of squares AIC becomes

$$AIC = 2k + [\ln(2\pi RSS / n) + 1]$$

BIC definition: $BIC = -2\ln(L) + k\ln(n)$

While calculating the residual sum of the square, the BIC becomes

$$BIC = n\ln(\frac{RSS}{n}) + k\ln(n)$$

SUSTAINED-RELEASE-DOSAGE FORM

USP divides tablets into three smaller categories: Conventional, delayed-release, and extended-release tablets [48]. Conventional tablets can be divided into smaller subgroups: chewable, molded, compressed, and coated tablets. Thus, the extended-release tabets, sustained release tablets, the prolonged-action tablets, and repeat-action tablets are included in the terminology for this dosage form.

USP defines that “extended-release tablets are formulated in such a manner as to make the contained medicament available over an extended period of time following ingestion”.

Controlled release drug dosage forms are “therapeutic systems” in which the rate of drug release is programmed and controlled through the design of the product formulation for specific treatment targets. This means the drug release kinetics are predictable and reproducible. Controlled drug release dosage forms have become popular, modern therapeutic drug delivery systems.

“Sustained release” is a narrow concept in the overall area of controlled drug release, which provides many advantages. First, sustained-drug-release dosage forms increase therapeutic efficiency. It is well documented that most drugs have a relatively stable therapeutic window (1); the concentration range in which the pharmacologic response is reasonably effective, and toxicity is at an acceptable low level. More clearly, within this therapeutic window, the toxicity index is reasonably low and the drug produces convincing clinical effects. The range of safe concentrations for a model drug is illustrated in Figure 2.2.

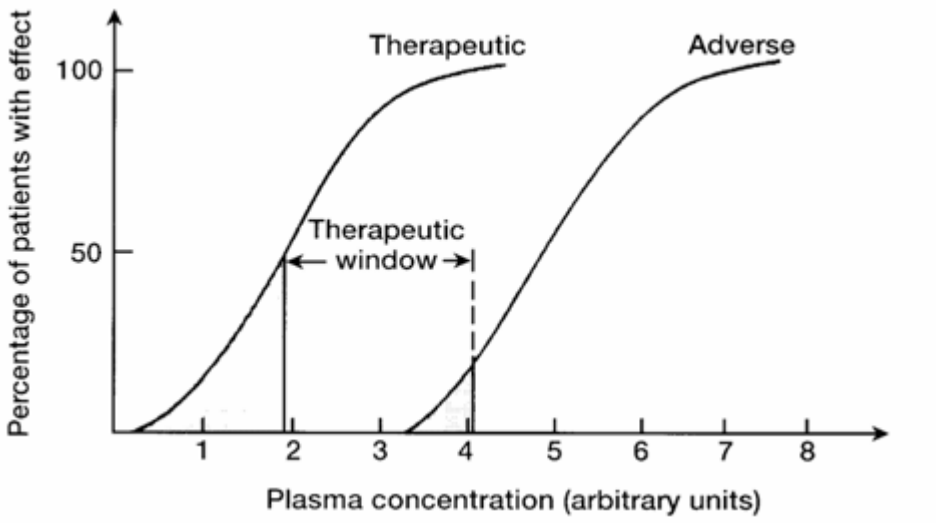

Figure 2.2. Relationship of incidence of toxicity and plasma concentration [49]

When the drug is administered into the body, plasma (and usually tissue) concentrations rise and then drop gradually with time. The dosing regimen chosen is a compromise between toxicity and effectiveness.

By keeping the plasma concentration of the drug within the therapeutic window, a sustained-release-dosage form may be more beneficial in treatment. Second, sustained-release-dosage forms bring more convenience to patients as the interval of the drug dosing can be lengthened, reducing the number of doses to be given. For some drugs, i.e. drugs treating hypertension, it is desirable to produce the maximum plasma concentration of the drug in the morning. If a sustained release dosage form with an appropriate lag time before the drug absorption begins is taken in the evening, the formulation may allow drug plasma concentrations to reach their maximum value in the morning.

Common oral sustained release dosage forms

One of the main objectives of our study is to prepare sustained release beads of acetaminophen residing inside a fast disintegrating tablet. The sustained beads belong to the category of sustained release dosage forms. The most common sustained release dosage forms are:

***Matrix Devices*:** The matrix is made up of single or multiple layers of the drug and a polymer. The unit of the matrix can be the pellets or the tablets. The dissolution of the drug into the outer medium may include mostly several mechanisms: swelling, erosion, and diffusion of the drug[50]. Using a biodegradable pH-dependent polymer is a promising method to prepare delayed or targeted-drug delivery dosage forms such as enteric and colon-targeting matrix tablets [51]. A delicate modification of the matrix

sustained-release-dosage form can lead to a desirable drug release such as a zero-order release of the drug from the dosage form [52].

Osmotically Controlled Systems: In this system, osmotic pressure provides the driving force for the drug's flow out of the tablet [53]. The system contains a semi-impermeable membrane. This membrane is permeable to water but not to the drug. Water penetrates into the tablet and dissolves the electrolytes or drug inside the device. The dissolution of the materials inside the device creates osmotic pressure; this force pushes the drug out of the device through a laser-drilled hole. The system can have one or several holes to release the drug. This system's advantage is that the osmotic driving force does not depend on the environment, and the drug release is not influenced by external forces such as GI pH, drug solubility, etc.

Ion-Exchange systems: Ion exchange drug delivery systems are generally used with resins composed of water-insoluble cross-linked polymers. The mechanism is very similar to ion exchange that occurrs in chromatographic column.

$$RESIN^{+} - DRUG + X^{-} \rightarrow RESIN^{+} - X^{-} + Drug^{-}$$
$$RESIN^{-} - DRUG + Y^{+} \rightarrow RESIN^{-} - Y^{+} + Drug^{+}$$

X^- and Y^- are ions in the GI tract. The freed drug then diffuses out of the resin slowly and creates the extended-release action [53].

Coated systems: Coating is a technique used to prepare sustained release beads of acetaminophen in this study.

Coating is a popular technique in preparing sustained-release dosage forms. It has been used for a long time and was originally used to mask the taste of a drug; it was probably first used for this purpose 1000 years ago. At present, coating is used for the following purposes:

To create controlled release properties

To maintain the physical integrity of the dosage form

To protect active pharmaceutical ingredients

To improve the appearance of the dosage form and mask the unpleasant taste

Coating equipment:

Pan coating usually is the technique using in both the hot-melt coating method and the film-coating, as well. The conventional pan is sub-globular with an opening in front for loading materials and for air flowing in and out. The pan normally tilts around 45^{o} with 25-40 rotations per minute. There have been modifications of the conventional coating pan as seen in Pellgrini, Hi-Coater, Accela-Cota, driacoater. The main improvements include: inlet and outlet air flow from perforated walls and atomized spraying nozzles (both nozzle position and the spraying rate).

Fluid-bed-spray coating**:** Fluidized beds, patented by Wurster is a widely used coating process [53-56]. The basic idea of this technique is that tablets or pellets are suspended by an upward stream of air. The heater in combination with the air flow in and out of the chamber dries the surface of the core beads or tablets quickly reducing agglomeration. The apparatus shown is a bottom-spray coater [57], but top-spray coating and tangential-spray coating machines are also available [58].

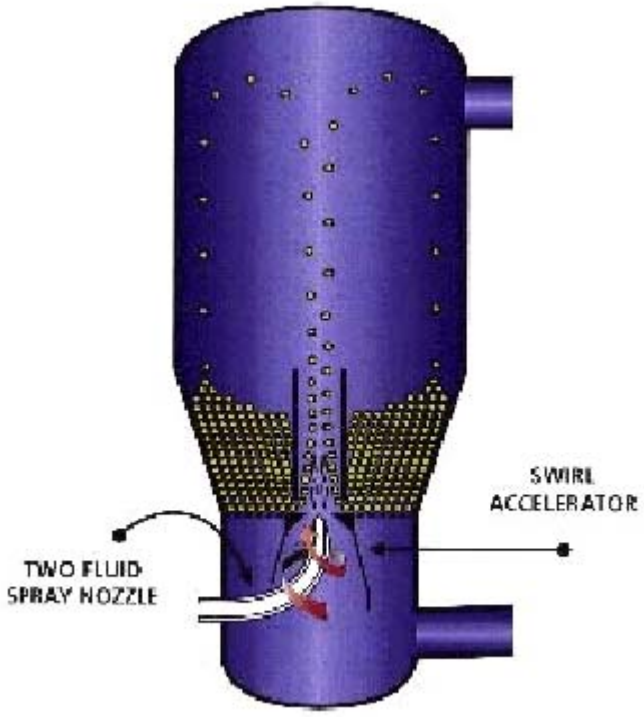

Figure 2.3. Bottom fluid-bed spray coater

Common coating agents for spray coating

Ethylcellulose (EC)

Ethyl cellulose is most widely used as a coating agent.

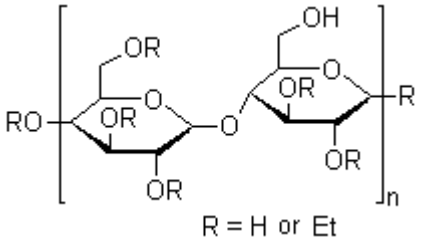

CAS: Cellulose ethyl ether [9004-57-3]

Ethyl cellulose is cellulose with varying degrees of ethoxyl substitution. EC is used as coating agent, binder, filler, and viscosity-increasing agent. Dispersions of

ethyl cellulose in water are popular for coating since the Clean Air Act calls for a reduction of volatile organic solvents emitted into the air [59].

Polymethacrylates

USP defines methacrylic acid copolymer as a fully polymerized copolymer of methacrylic acid and an acrylic or methacrylic ester. The polymer is biodegradable. In water, ester groups are hydrolyzed.

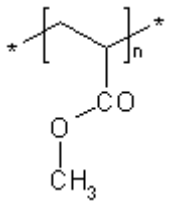

The substitution with different groups creating the ester linkage produces various categories of polymers. Each category is sensitive to a pH range. Based on pH-dependent properties, the formulators can select the appropriate polymers.

ORALLY DISINTEGRATING TABLETS (ODTs)

The orally disintegrating dosage form, ODT, has become more popular due to the market demand. Not only elderly people, small children, and in-bed patients but also healthy subjects prefer taking ODT [60].

In the Guidance for Industry, the FDA defines an orally disintegrating tablet as the following [61]:

A solid dosage form containing medicinal substances which disintegrates rapidly, usually within a matter of seconds when placed upon the tongue.

CDER also recommends that, *in addition to the original definition, ODTs be considered solid oral preparations that disintegrate rapidly in the oral cavity with an in vitro disintegration time of approximately 30 seconds or less, when based on the United States Pharmacopeia (USP) disintegration test method or alternative.*

…tablets that take longer than 30 seconds to disintegrate or are dosed with liquids may be more appropriately considered to be chewable or oral tablets.

The term fast-disintegrating, fast-melt, rapid-disintegrating and orally disintegrating tablet indicates the same dosage form.

According to Srikonda V. Sastry and Janakiram Nyshadham [62] and William R. [63], in general ODT brings to patients many benefits such as:

Clinical:

Improved drug absorption

Fast onset of action (headache, Parkinson)

Enhancing bioavailability

Minimized first-pass effect

Medical:

Better fed to patients than swallowing or chewing the dosage form

Better taste, no need to take with water

Improved safety and efficacy

Improved compliance

Currently, on the market, there are more than fifteen ODT products that are available [63]. The early ODTs had drawbacks. Initial poor-taste-masking ability limited the number of active pharmaceutical ingredients that could be used in ODTs; freeze-dried ODT's requires special packing and storage conditions creating a huge inconvenience for the general population and pushing the cost of ODT's out of the affordable range[64].

Popular methods for providing ODTs are listed by Fu Y. et al.: lyophylization, molding, sublimation, and compaction[65]. However, William R. added floss-based tableting technology [63, 66, 67]. Mesut et al. discovered a simple but effective way to prepare an orally-disintegrating capsule. By applying vacuum-drying to hard gelatin capsules, the capsules will absorb water rapidly and dissolve in water much faster than conventional capsules [68].

ODT's by conventional compressing

The convention-compression process to produce ODTs is a low-cost method that does not need special equipment, using a common combination of materials such as high-compressible polysaccharides (maltose, sorbitol, trehalose,maltitol, fructose) as binders with low-compressible polysaccharides (mannitol, maltodextrin, lactose, glucose, sucrose, erythritol), for superdisintegrants, and effervescent substances to facilitate rapid disintegration [67, 69].

Freeze-dried tablet

In this process, water inside the tablet is removed at a very low temperature under vacuum. Sublimation occurs when the water changes from the solid phase into vapor without passing through the liquid form. No heat treatment protects the drug or

proteins (vaccine) from degradation. The tablets prepared by the freeze-drying method are porous and hygroscopic. They disintegrate very rapidly in water. However, this is a high cost method, which needs packaging and storage conditions limiting the feasible marketing.

Floss-based compressing tablet

Polysaccharides such as sucrose, dextrose, lactose, fructose will create floss while undergoing quick heating to flash-melting under centrifugal force. The floss is fiber-like and can be used as a disintegrant in compressed tablets [62].

Rationales to develop orally disintegrating tablets

Melatonin is consumed widely as a medicine especially for autic and blind children. In the elderly, melatonin is used as natural sleeping aid. Orally disintegrating tablets would be much more convenient for such vulnerable subjects.

ODT of melatonin would be a promising product since not only patients prefer using ODTs but also healthy subjects use melatonin as a supplement.

Rationales to develop a sustained-release tabletof acetaminophen

Gwen M. Jantzen and Joseph R. Robinson [53] emphasize that to prepare a sustained-release dosage form, the drug should have a reasonable half life, usually shorter than 2 hours. A drug with a half-life longer than 8 hours is not appropriate for a sustained-release dosage form.

The area in the GI tract where the drug is absorbed also is a factor to which formulators need to pay attention. Drugs with an absorption window in the upper GI tract that is placed in a sustained-released dosage form may limit the absorption of the

drug by releasing the drug too slowly in the GI area it is absorbed and the dosage form may travel out of the absorption area of the drug without ample absorption of drug occurring. Gastric retention dosage forms could be a dosage form choice to overcome the drug's narrow absorption window of GI tract but none have been developed and marketed that work well [70].

As mentioned above, acetaminophen is stable in the GI tract. It has pretty short half-life, and it is absorbed well up to Ileum. In the colon, the fraction absorbed is lower but still very significant [36].

With regard to the dose size, 500mg of acetaminophen is administered to adults. A reasonable dose size for a sustained release dosage form is 500mg to 1000mg [71]. A double-dose size with an 8 hour extended-release is reasonable. On the market, there are many generic dosage forms of acetaminophen. The familiar product, Tylenol sustained-release lasts up to 8 hours [72].

The purpose of this study is to prepare the following: 1. a rapid disintegrating tablet for melatonin. 2. a rapid disintegrating tablet for acetaminophen that has been encapsulated in sustained-releases beads, wherein the sustained release properties of the beads containing acetaminophen is retained after tablet compression and disintegration in biological fluids.

MATERIALS AND METHODS

MATERIALS

Drug

Acetaminophen crystal form, 4-Acetamidophenol 98%, is from Acros Organics, lot: A017891801

Saccharides

D-Mannitol: A common monosaccharide. Powder and granule from Fisher Chemical Inc., Lot: 050176

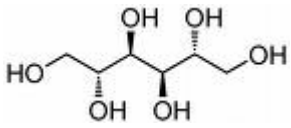

D(-)-Fructose: monosaccharide from Acros Organics lot: A0232221

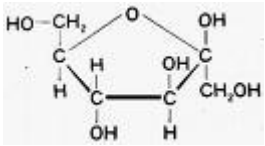

Maltose: Disaccharide, powder from Fisher Chemical Inc., Lot: AD-6017

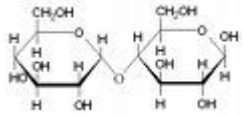

D-Sorbitol: powder from Acros Organics lot: A0204571001

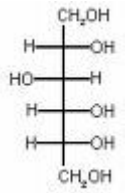

Sucrose: Disaccharide

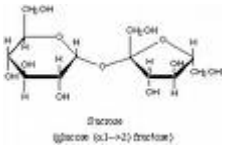

Sucralose:Disaccharides, from Fisher Chemical Inc.

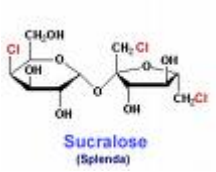

Aspartame: from Fisher Chemical Inc.

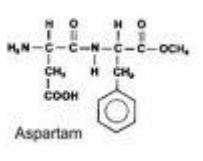

Saccharin: from Fisher Chemical Inc. Lot: B6956

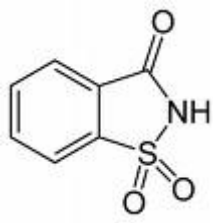

Superdisintegrants

Amberlite^{TM} IRP88: Polacrilin Potassium NF, from Rohm and Haas, lot: 0001574532

This resin is a cross-linked polymer of methacrylic acid and divinylbenzene, supplied as potassium salt.

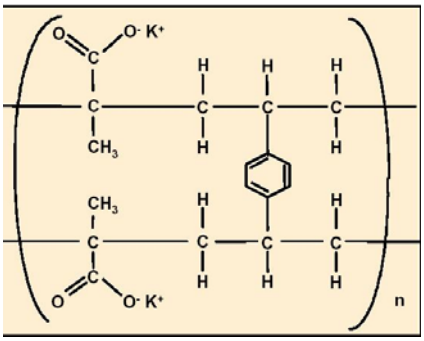

Croscarmellose Sodium, from Spectrum Chemical Mfg. Corp., lot: PA0436

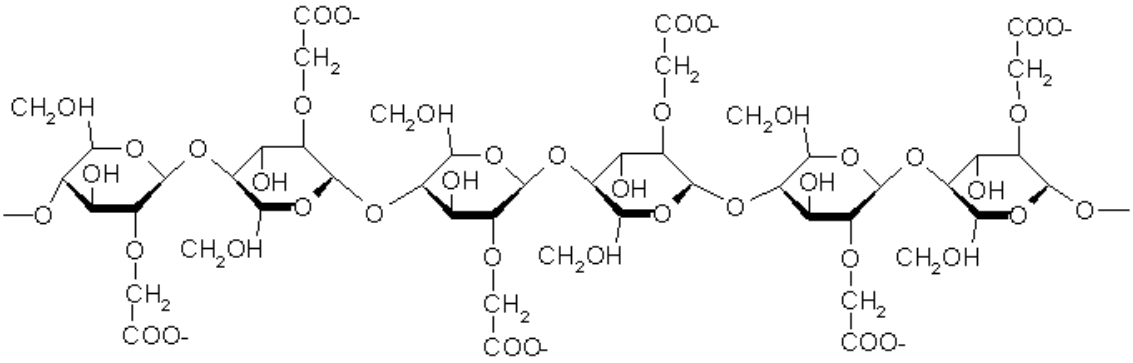

carboxymethyl cellulose sodium

Cross-linked polymers of carboxymethyl cellulose sodium

Polyplasdone® XL: Crospovidone NF, Cross-linked Polyvinylpyrrolidone, lot: 03300089744

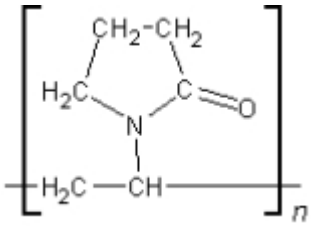

povidone

Crospovidone is a cross-linked polymer of povidone. Crospovidone is a water-insoluble tablet disintegrant. It is white to creamy-white, finely divided; free flowing, practically tasteless, odorless, and hygroscopic.

Emcosoy®: Natural superdisintegrants, soy polysaccharides, free sample from JRS Pharma

Explotab low pH: sodium starch glycolate, lot: E9631X

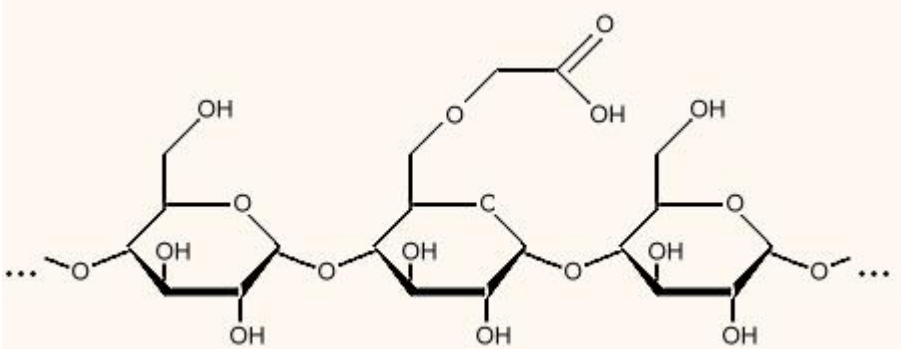

The polymer is a white or off white, odorless, tasteless, free flowing powder. It consists of oval or spherical granules.

Lubricant: Pruv Sodium Stearyl fumarate NF, from Mendell, lot 2 12-01
The polymer is a fine, white powder, with agglomerates of flat, circular-shaped particles.

Coating agent polymers and fillers

Polyox™ WSR N80 NF, from Dow Chemical Company lot: SJ0755S514

Methocel E5, hydroxypropyl methylcellulose, lot: 0A4013N22

Methocel E15, hydroxypropyl methylcellulose, lot: TK27012N22

Hydroxyproxyl methylcellulose is a partialy O-methylated and O-(2-hydroxypropylated) cellulose [73].

Structure molecule:

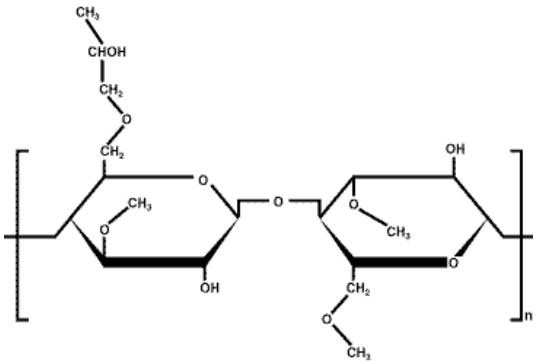

The HPMC can be divided according to viscosity. E5 has viscosity 4-6 mPas, E15 12-18mPas.

Surelease® :(Ethyl cellulose) aqueous suspension from Colorcon Inc.

Polywax: Emulsifying wax, is a preparation of higher fatty alcohols and represents an emulsified of self-bodying type. Polywax is from Croda Inc.

Avicel pH 102: Cellulose, microcrystalline from FMC Biopolymer

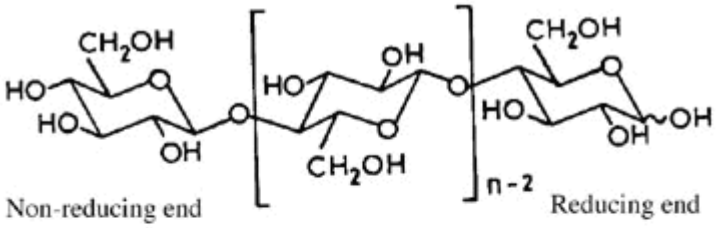

Sometimes shown as

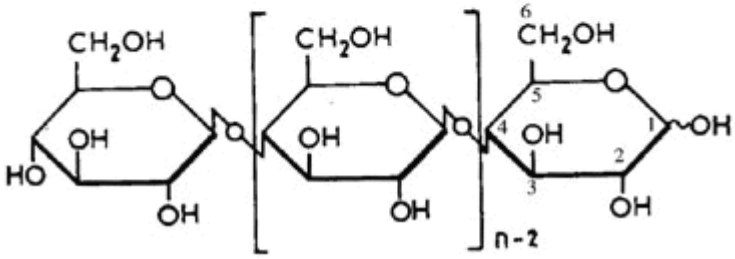

Used as a binder in the wetting-granulation method and as a disintegrating agent in the direct compression method of making tablets.

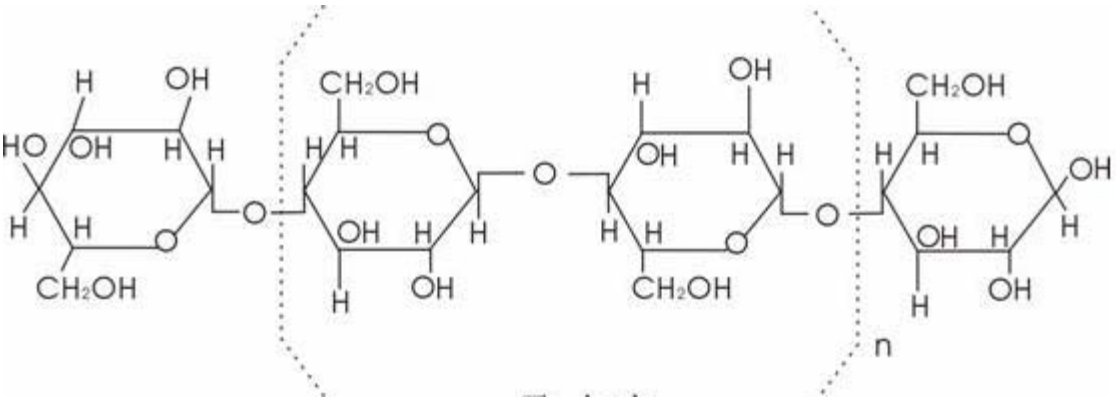

Kollicoat IR: Polyvinyl alcohol-polyethylene glycol graft copolymer. It has a low viscosity in water, and dissolves quickly in water.

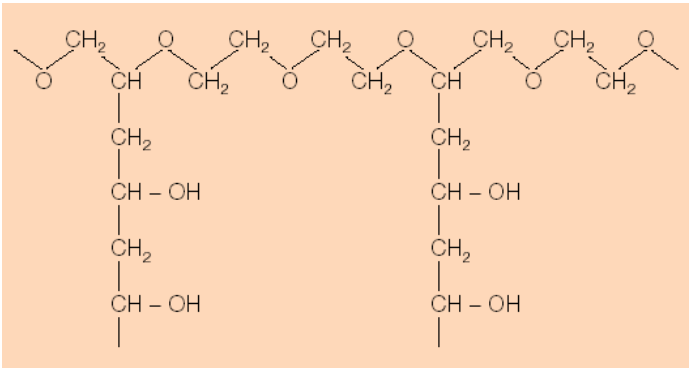

Stearic acid: Stearic acid is from Spectrum

USP[48] states that stearic acid is a mixture of stearic acid ($C_{18}H_{36}O_2$) and palmitic acid ($C_{16}H_{32}O_2$). Stearic is not less than 40%, and the sum of two acids is not less than 90.0%.

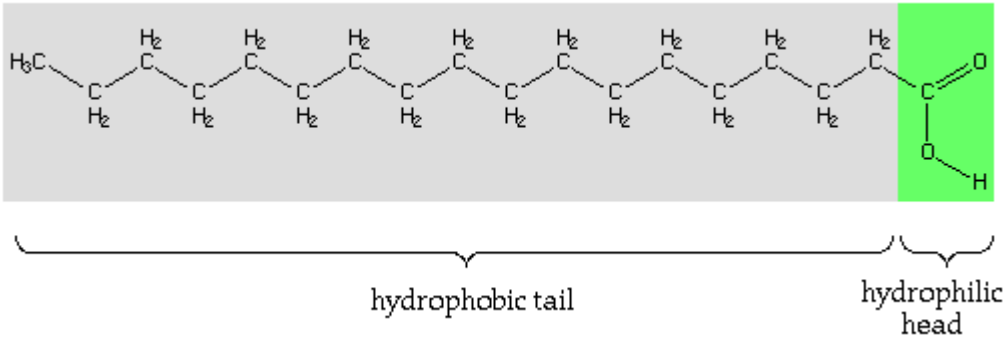

Amino acids

Glycine, from J.T. Baker, lot: H46715

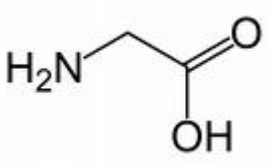

Glycine is the simplest amino acid. It freely dissolves in water and glycine, and it is used in pharmaceuticals as a sweetener and taste enhancer.

DL-Tryptophan, from J.T. Baker, lot: 928375

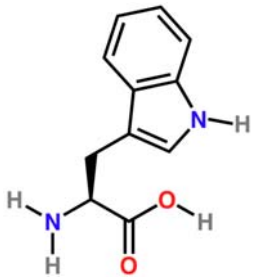

Tryptophan is one of the 20 standard amino acids, as well as an essential amino acid in the human diet.

L-Alanin, from J.T. Baker

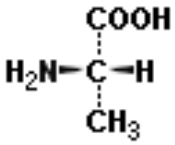

L-alanin dissolves in water (127.3g/l at 0^{o}C), is one of the 20 proteinogenic amino acids. It is a colorless crystal with a melting point of 314^{o}C.

L-Lysine hydrochloride from MP Biomedicals, Inc., lot: R20798. L-Lysine is crystalline in nature and soluble in water

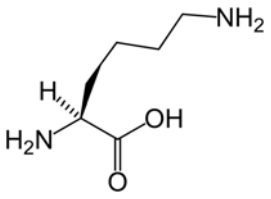

.HCl

L-Asparagine, from Sigma, lot: 121H5608. Asparagine is one of the 20 most common natural amino acids on Earth. It has carboxamide as the side chain's functional group. It is considered a non-essential amino acid. L-Asparagine is soluble in water, The substance is white crystalline powder, and freely soluble in water.

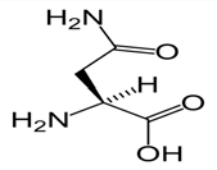

Flavors: A range of oil-based flavors and powder flavors were added to the tablets

Oil-based flavors: Orange, strawberry, from Spectrum

Powder flavors: Cherry, Apple, raspberry, spearmint from Spectrum

Low- melting fatty material:

Cocoa butter NF (β crystal form), from Spectrum, lot: PH0933. Cocoa butter is a pale-yellow, edible natural vegetable fat extracted from the cacao bean. The most common form of Cocoa butter has a melting point of around 34 to 38 degrees Celsius (93 to 100 degrees Fahrenheit), rendering chocolate a solid at room temperature that readily melts once inside the mouth. Cocoa butter displays polymorphism, having α, γ, β', and β crystals, with melting points of 17, 23, 26, and 35–37 °C respectively. The production of chocolate typically uses only the β crystal for its high melting point. A uniform crystal structure will result in smooth texture, sheen, and snap. Overheating

cocoa butter converts the structure to a less stable form that melts below room temperature. Given time, it will naturally return to the most stable β crystal form.

Gelucire 39/01: Gelucire 39/01 is glycerol esters of saturated C12-C18 fatty acids. The melting point is 39^{o}C. Gelucire are saturated polyglycolyzed glycerides that are obtained by polyglycosis of natural hydrogenated vegetable oils with polyethylene glycols (PEG). They are composed of a well-defined mixture of mono-, di- and tri-glycerides and fatty-acid esters.

APPARATUS

Extruder: Caleva, model: Exd 25

Spheronizer: Caleva, model: 120SPH

Friability tester: Vanderkamp Industrial Inc., model: 10809

Dissolution machine: model: VK7000 with auto sampler VK 8000

Spectrophotometer: Beckman DU 640

Bottom spray coater: Niro model Strea 1

METHODS

Preparing the core beads

The method of preparing core beads was as follows: The core beads contained acetaminophen, Polyox^{TM} WSR N80, Stearic acid, avicel pH 102 and are all displayed in Figure 2.4.

Figure 2.4. Acetaminophen mingled with other excipients of the core beads and water

Stearic acid was melted and the molten stearic acid was blended with acetaminophen, Polyox^{TM} WSR N80, and avicel pH 102. A stirrer was set up to make the mixture become homogenous. 10 ml water was added. The mixture was then extruded through an extruder with a 1mm screen. For the next step, the cylindrical extrudates of uniform shape and size were then cut into small pieces 1mm long. The extrudates were put on the gridded, fast spinning disc of the spheronizer. The extrudates were spheronized for 15 minutes.

Figure 2.5. Spheronizing beads

The last process, after the beads have undergone the spheronization process, was to collect and dry the collected beads at 35^{o}C for 6 hours yielding solid normal spherical beads.

Figure 2.6. The resultant uncoated beads loaded with the drug

Spray coating the beads

Uncoated beads were seized using sieves to eliminate beads smaller than 14 mesh size and larger than 28 mesh size.

The uncoated beads were put into the chamber of the bottom spray coater and spray coated. The coating agent can be HPMC, ethyl cellulose, Kollicoat®, or Polyox™ WSR N80.

For 100 g of uncoated beads, 10g HPMC E5 and 5g Polyox™ WSR N80 were mixed together. The mixture was dissolved into 100 ml of water at 60-70°C. The container was kept vigorously stirring on a hot plate. The process is illustrated in Figure 2.7.

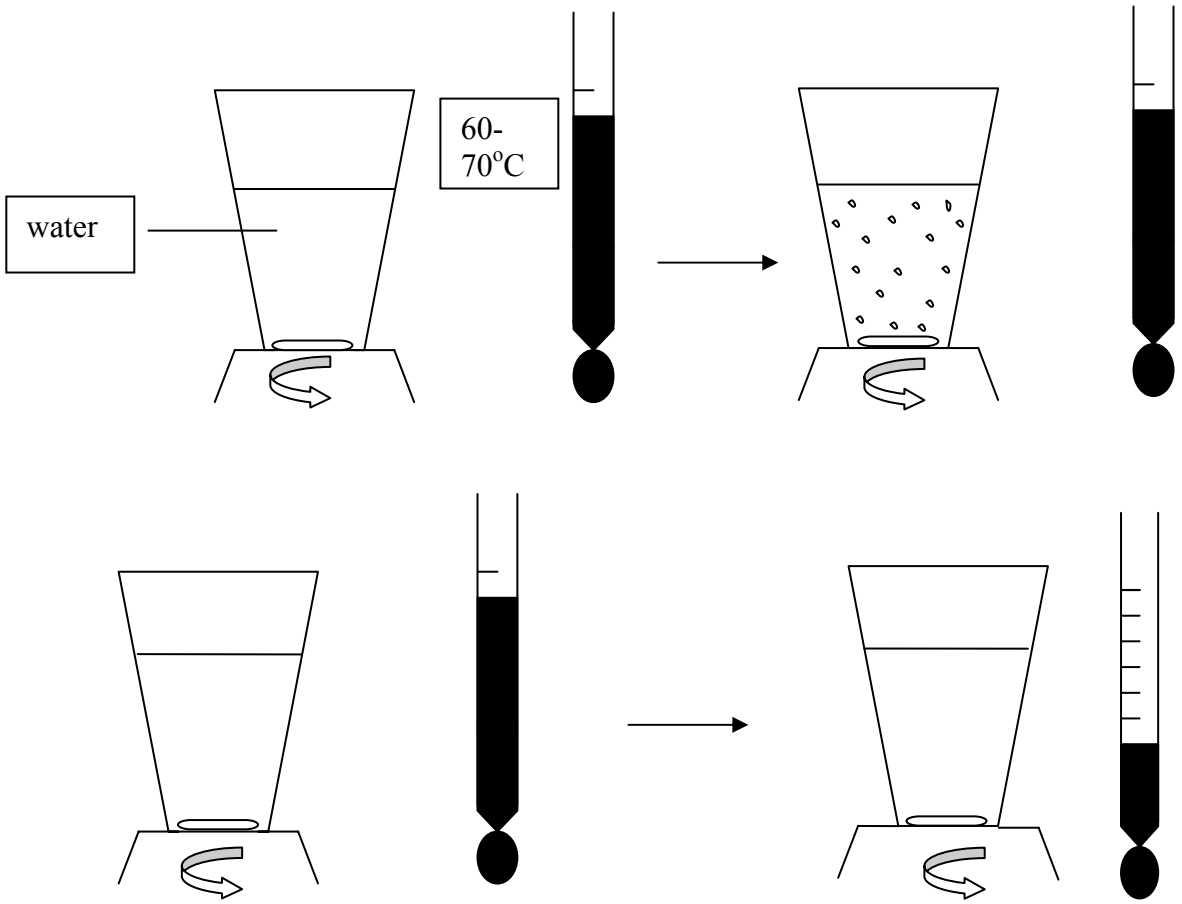

Figure 2.7. The process of dissolving the polymer in water

The HPMC concentration was 10% and polyox is 5%. When surelease was added to the solution, 10 ml of surelease is added to cool solution of HPMC and polyox. The surelease suspension 25% was diluted in water to obtain a 10% solution in the water. Kollicoat® was diluted in water at room temperature to obtain a 15% solution.

The conditions for spray-coating the beads in the Wurster chamber are presented in [74] Table 2.1.

Table 2.1. Spray coating conditions of the beads in fluid bed chamber

Solution	Inlet temperature	Outlet temperature	Rate of coating	Nozzle Diameter	Atomizing
HPMC 10% + polyox 5%	50	45	0.8ml/min	0.8mm	15-18
Surelease 10%	45	40	1ml/min	0.8mm	15-18
Kolicoat 15%	45	40	1ml/min	0.8mm	15-18

The coated beads scheme are drawn in Figure 2.8

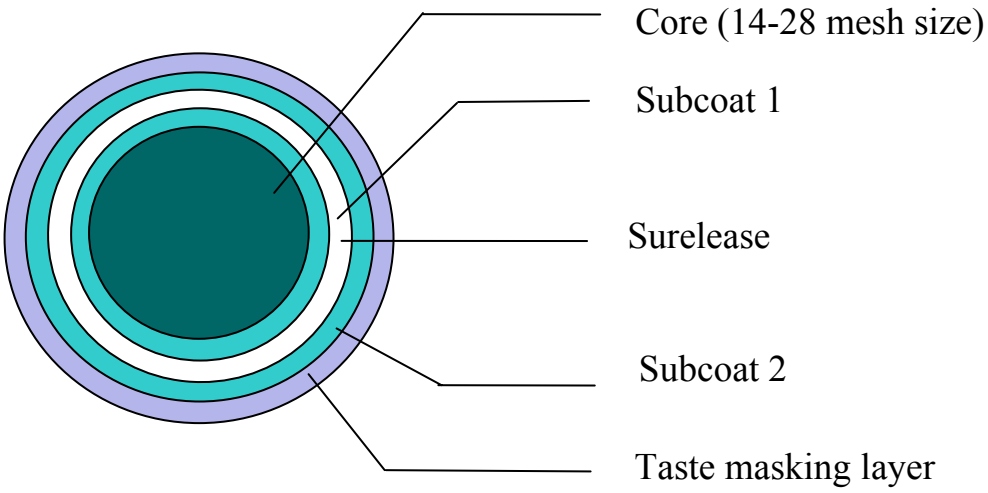

Figure 2.8. Coated beads scheme

The coating process in a fluid bed is present in Figure 2.9.

Figure 2.9. Spray coater used in the coating process, a fluid bed spray coater

Preparing orally disintegrating tablets of melatonin

Mannitol is the main filler in the tablet. Mannitol is granulated with 5% maltose. Other excipients such as superdisintegrants, amino-acids, flavors, and lubricants were added during blending and the blending continued until a thorough

mixture was achieved. Similarly, melatonin was dissolved in absolute ethanol, and then the solution was dispersed into the mixture. The mixture was kept at ambient air and room temperature for one hour to allow the ethanol to evaporate. Afterward, the whole mixture was compressed into tablets, 0.2g.

Figure 2.10. Melatonin tablets

Process for preparing orally disintegrating tablets containing acetaminophen sustained-release beads

The tablets containing sustained-release beads were prepared in a similar way as the orally disintegrating tablets of melatonin except that the sustained release beads were put into the tablet.

The sustained release beads of acetaminophen were mixed with mannitol and granulated by a maltose 5% solution in order to surround the mannitol around the sustained release beads. Consequently, this process prevents the beads from impacting

together during tablet compression. Before blending with other excipients (superdisintegrants, amino acids, flavors, lubricants), the granules were dried at 37^{o}C for 8 hours. The whole mixed finally was compressed to obtain the tablet; the tablet weighed from 0.57 to 0.72g.

Figure 2.11. A simple tablet compressor used to make tablets

The final tablet was keep at a low relative humidity <50%.

Figure 2.12. Acetaminophen tablets

Disintegration test

FDA industry guidance suggested that the traditional disintegration test should be carried out under the conventional method that is described in UPS uing the basket-rack assembly that can be seen in Figure 2.13.

The basket-rack assembly consists of 6 open-ended transparent tubes. The inner-diameter is 22 to 26 mm, and 7.75 ± 0.25 cm long. The tablet is held inside the tube, and the 6 tubes are immersed in a water bath at 37^{o}C. The baskets are raised and lowered in the water. The rate of basket immersion is between 29 to 32 cycles per minute, and the distance the tubes rise and lower is not less than 5.3 cm and not more than 5.7cm.

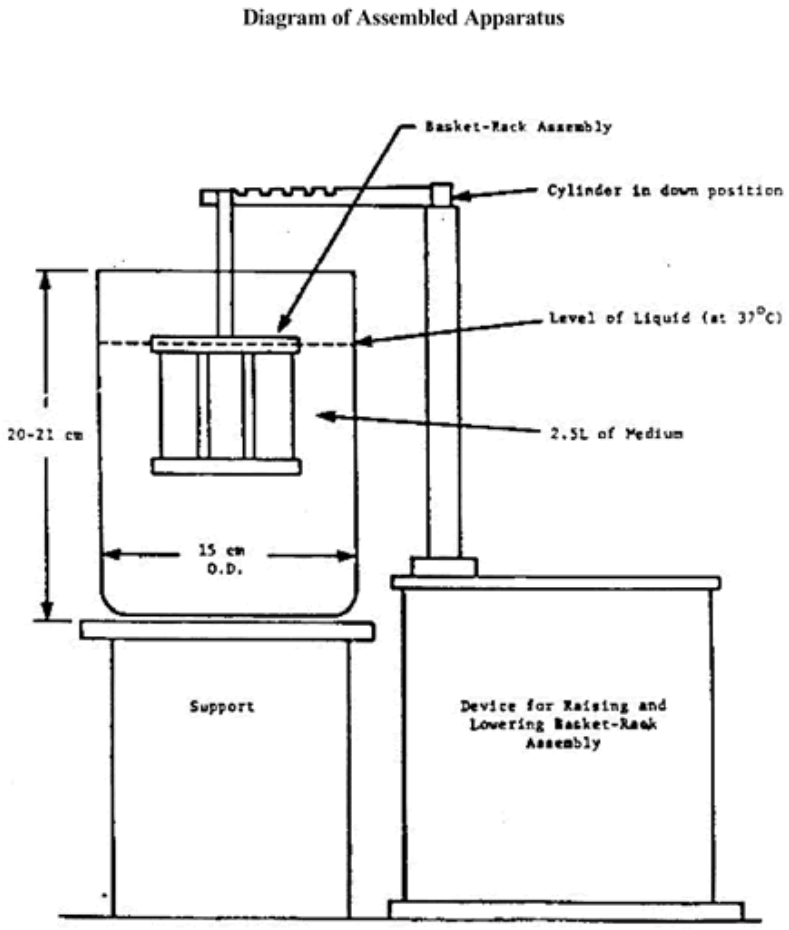

Figure 2.13. A basket rack assembly for tablet disintegration testing

Nevertheless, this method is not similar to the environment inside the mouth. The tongue's movement is not strong and fast compared to the conditions of the stomach. Thus, the immersion rate is likely too powerful for testing ODT's. In fact, the amount of water in the bath is excessive compared to the volume of saliva in the mouth. Consequently, the disintegration times tended to be shorter than the expected value.

A new, simple method is recommended to test the disintegration time of ODT's. A 25-ml cylinder containing water with a pH of 7.4 (the pH of saliva) may produce better results. The tablet is dropped from the top of the cylinder and allowed

to fall down to the bottom. The disintegration time is recorded when the tablet fully disintegrates. The procedure is depicted in Figure 2.14.

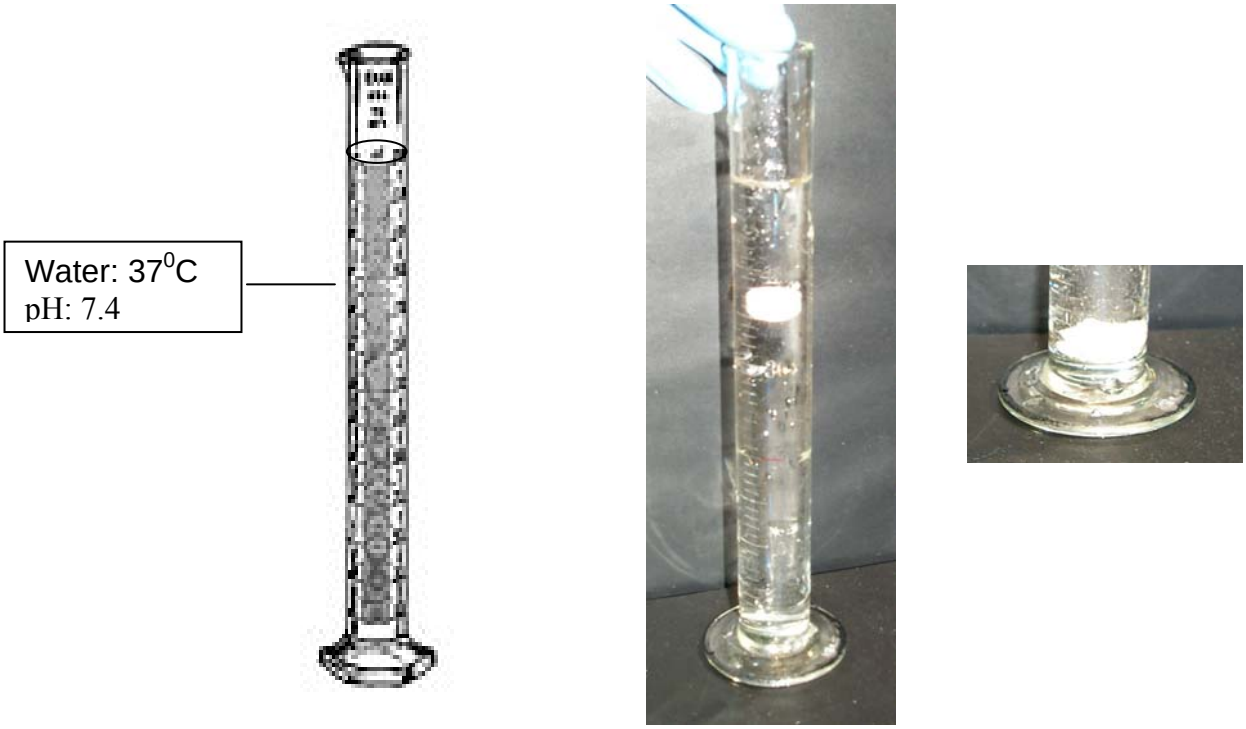

Figure 2.14. Disintegration test of ODTs using a 25ml cylinder

Friability Test

One of the tests that a tablet needs to endure is friability in accordance to the USP. Tablets were placed inside each side of the rotating drum.. The drum with an internal diameter from 283 to 291mm and a depth of 36-40mm is attached to a horizontal axis and rotated at 25 ± 1 rotations per minute. The tablets were tumbled 100 times in the rotating drum.

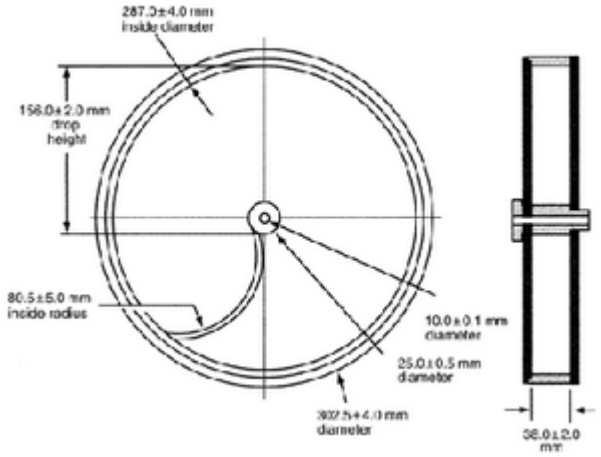

Figure 2.15. A friability tester

For tablets weighing equal to or less than 650mg, ten or more tablets of the sample formulation that yield a total weight of to 6.5 g were placed in the friabilator. For tablets weighing more than 650mg, ten tablets were used for testing.

After running 100 rotations in the friabilator, the reduction of the tablet weight must be less than 1% without cracking to pass the test.

Hardness test

The hardness of the tablet is measured by a tablet-hardness tester that is displayed in Figure 2.16. A tablet is placed under two high pressure plates. The pressure is increased until the tablet is broken.

Figure 2.16. A tablet-hardness tester

The units of force in the hardness tester are recorded in dial. 1dial =1.6kg

Dissolution test

Dissolution test for melatonin

Since melatonin in the ODTs was expected to dissolve very quickly after being put into the mouth, the dissolution test was run with simulated a gastric fluid medium; it had a pH 1.4±0.1 with 900 ml. Apparatus 2, the paddle method was employed with 75 rpm at 37^{o}C. The melatonin sample was withdrawn at 5, 10, 15, 20, 30 minutes and 1, 2, 3, 4 hours. The melatonin concentrations from the samples were measured using 254 nm wavelength in the UV spectrophotometer. As the melatonin dose was small, the dissolution test was performed in the 900 ml per flask with the gastric-fluid medium using 10-20 tablets for each flask bowl.

Dissolution test for acetaminophen

The dissolution test of acetaminophen beads or tablets was performed as described in UPS 28, NF25. The Apparatus 2, the paddle method was employed. The solution medium was a simulated gastric medium pH 1.4 ± 0.1 with 900 ml placed in a dissolution flask. The dissolution apparatus was set up at 75 rotations per minute and at a temperature at 37 ^{o}C. The test amount of acetaminophen in the beads or in the tablet ranged from 250-500mg depending on acetaminophen concent.

At the specified time points: 5, 15, 30 minutes, 1, 2, 3, 4, 5, 6, 8, 10, 12, 14, 16, 18, 20, 22, 24 hours, 2.5ml samples were withdrawn. The samples were then diluted to the ratio 1/20 using dissolution media, and the acetaminophen concentrations were measured by UV detection at 244 nm in a spectrophotometer. Simulated gastric fluid was the blank sample. The dissolution apparatus is shown in the Figure 2.17.

A reference sample was produced by totally dissolving tablets. Three tablets were dissolved in three volumetric flasks having a volume of 500 ml. The samples were sonicated for 24 hours to allow resident acetaminophen to dissolve completely in the gastric fluid. The supernatant was then filtered after diluting the sample to a ratio of 1:20 in the gastric fluid. Finally, the solution was measured by UV detection in a spectrophotometer at 244 nm. The blank sample was simulated gastric fluid.

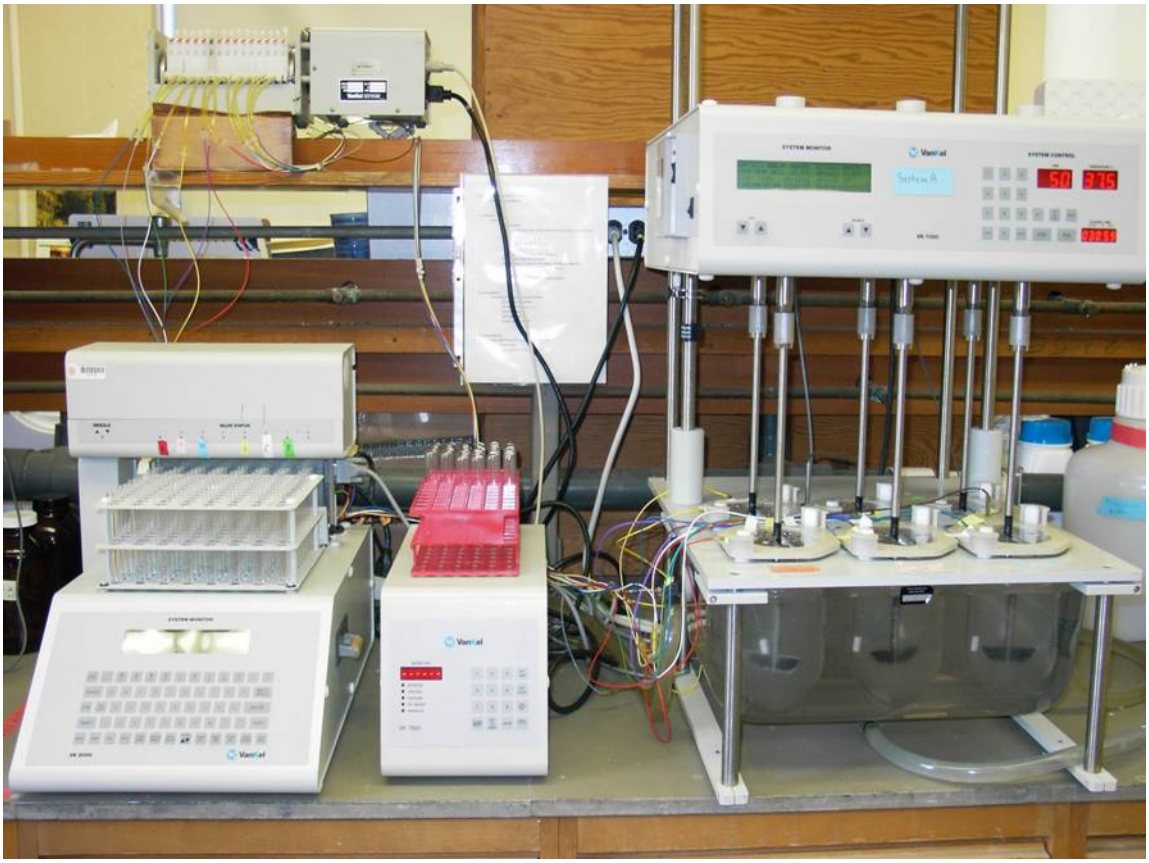

Figure 2.17. Dissolution machine, apparatus 2, to conduct dissolution studies on melatonin and acetaminophen tablets

The average values of three replications in the three drug flasks used for dissolution were calculated. The concentration of the drug was determined using a standard curve. The actual amount of acetaminophen in the tablets was used as the reference to evaluate the percentage of drug release.

Single-beam spectrophotometer is presented in Figure 2.18.

Figure 2.18. A spectrophotometer- Model Beckman DU 640

Statistical analysis

Basic statistics tests such as two sample t tests, ANOVA and linear and non-linear regression for fitting were applied to analyzed data. All statistics test were performed on an S-plus version 8.0, Sigma Plot 10.0.

Two-sample t tests were used to compare two individual, independent samples. An F test was used to find a significantly different sample from a group of samples. These types of tests could be used for disintegration time, drug concentrations, and thickness of the membrane. Linear and non-linear regression is employed to fit drug-dissolution profiles.

Convolution

In mathematics, in particular, functional analysis, convolution is a mathematical operator which takes two functions *f* and *g* and produces a third function , which, in a sense, represents the amount of overlap between *f* and a reversed and translated version of *g*.

The system consists of a black box, a physical entity that transforms an input into output [75].

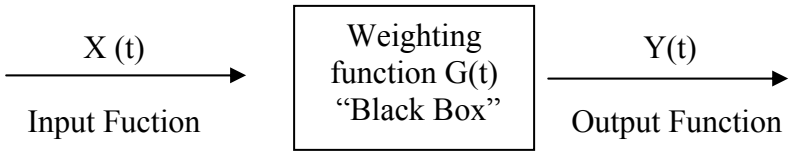

X(t) is the input function, Y(t) is the out put function, G(t) is called the weighting function of the black box, such that:

$$Y(t) = \int_0^t G(t-T)X(T)dT$$

It is stated that Y(t) is given by the convolution between G(t) and X(t) where 0<T<t. The relationship of three functions can be displayed by the laplace transformation:

$$y(s) = g(s)x(s)$$

Where y(s), g(s), x(s) are the laplace transforms of Y(t), G(t) and X(t). The function g(s) is called the transfer function and its matrix is called the transfer matrix of the black box. In fact, applied in pharmacokinetics, Y(t) is the function describing the plasma (serum or whole blood concentration time curve following extravascular administration), G(t) is the function describing the concentration-time curve following bolus intravenous administration and X(t) is the function describing the drug's input. In convolution the desirable result Y(t), usually the predicted plasma concentration, is

obtained using the input function X(t), the dissolution profile of the drug; and G(t), the function describing IV plasma concentration.

To run convolution some assumptions are applied: First, the rate of drug absorption should be fast and the amount of the drug absorbed *in vivo* must be similar to *in vitro* drug dissolution. Consequently, convolution is applied to drugs falling into class I and class II in the biopharmaceutics classification system Figure 2.19 [76]. Second, for the administered dose, the drug must obey linear pharmacokinetics.

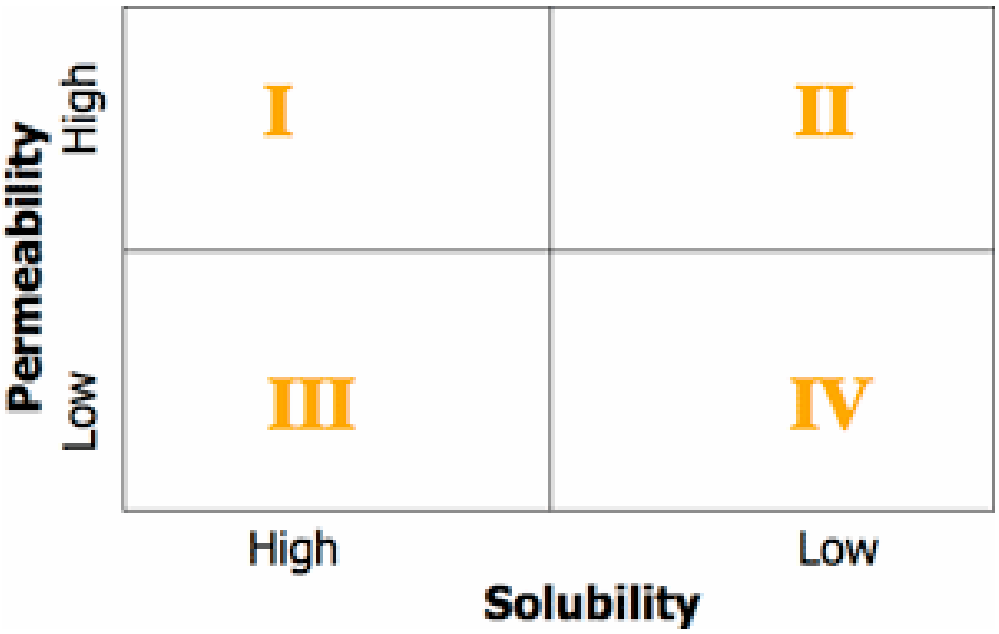

Figure 2.19. Biopharmaceutic drug-classification system

Kinetica® is a commercial software program for pharmacokinetics from Thermo Scientific. The academic package contains common PK-PD models: non-compartmental analysis, compartmental analysis, simulation: convolution and deconvolution. The obtained drug-plasma concentration obtained from convolution with Kinetica® was used to run the "non-compartmental analysis". The parameters

obtained were half life ($t_{1/2}$), mean residence time (MRT), area under the curve (AUC), C_{max}, T_{max}, and clearance (Cl) for comparison.

Non-compartmental analysis

Non-compartmental analysis is an independent approach model in pharmacokinetic modeling in which the number of compartments to describe drug disposition is ignored. Using the area under the first moment curve and the area under the curve of the drug concentration versus time curve and analysis of the terminal elimination phase of drug-disposition profile, some pharmacokinetic parameters were calculated and extrapolated. The common pharmacokinetic parameters obtained were half-life ($t_{1/2}$), Mean Residence Time (MRT), Area Under the Curve (AUC), maximum concentration (C_{max}), time of maximum concentration (T_{max}), and Clearance (Cl).

The simulated, plasma concentration versus time curves for melatonin and acetaminophen were obtained by running convolution and were analyzed by non compartmental analysis both with optimal formulations of the drug and the immediate-release dosage forms. The pharmacokinetic parameters of two the formulations were compared to clarify the differences between the two formulations.

RESULTS AND DISCUSSION

EFFECT OF DISINTEGRANTS

Definition: An agent used in pharmaceutical preparation of tablets, which on contact with moisture especially GI fluids causes the tablets to disintegrate and release their medicinal substances.

Mechanisms that facilitate the activity of a disintegrant.

Capillary Action of aqueous fluids (wicking)

Disintegrants are hydrophilic agents with low free-energy surfaces. Water penetrating into the tablet exerts forces between the particles compressed within a tablet pore causing expansion. Disintegrants enhance these forces and allow the water to penetrate quickly. This rapid penetration of the water rapidly expands the tablet producing fast-tablet disintegration.

Swelling with minimal gelling

Many disintegrants are also gelling agents. They swell and eventually form a gel. Swelling also lets water penetrate into the tablet quickly. Water penetration, swelling, and gel formation by the disintegrant is the balance that is to be achieved for a disintegrant to work well, especially for rapid disintegration.

The gel layer forms a viscous mass that water needs to pass through in order to penetrate deeply into the tablet. Rapid-gel formation inhibits tablet disintegration. Consequently, gel formation prevents the inner part of the tablet from contacting the water. A good disintegrant should not create a gel too rapidly.

Deformation

An excipient in a tablet, during tablet formation, is deformed under the pressure of compression that forms the tablet. A compressed excipient will release the energy that it has from its deformed state when the tablet is put into water due to deformation recovery.

Multiple combinations of mechanisms usually occur when a disintegrant contacts water. For example Polyplasdone's mechanism of action is water wicking, swelling, and possibly some deformation recovery. Crocarmellose demonstrates wicking due to its fibrous structure and swelling with minimal gelling. Amberlite™ IRP 88 is a very fast wicking material and has an excellent deformation recovery without adhesion.

To test the activity of disintegrants, a range of formulations were prepared with common super-disintegrants. All formulations consisted of a mannitol granule 5 g and pruv as the lubricant 1%. The disintegration times and hardnesses of the 0.5g tablets is recorded in Table 2.2.

Table 2.2. Effect of disintegrants on the disintegration time

Formulation	**Mannitol granules**	**Disintegrants**	**Pressure 2000lbs**		**Pressure1000lbs**	
			Time (second)	Hardness (dial)	Time (second)	Hardness (dial)
1	5g+0.05g pruv	Crosscamellose Na 0.1g	35 36	10 10.2	27 28	6.4 6.5
			35	10.3	27	6.8
		mean	**35.3**	**10.2**	**27.3**	**6.57**
		SE	0.333	0.088	0.333	0.120
2	5g+0.05 pruv	Crosscamellose Na 0.05	39 40 39	11.1 10.8 10.5	35 36 35	6.1 6.7 6.8

		mean	**39.3**	**10.8**	**35.3**	**6.53**
		SE	0.333	0.173	0.333	0.219
3	5g+0.025g pruv	Polyplasdone XL 0.05g	31	10.3	23	6.6
			30	10.2	24	6.5
			31	10.3	23	6.6
		mean	**30.7**	**10.3**	**23.3**	**6.57**
		SE	0.333	0.033	0.333	0.033
4	5g+0.025g pruv	Polyplasdone XL-10 0.05g	32	11.5	24	7.0
			33	9.8	25	6.8
			30	10.5	24	6.6
		mean	**31.7**	**10.6**	**24.3**	**6.8**
		SE	0.882	0.493	0.333	0.116
5	5g+0.025g pruv	Avicel pH 102 0.05g	76	11	64	7.5
			81	11.5	68	7.5
			78	11.8	70	7.1
		mean	**78.3**	**11.4**	**67.3**	**7.37**
		SE	1.45	0.233	1.76	0.133
6	5g+0.025g pruv	Explotab low pH 0.05g	47	12	31	7.2
			48	11.1	32	6.8
			47	10.3	33	6.5
		mean	**47.7**	**11.1**	**32**	**6.83**
		SE	0.333	0.491	0.577	0.203
7	5g+0.025g pruv	Amberlite IRP 88 0.025g	33	11	23	7.0
			31	10.5	23	7.3
			31	10.8	22	7.5
		mean	**31.7**	**10.8**	**22.7**	**7.27**
		SE	0.667	0.145	0.333	0.145
8	5g+0.025 pruv	Amberlite IRP 88 0.05g	31	9.8	22	7.0
			29	10.6	23	6.7
			30	10.9	21	6.8
		mean	**30**	**10.4**	**22**	**6.83**
		SE	0.577	0.328	0.5773	0.0882
9	5g+0.025g pruv	Emcosoy 0.05g	45	11.2	27	7.3
			39	10.9	29	6.9
			40	10.8	30	6.5
		mean	**41.3**	**10.9**	**28.7**	**6.9**
		SE	1.856	0.120	0.882	0.231

ANOVA output shows that the disintegration time was remarkably different among the entire test groups having a disintegrant of ($p<0.0001$) whether the tablets

were formed using either 2000 or 1000 lbs compression forces. However there is no clear convincing differences observed in the hardnesses of the tablets of the test groups (p= 0.08 for 2000lbs group and 0.04 for 1000lbs group).

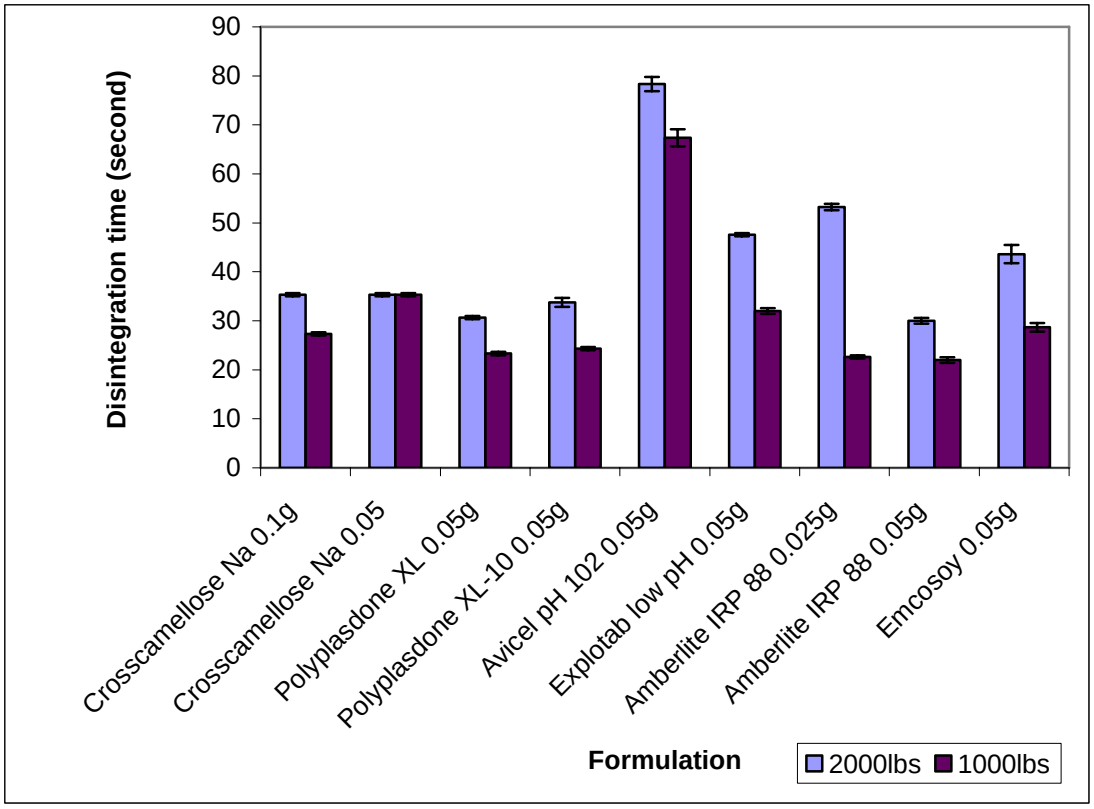

Figure 2.20. Effect of different disintegrants on disintegration times of the tablets

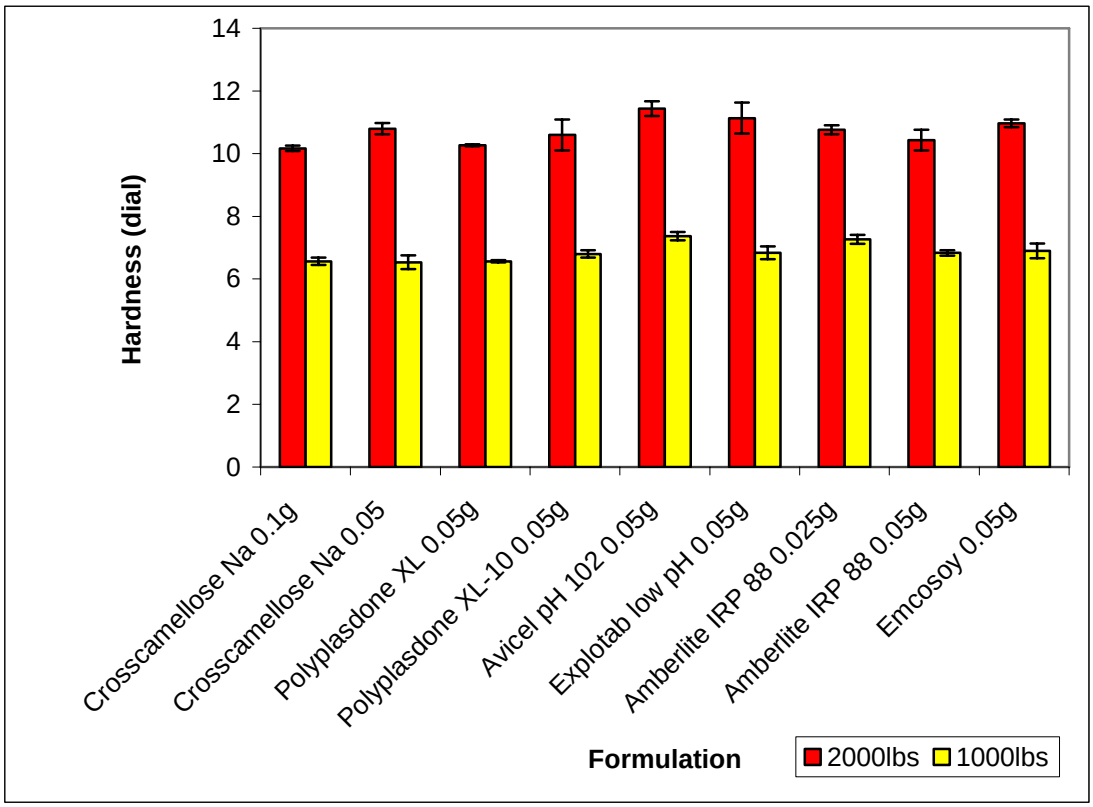

Figure 2.21. Hardnesses of tablets containing different disintegrants

The comparison of tablet disintegration times, when the same amount of different disintegrants were used, showed Amberlite IRP 88 and polyplasdone produced the best activity. Ranking the ability to break apart tablets yields: Amberlite IRP 88 ~ Polyplasdone XL > Croscarmelose Na > Emcosoy STS IP > Explotab > Avicel pH 102. The results in Figure 2.20 and 2.21 reveal that Avicel pH 102 (microcrystalline cellulose) was least effective in reducing the disintegration time of the tablet. The results are not surprising as Avicel is not considered a super-disintegrant. Amberlite IRP 88, Polyplasdone XL, croscarmelose Na and Emcosoy STS are all considered super-disintegrants and are used widely. These disintegrants enhanced tablet disintegration.

Microparticle-sized particles disperse evenly throughout the whole tablet. A previous study showed that polyplasdone loses its activity after wet granulation [77]. No similar investigation had been carried out for the Amberlite IRP 88. From the results found on formulating with polyplasdone, it is recommended that super-disintegrants should be added after mannitol granulation. Thus, both the Amberlite IRP 88 and polyplasdone XL were mixed with mannitol granules.

The tablet hardness tests also showed that Avicel pH102 produced tablets with greater hardness. However, other solid disintegrants did not have remarkable effects on the hardness of the tablet.

To investigate the optimal concentration of disintegrants and the combination of disintegrants, a range of concentrations of the disintegrant Amberlite IRP 88 was put into tablet. The formulation:

Mannitol 10g
Sucralose 0.05 g
Sustained release beads of acetaminophen 10g
Pruv 0.1g

Mannitol was mixed with sucralose and granulated with sustained release beads. Tablets were compressed under 1000lbs pressure; each tablet's weight was kept constant at 0.4g.

The disintegration times of the tablets were tested by placing them in a 25-ml cylinder containing water and allowing them to settle to the bottom of the cylinder. The method is mentioned in the materials and methods section. The final results are shown in Table 2.3 and Figure 2.22.

Table 2.3. Disintegration times and the percentages of Amberlite IRP 88 used in tablets

Amberlite IRP 88	1%	2%	3%	4%	5%	6%	7%
1	33	30	25	28	30	31	29
2	33	32	30	30	30	29	30
3	35	34	29	28	29	28	30
Mean	**33.7**	**32**	**28**	**28.7**	**29.7**	**29.3**	**29.7**

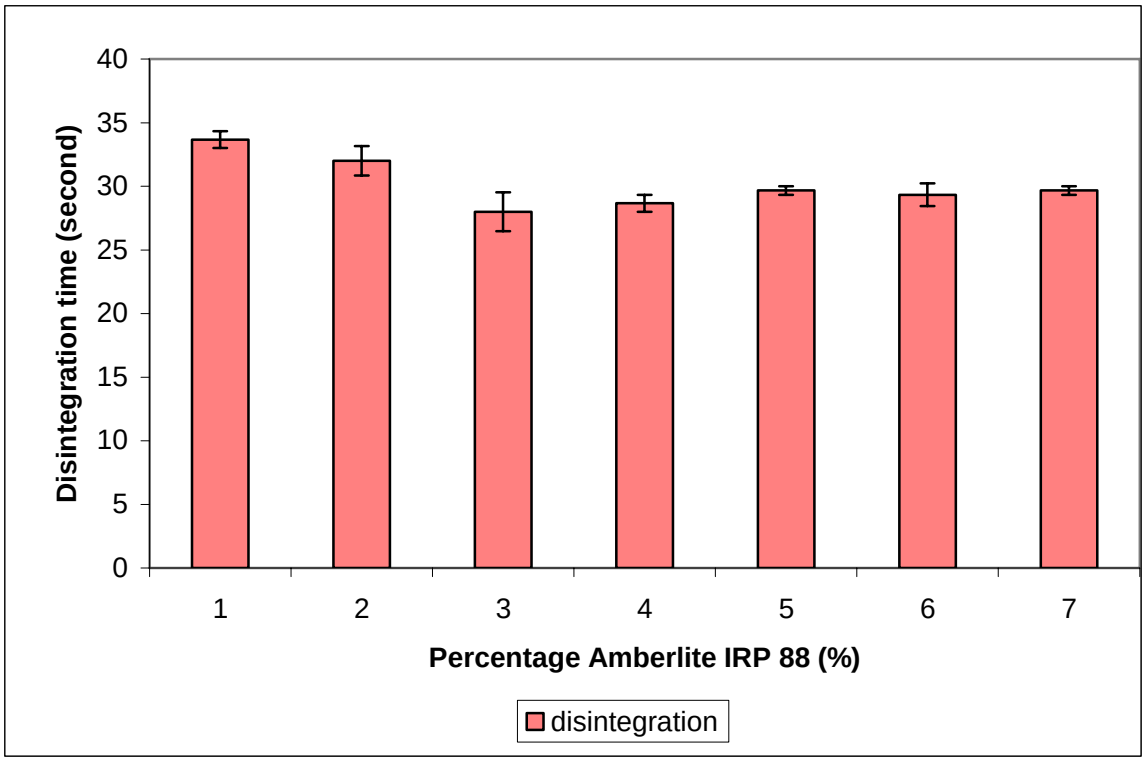

Figure 2.22. The effect of the concentration of Amberlite IRP 88 on disintegration times of tablets

The tablet-disintegration time declined until Amberlite IRP 88 reached 3% (F test ($p<0.05$) and then remained stable up until the amount of Amberlite IRP 88

reached 7% ($p>0.05$). Higher concentrations of disintegrants did not produce any improvement in disintegration times of the tablets.

To test the effect of a combination of disintegrants on tablet disintegration times, Ambertlite IRP 88 was combined with other disintegrants in tablets. The levels of disintegrants used in tablets can be seen in Table 2.4.

Formulation:

Mannitol 10g
Sucralose 0.05 g
Pruv 0.1g
Amberlite IRP 88 3%

Tablet weight is 0.2g, compress under 1000lbs

Table 2.4. Test of the combination of disintegrants

Formulation	Disintegrant	Disintegration time
1	Crosscarmellose 3%	28
		29
		28
	mean	**28.3**
2	Explotab3%	29
		30
		30
	mean	**29.7**
3	Polyplasdone XL 3%	24
		23
		24
	mean	**23.7**

The results in Table 2.4 shows convincing evidence ($p<0.01$) that a combination of polypladone XL and Amberlite IRP 88 produces a synergic activity of disintegants in breaking apart tablets.

A COMBINATION OF HIGH COMPRESSIBLE AND LOW COMPRESSIBLE SUGARS

Although mannitol is used widely in ODT's both as the disintegrant and sweetener, mannitol is a low-compressible sugar. Specifically, the hardness of the mannitol tablets reached a plateau level with increased compression pressure. Conversely, the hardness of the maltose tablet increased sharply when the compression pressure was increased [78].

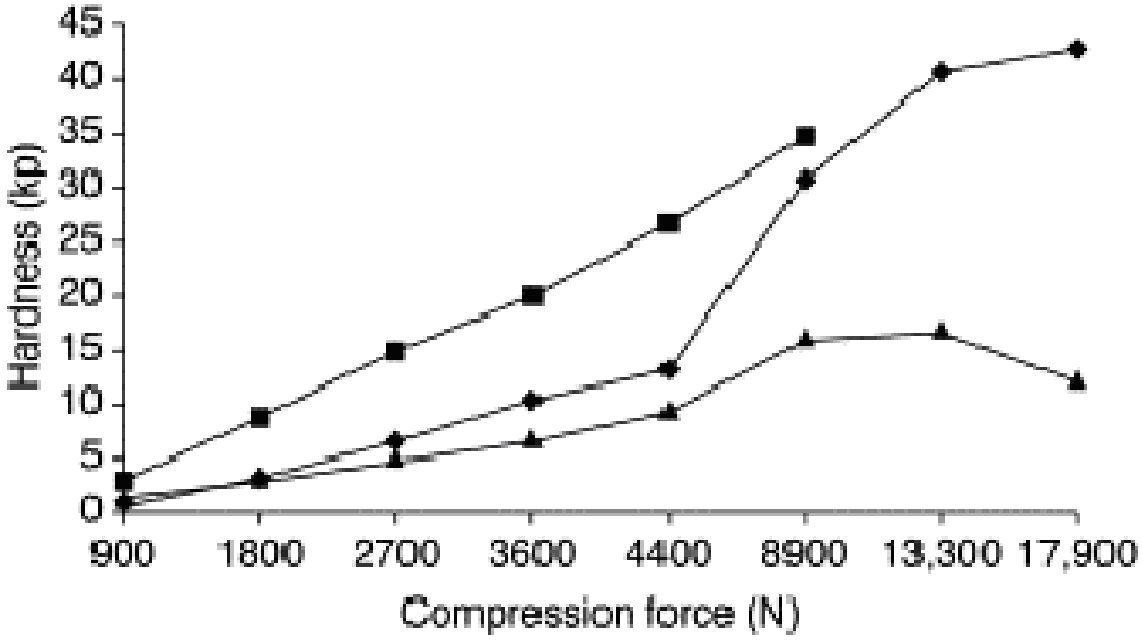

Figure 2.23. Correlation between compression force and hardness of a 400mg maltose tablet (♦), granular mannitol (▲) and 100% microcrystalline cellulose (■) [77]

The Surface energy and the contact angle have a close relationship according to Kaeble's equation:

$$\frac{1+\cos\theta}{2}\frac{\gamma L}{\sqrt{\gamma_L{}^d}} = \sqrt{\gamma_S{}^p}\sqrt{\frac{\gamma_L{}^p}{\gamma_L{}^d}} + \sqrt{\gamma_S{}^d}$$

γ_L and γ_S are the surface-free energy of the liquid and the solid, respectively. The symbol p and d represent polar and dispersion components of the surface-free energy. The surface energy also has a relationship with the compressibility of polysaccharides. More precisely, the surface free energy of the polar component of high-compressible saccharides are over 47 mJ/m^2, including (maltose, sorbitol, trehalose, multitol). Low-compressible saccharides have surface energies of polar components under 38 mJ/m^2 (Figure 2.24).

An improvement in the compressibility of mannitol is necessary for ODTs to be possible. For this purpose, mannitol granulated with a maltose solution is recommended [77].

Takao Mizomoto et al.[79] used a15% maltose solution for granulating mannitol powder. However, the mannitol granules obtained were sticky following normal granulation, and a higher mingle rate is required to avoid agglomeration with maltose 15%.

Maltose and sorbitol are the common saccharides used in the pharmaceutical industry. To compare the effectiveness of maltose and sorbitol to improve compressibility when mixed with mannitol, two formulations are prepared. The excipients used are in Table 2.5, and the tablets were compressed under 1000lbs and 2000lbs pressure. Tablet weight is 0.2g.

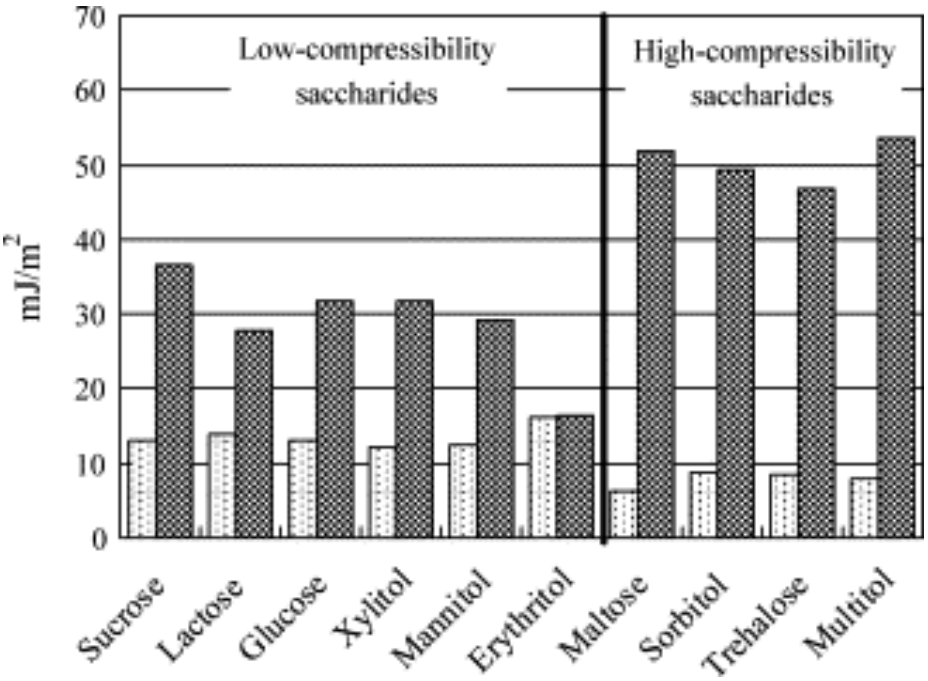

Figure 2.24. The surface free energy of the dispersive component and the polar component of the low- and high-compressibile saccharides. The surface-free energy of the dispersive component (▒) and the polar component (▓)

Table 2.5. Formulations to test the combination of high-compressible polysaccharides and low-compressible polysaccharides in combination with mannitol

Formulation	1	2	3
Mannitol powder	10g	10g	
Sorbitol solution 15%	2ml		
Maltose solution 15%		2 ml	
Maltose solution 5%			2ml
Pruv	0.1g	0.1g	

The hardness and disintegration time of the tablets are presented in Table 2.6 and Figure 2.25, and Figure 2.26.

Table 2.6. Disintegration time and hardness of sorbitol 15%, maltose 15%, maltose 5% solution for mannitol granulation

Formulation	Disintegration time (second)		Hardness (dial)	
	2000lbs	**1000lbs**	**2000lbs**	**1000lbs**
1	35	27	6.7	3.5
	36	27	6.8	3.6
	35	28	6.9	3.8
Mean	**35.3**	**27.3**	**6.8**	**3.63**
SE	0.333	0.333	0.058	0.088
2	36	28	6.8	3.6
	34	26	7	3.5
	35	26	6.7	3.9
Mean	**35**	**26.7**	**6.83**	**3.67**
SE	0.577	0.667	0.088	0.120
3	30	25	6.4	3.5
	31	24	6.4	3.4
	32	23	6.3	3.1
Mean	**31**	**24**	**6.37**	**3.33**
SE	0.577	0.577	0.033	0.120

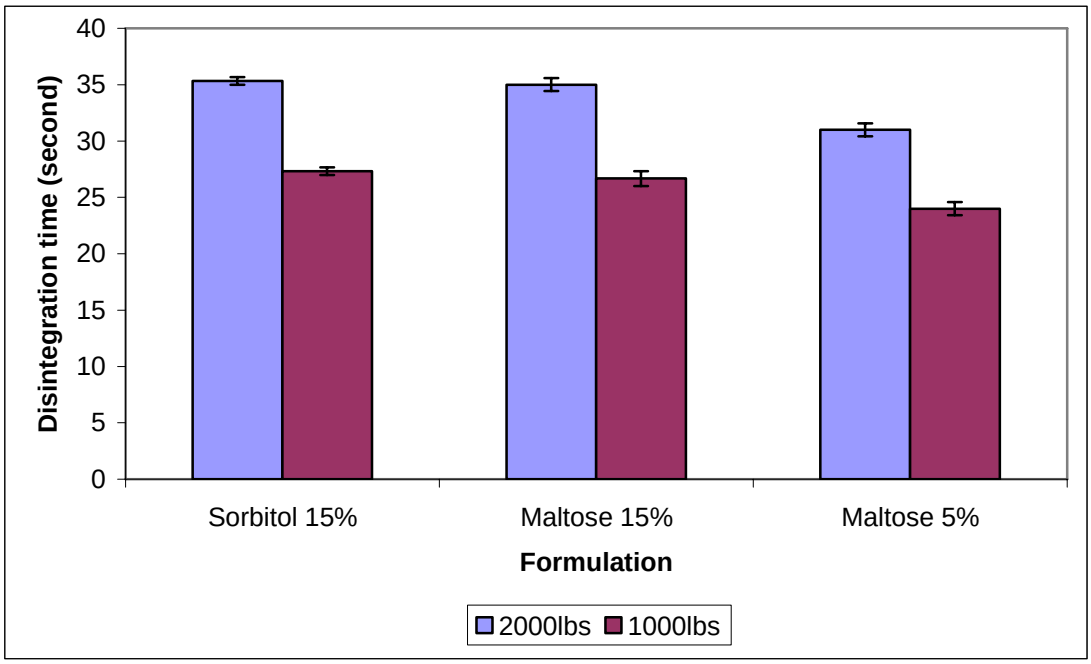

Figure 2.25. The disintegration times of formulations granulated with sorbitol 15%, maltose 15% and maltose 5% with mannitol

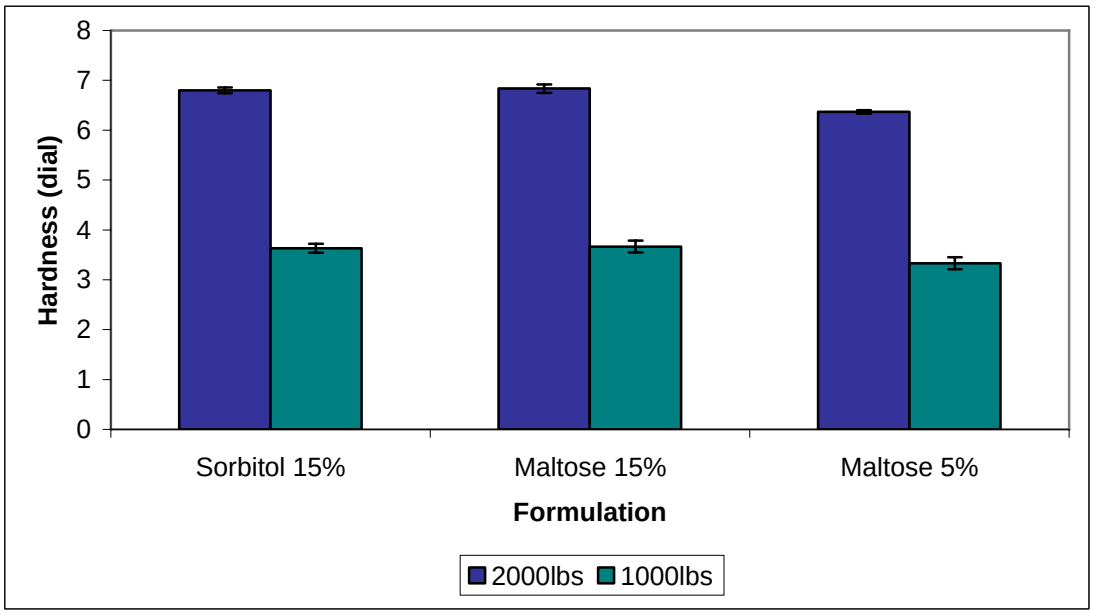

Figure 2.26. The hardnesses of formulations granulated with sorbitol 15%, maltose 15% and maltose 5% with mannitol

There is suggestive evidence ($0.05<p<0.1$) that the formulation with maltose is better than that of the sorbitol in granulation.

A five-percent maltose solution is sufficient to granulate with mannitol to obtain a fast-disintegration time with little reduction in tablet hardness.

EFFECTS OF SWEETENERS

Taste is a chemical reaction derived from the sensor response. Physiological concepts covering basic tastes include salt, sour, bitter, sweet. Two other perceptions, umami and trigeminal are also included for taste.

Umami is the taste sensation that is produced by several amino acids and nucleotides; umami is a meaty or savory taste. Trigeminal is the burning sensation derived from such foods as spicy materials and peppers.

Contrary to popular understanding that different tastes map to different areas of the tongue, taste qualities are found an all areas of the tongue [80, 81].Even the density of each taste-bud type distributed over main locations. Six tastes on the tongue[60] are shown in Figure 2.27.

Olfaction contributes synergically to the taste. The aromas releasing from the dosage forms evaporate into the nasal cavity. The signal of taste and smell is transferred to the brain. In the brain, the signal is interpreted as a combined process. Therefore, an adjustment of both taste and smell is necessary to obtain a good mouthfeel.

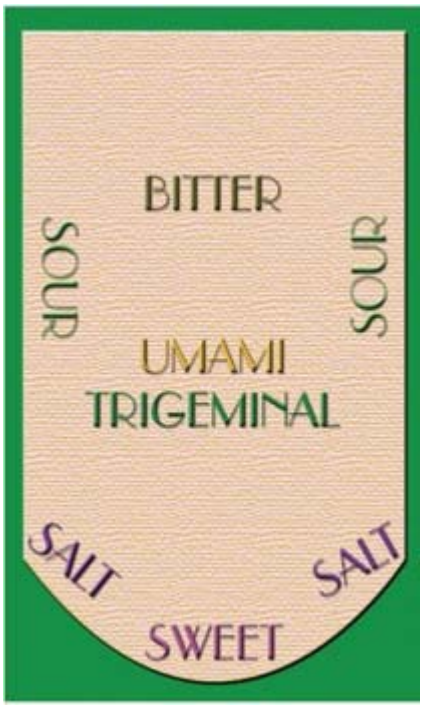

Figure 2.27. The taste locations on the tongue

Market surveys also show that most patients that have experienced an ODT will prefer to have an ODT again when they select between conventional tablets and ODTs [60].

In this study, melatonin and sustained release beads of acetaminophen do not have extensive problems of taste. Adding sugar to the formulation, however is to improve the mouthfeel.

Currently, there are many natural and synthetic polysaccharides available to sweeten formulations. A range of common sugars used as the sweeteners for tablets are presented in Table 2.7.

A series of tablets were prepared.

Formulation:

Mannitol 3.9g
Pruv 0.05g
Amberlite 0.6g
Cherry flavor 0.4g
Beads 5g
Sweetener

Tablets 0.8g were compressed under 2000lbs force.

Table 2.7. Effect of sweeteners on disintegration times and hardness of the tablets

Formulation	**Sweeteners**	**Sweet scale (Reference: sucrose)**	**Pressure 2000lbs (0.5g)**	
			Time (second)	Hardness (dial)
1	Sucralose 0.025g	600	24	4.2
			23	4
			24	4.2
		mean	23.7	4.13
2	Sucralose 0.0125g	600	22	4.3
			21	4.1
			25	4.2
		mean	22.7	4.2
3	Aspartame 0.09g	180	22	4.1
			23	4.2
			26	4.5
		mean	23.7	4.27
4	Fructose 0.5g	1.2-1.8	310	6.2
			326	6.5
			341	6.6
		mean	326	6.43
5	Fructose 0.1g	1.2-1.8	200	6.1
			187	6.1
			165	6.0
		mean	184	6.07
6	Saccharin 0.025g	300	23	4.3
			24	4.1
			23	4.2
		mean	23.3	4.2

The taste test set up to measure the amount of sweetener needed in the formulation was carried out using 3 healthy subjects. The acceptable amount of sweeteners is listed in Table 2.7. The disintegration time of the tablets containing fructose was statistically different from other tablets utilizing other sweeteners both in the disintegration time and hardness time (ANOVA method with $p<0.01$).

Fructose is only 1.2-1.8 times sweeter than sucrose. To obtain the desired sweetness, the amount of fructose needed in the tablet was too high. Fructose is also known as a strong binder. Accordingly, fructose was not an adequate sweetener since the disintegration time was too long. Using a small amount of synthetic sugar that is many times sweeter than sucrose was a better choice to avoid the prolonged disintegration time fructose exerts. Aspartame and saccharin are common sweeteners that are widely used in the pharmaceutical and food industry. The FDA approved the use of sucralose in 15 beverage categories in 1998. In 1999 the approval was extended to supplements in general foods and pharmaceutical products. The data in Table 2.7 show that sucralose, aspartame, and saccharin can be used to improve the taste without interfering with the tablet-disintegration time.

EFFECTS OF AMINO ACIDS

Amino acids are chemically defined as a molecule that contains both amine and carboxyl functional groups. Many amino acids are essential in protein-building and physiological processes.

Simple amino acids are soluble in water and their high dissolution rate may stimulate the disintegration of the tablet.

The amino acids L-Glycine, L-Lysine, L-Asparagine, Aspartic acid, L- tryptophan were added to the tablet.The rest excipients are the same.

Mannitol granules 5g
Pruv 0.05g
Amberlite IRP 88 0.1g

Table 2.8 Effects of simple amino acids on the disintegration time of tablets

Formulation	**Amino acids**	**Pressure 2000lbs**	
		Time (second)	Hardness (dial)
1	0	28	7
		29	7.2
		29	6.9
	mean	**28.7**	**7.03**
	SE	0.333	0.088
2	L-Asparagin (0.2g)	29.7	7.4
		26	7.6
		27	7
	mean	**27.6**	**7.33**
	SE	1.09	0.176
3	Aspartic acid (0.2g)	28	7.1
		29	7.2
		25	6.8
	mean	**27.3**	**7.03**
	SE	1.20	0.120
4	Glycine (0.2 g)	22	6.9
		21	7.1
		21.3	6.93
	mean	**21.4**	**6.98**
	SE	0.294	0.062
5	Tryptophan (0.2g)	28	7.2
		27	7.3
		27	7.4
	mean	**27.3**	**7.3**
	SE	**0.333**	**0.058**

6	L-lysine	28	7.1
		27	7.0
		28	7.2
	mean	**27.7**	**7.10**
	SE	**0.817**	**0.263**

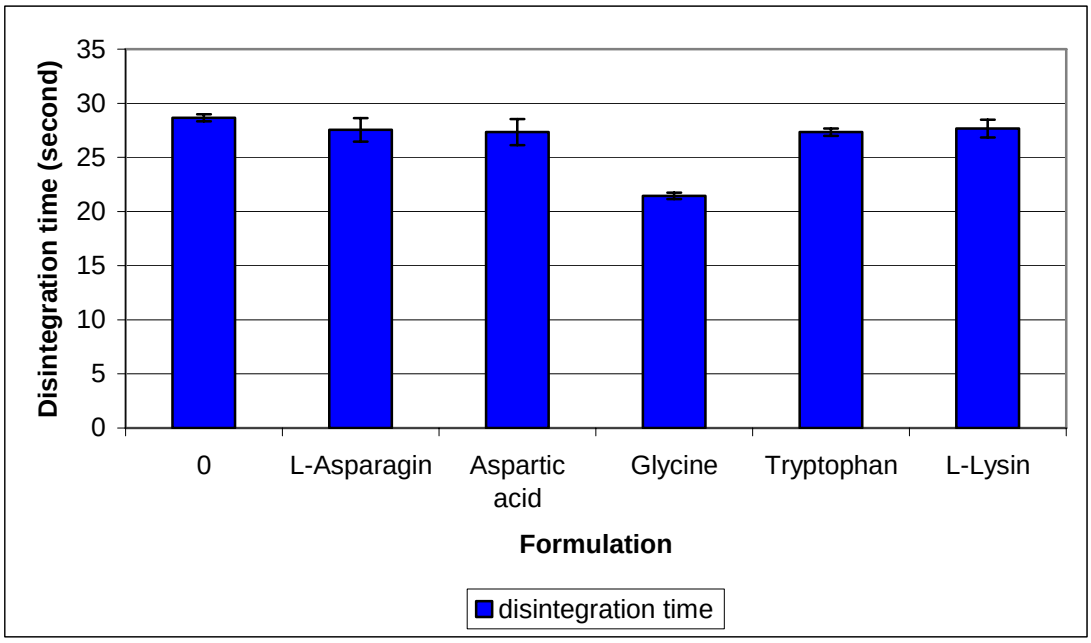

Figure 2.28. The disintegration times of tablet formulations containing amino acids

L-Glycine, the simplest amino acid reduced the tablet disintegration time more than the other amino acids. This effect may be due to the hygroscopic properties of L-glycine that allow it to dissolve quickly in water.

EFFECTS OF LOW MELTING WAXES

Low-melting-point triglycerides such as cocoa butter have been added into suppositories for many years. The synthetic polymer PEG's are also used as excipients to improve suppositories.

Table 2.9. The effects of the inclusion of low-melting-point waxes on the disintegration times of tablets

Waxes	Taste	Pressure 1000lbs (0.25g)		Pressure 1500lbs (0.25g)		Pressure 2000lbs (0.25g)		Pressure 2500lbs (0.25g)	
		Time (second)	Hardness (dial)	Time (second)	Hardness (dial)	Time (second)	Hardness (dial)	Time (second)	Hardness (dial)
0	**good**								
		20	5	25	6.2	32	6.8	36	8
		19	4.9	26	5.9	33	7	38	7.5
		26	4.4	25	5.5	34	7.1	39	7.4
	mean	**21.7**	**4.77**	**25.3**	**5.867**	**33**	**6.97**	**37.7**	**7.63**
	SE	**2.19**	**0.186**	**0.333**	**0.203**	**0.577**	**0.088**	**0.882**	**0.186**
Cocoa butter	**smooth**								
		18	1.5	19	1.8	27	3.6	33	4.5
		19	1.6	22	1.9	31	3.8	36	4
		18	1.7	21	2	26	3.4	32	4.1
	mean	**18.3**	**1.6**	**20.7**	**1.9**	**28**	**3.6**	**33.7**	**4.2**
	SE	**0.333**	**0.058**	**0.882**	**0.058**	**1.528**	**0.116**	**1.202**	**0.153**
Gelucire 39/01	**Terrible**								
		28	2	32	2.7	42	6.6	56	6.5
		29	2.3	33	2.6	46	7.1	62	7.5
		33	2.5	31	2.8	49	6.8	66	7.3
mean		**30**	**2.267**	**32**	**2.7**	**45.7**	**6.83**	**61.3**	**7.1**
SE		**1.528**	**0.145**	**0.577**	**0.058**	**2.03**	**0.145**	**2.91**	**0.306**
PEG1000	**Terrible**								
		64	2.9	68	3.1	59	5.5	65	5.7
		65	3.3	72	3.7	65	5.6	68	6.8
		69	3.1	70	3	68	6.2	63	6.6
	mean	**66**	**3.1**	**70**	**3.27**	**64**	**5.77**	**65.3**	**6.37**
	SE	**1.528**	**0.116**	**1.15**	**0.219**	**2.65**	**0.219**	**1.45**	**0.338**

Three tablet formulations containing either cocoa butter, PEG 1000 or gelucire 39/01, respectively were prepared.

Formulation:

Mannitol powder 4.7g
Pruv 0.05g
Amberlite 0.1g
Glycine 0.25
Cherry flavors 0.1
Sucrose 15% solution (1ml)

Mannitol powder was granulated using a 15%-sucrose solution. Cocoa butter, PEG or Gelucire 39/01 was melted using 42°C and then mixed with granules, disintegrants, flavors, and lubricants. Finally, the whole mixture is compressed into a tablet, 0.25g.

All tablet formulations are listed in Table 2.9.

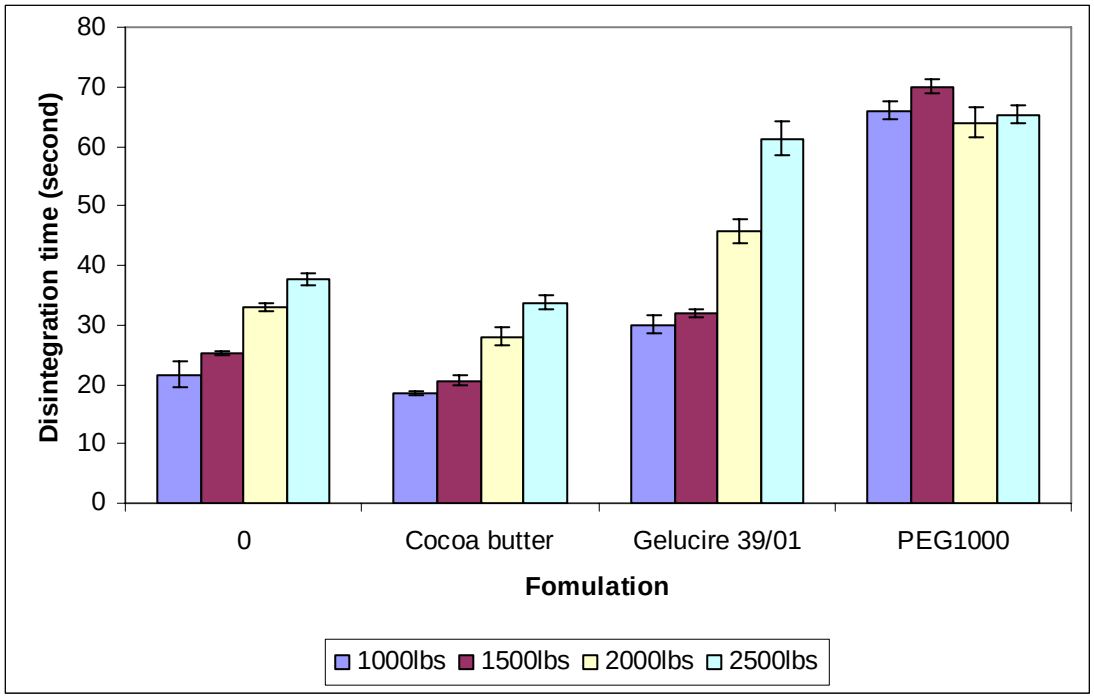

Figure 2.29. The disintegration times of tablet formulations containing low-melting-point waxes

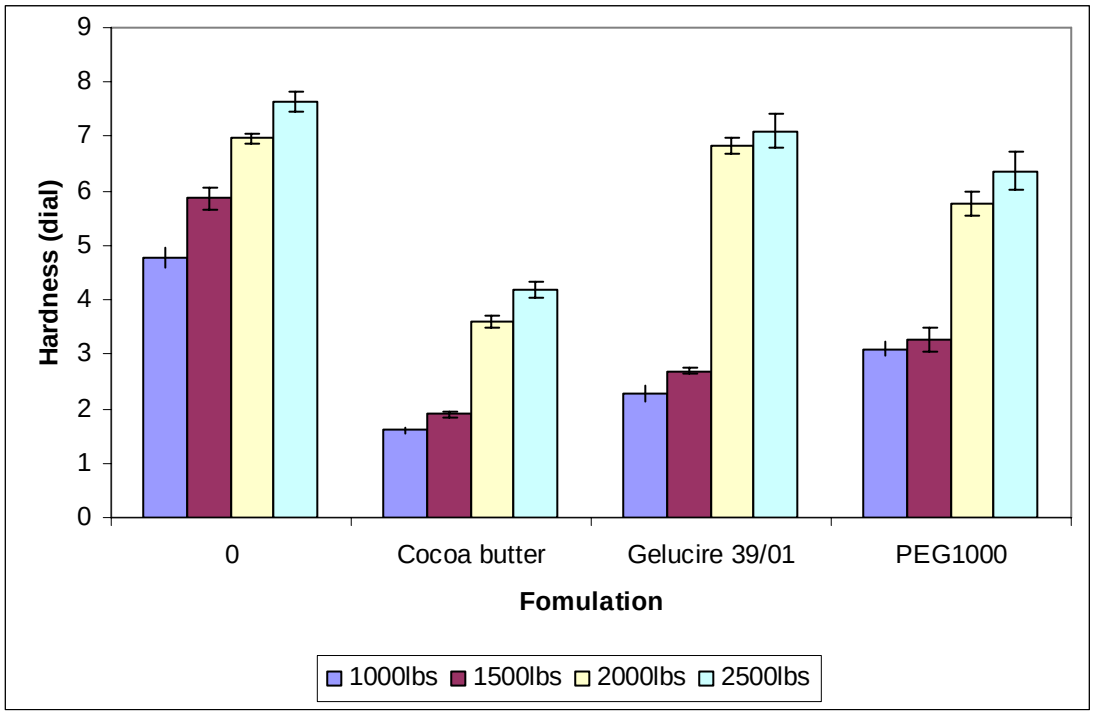

Figure 2.30. The hardnesses of tablets containing low-melting-point waxes

Cocoa butter added good taste to the tablet. Thus, a tablet with a low hardness but a good taste might be another choice for formulators. The other excipients gelucire 39/01 and PEG 1000 did not produce satisfactory results in either the taste or hardness criteria. Cocoa butter melted very fast and reduced the disintegration time significantly; however, the hardness of the tablet dropped sharply.

The rate of melting of gelucire, or PEG 1000 was not rapid enough to reduce the disintegration time. The semi-solid that gelucire and PEG forms at room temperature prevents the activity of disintegrants; thus, the disintegration time is longer than expected.

Cocoa butter exists naturally in several polymorphism: α, γ, β', and β crystals with melting-point temperatures of 17, 23, 26 and 35-37^{o}C respectively. By heating cocoa butter to high temperatures, the β form transforms to other crytalline forms with

lower melting points. When cooled at room temperature, α, γ, β' gradually transitions back to β form. To test the effects of elevated temperature on the cocoa-butter polymorphism, the compressed tablet was kept at room temperature in a hermitically-sealed container to prevent tablet exposure to humidity for one week. The disintegration time and the hardness of the tablet were then compared to initial values.

Table 2.10. The efffect of cocoa butter on tablet-disintegration time and hardness with and without one-week curing

Sample	**Pressure 1000lbs** (Cocoa butter no curing)		**Pressure 1000lbs** (Cocoa butter after curing)		**Pressure 2000lbs** (Cocoa butter no curing)		**Pressure 2000lbs** (Cocoa butter after curing)	
	Time (sesond)	Hardness (dial)	Time (sesond)	Hardness (dial)	Time (sesond)	Hardness (dial)	Time (sesond)	Hardness (dial)
1	18	3	18	3.3	29	4.8	31	5.3
2	19	3.2	20	3.3	31	4.5	32	5.6
3	20	2.9	21	3.8	31	5.4	28	4.5
4	17	3.1	20	3.7	32	5.1	27	4.6
5	16	3	17	3.9	27	5.2	32	6
Mean	**18**	**3.0**	**19.2**	**3.6**	**30**	**5**	**30**	**5.2**
SE	**0.070**	**0.051**	**0.735**	**0.127**	**0.894**	**0.158**	**1.049**	**0.288**

The data in Table 2.10 shows that there is an increase in the hardness of the tablet upon one week storage, but the increase is not significant. Two sample t-test applied to tablets made under pressures 1000 lbs and 2000 lbs show that there is no difference between the original tablets or cured tablets even though the mean values for the tablet hardness and disintegration times are higher after curing. The data suggests that the β form of cocoa butter did not transform to a significant extent of polymorphic forms if the temperature was not raised too high and for a short of time.

Effects of Effervescent Materials

Effervescence consists of the mixing of an acid with a salt of carbonic acid, i.e. sodium bicarbonate, into a tablet and placing the tablet in water. The effervescent materials, the acid and the salt of carbonic acid, react in the water and release carbon dioxide that bursts out and the resulting eruption of the carbon dioxide gas causes the tablet to disintegrate in a short period of time. Nevertheless, the presence of the salt in carbonic acid salt and acid can alter the taste of the tablet. Acid increases the sour taste; sodium salt provides a salty taste. The adding of a small amount of effervescent materials to tablets were tested both for their effect on tablet disintegration time and taste of the tablet.

Two formulations containing the same excipients except that one had effervescent materials. The ingredients are listed in Table 2.11.

Tablet A:

Melatonin	5mg or 10mg
Maltose 5% 2ml	
Sucralose 0.5%	0.025g
Glycine 6%	0.3g
Pruv 1%	0.05g
AmberliteTM 3%	0.15g
Polyplasdone XL 3%	0.15g
Cherry flavors 2%	0.1g
Mannitol 85%	4.25g

Tablet B:

Melatonin	5mg or 10mg
Maltose 5% 2ml	
Sucralose 0.5%	0.025g
Glycine 6%	0.3g
Pruv 1%	0.05g
AmberliteTM 3%	0.15g
Polyplasdone XL 3%	0.15g
Cherry flavors 2%	0.1g
Mannitol 79%	4.17g

NaHCO3 1%	0.05g
Citric acid 0.5%	0.03g

The whole mixture was compressed into a tablet 0.2g

Table 2.11. The effects of effervescent materials on disintegration time and hardness of tablet

		Effervescent substance	**Pressure 1000lbs**	
	Sample		Time (second)	Hardness (dial)
A	1	0	20	4
	2		22	4.5
	3		21	4.2
		mean	**21**	**4.23**
		SE	**0.333**	**0.084**
B	1	NaHCO3+ Citric acid	18	4.5
	2		17	4.5
	3		18	4.8
		mean	**17.7**	**4.6**
		SE	**0.193**	**0.058**

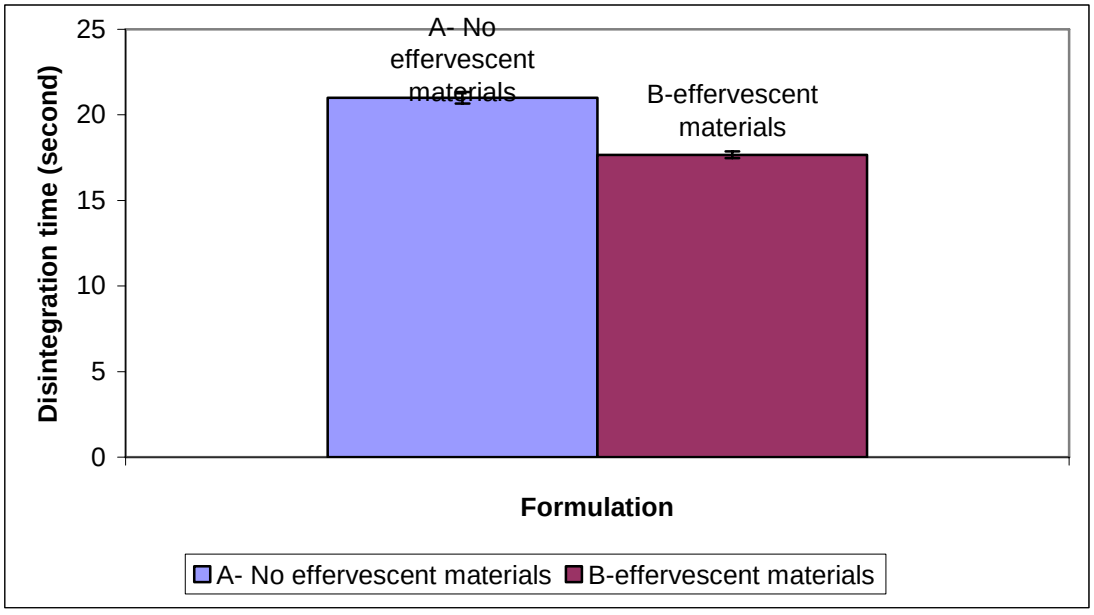

Figure 2.31. The disintegration times of formulations containing effervescent materials versus those not containing effervescent materials

The tablet containing effervescent materials produced a significantly shorter disintegration time, two-sample t tests, $p<0.01$; whereas, the hardness of the tablet did not change, $p>0.1$.

MELATONIN AND ACETAMINOPHEN STANDARDS

Standard solution of melatonin

Since melatonin is unstable under non-sterile condition, a stock solution of melatonin was prepared in ethanol for whenever standard solutions were needed, due to its instability in non-sterile solutions. Three standard solutions of melatonin were prepared of 100μg/ml and measured by UV-VIS on a spectrophotometer within 24 hours as the references for melatonin dissolution study.

Standard curve of acetaminophen

A stock solution of acetaminophen was prepared of approximately 100 μg/ml. From the acetaminophen stock solution, a range of acetaminophen solutions were prepared ranging in concentration of 1 to 50 μg/ml. The acetaminophen concentrations and the absorbances of a standard curve is listed in Table 2.10. The linear-regression fitting and the R^2 is shown on Figure 2.32.

The UV-VIS spectrophotometric method was validated for accuracy and precision. “Accuracy”: To evaluate the accuracy of a method, a mixture made with known quantities of samples and a known quantity of the component (acetaminophen) was mingled together into one solution. The measured amount of the sample component after subtracting the known amount of the drug in the sample must lay within 99-101% of the original component quantities.

Table 2.12. Acetaminophen concentrations and respective absorbance of the standard solutions

Number	Concentration (μg/ml)	Absorbance
1	1.008	0.0685
2	2.016	0.1347
3	3.024	0.2025
4	5.04	0.3346
5	10.08	0.672
6	15.12	1.0066
7	20.16	1.3446
8	30.24	2.0154
9	50.4	3.3017

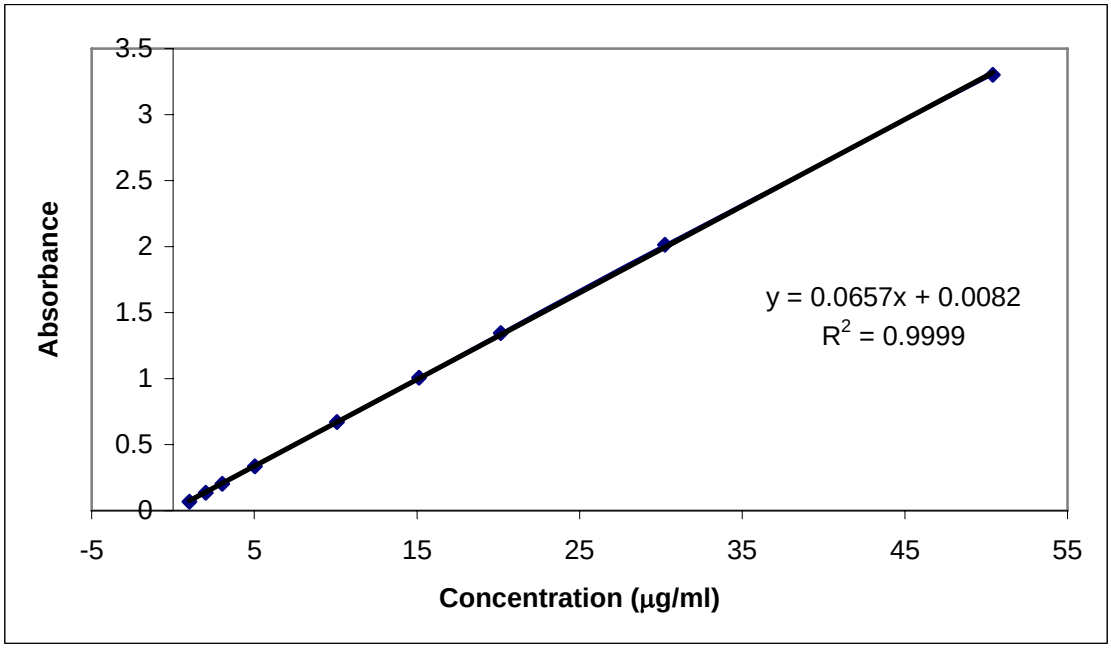

Figure 2.32. The standard curve of acetaminophen within the linear range

"Precision": precision refers to the *repeatability* of the results of a sample running with the same method over a short time, *intermediate precision* for a long time.

The standard curve was repeated three times to evaluate the precision and the linearity of the curve. The linearity also showed the accuracy of the method.

For a standard curve to reflect an intermediate precision, the standard curve should be repeated several times and provide the same precision for 4 months.

THE COATING CORE OF ACETAMINOPHEN

To improve the taste of the ODT's, the desirable beads size should be minimized to as small a size as possible. Within the lab scale, the smallest size bead the extruder can produce is around 20 mesh size. The core of the beads must also be strong enough to withstand the coating process. The recommended core bead formulations are presented in Table 2.11.

Excipients such as Avicel pH 102, Polyox^{TM} WSR N80 in the core beads provide several roles such as that of binders and diluents. Avicel is a strong binder without being sticky after wet granulation producing physically stable beads. Avicel PH 102 has excellent properties that enhance the production of smooth spheroids beads that arew ready for coating. Avicel PH 102 also creates the adequate hardness for the beads so they withstand the coating process. Polyox^{TM} WSR N80 is a hydrophilic polymer that soluble in water. At high concentrations in core beads, there is an increased possibility the polymer will cause stickiness and hinder the granulation process. A small amount of Polyox^{TM} WSR N80 increases the binding in beads and combines acetaminophen and other excipients into a homogenous mixture in the beads.

The dissolution profiles of three core beads reveal that acetaminophen releases quickly from the core beads. Stearic acid slightly delays the release of the drug since it is a lipophillic agent, and it hinders water penetration. Stearic acid also acts as a

plasticizer since stearic acid is lipophilic and it increases elasticity in the beads. Stearic makes the beads softer when wetting, but dry beads are sufficiently hard with stearic acid levels under 5%.

Table 2.13. The ingredients used for three different core beads

Ingredient	Core 1	Core 2	Core 3
Acetaminophen	65	70	70
Avicel pH 102	30	25	20
Polyox™ WSR N80	5	5	5
Stearic acid	0	0	5

Drug released from all three beads are displayed in Table 2.13 and Figure 2.33

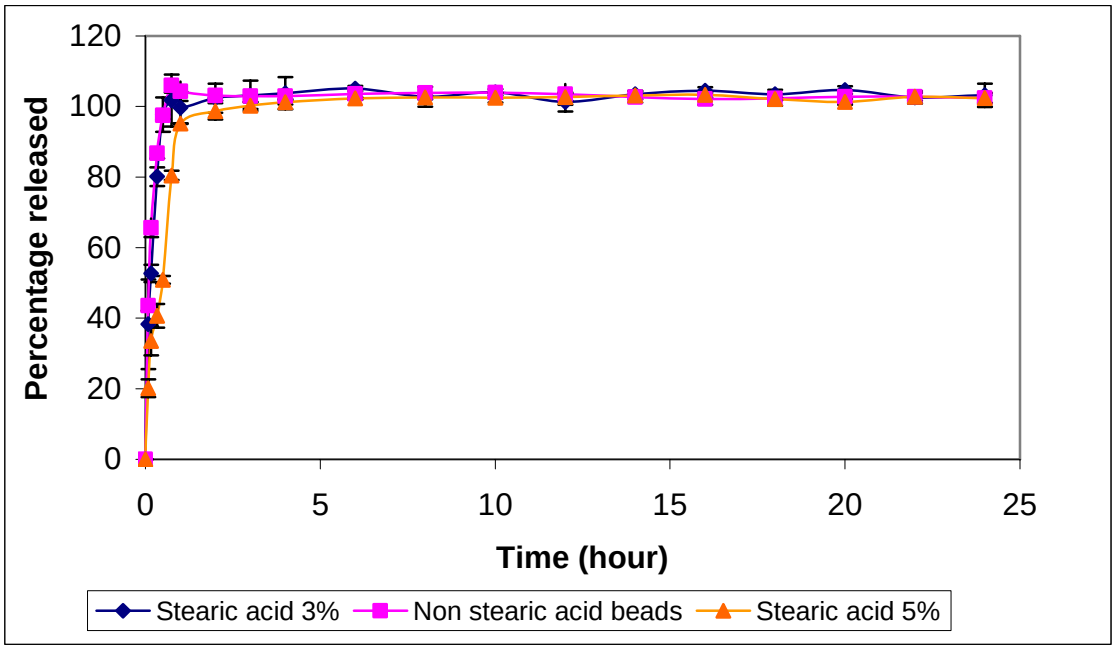

Figure 2.33. The dissolution profiles of acetaminophen from three core beads

All the core beads were hard enough for the coating process in a fluid-bed coating machine with less than 1% of the beads breaking off after 6 hours of coating.

Table 2.14. The dissolution of acetaminophen from three different core beads

Time (hour)	Non stearic beads' release (%)	3% stearic beads' release (%)	5% tearic beads' release (%)
0	0	0	0
0.083333	43.56	38.281	20.14
0.166667	65.592	52.678	33.56
0.333333	86.767	80.116	40.65
0.5	97.506	97.712	50.89
0.75	105.969	101.716	80.457
1	104.296	99.683	95.145
2	103.138	102.356	98.65
3	102.965	103.064	100.23
4	102.932	103.751	101.23
6	103.527	105.086	102.32
8	103.833	102.729	102.568
10	103.876	103.987	102.475
12	103.422	101.299	102.654
14	102.666	103.489	103.147
16	102.112	104.472	103.254
18	102.331	103.506	102.142
20	102.736	104.663	101.254
22	102.776	102.602	102.776
24	102.410	103.175	102.410

THE EFFECTS OF SURELEASE ON DRUG RELEASE FROM THE CORE BEADS

Surelease dispersion-coating levels in water, Formula No: E-7-19010 consists of ethyl cellulose, oleic acid, and dibutyl sebacate. Two later substances are plasticizers used to lower the glass transition temperature of ethyl cellulose.

Ethyl cellulose which impedes water permeation through it has a glass-transition temperature lower than 50^{o}C when mixed with oleic acid and dibutyl sebacate. This temperature is ideal for temperatures inside a fluid-bed spray coater.

A range of coating thickness of surelease as a measurable weight gain was applied to the coated beads. The all had the same core:

Acetaminophen: 65g
Avicel PH 102: 30 g
Polyox: 5g
Layer 1: HPMC 8.5% weight gain
Layer 2: surelease

The effects of the surelease coating levels that retard water penetration that will dissolve the drug in the core beads are presented in Table 2.15. The dissolution profiles are in Figure 2.34.

Table 2.15. The percentage acetaminophen released from surelease coated beads

Time (hr)	Surelease 15.2%	SE	Surelease 12.2%	SE	Surelease 7.5%	SE	Surelease 8.3%	SE
0	0	0	0	0	0	0	0	0
0.083333	0	0	1.026	0.649	1.845	1.038	3.778	1.168
0.166667	0	0	3.050	0.460	3.758	0.831	5.139	1.444
0.333333	0.107	0.084	2.365	0.656	5.554	1.331	8.917	2.216
0.5	0.289	0.105	2.517	0.697	7.099	1.781	13.104	2.587
0.75	0.672	0.170	3.175	0.770	8.647	1.891	16.118	4.422
1	1.041	0.171	3.928	0.840	11.030	1.870	18.318	2.441
2	2.742	0.298	6.022	0.747	16.006	2.418	24.174	4.850
3	4.135	0.504	8.211	0.808	21.106	2.429	28.836	4.533
4	5.479	0.455	9.716	1.010	26.099	2.333	33.095	4.812
6	8.029	0.612	12.874	1.138	34.015	2.561	38.526	8.710
8	10.103	0.709	16.372	1.094	42.246	2.199	44.289	3.023
10	11.657	0.734	18.458	2.250	47.434	2.232	48.413	3.013
12	12.846	0.783	21.295	1.182	53.133	2.164	52.115	2.108
14	14.140	0.831	23.558	0.871	54.564	3.011	55.381	1.963
16	15.234	0.772	25.724	1.148	60.049	1.919	56.979	1.848
18	16.098	0.808	27.557	1.954	63.368	2.170	58.971	2.057
20	17.135	0.819	29.580	2.644	71.002	1.921	61.403	2.318
22	17.719	0.769	32.358	2.313	71.127	1.928	63.551	2.368
24	19.121	1.007	32.825	0.597	70.475	1.927	64.744	1.929

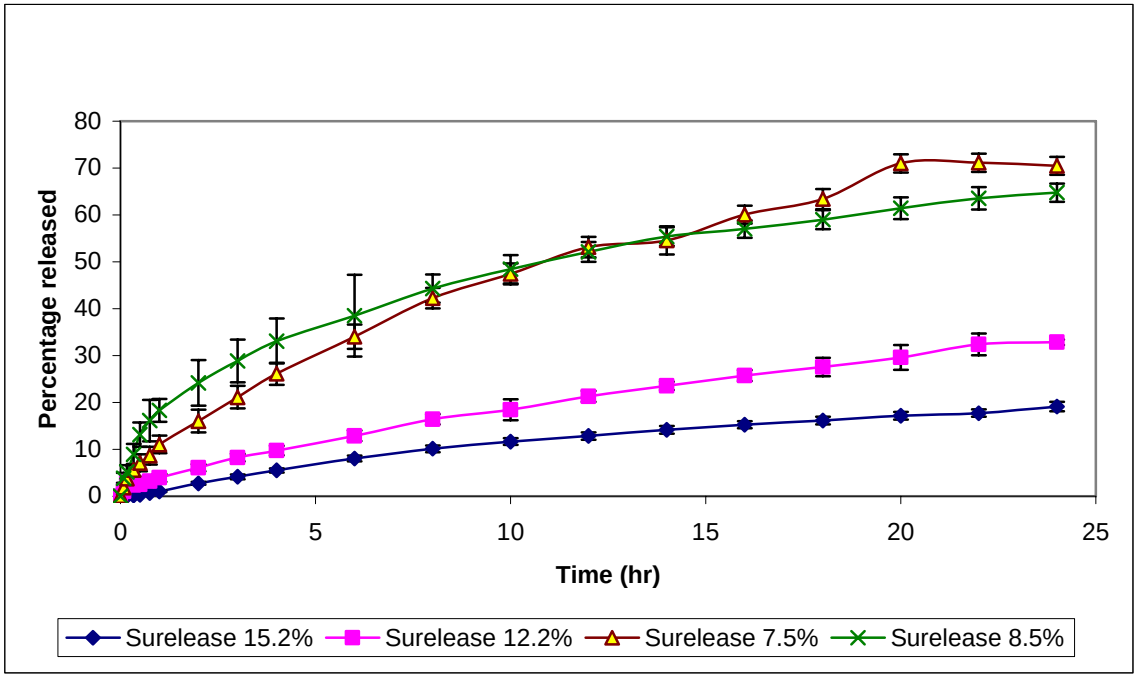

Figure 2.34. Dissolution profiles of acetaminophen from coated beads with different levels of the coating with surelease

At a high weight gain, the small particles of ethyl cellulose, that impinge on the surface core beads during spray coating, create a complete membrane around the core beads when placed under heat. This is due to the high temperature in the fluid-bed spray coater as the temperature rises above the glass transition temperature of ethyl cellulose. Acetaminophen diffuses through the membrane coating of the beads following the Fick's-law of diffusion. The drug-diffusion profiles may closely follow zero-order kinetics under certain conditions. With less weight gain, the coating layer does not cover the entire surface of the beads. Water can then be absorbed readily from the outside and into the beads and, thus, dissolve the drug. The dissolution profiles diverge from zero order kinetics.

The fitting-power-law equation: $y = kx^n$ using the non-linear regression method.

Table 2.16. Power law fitting with different surelease weight gain

Parameter	Surelease 7.5%	Surelease 8.5%	Surelease 12.2%	Surelease 15.5%
k	18.0182 ± 0.5359	11.8975 ± 0.5594	4.0122 ± 0.1481	2.1031 ± 0.1895
n	0.4140 ± 0.0112	0.5810 ± 0.0170	0.6677 ± 0.0132	0.7053 ± 0.0320

The "n" values increase as weight gain of Surelease on to the beads increases and approaches 1.The closer n approaches to 1, the closer the drug release is to zero-order kinetics. A compromise takes place between the ratio of the amount of surelease applied to the beads and the amount of beads necessary to obtain a desirable drug release. Since the beads used in this study are small, the surface area of the beads is large, a high weight gain is thus predicted for the coating beads.

SUBCOATING LAYER

As the Ayres et al.'s patent indicates [82], hydrophilic gel-forming materials can be used as self-sealing agents in coated beads to prevent the drug leaking out from cracks produced in the beads during the high-pressure compression of the tablet formation. The protecting mechanism of the subcoat is presented in Figure 2.35.

When coated beads are placed in with excipients and compressed into tablets, cracks occur in the coating surrounding the beads. The cracks allow water to penetrate readily and release the drug as though no coating had been applied. A subcoating material has been applied so that when the water enters the bead, the subcoating material swells and seals crack sites in the beads. This subcoating reseals the coating

and maintains the sustained-release characteristics of the coating surrounding the beads.

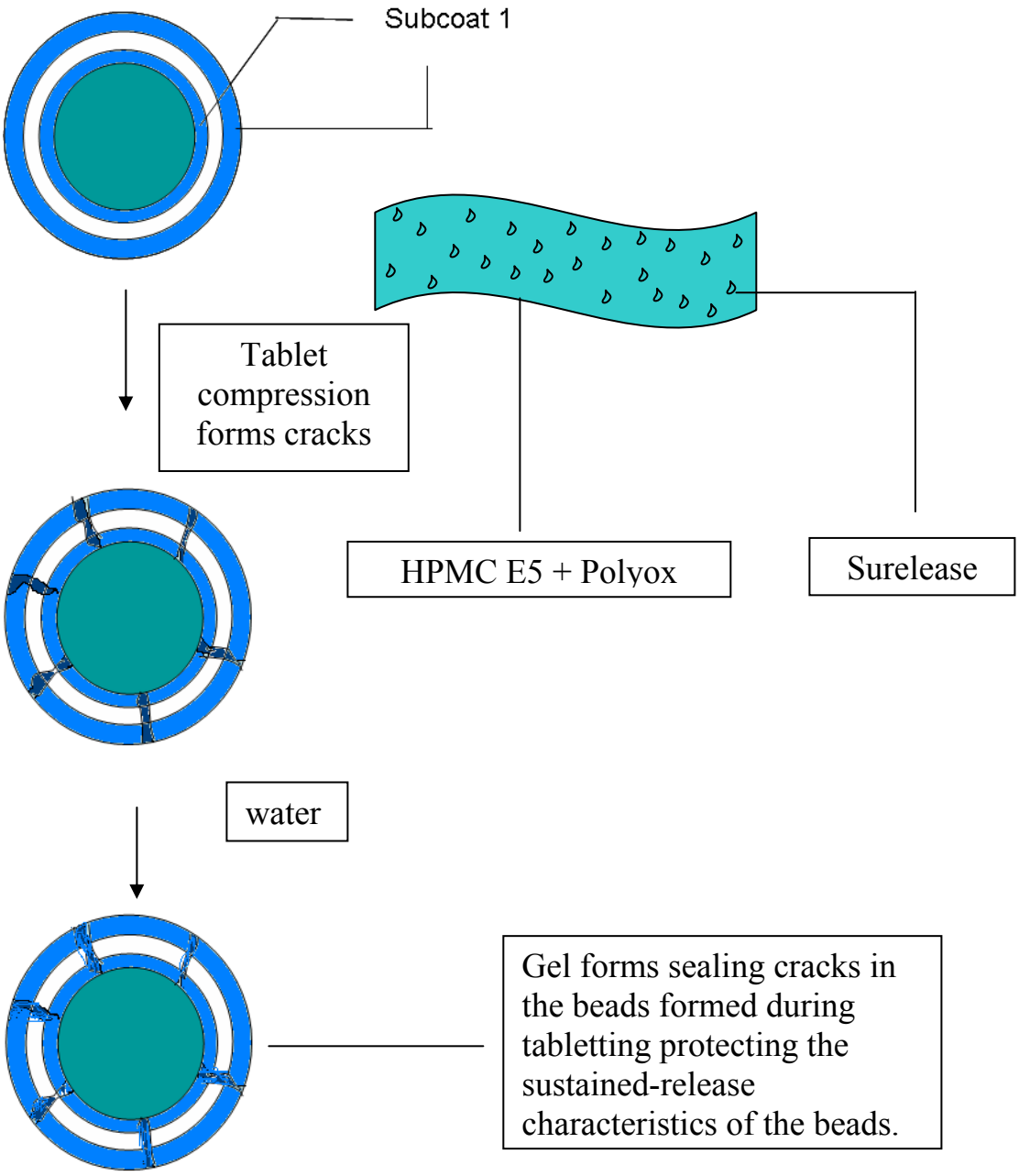

Figure 2.35. Hydrophilic gel polymers create a gel to protect compressed beads

The protecting of the sustained-release characteristics of the beads depends on the rate the gel forms and the viscosity of the gel layer formed. The polymer must

create the gel quickly. Hydrophilic polymers that produce a high viscosity when dissolving in water were preferred. HPMC, Polyox™ WSR N80 can form gels quickly. However, a high molecular weight that produces a high viscous polymer in water causes difficulty in the coating process. The polymer must be dissolved in water at low concentrations and the coating process in the fluid-bed-spray coater was performed slowly with low spray flow rate. A mixture of high-viscous polymer and low viscous polymer at a ratio that faciliates spray coating and can produce the viscosity that is high enough to protect sustained release characteristics of the beads is desirable. The ratio HPMC E5 and Polyox™ WSR N80 at 2:1 is suitable for the coating process.

To investigate the effect of various polymers on their ability to coat beads and maintain the sustained release characteristic of the beads after tabletting has disrupted the coated beads, a number of formulations were prepared, and the beads were compressed into a tablet under 1000lbs pressure.

The core beads: Acetaminophen: 65g
Avicel PH 102: 30 g
Polyox: 5g

Table 2.17. Polymer tested as sealing agents for coated beads

Formulation	Layer 1	Layer 2	Layer 3
1	HPMC E10 8.4%	Surelease 6.3%	
2	HPMC E10 8.4%	Emulsified wax 4%	Surelease 3.3%
3	HPMC E10 8.4%	Stearic beads 4%	Surelease 4%
4	HPMC E10 8.4%	PEG 5%	Surelease 7%
5	HPMC E10 8.4%	PEG 5%	Surelease 7%, then stearic acid 5%

The dissolution of acetaminophen from coated beads is displayed in Figure 2.36.

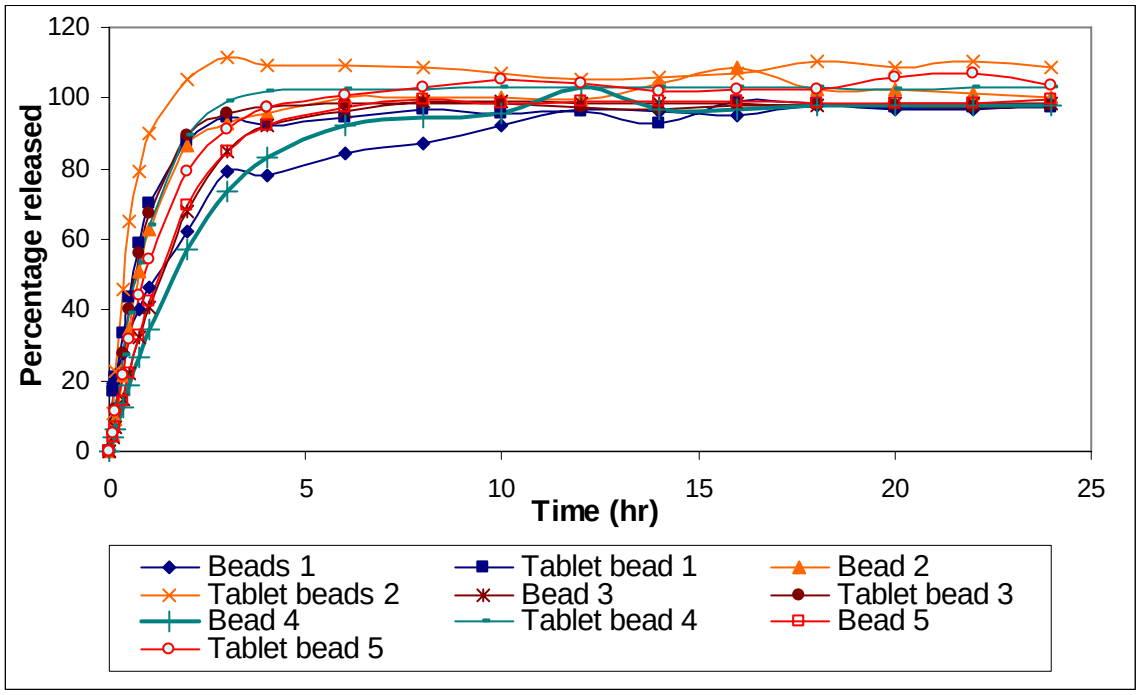

Figure 2.36. The sealing effect of some coating agents on acetaminophen-loaded beads

PEG and emulsified wax do not protect the sustained-release properties of the beads in the tablet. Adding stearic acid to the outer-coating layer improved the durability of the beads.

To investigate the sealing effect that various coating materials have in resealing ethyl cellulose coats on beads, 6 formulations with or without a sealing layer were prepared and compressed into tablets. The beads were compressed into tablets under a range of pressures 500lbs, 1000lbs, 200lbs, 3000lbs, 3500lbs.

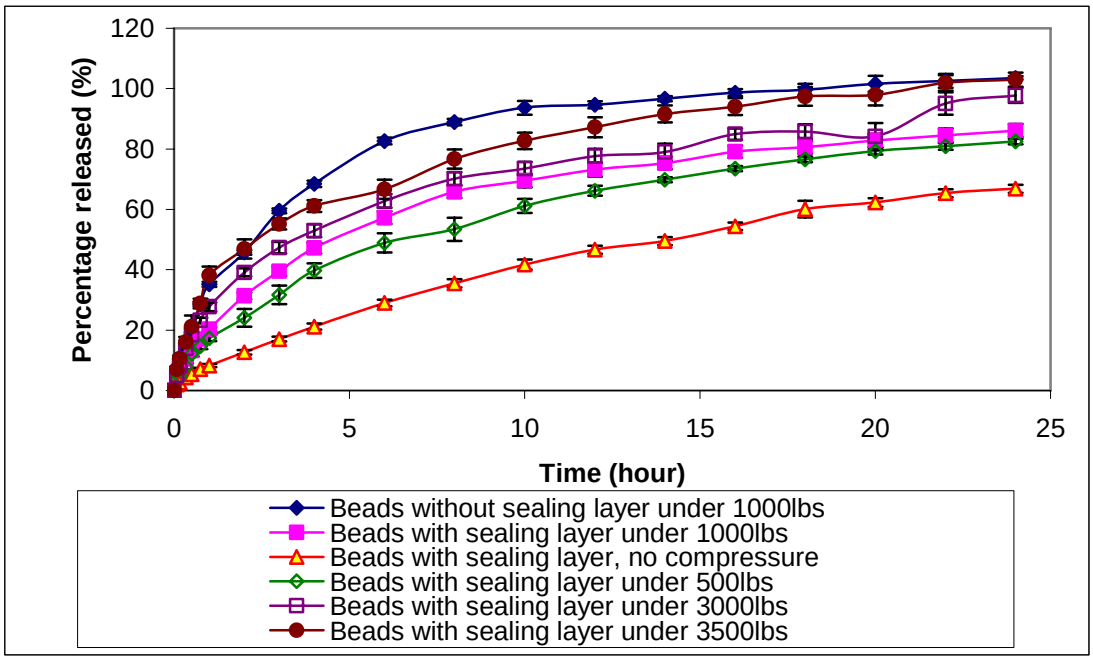

Figure 2.37. Effects of compression pressure on the ability of the sealing sub-coat to reseal beads and maintain the sustained action of the coated beads in releasing acetaminophen

Formulation:

Core beads:

Acetaminophen: 70g
Avicel PH 102: 20 g
Polyox: 5g
Stearic acid: 5g

Coating layer 1: HPMC E5 9%+Polyox 4.5%
Coating layer 2: Surelease 38ml, weight gain is 9.2%
Coating layer 3: E5 3.6g+20ml surelease
Coating layer 4: Kolicoat® IR 2.5g + mannitol 2.5g

The results are shown in Figure 2.37.

Sealing beads compared to non-sealing beads

Power-law fitting by sigma plot render the final n values of 0.3814 for non-sealing-coating layer beads and 0.4235 for sealing-coated beads.

Table 2.18. Power-law fitting for beads under different pressures

Parameter	w/ sealing, no compression	w/o sealing 1000lbs	w/ sealing 500 lbs	w/ sealing 1000lbs	w/ sealing 3000lbs	w/ sealing 3500lbs
k	9.126 ± 0.352	33.598 ± 2.831	19.173 ± 0.884	24.085 ± 1.473	28.614 ± 1.326	34.082 ± 1.456
n	0.641 ± 0.018	0.381 ± 0.032	0.478 ± 0.017	0.424 ± 0.023	0.390 ± 0.018	0.365 ± 0.016

Since the formula $y = kt^n$ can be converted into log transformation:

$$\log(y) = \log(k) + n\log(x)$$

The log(k) and n have a normal distribution. Confidence interval (CI) 95% of "log(k)" value of w/o sealing 1000lbs: log(33.598) ± $t_{18,0.975}$ * log(2.831) = 3.514 ± 2.101*1.041 =3.142 ↔ 6.656. Convert back to log transformation CI 95% of k is 23.142↔777.513. This CI 95% does not include "n" value of w/ sealing 1000lbs

CI 90% of "n" of w/o sealing 0.381 ± 2.101*0.032 = 0.381 ± 2.101 * 0.032 = 0.381 ± 0.067=-0.314 ↔ 0.448. This one does include "n" values of w/ sealing. The data of Table 2.18 shows there is statistically significant difference in k values of the sub-coat layer protecting the sustained-release characteristics of beads from compression forces of tabletting, but the n values are not significantly different.

Compression effects on sealing beads

Under 3500lbs, CI 95% "log(k)" value of sealing beads is log(34.082) ± $t_{18,0.975}$*log(1.456) = 3.529 ± 2.101*0.376 = 3.529 ± 0.789 = 2.740 ↔ 4.318. Convert back to log transformation CI 95% of k is 15.484 ↔ 5.023.

CI 95% of "n" value is 0.365 ± 2.101*0.016 = 0.330 ↔ 0.399. The CI95% does not include the n value of n under1000 lb.

Tablets formed with high-impact compression forces showed the tablet cracked remarkably. However, the beads in the tablets compressed under the force of 3000 and

3500 lbs. revealed that the beads were still less broken or cracked than the non-sealed beads compressed with pressures under 1000lbs.

Effects of stearic acid on the dissolution profile of acetaminophen from the core beads of coated beads.

Stearic acid plays a role as a binder to make the core beads stronger. The presence of stearic acid in the core beads also works as a weak-rate controlling drug-release agent in the core and delays acetaminophen release slightly from the beads, yet it does not enhance the sustained release characteristics of the beads. However, the stearic acid might provide elasticity to protect the beads.

To test the difference in drug-release profiles, two formulations, non-stearic-acid-containing beads and stearic-acid-containing beads, which produce total drug release that is similar after 24 hours of dissolution testing are investigated.

Formulation:

Non-stearic beads:

Core bead: Acetaminophen: 70g
Avicel PH102: 23 g,
Polyox: 7g
Layer 1: HPMC E5 10g + Polyox 5g + surelease 10ml
Layer 2: surelease 42ml
Layer 3: E15 3.6g+20ml surelease
Layer 4: Kolicoat® IR 2.5g + mannitol 2.5g

Stearic beads:

Core bead: Acetaminophen: 70g
Avicel PH102: 20 g,
Polyox: 7g
Stearic acid: 3g
Layer 1: HPMC E5 10g + Polyox 5g + surelease 10ml
Layer 2: surelease 36ml
Layer 3: E15 3.6g+20ml surelease
Layer 4: Kolicoat® IR 2.5g + mannitol 2.5g

Table 2.19. The percentage of acetaminophen dissolved versus time from beads containing stearic acid and beads not containing stearic acid

Time	Non-stearic beads (%)	SE	Stearic beads (%)	SE
0	0	0	0	0
0.083333	3.117	0.565	1.172	0.153
0.166667	2.401	0.432	1.268	0.161
0.333333	3.128	0.440	1.582	0.211
0.5	3.143	0.300	1.982	0.217
0.75	4.063	0.441	2.740	0.267
1	4.527	0.519	3.561	0.337
2	6.727	0.467	6.893	0.425
3	9.384	0.541	10.240	0.686
4	11.761	0.866	13.254	0.830
6	15.634	0.530	18.494	0.979
8	19.565	0.753	23.357	1.087
10	22.250	0.893	26.407	1.248
12	26.128	1.107	28.592	1.197
14	28.094	0.273	30.569	1.246
16	30.713	0.622	32.558	1.193
18	33.251	1.257	34.418	0.956
20	35.063	1.137	36.290	1.255
22	38.250	1.547	37.507	1.176
24	39.798	1.575	39.202	1.181

From the dissolution profiles in Table 2.19 and Figure 2.38, stearic acid in the core beads provides a better linear drug-release pattern than beads not containing stearic acid.

After 24 hours of dissolution testing, the two formulations released about 40% of the drug loaded in the beads. However, the dissolution profiles of the two formulations were different. The acetaminophen-dissolution curve of the beads containing stearic acid was close to zero-order compared to the curve for the formulation not containing stearic beads.

Fitting the data of drug release from the dissolution curves to the power law equation supports this observation. The “n” value of the beads not containing stearic acid is smaller than that of the stearic-acid-containing beads. To obtain the same rate

and amount of the drug release over time, the formulation having core beads that did not have had stearic acid should have more of the rate-controlling polymer, surelease, applied to its beads.

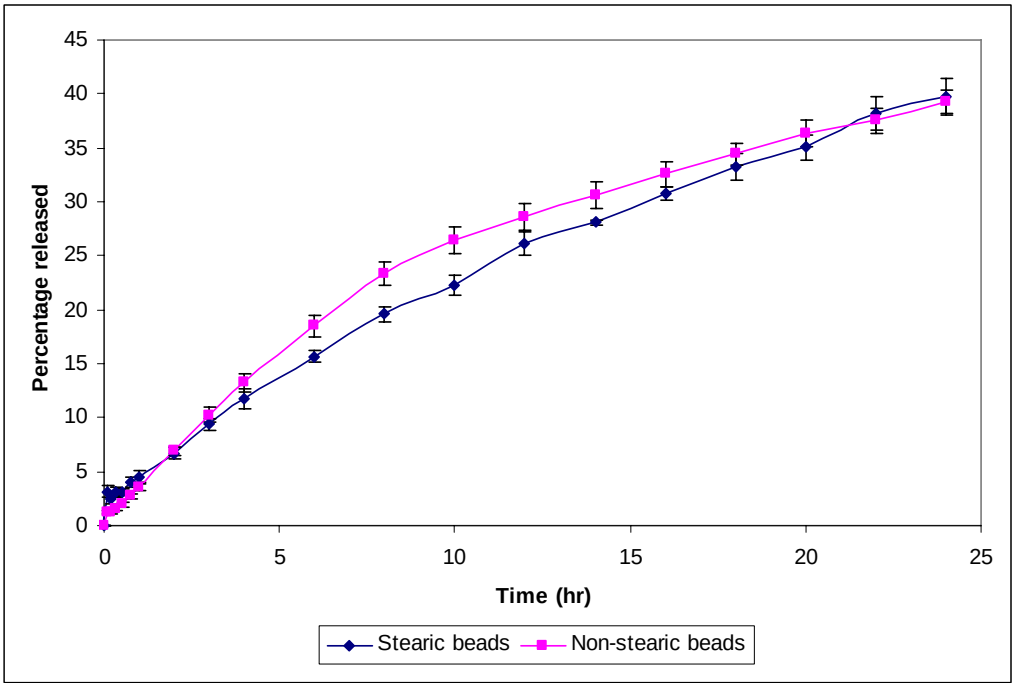

Figure 2.38. The dissolution profiles of acetaminophen release from stearic acid containing and non-stearic acid coating beads

Table 2.20. Power-law fitting acetaminophen-dissolution parameters of stearic-acid-containing beads and non-stearic- acid-containing beads

Parameter	Stearic acid beads	Non Stearic beads
k	4.813 ± 0.195	5.679 ± 0.444
n	0.667 ± 0.014	0.624 ± 0.028

The log(k) and n have a normal distribution. CI 95% of "k" value of stearic beads is $\log(4.813) \pm t_{18,0.975} * \log(0.195) = 1.571 \pm 2.101 * (-1.637) = 1.571 \pm (-3.440) = -1.869 \leftrightarrow 5.011$. Transform back to normal scale, CI 95% is $0.154 \leftrightarrow 150.061$ does not include "a" value of non stearic acids beads.

CI 95% of "n" value of w/o sealing is 0.667 ± 2.101*0.014 = 0.667 ± 0.030 = 0.637 ↔ 0.698. This CI 95% does not include the value of stearic sealing beads.

All the parameters obtained by fitting the dissolution curves to the power law equation for the two formulations are significantly different. This implies that beads containing stearic acid produce drug dissolution profiles closer to zero order release due to its hydrophobic nature and flexibility.

TASTE MASKING LAYER

As Brown et al. stated, the taste of the oral product is more important than the speed of the disintegration of an ODT [60]. This implies the importance of the tablet's taste to patients. For melatonin tablets, sweeteners and flavors can improve the taste of the tablet. For the ODT of acetaminophen, besides the taste, the surface of the sustained beads have an important additional impact on the taste of the whole tablet. The beads must be small, smooth, and sweet.

The lowest limit to prepare beads in the lab is a 20 mesh screen size that is small enough for the patients to accept the beads without difficulty in swallowing and having an unpleasant mouthfeel.

Coating the beads with a low viscosity polymer mix that includes a sweetener might be a good choice. An insoluble ethyl cellulose coating reduced the unpleasant taste of the beads but the surface was rough. An additional masking layer was necessary to improve the taste and feel of the beads' rough surface.

The beads were coated with an outermost layer of HPMCE5, E15 or Kollicoat® IR as the polymer coating, but they had sugar added to improve the taste.

Table 2.21. Trial polymers and sweeteners for the taste masking layer

Polymer	Sweeteners	Taste
Ethyl cellulose	0	Un pleasant, no sticky
Stearic acid	0	Neutral, no sticky
HPMC E15 2.5%	Mannitol 2.5%	Good, sticky on the tongue
HPMC E5 2.5%	Mannitol 2.5%	Good, sticky on the tongue
HPMC E15 2.5%	Mannitol 2.5%	Good, sticky on the tongue
HPMC E 2.55 %	Fructose 1%	Good, sticky and beads agglomerate
Kollicoat® IR 2.5%	Fructose 1%	Good, sticky, beads agglomerate
Kollicoat® IR 2.5%	Mannitol 2.5%	Good, smooth slippery, no sticky,

The taste test showed that the HPMC E5 or E15 produced a sticky surface on the tongue. The Kollicoat® IR solution in water had a low viscosity and could be applied easily to the surface of the beads. Mixing the polymer coating agent with mannitol provided a good taste; the addition of a sweet sugar improved the olfactory sensation of the beads in the mouth. Fructose also acted as the binder causing the beads to agglomerate during tablet compaction. Fructose also enhanced the stickiness of the beads on the tongue, even though the fructose brought sweetness to the tablet. Besides mannitol, the sacchrides' high sweetness scale could be used in small quantities as they did not alter the stickiness of the coating polymer, Kollicoat® IR.

HARDNESS AND FRIABILITY OF THE TABLET CONTAINING THE BEADS

An illustration of the difference of a tablet not containing and a tablet containing sustained release beads is given in Figure 2.39.

As described in the materials and method section, the acetaminophen tablet was prepared by adding small sustained release beads into a mixture of mannitol granules and other excipients in the ratio 1:1. Putting sustained-release beads into a tablet can alter the disintegration time of the ODT's. To investigate the impact of the sustained release beads on the disintegration time and the hardness of tablets

containing sustained release beads, two types of tablets were prepared, tablets with sustained release beads and tablets without sustained release beads.

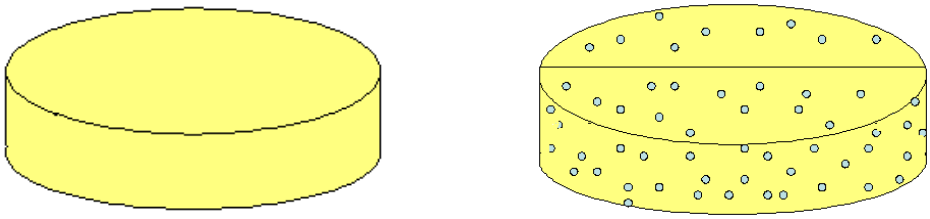

Figure 2.39. The tablets containing sustained-release beads and without sustained release beads

Tablet without the beads:

Mannitol powder 4.7g
Pruv 0.05g
Amberlite 0.1g
Glycine 0.25
Cherry flavors 0.1
Maltose 5% solution (0.5ml)

Mannitol is granulated into using a 5% maltose solution. After thoroughly mixing, other excipients were added. The mixture was compressed into various tablets with 1000 lbs, 2000lbs, 3000lbs, 3500lbs pressure. The final tablet weight was 0.8g.

To prepare the tablet with beads, sustained beads were blended with mannitol granules, an amino acid, lubricant, and a flavor.

The tablets were made by compressing the mixture under 1000lbs, 2000lbs, 3000lbs pressure. The tablets from two groups were measured for hardness, disintegration time, and friability. The results are presented in Table 2.22.

From the data, there is a convincing evidence (t test for disintegration time ($p<0.01$)) that the disintegration time of the tablets containing sustained release beads is shorter than tablets without the beads.

Table 2.22. The disintegration time, hardnesses and friability of tablets containing beads and not containing beads

Formulation			1000lbs	2000lbs	3000lbs	3500lbs
w/o beads						
1	Hardness (dial)		5.1	8.0	10	11
	Disintegration time (second)		32	35	40	21
	Friability (<1%)		passed	passed	passed	passed
2	Hardness (dial)		4.9	7.6	8.8	11.2
	Disintegration time (second)		31	35	41	45
	Friability (<1%)		passed	passed	passed	passed
3	Hardness (dial)		4.8	7.5	11	11.5
	Disintegration time (second)		30	36	42	44
	Friability (<1%)		passed	passed	passed	passed
	Hardness (dial)	**Mean**	4.933	7.7	9.933	11.233
		SE	0.088	0.153	0.636	0.145
	Disintegration time (second)	**Mean**	31	35.333	41	36.667
		SE	0.577	0.333	0.577	7.839
	Friability (<1%)	**Mean**	passed	passed	passed	passed
w/ beads						
1	Hardness (dial)		2.8	3.6	5.3	6.0
	Disintegration time (second)		22	27	33	35
	Friability (<1%)		failed	failed	failed	passed
2	Hardness (dial)		2.9	3.8	5.6	6.2
	Disintegration time (second)		23	28	32	34
	Friability (<1%)		failed	failed	failed	passed
3	Hardness (dial)		2.8	3.7	5.5	6.4
	Disintegration time (second)		21	27	34	36
	Friability (<1%)		failed	failed	passed	passed
	Hardness (dial)	**Mean**	2.833	3.7	5.467	6.2
		SE	0.033	0.058	0.088	0.116
	Disintegration time (second)	**Mean**	22	27.3333	33	35
		SE	0.577	0.333	0.577	0.577
	Friability (<1%)	**Mean**	failed	failed	failed	passed
		SE				

The hardness and friability of the tablet with the beads is much lower than that of the tablet without the beads. At 3000 lbs compression force, the tablets formed with sustained-release beads reached an adequate hardness.

Friability is a strict and difficult test that an ODT has to pass. Under pressure 3500 lbs for tablet formation, the tablet with the beads passed the friability test. However, under this high pressure, the disintegration time was longer and the number of cracked beads also increased.

The optimal formulations

The orally disintegrating tablet of melatonin

From the results obtained in the primary investigations the optimal formulation for the melatonin tablet and the acetaminophen tablet was.

Maltose	5% 0.5ml
Sucralose 0.5%	0.025g
Glycine 6%	0.3g
Pruv 1%	0.05g
AmberliteTM 3%	0.15g
Polyplasdone XL 3%	0.15g
Cherry flavors 2%	0.1g
Mannitol 85%	4.25g
NaHCO3 1%	0.1g
Citric acid 0.5%	0.06g

The melatonin was dissolved in absolute ethanol at a low concentration of 1% (w/v). The melatonin was then added into the excipients' mixture depending on the dose size of the melatonin (1mg, 3mg and 5mg). The small amount of melatonin does not affect physio-chemical properties of the tablets.

The tablet size was 0.2g and compressed into a tablet under a force of 1000 lbs of pressure. The melatonin content in each tablet was 5mg or 10mg. The disintegration

time of optimal melatonin formulation was between 18 – 20 seconds and the hardness of the tablet is around 5.5 dials.

The orally disintegrating sustained- release tablet of acetaminophen

Core Beads:

Acetaminophen	70g
Avicel	20g
Stearic acid	5 g
Polyox™ WSR N80	5g

Surelease is ethyl cellulose 25% suspension.

The core beads are coated with four layers
Layer 1: HPMC E5 10g Polyox™ WSR N80 + surelease 10ml
Layer 2: surelease 36ml
Layer 3: E15 3.6g+20ml surelease
Layer 4: Kolicoat® IR 2.5g + mannitol 2.5g

Exipients that were the same as those used for the melatonin tablets and beads were mixed together to form the tablet in a manner similar to prepared melatonin tablets. The ratio of the beads to the excipients was 1:1. The theoretical acetaminophen content in the tablets was 35%. To obtain a tablet 0.2 or 0.25g of acetaminophen, the tablet's weight had to be 0.57g and 0.72g, respectively.

The tablet was made by compressing beads and excipients under a force of 3500 lbs pressure. The disintegration time of the optimal tablet of acetaminophen was around 30 seconds and the hardness is around 6.3 dial.

SIMULATION

The dissolution profiles of optimal formulations described in the previous section were used to run the convolution to predict plasma concentration versus time profiles for melatonin and acetaminophen.

Melatonin tablet

Table 2.23. Melatonin release from an orally disintegrating tablet

time (hr)	Percentage released (%)	SE
0	0	0
0.083333	13.242	4.542
0.166667	27.654	3.541
0.333333	45.365	2.321
0.5	68.655	3.215
0.75	90.365	2.214
1	98.654	1.201
2	99.654	1.654
3	100.365	1.254
4	101.655	0.541

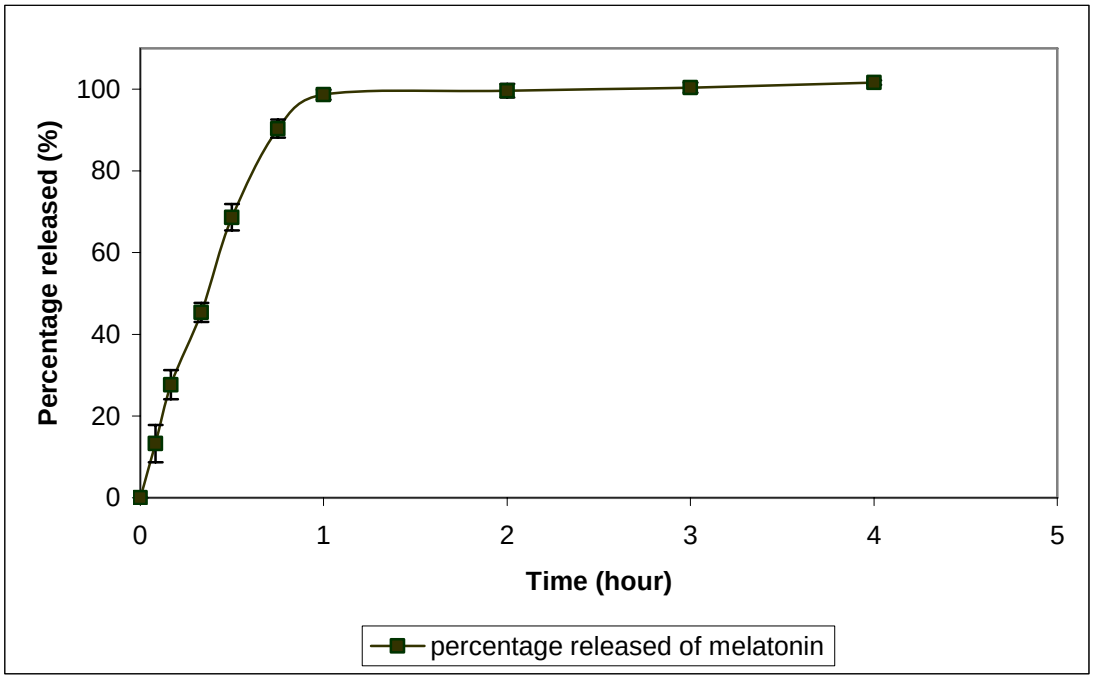

Figure 2.40. The dissolution profile of melatonin from tablets

An acetaminophen-dissolution profile of the optimal formulation produced under a compression pressure of 3500 lbs is shown in Figure 2.37.

Melatonin is an endogenous hormone not a xenobiotic, and it is administered as a supplement. To simulate exactly the melatonin plasma concentration, knowledge of both sources of melatonin is required, exogenous and endogenous sources. With limited only data for the exdogenous administration of melatonin, there is unfortunately, not enough information to properly perform a convolution for a prediction of plasma melatonin concentration. Therefore, a simulation for melatonin plasma concentrations after tablet administration was not performed.

Acetaminophen tablet

Because no published papers detailing IV administration of acetaminophen could be found, pharmacokinetic parameters for acetaminophen on IV plasma concentration versus time profiles was generated using pharmacokinetic parameters [23].

V	1L/kg
Dose	200mg
Children Weight	15kg

$$C_{\max} = \frac{D}{V} = \frac{200}{15} = 13.33$$

$$\beta = \frac{\ln(2)}{t_{1/2}} = \frac{\ln(2)}{2}$$

$$C_t = C_{\max} e^{-\beta t}$$

Dissolution profiles are of immediate release formulations of acetaminophen in Figure 2.42. Acetaminophen tablet 500mg, Lot: 7300-999-11-2, distributed by BI-

MART. Each dissolution profile will have a respective output by running a convolution.

Table 2.24. Theoretical data generated for acetaminophen-plasma concentration after IV administration

Time (hour)	Plasma concentration (mg/L)
0	13.333
0.083333	13.029
0.166667	12.731
0.333333	12.156
0.5	11.607
0.75	10.830
1	10.105
2	7.658
3	5.804
4	4.398
6	2.526
8	1.451
10	0.833
12	0.479
14	0.275
16	0.158
18	0.091
20	0.052
22	0.030
24	0.017

IV data is in Table 2.21 and Figure 2.41

All of the required input and convolution was run using a Kinetica® 2000 software package. The output, the plasma concentration versus time profile, is displayed in Figure 2.43.

The acetaminophen-plasma concentrations should be over 1mg/L. The immediate release acetaminophen tablets produced plasma concentrations above 1mg/L for 9 hours whereas the optimal acetaminophen sustained-release beads in a tablet formulation produced under a compression force of 3500 lbs produced plasma concentrations above 1mg/L for 15 hours.

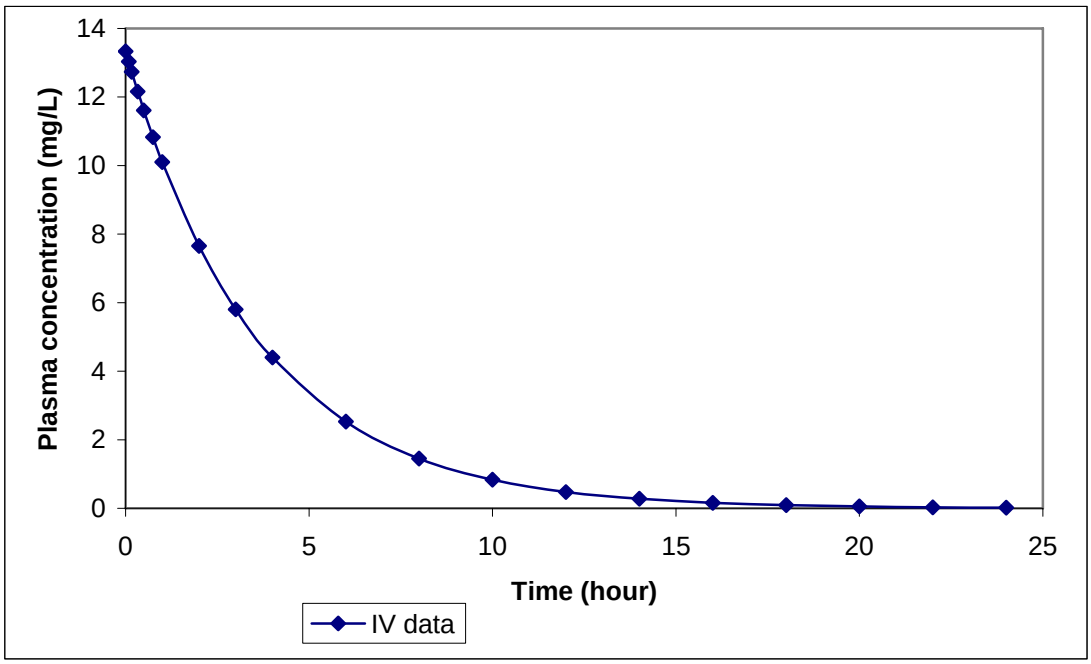

Figure 2.41. Theoretical plasma concentration after IV administration for the convolution process of acetaminophen tablets

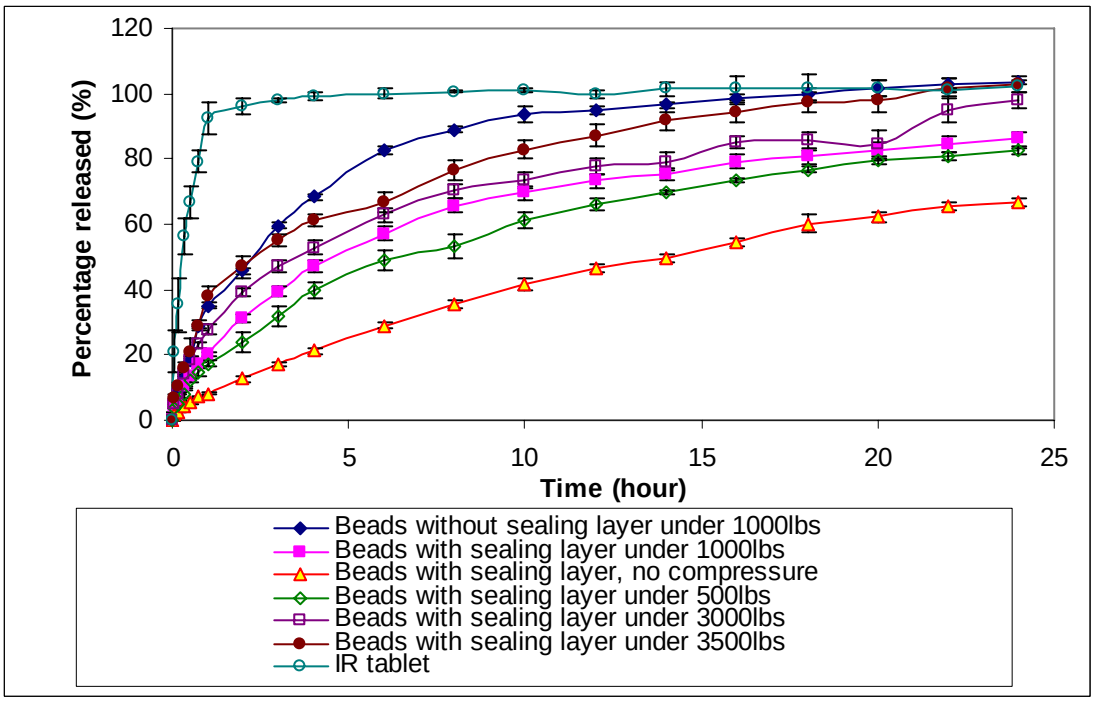

Figure 2.42. The dissolution profile of tested formulations and an IR tablet of acetaminophen

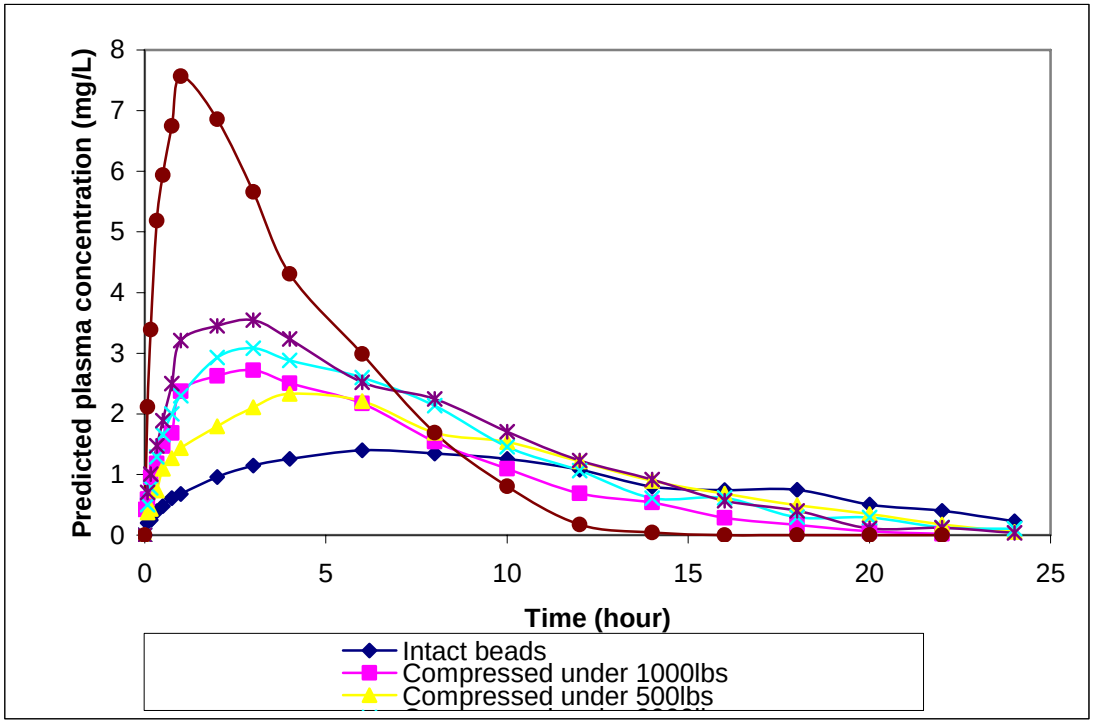

Figure 2.43. Predicted plasma concentrations of acetaminophen with different pressures

Table 2.25. Pharmacokinetic parameters from the non-compartmental analysis of acetaminophen from an IR tablet and a tablet produced under 3500lbs

Dosage form	C max (mg/L)	T max (hour)	AUC (0-24 hour) (hour*mg/l)	AUC (0-inf) (hour*mg/l)	$t_{1/2}$ (hour)	MRT (hour)	Clearance (L/hour)
Optimal Formulation	3.545	3.000	34.974	35.106	2.568	6.815	5.697
IR tablet	7.570	1.000	39.769	39.990	2.032	3.818	5.001

The pharmacokinetic parameters from the non compartmental pharmacokinetic analysis of the predicted acetaminophen-plasma concentration versus time curves reveal significant differences in pharmacokinetic parameters between the immediate-release and sustained-release acetaminophen tablets. The C_{max} of sustained-release is

less than half of the value observed in the immediate release tablet. T_{max} occured 2 hours later. Other values like half life and clearance were similar. Mean Residence Time (MRT) of the sustained-release dosage form was longer compared to the immediate release tablet.

CONCLUSIONS

To prepare an orally disintegrating tablet of melatonin with acceptable hardness and friability, a combination of two superdisintegrants and other excipients in one tablet produced a successful formulation when the tablet was compressed under a pressure of 1000lbs. The melatonin tablet's weight of 0.2g produced the shortest disintegration time.

To accomplish the goal of putting sustained release beads into an orally disintegrating tablet, the application of a high compression pressure of 3500l bs was needed to form the tablet so that it could pass the friability test and obtain the appropriate hardness. The acetaminophen tablet produced a longer disintegration time compared to the melatonin tablet due to the high compression-pressure force needed to form the tablet and the larger size of the tablet.

REFERENCES

1. Caniato R., F.R., Piovan A., Puricelli L., Borsarini A., Cappelletti E., *Melatonin in plants.* Advanced Expermental Medical biology, 2003. **527**: p. 593-597.
2. Altun A, U.-A.B., *Melatonin: therapeutic and clinical utilization.* Journal of International Clinical Practice, 2007. **61**(5): p. 835-845.
3. Boutin J., A.V., Ferry G., Delagrange P., *Molecular tools to study melatonin pathways and actions.* Trends Pharmacology Science, 2005. **26**(8): p. 412-419.
4. Muñoz-Hoyos A., B.-P.A., Avila-Villegas R; González-Ripoll M; Uberos J; Florido-Navío J; Molina-Carballo A, *Melatonin levels during the first week of life and their relation with the antioxidant response in the perinatal period.* Neonatology, 2007. **92**(3): p. 209-216.
5. Sliwinski T., R.W., Morawiec-Bajda A., Morawiec Z., Reiter R., Blasiak J., *Protective action of melatonin against oxidative DNA damage: chemical inactivation versus base-excision repair.* Mutation research, 2007. **634**(1-2): p. 220-227.
6. Liu W., Z.Y., Ma L., *The oxidative DNA damage of monocytes and its in vitro repair by melatonin in patients with tuberculous pleurisy.* Chinese Journal of Internal Medicine, 2007. **46**(3): p. 213-216.
7. Palm L., B.G., Wetterberg L., *Long-term melatonin treatment in blind children and young adults with circadian sleep-wake disturbances.* Developmental medicine and child neurology, 1997. **39**(5): p. 319-325.
8. Gupta M., A.S., Kohli K., *Add-on melatonin improves sleep behavior in children with epilepsy: randomized, double-blind, placebo-controlled trial.* Journal of Child Neurology, 2005. **20**(2): p. 112-115.
9. A. Cavallo, M.H., *Stability of melatonin in aqueous solution.* Journal of Pineal Research, 1995. **18**(2): p. 90-92.
10. Anita Cavallo, W.A.R., *Pharmacokinetics of Melatonin in Human Sexual Maturation.* Journal of Clinical Endocrinology and Metabolism, 1996. **81**(5): p. 1882-1886.
11. Lane E.A., M.H.B., *Pharmacokinetics of Melatonin in Man: First pass Hepatic Metabolism.* Journal of Clinical Endocrinology and Metabolism, 1985. **61**(6): p. 1214-1216.
12. Pontes G.N., C.E.C., Carneiro Sampaio M.M., Markus R.P., *Pineal melatonin and the innate immune response: the TNF-alpha increase after cesarean section suppresses nocturnal melatonin production.* Journal of pineal research, 2007. **43**(4): p. 365-371.
13. Markus R.P., F.Z.S., Fernandes P.A., Cecon E., *The immune-pineal axis: a shuttle between endocrine and paracrine melatonin sources.* Neuroimmunomodulation, 2007. **14**(3-4): p. 126-133.
14. Aronoff DM, O.J., Boutaud O, *New insights into the mechanism of action of acetaminophen: Its clinical pharmacologic characteristics reflect its inhibition*

of the two prostaglandin H2 synthases. Clinical Pharmacology Therapy, 2006. **79**(1): p. 9-19.

15. Graham GG, S.K., *Mechanism of action of paracetamol. American journal of therapeutics*, 2005. **12**(1): p. 46-55.
16. Roberts, L.J.I.M., J.D, *Analgesic-antipyretic and Antiinflammatory Agents and Drugs Employed in the Treatment of Gout.* The Pharmacological Basis of Therapeutics, 2001: p. 687-731.
17. Högestätt ED, J.B., Ermund A, *et al*, *Conversion of acetaminophen to the bioactive N-acylphenolamine AM404 via fatty acid amide hydrolase-dependent arachidonic acid conjugation in the nervous system.* The Journal of biological chemistry, 2005. **280**(36): p. 31405-12.
18. Köfalvi A., *Chapter 9: Alternative interacting sites and novel receptors for cannabinoid ligands.* 'Cannabinoids and the Brain, 2008: p. 131-160.
19. Borne, R.F., *Nonsteroidal Anti-inflammatory Drugs*. *Principles of Medicinal Chemistry*, Fourth Edition. 1995. 544-545.
20. John T. Slattery, J.M.W., Thomas F. Kalhorn, Sidney D. Nelson, *Dose-dependent pharmacokinetics of acetaminophen: Evience of glutathione depletion in humans.* Clinical Pharmacology, 1987. **41**(4): p. 413-418.
21. Martha M. Rumore, R.G.B., *Influence of Age-Dependent Pharmacokinetics and Metabolism on Acetaminophen Hepatotoxicity.* American Pharmaceutical Association, 1982. **81**(3): p. 1982.
22. Chandrahas G, S., James W. Ayres, *Multiple-Dose Acetaminophen Pharmacokinetics.* 1991. **80**(9): p. 855-860.
23. Kenneth S. Albert, A.J.S., John G. Wagner, *Pharmacokinetics of Orally Administered Acetaminophen in Man.* Journal of Pharmacokinetics and Biopharmaceutics, 1974. **2**(5): p. 381-393.
24. R. Don Brown, J.T.W., Gregory L. Kearns, Calerie F. Eichler, Virginia A. Johnson, and Karl M. Bertrand, *Single-Dose Pharmacokinetics of Ibuprofen and acetaminophen in febrile children.* Journal of Clinical Pharmacology, 1992. **32**: p. 231-241.
25. Gerhard Levy, N.N.K., David M. Soda, *Pharmacokinetics of Acetaminophen in Human Neonate: Formation of Avetaminophen Glucuronide and Sulfate in Relation to Plasma Bilirubin Concentration and D-Glucaric Acid Excretion.* Pediatrics, 1975. **55**(6).
26. Robert G. Peterson, B.H.R., *Pharmacokinetics of Acetaminophen.* Padiatrics, 2001. **62**(5): p. Suppl: 877-879.
27. Shigeo Shinoda, T.A., Yukio Aoyama, Sachiko Tomioka, Yoshiaki Matsumoto, Yoko Oche, *Pharmacokinetics/Pharmacodynamics of Acetaminophen Analgesia in Japanese Patients with Chronic Pain.* Biological & pharmaceutical bulletin, 2007. **30**(1): p. 157-161.
28. Joseph M. Scavone, G.T.B., David J. Greenblatt, *Lack of Effect of Influenze Vaccine on the Pharmacokinetics of Antipyrine, Alprozolam, Paracetamol (Acetaminophen) and Lorazepam.* Clinical Pharmacokinetics, 1989. **16**: p. 180-185.
29. Alan K. Fritz, D.P.B., James E. Peterson, George B. Park, Jerome Adelson, *Relative Bioavailability and Pharmacokinetics: A Combination of Pentazocine*

and Acetaminophen. Journal of Pharmaceutical Sciences, 1984. **73**(3): p. 326-331.

30. Janne RØmsing, D.Ø., Thomas Senderovitz, Mominika Drozdziewicz, Jesper Sonne, Grete Ravn, *Pharmacokinetics of oral diclofenac and acetaminophen in children after surgery.* Paediatric Anaesthesia, 2001. **11**: p. 205-213.
31. Roger H. Rumble, M.S.R., Michael J. Denton, *Effects of Posture and Sleep on the Pharmacokinetics of Paracetamol (Acetaminophen) and Its Metabolites.* Clinical Pharmacokinetics, 1991. **20**(2): p. 167-173.
32. Winston H. Lee, W.G.K., George E. Granville, *The Effect of Obesity on Acetaminophen Pharmacokinetics in Man.* Journal of Clinical Pharmacology, 1981. **21**: p. 284-287.
33. David T. Lowenthal, S.Ø., John C. Van Stone, *Pharmacokinetics.* Journal of Pharmacology and Experiment Therapeutics, 1976. **196**(3): p. 570-578.
34. Igor Loniewski, M.S., Andrzej Pawlik, Jerzy Wójcicki, Marek Drozdzik, *Lack of Effect of Physical exercise on.* Acta Plonia Pharmaceutica-Drug Research, 2001. **58**(2): p. 141-144.
35. Binh T. Ly, A.B.S., Richard F. Clark, *Effect of Whole Bowel Irrigation on the Pharmacokinetics of an Acetaminophen Formulation and Progression of Radiopaque Markers through the Gastrointestinal Tract.* Toxicology/Original Research, 2004. **43**(2): p. 189-195.
36. B.J. Anderson, N.H.G.H., *Rectal Acetaminophen Pharmacokinetics.* Anesthesiology, 1998.
37. Ralph F. Shangraw, W.D.W., *Effect of Vehicle Dielectric Properties on Rectal Absorption of Acetaminophen.* Journal of Pharmaceutical Sciences, 1971. **60**(4): p. 600-602.
38. Patrik K. Birmingham, M.J.T., Thomas K. Henthorn, Dennis M. Fisher, Maura C. Berkelhamer, Fredrick A. Smith, Kaaren B. Fanta, R. N., Charles J. Cote, *Twenty-four-Hour Pharmacokinetics of Rectal Acetaminophen in Children.* Anesthesiology, 1997. **87**: p. 244-252.
39. Richard A. van Lingen, H.T.D., Coby M.E. Quak, Albert Okken, Dick Tibboel, *Multiple-dose pharmacokinetics of rectally administered acetaminophen in term infants.* Clinical Pharmacology & Therapeutics, 1999. **66**(5): p. 509-515.
40. Ying Liu, J.B.S., Roger L. Schnaare, *A Multimechanistic Drug Release Approach in a Bead Dosage Form and In Vitro Predictions.* Pharmaceutical Development and Technology, 2003. **8**(2): p. 163-173.
41. Martin, A., *Martin's Physical Pharmacy and Pharmaceutical Sciences: Physical Chemical and Biopharmaceutical Principles in the Pharmaceutical Sciences*. Diffusion, ed. P.J. Sinko. 2006. 301-335.
42. Ying Liu, J.B.S., Roger L. Schnare, Edwin T. Sugita, *A multi-mechanistic Drug Release Approach in a Bead Dosage and In Vivo Predictions.* Pharmaceutical Development and Technology, 2003. **8**(4): p. 419-430.
43. Korsmeyer R. W., G.R., Doelker E., Buri P., Peppas, *Mechanism of solute from porous hydrophilic polymers.* Internnational Journal of Pharmaceutics, 1983. **12**: p. 25-35.

44. E.Rinaki, G.V., P. Macheras, *The power law can describe the entire drug release.* Internnational Journal of Pharmaceutics, 2003. **255**: p. 199-207.
45. Peppas N. A., S.J.J., *A simple equation for the descriptionof solute release: III Couple of diffusion and relaxation.* Internnational Journal of Pharmaceutics, 1989. **57**: p. 169-172.
46. Hixson A. W., C.J.H., *Dependence of Reaction Velocity upon Surface and Agitation.* Industrial and Engineering Chemistry, 1931. **23**(9): p. 923-931.
47. Ramsey F. L., S.D.W., *The Statistical Sleuth: Acourse in Methods od Data Analysis*. 2002.
48. Inc., T.U.S.P.C., in *The United States Pharmacopeia 28-The National Formulary NF-23*. 2005.
49. Muller, H. and R. Hilger, *Curative and palliative aspects of regional chemotherapy in combination with surgery.* Support Care Cancer, 2003. **11**(1): p. 1-10.
50. Per Borgquist, A.K., Lennart Picylell, anette Larsson, Anders Axelsson, *A model for the drug release from a polymer matrix tablet-effects of swelling and dissolution.* Journal of Controlled Release, 2006. **113**: p. 216-225.
51. Maria Antonietta casadei, G.P., Rossella Calabrese, Patrizia Paolicelli, Gaetano Giammona, *Biodegradable and pH-Sensitive Hydrogels for Potential Colon-Specific Drug Devilvery: Characteriazation and In Vitro Release Studies.* Biomacromolecules, 2008. **9**: p. 43-49.
52. Vijayalakshmi P, D.V., Narendra C, Srinagesh S, *Development of extended zero-order release gliclazide tablets by central composite design.* Drug development and industrial pharmacy, 2008. **34**(1): p. 33-45.
53. Robinson, G.M.J.a.J.R., *Sustained- and Controlled-Release Drug Delivery*, in *Morden Pharmaceutics*, G.S.B. Christopher, Editor. 1996, Marcel Dekker. p. 575-609.
54. R. K. Chang, C.H.H., J. R. Robinson, *A Review of Aqueous Coating techniques and Preliminary data on release from a Theophylline product.* Pharmaceutical Technology, 1987. **11**(3): p. 56-58.
55. M. Hossain, J.W.A., *Variables that influence coat integrity in laboratory spray coater.* Pharmaceutical Technology, 1990. **14**(10): p. 72-82.
56. Yuh-Fun Maa1, C.I., Mahmoud Ameri, Robert Rigney, Lendon G. Payne, Dexiang Chen, *Spray-Coating for Biopharmaceutical Powder Formulations: Beyond the Conventional Scale and Its Application.* Pharmaceutical Research, 2004. **21**(3): p. 515-523.
57. Chang X. X., T.R., *The prediction of variability occurring in fluidized bed coating equipment. I. The measurement of particle circulation rates in a bottom-spray fluidized bed coater.* Pharmaceutical development and technology, 2000. **5**(3): p. 311-322.
58. Vecchio C, F.F., Sangalli ME, Zema L, Gazzaniga A, *Rotary tangential spray technique for aqueous film coating of indobufen pellets.* Drug development and industrial pharmacy, 1998. **24**(3): p. 269-274.
59. Agency, E.P., *Clean Air Act*. 1970.
60. Brown, D., *Orally Disintegrating Tablets – Taste Over Speed.* Drug Delivery Technology, 2001. **3**(6): p. 58-61.

61. Food and Drug Administration, C.F.D.E.a.R., *Guidance for Industry: Orally Disintegrating Tablets*. 2007.
62. Srikonda V. Sastry, J.N., *Process develpment ans Scale-Up of Oral Fast-Dissolving Tablets*. Drug Delivery to the Oral Cavity: Molecules to Market, ed. W.R.P. Tapash K. Ghosh. 2005. 311-336.
63. William R. Pfister, T.K.G., *Orally Disintegrating Tablets: Products, Technology and Development Issues.* Pharmaceutical Technology, 2005. **29**(10): p. 136-150.
64. Harmon, T.M., *Orally Disintegrating Tablets: A Valluable Life Cycle Management Strategy.* Pharmaceutical Commerce, 2007. **3**.
65. Fu Y, Y.S., Jeong SH, Kimura S, Park K, *Orally fast disintegrating tablets: developments, technologies, taste-masking and clinical studies.* 2004. **21**(6): p. 433-476.
66. S. Indiran Pather, R.K., John Siebert, *Quick-Dissolving Intraoral Tablets*. Srug Delivery to the Oral Cavity: Molecules to Market, ed. W.R.P. Tapash K. Ghosh. 2005.
67. Ed L. Hamilton, E.M.L., *Advanced Orally Disintegrating Tablets Bring Significant Benefits to Patients & Product Life Cycles.* Drug Delivery Technology, 2005. **5**(1): p. 34-37.
68. Mesut Ciper, R.B., *Modified conventional hard gelatin capsules as fast disintegrating dosage form in the oral cavity.* European Journal of Pharmaceutics and Biopharmaceutics, 2006. **62**: p. 178-184.
69. Y. Gonnissen, J.P.R., C. Vervaet, *Effect of maltodextrin and superdisintegrants in directly compressible powder mixtures prepared via co-spray drying.* European Journal of Pharmaceutics and Biopharmaceutics, 2008. **68**: p. 277-282.
70. J Goole, D., F. Vanderbist, K. Amighi, *New Levodopa Sustained release Floating minitablets coated with Insoluble acrylic polymer.* European Journal of Pharmaceutics and Biopharmaceutics, 2008. **68**: p. 310-318.
71. Eriksen, S., in *In the Thepry and Practice of Industrial Pharmacy*, H.A.L. L. Lachman, J.L. Kanig, Editor. 1970. p. 408.
72. *Physician's Desk Reference*, ed. K.D. Sanborn. 2007: Thomson. 1870-1872.
73. *Handbook of Pharmaceutical Excopients*. Hydropropyl Methylcellulose, ed. A.H. Kibbe. 2000. 252-255.
74. *Spray coating conditions in fluid bed chamber*.
75. Wagner, J.G., *Pharmacokinetics for the Pharmaceutical Scientist*. Noncompartmental and System Analysis. 1993: Technomic. 96-99.
76. Food & Drug Administration, C.-O.o.P.S., *The Biopharmaceutics Classification System (BCS) Guidance.* 2007.
77. Na Zhao, L.L.A., *The Influence of Granulation on Super Disintegrant Performance.* Pharmaceutical Development and Technology, 2006. **11**(1): p. 47-53.
78. Bowe, K.E., *Recent advances in sugar-based excipients.* Pharmaceutical Sciences Technology, 1998. **1**(4): p. 166-173.
79. Mizumoto, T., et al., *Formulation design of a novel fast-disintegrating tablet.* Int J Pharm, 2005. **306**(1-2): p. 83-90.

80. Huang, A.L., et al., *The cells and logic for mammalian sour taste detection.* Nature, 2006. **442**(7105): p. 934-8.
81. Roberts, D., *Signals and Perception: The Fundamentals of the Human Senses*. 2002: Palgrave Macmillan.
82. Ayres et al.., *Compactable Self-sealing Drug Delivery Agents*, U.S. Patent, Editor. 1998, Oregon State University: USA.

CHAPTER 3

PHARMACOKINETICS OF TERBINAFINE IN PENGUINS

Hang Le, John Mark Christensen, Ursula Bechert

ABSTRACT

Purposes: Aspergillosis is a common disease in penguins. Terbinafine is an anti-fungal medicine that is administered in humans by oral administration to treat some other types of fungal infections such as dermatophytes, and aspergillosis. This study investigated pharmacokinetic properties in penguins to determine the pharmacokinetic parameters and the dose of Terbinafine to treat aspergillosis in penguins. **Method:** Terbinafine was administered in African penguins (*Spheniscus demersus)* in three different treatments of single dosing: 3mg/kg, 7mg/kg, 15mg/kg and one treatment of multiple dosing: 15.mg/kg each every 24 hours. The blood samples were collected at specific time points and analyzed by HPLC. The data was analyzed on a WinNonlin pharmacokinetic software package. **Results:** In penguins**, the** Terbinafine follows a two-compartmental open model with a long half-life termination phase from the adipose tissues. The elimination phase from the deep-tissue compartment was detected by accumulation of the trough concentration in the multiple dosing treatment. The recommended dose for the multiple dosing of Terbinafine every 24 hours was 15mg/kg. **Conclusion:** Terbinafine can be administered orally in penguins to treat aspergillosis at a reasonable dose. The suggested dose is probably a guideline to develop an appropriate oral dosage form.

INTRODUCTION

PENGUINS

According to the classification of living things, penguins belong to the class Aves. This class includes all birds which have an outer covering of feathers, are endothermic (warm-blooded), have front limbs modified as wings, and lay eggs. Penguins are from the lower level inside this class. Penguins belong to the order Sphenisciformes, which includes all living and extinct penguins. The family is called spheniscidae. Spheniscidae includes all penguins, living and extinct, and is the only family classification in the order Sphenisciformes. According to del Hoyo, et al., 1992, there are 17 species of penguins and 32 extinct species [1-4].

- emperor *Aptenodytes forsteri*
- king *Aptenodytes patagonicus*
- Adélie *Pygoscelis adeliae*
- gentoo *Pygoscelis papua*
- chinstrap *Pygoscelis antarctica*
- rockhopper *Eudyptes chrysocome*
- macaroni *Eudyptes chrysolophus*
- royal *Eudyptes schlegeli*
- Fiordland crested *Eudyptes pachyrhynchus*
- erect-crested *Eudyptes sclateri*
- Snares Island *Eudyptes robustus*
- yellow-eyed *Megadyptes antipodes*

- fairy (also known as little blue) *Eudyptula minor*
- Magellanic *Spheniscus magellanicus*
- Humboldt *Spheniscus humboldti*
- African (formerly known as black-footed) *Spheniscus demersus*
- Galapagos *Spheniscus mendiculus*

The penguins used in the study were african penguins or Jackass Penguin. The Latin name is Sphenicus demersus.

Geographic distribution

African penguins live off the coast of South Africa. They breed on twenty-four islands offshore between Namibia and Port Elizabeth, South Africa. On the mainland, there are colonies of penguins at Betty's Bay and Simonstown, South Africa, and in Namibia [5].

The habitat of African penguins

African penguins live in the warm climates region between twenty to forty degrees south on the rocky shores where they reproduce and take care of their young.

The world population is about 70,000 pairs. The current population is less than 10% compared to the number in 1900. The annual rate of decline is approximately 2%. The reduction in population is mostly due to the over exploitation of penguin eggs for food, guano collection at breeding colonies**,** over fishing for pelagic fish prey, and oil pollution [6].

Physical Description

The African penguin is 30 to 100 cm in height (average 68cm length) and its weight is between 2.1 to 3.7 kg. They are black on their dorsal side, face, flippers, and the top of their head. Their entire ventral side and lateral parts of the head and torso are white. Along the chest and sides are black horseshoe-shaped stripes. The body of the African Penguin is shaped like a bowling pin, and its feet are webbed [5].

Figure 3.1. An African penguin [6]

Behavior

African Penguins are monogamous, and the same pair will generally return to the same colony and often the same nest site each year**.** Both parents continue to brood the chicks, and for about the first 15 days, the chicks are constantly brooded by one of the

adults. The juveniles remain away from their natal colonies for anywhere from 12 to 22 months, after which time they return, normally to their natal colony, to moult into adult plumage. African Penguins have adapted to terrestrial life in the temperate zone confining their activities at breeding sites largely to dawn and dusk periods. Breeding birds nest mostly in burrows or under some other form of shelter, such as boulders and bushes, which provide some protection from the intense solar radiation during the day [6].

Fungal infection in penguins

Aspergillosis sometimes becomes an outbreak in penguins. This infection can lead to a weakness and may cause mortality in penguins. This disease is one of the most common diseases in penguins especially in penguins kept in public institutions. The purpose of this study is to investigate the pharmacokinetics of Terbinafine in penguins in the hope that Terbinafine can be used to treat aspergillosis [7].

TERBINAFINE

Tebinafine is an allylamine antifungal agent [8, 9], which is used to treat nail infections of onycomycoses and tinea pedis in humans caused by dermatophytes [9-15]. Onycomycoses are superficial fungal infections on the skin and keratinized tissues, which affect millions of people worldwide [10]. Approximately 90% of fungal nail infection cases are caused by dematophytes that commonly are Trichophyton spp., Microsporum spp. and Epidermophyton spp. [10-12]. Dermatophytes infect the stratum corneum layer of the epidemis and keratinised tissues derived from it like the hair and nails. Tinea pedis is the most common fungal infection caused by Trichophyton rubrum or Trichophyton

metegrophytes [9, 10]. The infection may be worse due to the intrudence of bacteria such as Streptoccoccus [10].

Terbinafine was discovered in 1983. It is originally from naftidine. The replacement of the phenyl ring in the naftidine molecule by the tert-butylacetylene group creates a stronger antifungal and broader spectrum compound.

The chemical structure of Terbinafine:

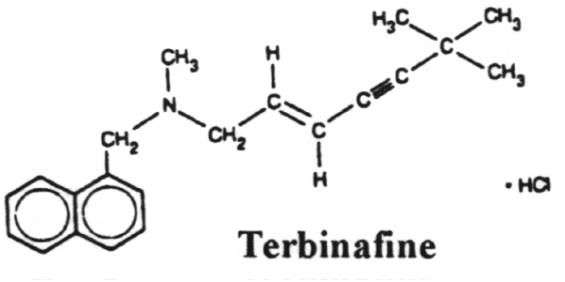

Figure 3.2. The chemical structure of Terbinafine

The oral form was approved by FDA in 1996 [12].

Mechanism of action

Terbinafine inhibits the fungal enzyme squalene epoxidase which plays an important role in ergosterol biosynthesis. Since ergosterol is the essential component of the fungal cell wall, it will lead to the toxic accumulation of squalene, and the fungal cell will become weak [9, 10, 13, 14]. The extent of the sterol biosynthesis in fungal cells is much greater than that in mammalian cells [12]. No effect of Terbinafine has been observed on other enzymes of the ergosterol pathway [9]. The inhibition of Terbinafine on induced ergosterol depletion is fungistatic and fungicidal [12, 16]. No direct inhibitory effect on protein, nucleic acid, cell wall biosynthesis, or cell membrane activity has been reported with Terbinafine given to Candida and Trichophyton [9].

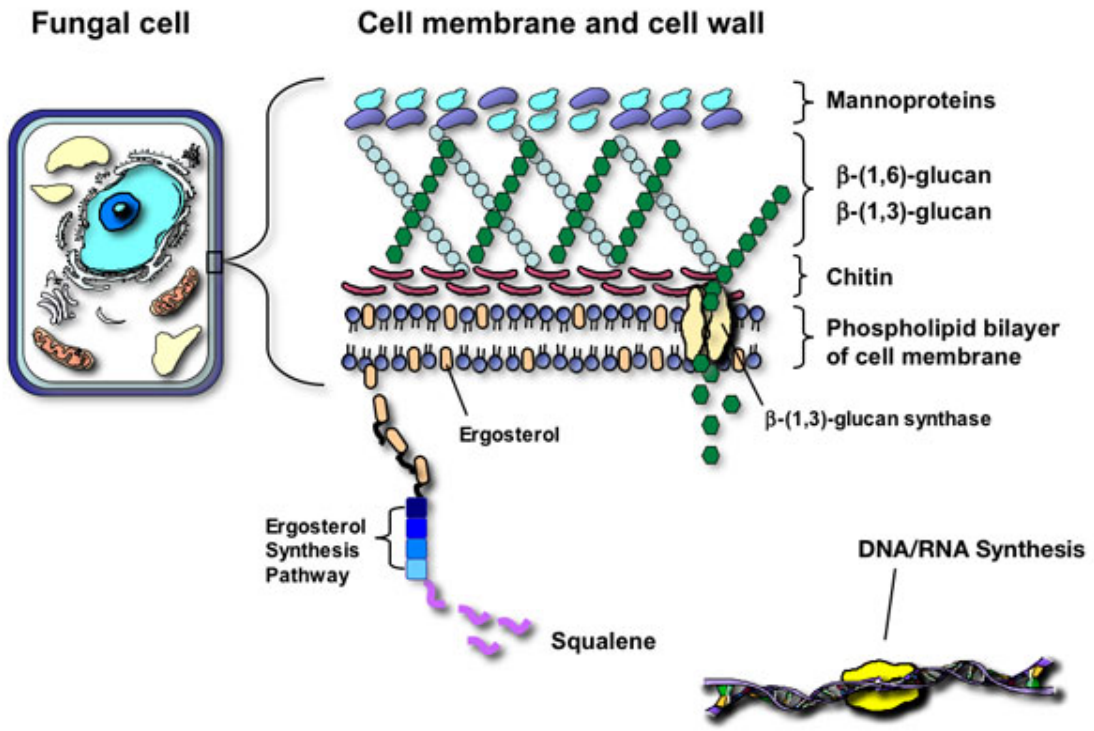

Figure 3.3. The mechanism of action of Terbinafine

Clinical Mycology

Various fungal species were tested to determine the MIC_{95} (minimum inhibitory concentration) with Terbinafine. However the MIC_{95} varied considerably due to a lack of a standardized method, and there is no direct relation between *in vitro* activities and in vivo efficacies [12]. Terbinafine shows remarkable inhibition activity against dematophytes *in vitro*. Pretyani et al. reported the results of MIC_{95} values of 112 clinical isolates which ranged from 0.0015 to 0.01 (Table 3.1)[17]. However, with Aspergillus spp., the observed MIC was much higher [14].

Table 3.1. MIC and MFC of Terbinafine on Aspegillus spp.

Species	Inoculum	MIC			MFC		
		Range	50%	90%	Range	50%	90%
A.fumigatus	Low	0.8-1.6	0.8	1.6	0.8-3.2	0.8	1.6
	High	0.8-1.6	1.6	1.6	0.8-3.2	1.6	1.6
A. flavus	Low	0.025-0.4	0.2	0.4	0.025-0.4	0.4	0.4
	High	0.4-0.8	0.8	0.8	0.4-0.8	0.8	0.8
A. niger	Low	0.025-0.4	0.1	0.4	0.05-0.4	0.1	0.4
	High	0.05-0.4	0.8	1.6	0.05-0.4	0.2	0.4

Julia Balfour reported *in vitro* MIC_{95} of Terbinafine on fungal species [9]. From Table 3.2, high concentrations of Terbinafine are necessary to inhibit Aspergillus and Candida spp.

Table 3.2. MIC_{95} of Terbinafine on fungi

	Inhibitory concentration (mg/L)	
Species	Fungal growth	Sterol Biosynthesis
Trichophyton rubrum	0.003	0.02
T. mentagrophytes	0.003	0.04
Aspergillus fumigatus	0.8	1.2
Candida parasilosis	0.4	0.3
Candida albicans	3.1	0.9
Candida glabrata	100	0.9

It also indicates that Terbinafine inhibits the Trichophyton species at low concentrations. Terbinafine has a weak inhibition of Candida species and Aspergillus. Other studies showed that Terbinafine demonstrates less potency against all strains of Candida compared to azoles-derivative antifungals [12, 17].

Pharmacokinetics on humans

Absorption

In humans, Terbinafine is absorbed well [12, 18, 19] with more than 70% being absorbed after oral administration. Forty seven percent is metabolized by the first-pass

effect, and the C_{max} is about 0.8 to 1.5 mg/L and the T_{max} is around 1.3 to 2 hours after a 250 mg oral dose. Multiple-dose regimens in healthy volunteers show that the C_{max} is about 25% of the predicted concentration at steady state [12]. The AUC ranged from 3.14 to 4.74 mg*hour/L [14]. The presence of food prolongs the absorption process [14, 20]. In children (age 5-11 years), the AUC is higher than young adults but concentrations are lower at similar doses based on mg/kg. AUC is also higher in elderly than young subjects [13, 18, 20, 21]. The AUC is also higher in the elderly than in young adults, patients with dysfunction, and patients with renal impairment [12, 14].

Distribution

Ninety-nine percent of Terbinafine is bound to plasma proteins, mainly to albumin and high and low- density proteins. This non-specific binding reduces the Terbinafine inhibitory activity of ergosterol biosynthesis *in vitro* [12-14, 22]. However, the extensive plasma-protein binding of Terbinafine is considered an advantage in the drug absorption process since the binding process contributes to producing large concentration gradients from the GI lumen to blood. This facilitates drug absorption. The high affinity of the Terbinafine to plasma proteins and adipose tissue produces a "sink" condition which creates a "Terbinafine reservoir" from which Terbinafine is gradually provided to poorly diffused tissues. Terbinafine is distributed extensively to body tissues and fluids. Volume distribution at steady state is approximately 950 L [14]. A multiple-dosing study of Terbinafine in humans indicates the highest concentrations were observed in the sebum and the hair, at levels ten times that seen in the skin and nails, while the lowest concentrations were observed in plasma after 30 days of multiple dosing regimens [22, 23].

An analysis of Terbinafine concentration in various tissues of rats found that Terbinafine has a high affinity for skin and adipose tissue. Terbinafine is rapidly delivered to the skin's stratum corneum [14, 17]. Its concentration remains high 50 hours after administration; whereas drug concentrations decline rapidly in other tissues. Of total Terbinafine, the V_{ss} value uptake into adipose tissue and skin represents 52.3% and 41.4% of the total V_{ss} value respectively [24]. Terbinafine is first detected in the nails within one week of oral administration [13]. Diffusion of Terbinafine in the nails is thought as the only way that Terbinafine can reach this tissue. The concentration of Terbinafine in the nails becomes constant after 12 weeks of oral dosing. No difference in Terbinafine levels were observed in uninfected nails and infected nails [12, 13, 22]. Because Terbinafine is lipophilic, the log (octanol/water) partition coefficient is 3.3 [21]. It has a high affinity to adipose tissue and strong protein binding. This leads to a very long terminal elimination half life of Terbinafine, 90-200 hours. The long terminal half life of Terbinafine is due to the drug presence and its affinity to adipose and skin providing a large reservoir of the drug after the cessation of the administration that allows continuing detection of Terbinafine up to 24 weeks. Isotope ^{14}C used to test the drug's pharmacokinetic profile indicates that a three-compartmental model best describes Terbinafine in the *in vivo* disposition. The half-life of the absorption phase is 0.8-1.2 hours. The effective half life is 16-26 hours after drug's administration and the terminal elimination's half life of 90-200 hours for Terbinafine is due to the deep tissue elimination phase. However, the Terbinafine concentrations are under the MIC, and it is likely not effective anymore [21, 23].

Metabolism and Elimination

Terbinafine undergoes extensive metabolism by the liver [12, 14]. At least 7 CYP enzymes are involved in Terbinafine metabolism[13]. Fifteen distinct metabolites have been identified. The biotransformation is mostly by oxidation, and phase II conjugation occurs with oxidized metabolites [12, 21]. The major pathway and the kinetics of metabolism were also known for Terbinafine and its five major metabolites [11, 21, 22]. The major pathways are N-demethylation of the central nitrogen atom of the allylamine; oxidative N-dealkylation of the allyamine (these are conjugated and then eliminated or further oxidized to carboxylic acids); and N-dealkylation at the allylic position. Some other less important pathways are recorgnizied: N-dealkylation at the aromatic ring; arene oxide formation; aliphatic oxidation; aromatic oxidation [21], reduction of the olefinic double bond; and aldehyde reduction. Conjugation with alcohol, dihydrol and phenol is described [13, 23]. None of metabolites are active.

It is postulated that CYP 2C9, CYP 1A2, and CYP 3A4 are the major enzymes participating in Terbinafine metabolism. In the liver, unlike azole drugs Terbinafine has less effects on the pharmacokinetics of other drugs [22]. There is some evidence that Terbinafine is a CYP 2D6 inhibitor. It is reported that some drugs that are substrates of CYP 2D6 interact with Terbinafine. Some patients have developed nortriptyline toxicity similar to an overdose of nortriptyline when given in combination with Terbinafine. This toxicity is thought to be attributed to Terbinafine's inhibition of CYP 2D6 since nortriplyline is mainly metabolized by CYP 2D6 [25]. Furthermore, It was obseved that Terbinafine has a favorable pharmacophore to be a CYP 2D6 inhibitor [26, 27]. Clearance of theophylline declines with concomitant administration with Terbinafine [28]. Another

report suggests that Terbinafine inhibited CYP 1A2 and decreases theophyline clearance. Terbinafine also reduced caffeine clearance by 21%, and it attributed to CYP 1A2 inhibition, as well. Xanthines delayed metabolism and is thought to be attributed to inhibition of CYP 1A2 by Terbinafine [12]. Terbinafine also interacts with thioridazine, desipramine, paroxetine, venlafaxine, dextromethorphan, codeine, cardiovascular drugs such as metoprolol, encainide, flecainide, tpropanfenone and metilitine, **n**ortriptyline, and also with cyclosporine [12, 14, 28-30]. Other drugs that inhibit or induce the cytochrome P450 system enzymes can interfere with Terbinafine clearance. Cimetidine reduces the elimination of Terbinafine, and rifampicin has the opposite effect of increasing the elimination of Terbinafine [14].

The effective terminal half life of Terbinafine is 27-29 hours, and 80% of Terbinafine metabolites are excreted into the urine with a small amount excreted in the feces [13, 14, 31, 32]. The Terbinafine dose should be reduced in case of hepatic dysfunction or severe renal impairment.

Dosage form

Both a topical and an oral dosage form of Tebinafine are available to treat onychomycosis [33]. Terbinafine HCl 1% cream produced a good effect in clinical trials with an improvement rate of up to 90-100% after 12 weeks of treatment [14, 15, 19]. In addition, an emulsion gel, a solution and a spray formulation exist. A Terbinfafine HCl tablet was administered at 250 mg once daily for 12 weeks [17]. Terbinafine is preferred to treat onychomycosis in patients with acquired diabetes mellitus because there is no reported Terbinafine interaction with anti-diabetes medicines [15], and one third of

patients with diabetes have toenail onychomycosis. Oral Terbinafine has a superior cost effectiveness ratio in treatment compared to that of itraconazole, ketoconazole, and griseofulvin treatments [12, 14].

NON-LINEAR REGRESSION

Data such as plasma concentrations versus time are fitted to pharmacokinetic models. The WinNonlin reference guide defines two types of fitting methods for these pharmacokinetic models: Linear regression and non-linear regression. Linear regression is a regression model in which parameters to be determined by the fitting process appear only as coefficients of the independent variables [34]. For example:

Simple linear regression

$Y = A+BX+C$

Polynomials regression

$Y = A_1+A_2X + A_3X^2 + A_4X^3 +C$

Multiple linear regression

$Y = A_1 + A_2X_1+A_3X_2 + A_4X_3 + C$

In nonlinear models, at least one of the parameters to be determined by the regression process appears as other than a coefficient.

Decay curve is the simple example of nonlinear regression.

$Y = Y_0 \exp(-BX)$

$Y = A_1\exp(-B_1X) + A_2\exp(-B_2X)$.

These models can be converted into linear models by simple transformation. All pharmacokinetic models are derived from a set of basic differential equations that can be

integrated to algebraic equations. Besides that, the curves can be fitted to numerical equations. The WinNonlin can be used to fit data to pharmacokinetic models defined in terms of algebraic equations or models defined in terms of differential equations as well as combinations of both types of equations. Two methods are used to fit data to pharmacokinetic models: The maximum likelihood and least squares. In general, least square is not appropriate for non-linear regressions. To apply the leastsquare method to a non-linear equation, an iterative procedure must be used. First, initial estimates of the pharmacokinetic parameters are made, and then in some way these initial estimates are modified to give a better estimate which results in a smaller sum of squares' deviations. The iteration continues until hopefully the minimum (or least) sum of squares is reached. For pharmacokinetic models with random effects, the more general method of maximum likelihood must be employed.

WEIGHTING

As mentioned above, most concentration time curves can be expressed by a non linear equation. To fit the equation by the maximum likelihood method or least square method, the equation needs to be transformed into another equation. In essence the function or equation that best fits the transformed data will give the best approximation of the data. The distribution of the data and the transformed variables are likely different.

Weighting is used to adjust the mean square error of the transformed least square method. If y is the original variable and Y is the transformed variable. Marian Karolczak et al. [35] indicated that when fitting transformed data to a function by the least square

method is likely to minimize $\sum_{i=1}^{n}(Y-Y_i)^2$ while we desire to minimize $\sum_{i=1}^{n}(y-y_i)^2$.

Assuming that the errors are small, the relationship of Y and y is the following:

$$\Delta y_i \approx \frac{dy_i}{dY_i}\Delta Y_i$$

$$w_i = \left(\frac{1}{dY_i / dy_i}\right)^2$$

$$\Delta y_i = w_i^{1/2}\Delta Y_i$$

As the result of definition

$$\sum_{i=1}^{n}(Y-Y_i)^2 = \sum_{i=1}^{n}(y-y_i)^2$$

If the w_i is employed to pharmacokinetics. As seen in the previous section the fitting of the data to an equation is by using non-linear regression that follows an exponential relation. For example:

$$y = Y_0 \exp(-BX)$$

$$Y = \ln(y) = \ln Y_0 - BX$$

$$w_i = \left(\frac{1}{d(\ln y_i / dy_i)}\right)^2 = y_i^2$$

Weighting is necessary to provide better fitting of the data to an equation. The WinNonlin program provides various choices of weightings. Thus, to weight data:

$$\frac{\Delta y_i}{w_i^{1/2}} = \Delta Y_i = \frac{\Delta y_i}{y_i}$$

It means 1/yi is the weighting value that is needed to multiply the data points by, before the transformation process.

Weighted least squares

The general weighting formula is Y^n; where n can be positive or negative numbers. The common value of n is 0 (no weighting,-1, -2). The WinNonlin, program requires choosing a weight for each pharmacokinetic model before fitting the data.

Iterative weighting

Besides the fixed weighting, there is another type of weighting that is provided by WinNonlin, iterative re-weighting. The general form of iterative re-weighting is $\hat{Y}^n$ where n can be positive or negative. The common values in pharmacokinetics models are 0, -1, -2.

Scaling of weight or normalization of weight: Because the scaling of weight has no effect on the model being fitted software can use different techniques to set up the scaling of weight. A simple way of normalization is

$$W_i = \frac{w_i}{\sum (w_i / n)}$$

This means the sum of weights for each function is equal to the number of data values

$$\sum W_i = \sum \frac{w_i}{\sum (w_i / n)} = n$$

ARITHMETIC MEAN AND HARMONIC MEAN

The variance and standard error of a population is

$$\sigma^2{}_Y = \frac{\sum_{i=1}^{n} (Y_i - \overline{Y})^2}{n-1}$$

$$\sigma_Y = \sqrt{\frac{\sum_{i=1}^{n} (Y_i - \overline{Y})^2}{n-1}}$$

The variance calculated for a sample is

$$s^2{}_Y = \sqrt{\frac{\sum_{i=1}^{n} (Y_i - \overline{Y})^2}{n-1}}$$

Arithmetic mean

Y_1, Y_2, $Y_{3...,}$ Y_n are the random variables from a normal population. The average $\overline{Y}$ or arithmetic mean is calculated by formula:

$$\overline{Y} = \frac{\sum_{i=1}^{n} Y_i}{n}$$

Variance of $\overline{Y}$:

$$\sigma^2_{\overline{Y}} = \frac{\sigma^2_{\overline{Y}}}{n}$$

$$\sigma^2_{\overline{Y}=} \frac{\sum_{i=1}^{n} (Y_i - \overline{Y})^2}{n(n-1)}$$

The standard error of a population:

$$\sigma_{\overline{Y}} = \frac{\sigma_{\overline{Y}}}{\sqrt{n}}$$

$$\sigma_{\overline{Y}=} \sqrt{\frac{\sum_{i=1}^{n} (Y_i - \overline{Y})^2}{n(n-1)}}$$

Standard error for the sample:

$$SE_{\overline{Y}=} \sqrt{\frac{\sum_{i=1}^{n} (Y_i - \overline{Y})^2}{n(n-1)}}$$

The central limit theory states that for any type population, when the number of samples converge to infinity, the distribution of the averages converge to a normal distribution and the average value converges to the mean of the population and the s^2 value converges to σ^2 value [36].

This theorem allows the approximate calculation of means and variations when the sample size is large (over 30). In pharmacokinetic studies, most of the time there is

only a limited number of samples (normally smaller than 30 subjects), so the average of a sample is considered to have a t distribution with n-1 degrees of freedom. For example, the elimination constant, beta value, is obtained from the curve stripping of each subject. If we consider each subject as treated independently in the experiment, the Beta values are considered the random sample from a population and the value calculated for the average and standard error are (standard deviation according formula):

$$\overline{\beta} = \frac{\sum_{i=1}^{n} \beta_i}{n}$$

Standard error:

$$s_{\overline{\beta}=} \sqrt{\frac{\sum_{i=1}^{n} (\beta_i - \overline{\beta})^2}{n(n-1)}}$$

Other pharmacokinetic parameters such as A and alpha are considered random variables and the way to calculate the average value and standard error is similar to that of beta.

Mean residence time (MRT), Half-life ($t_{1/2}$), Clearance (Cl_F), Volume of distribution (V_F) are calculated by the formulae:

$$MRT = \frac{AUMC}{AUC}$$

$$t_{1/2} = \frac{\ln(2)}{\beta}$$

$$Cl\_F = \frac{D}{AUC}$$

$$V\_F = \frac{Cl}{\beta}$$

All of the pharmacokinetic parameters are calculated by formula with beta or AUC in the denominator. The distribution of these variables is not a t distribution

anymore. To apply t distribution to calculate the standard error or (100-α)% or (100-α/2)% confidence interval, F.C Lam, C.T. Hung, D. G. Perrier [37] have recommended using the harmonic mean to replace the arithmetic mean. The harmonic mean is determined by the following formulae:

$$\frac{1}{\overline{Y}} = \frac{1}{n}\sum_{i=1}^{n}\frac{1}{Y}$$

Stadard error of $\overline{Y}$:

$$\overline{Y} = \frac{n}{(\frac{1}{Y_1}+\frac{1}{Y_2}+....+\frac{1}{Y_n})}$$

$$\overline{Y_i} = \frac{n-1}{(\frac{1}{Y_1}+\frac{1}{Y_2}+....+\frac{1}{Y_{i-1}}+\frac{1}{Y_{i+1}}+\frac{1}{Y_n}}$$

$$SE_{\bar{Y}} = \sqrt{\frac{n-1}{n}\sum_{i=1}^{n}(\overline{Y}_i - \overline{Y})^2}$$

These formulae can be applied for $t_{1/2}$, Cl_F, V_F, MRT to get the harmonic mean and the standard error [38].

Pseudo -standard error

There is a harmonic function on Excel, Matlab. On both Matlab and Excel this function is “harmean (). However, in either program there is no function to calculate the variance or standard error; it is not available. Aother program can be used to calculate standard error:

Matlab code:

```
function HarmonicSD(filename);
data=dlmread(filename,',',3,0);
[17]=size(data);
```

```
harmonicMean=zeros(1,col);
harmonicMeanSD=zeros(1,col);

for j=1:col
    N=0;
    for i=1:row
        if data(i,j)~=0
            N=N+1;
        end
    end

    %compute harmonic mean

    Ybar=0;

    for i=1:row
        if data(i,j)~=0
            Ybar=Ybar+1/data(i,j);
        end
    end

    Ybar=N/Ybar;

    harmonicMean(j)=Ybar;

    %compute the SD
    SS=0;
    for i=1:row
        if data(i,j)~=0
            SS=SS+1/data(i,j);
        end
    end

    YYbar=zeros(1,N);
    index=0;
    for i=1:row
        if data(i,j)~=0
            index=index+1;
            YYbar(index)=(N-1)/(SS-1/data(i,j));
        end
    end

    SQ_YY=(YYbar-Ybar).^2;
    SD_SUM=sum(SQ_YY);
    h_SD=sqrt((N-1)/N*SD_SUM);

    harmonicMeanSD(j)=h_SD;
end

dlmwrite(filename,' ','-append');
dlmwrite(filename,harmonicMeanSD,'-append');
```

AKAIKE'S INFORMATION CRITERION (AIC) AND SCHARZ BAYSIAN (BSC) OR BAYESIAN INFORMATION CRITERION (BIC)

Akaike's information criterion, developed by Hirotsugu Akaike under the name of "an information criterion" (AIC) in 1971 and proposed in Akaike (1974), is a measure of the goodness of fit of an estimated statistical model [39].

AIC is defined according to the formula:

$$AIC = 2k - 2\ln(L)$$

Here k is the number of parameters in the statistical model

L is the maximized value of the likelihood function for the statistical model

As regard to the residual sum of squares AIC becomes:

$$AIC = 2k + n[\ln(2\pi RSS / n) + 1$$

n is the number of observations, or equivalently, the sample size.

AIC is used to avoid over fitting [40] because the fomula is the sum of two factors: the residual sum of the square and number of parameters. When the number of parameters increases, the residual sum of squares decreases, AIC is the trade off of penalty factor and the benefit factor.

SBC or BIC

$$BIC = -2\ln L + k\ln(n)$$

$$BIC = n\ln\left(\frac{RSS}{n}\right) + k\ln(n)$$

Similar to AIC, BIC contains both the penalty and benefit factors. The BIC penalizes free parameters more strongly than does the AIC.

ACCELERATED CONVERGENCE METHOD

The dosing interval (the time between doses given) in multiple dosing affects the plasma drug concentration at a steady state. A shorter dosing interval produces higher plasma concentrations at a steady state. However, time to reach steady state-plasma drug concentration depends only on the terminal elimination rate constant or half life of the drug. In other words, the way plasma concentrations reach the steady state is independent of the interval of dosing and dependent upon the half-life of the drug. It is well-known that Terbinafine in humans has a long terminal-elimination half life due to its affinity to adipose tissue (100-200 hours). The single dose data collected in the study does not allow calculation of this terminal half life since the last sample point was taken 48 hours after drug administration. However, another alternative method can be used to estimate the value of Terbinafine's terminal elimination rate constant and half-life, the accelerated convergence method [41].

Y_i is variable approaching an asymptote Y_∞ and it obeys first order kinetics from time t', thus following we have the equation:

$$Y_i = Y_\infty[1 - e^{-\lambda_1(t_i - t')}]$$

For three equally spaced points, at intervals, Δt, the above equation can be written:

$$Y_1 = Y_\infty[1 - e^{-\lambda_1 \Delta t}]$$
$$Y_2 = Y_\infty[1 - e^{-2\lambda_1 \Delta t}]$$
$$Y_3 = Y_\infty[1 - e^{-3\lambda_1 \Delta t}]$$

On the two dimension abscissa, $Y = Y_i$ vs. $X = Y_{i+1}-Y_i$. The linear equation $Y = a + bX$

Two points on the line are (Y_2-Y_1) and (Y_3-Y_2). At the same intervals, it is always that $Y_1<Y_2<Y_3$ and $(Y_2-Y_1) > (Y_3-Y_2)$. The intercept and slope of the equation is:

$$b = \frac{(Y_2 - Y_3)}{(Y_2 - Y_1) - (Y_3 - Y_2)} = \frac{Y_3 - Y_2}{Y_3 - 2Y_2 + Y_1}$$

When $Y=Y_3$ the equation becomes:

$$Y_3 = Y_\infty + [\frac{Y_3 - Y_2}{Y_3 - 2Y_2 + Y_1}](Y_3 - Y_2) = Y_\infty + \frac{(Y_3 - Y_2)^2}{Y_3 - 2Y_2 + Y_1}$$

Rearrange the equation the formula becomes:

$$Y_\infty = Y_3 - \frac{(Y_3 - Y_2)^2}{Y_3 - 2Y_2 + Y_1}$$

Generating the equation above for Y_i yields

$$Y_i = Y_\infty - slope(Y_{i+1} - Y_i)$$

The intercept is the Y_∞. Y_∞, the elimination rate constant can be calculated by

$$e^{-\lambda(t_i - t')} = 1 - \frac{Y_i}{Y_\infty}$$

$$\lambda = \frac{\ln(1 - \frac{Y_i}{Y_\infty})}{t_i - t'}$$

This method can be employed to calculate the first order pharmacokinetic parameters such as AUC, plasma concentration, or, in this instant, the terminal elimination rate constant.

RESULTS AND DISCUSSION

SINGLE DOSING PHARMACOKINETIC

Penguins were administered oral Terbinafine tablets. Three single oral Terbinafine treatments of 3mg/kg, 7mg/kg and 15mg/kg were given to each bird.

All pharmacokinetics analysis was calculated without regard to the fraction of the dose absorbed. The clearance was the overall clearance or apparent clearance. Each penguin was identified by a number.

Table 3.3. Plasma concentrations versus time of Terbinafine in each Penguin (3, 7 and 15mg/kg single oral dose)

Penquins-Aug 2004

		Treatment 1 Dose: 3mg/kg												
Time (hr)	**Samples**	**C (mg/L)**	**Time (hr)**	**Samples**	**C (mg/L)**	**Time (hr)**	**Samples**	**C (mg/L)**	**Time (hr)**	**Samples**	**C (mg/L)**	**Time (hr)**	**Samples**	**C (mg/L)**
0	105079-1	<0.01	0	105114-1	<0.01	0	104721-1	<0.01	0	104986-1	<0.01	0	104708-1	<0.01
0.25	105079-2	0.033	0.25	105114-2	0.06	0.25	104721-2	<0.01	0.25	104986-2	<0.01	0.25	104708-2	<0.01
0.5	105079-3	0.056	0.5	105114-3	0.016	0.5	104721-3	<0.01	0.5	104986-3	<0.01	0.5	104708-3	<0.01
0.75	105079-4	0.07	0.75	105114-4	0.03	0.75	104721-4	0.046	0.75	104986-4	0.022	0.75	104708-4	<0.01
1	105079-5	0.065	1	105114-5	0.025	1	104721-5	0.05	1	104986-5	0.018	1	104708-5	<0.01
2	105079-6	0.058	2	105114-6	0.073	2	104721-6	0.045	2	104986-6	0.089	2	104708-6	<0.01
4	105079-7	0.183	4	105114-7	0.036	4	104721-7	0.044	4	104986-7	0.088	4	104708-7	<0.01
10	105079-8	0.019	10	105114-8	0.039	10	104721-8	<0.01	10	104986-8	0.147	10	104708-8	<0.01

12	105079-9	0.015	12	105114-9	0.21	12	104721-9	<0.01	12	104986-9	0.01	12	104708-9	<0.01
24	105079-10	0.012	24	105114-10	0.012	24	104721-10	<0.01	24	104986-10	<0.01	24	104708-10	<0.01

Time (hr)	Samples	C (mg/L)	Time (hr)	Samples	C (mg/L)	Time (hr)	Samples	C (mg/L)	Time (hr)	Samples	mg/L	Time (hr)	Samples	C (mg/L)
0	105297-1	<0.01	0	104757-1	<0.01	0	104903-1	<0.01	0	105040-1	<0.01	0	104720-1	<0.01
0.25	105297-2	0.01	0.25	104757-2	0.021	0.25	104903-2	0.016	0.25	105040-2	<0.01	0.25	104720-2	<0.01
0.5	105297-3	0.029	0.5	104757-3	0.029	0.5	104903-3	0.033	0.5	105040-3	<0.01	0.5	104720-3	<0.01
0.75	105297-4	0.031	0.75	104757-4	0.031	0.75	104903-4	0.045	0.75	105040-4	0.08	0.75	104720-4	0.036
1	105297-5	0.026	1	104757-5	0.034	1	104903-5	0.068	1	105040-5	0.025	1	104720-5	0.067
2	105297-6	0.162	2	104757-6	0.018	2	104903-6	0.075	2	105040-6	0.013	2	104720-6	0.084
4	105297-7	0.157	4	104757-7	0.052	4	104903-7	0.067	4	105040-7	0.049	4	104720-7	0.146
10	105297-8	0.028	10	104757-8	0.038	10	104903-8	0.07	10	105040-8	0.023	10	104720-8	<0.01
12	105297-9	0.016	12	104757-9	0.027	12	104903-9	<0.01	12	105040-9	0.013	12	104720-9	<0.01
24	105297-10	0.011	24	104757-10	<0.01	24	104903-10	<0.01	24	105040-10	<0.01	24	104720-10	<0.01

Treatment 2
Dose 7mg/kg

Time (hr)	Samples	C (mg/L)	Time (hr)	Samples	C (mg/L)	Time (hr)	Samples	C (mg/L)	Time (hr)	Samples	C (mg/L)	Time (hr)	Samples	C (mg/L)
0	2-104720-1	<0.01	0	2-104993-1	<0.01	0	2-104763-1	<0.01	0	2-105079-1	<0.01	0	3-1047121-1	<0.07
0.25	2-104720-2	0.081	0.25	2-104993-2	0.016	0.25	2-104763-2	0.021	0.25	2-105079-2	0.036	0.25	3-1047121-2	<0.07
0.5	2-104720-3	0.176	0.5	2-104993-3	0.059	0.5	2-104763-3	0.021	0.5	2-105079-3	0.056	0.5	3-1047121-3	0.126
0.75	2-104720-4	0.204	0.75	2-104993-4	0.104	0.75	2-104763-4	0.049	0.75	2-105079-4	0.071	0.75	3-1047121-4	0.181
1	2-104720-5	0.197	1	2-104993-5	0.13	1	2-104763-5	0.042	1	2-105079-5	0.058	1	3-1047121-5	0.14
2	2-104720-6	0.185	2	2-104993-6	0.125	2	2-104763-6	0.036	2	2-105079-6	0.062	2	3-1047121-6	0.134
4	2-104720-7	0.262	4	2-104993-7	0.181	4	2-104763-7	0.098	4	2-105079-7	0.318	4	3-1047121-7	no sample

10	2-104720-8	0.101	10	2-104993-8	0.102	10	2-104763-8	0.05	10	2-105079-8	0.106	10	3-1047121-8	0.145
12	2-104720-9	0.085	12	2-104993-9	0.082	12	2-104763-9	0.023	12	2-105079-9	0.148	12	3-1047121-9	0.119
24	2-104720-10	0.039	24	2-104993-10	0.046	24	2-104763-10	0.03	24	2-105079-10	0.116	24	3-1047121-10	0.071
48	2-104720-11	0.016		2-104993-11	0.017	48	2-104763-11	<0.01	48	2-105079-11	0.098	48	3-1047121-11	<0.07

Time (hr)	Samples	C (mg/L)	Time (hr)	Samples	C (mg/L)	Time (hr)	Samples	C (mg/L)	Time (hr)	Samples	C (mg/L)	Time (hr)	Samples	C (mg/L)
0	2-104708-1	<0.01	0	2-105297-1	<0.01	0	2-105114-1	<0.01	0	3-104759-1	<0.07	0	3-105041-1	<0.07
0.25	2-104708-2	0.37	0.25	2-105297-2	<0.01	0.25	2-105114-2	0.024	0.25	3-104759-2	<0.07	0.25	3-105041-2	0.085
0.5	2-104708-3	1.156	0.5	2-105297-3	0.084	0.5	2-105114-3	0.067	0.5	3-104759-3	<0.07	0.5	3-105041-3	0.133
0.75	2-104708-4	1.035	0.75	2-105297-4	0.082	0.75	2-105114-4	0.086	0.75	3-104759-4	0.125	0.75	3-105041-4	0.124
1	2-104708-5	0.928	1	2-105297-5	0.137	1	2-105114-5	0.11	1	3-104759-5	0.11	1	3-105041-5	0.119
2	2-104708-6	0.362	2	2-105297-6	0.125	2	2-105114-6	no sample	2	3-104759-6	0.074	2	3-105041-6	0.109
4	2-104708-7	0.299	4	2-105297-7	0.731	4	2-105114-7	0.129	4	3-104759-7	0.116	4	3-105041-7	0.392
10	2-104708-8	0.178	10	2-105297-8	0.198	10	2-105114-8	0.224	10	3-104759-8	0.106	10	3-105041-8	0.084
12	2-104708-9	0.123	12	2-105297-9	0.01	12	2-105114-9	0.141	12	3-104759-9	0.095	12	3-105041-9	0.085
24	2-104708-10	0.037	24	2-105297-10	0.087	24	2-105114-10	0.058	24	3-104759-10	<0.07	24	3-105041-10	<0.07
48	2-104708-11	<0.01	48	2-105297-11	0.029	48	2-105114-11	0.01	48	3-104759-11	<0.07	48	3-105041-11	<0.07

Treatment 3
Dose: 15mg/kg

Time (hr)	Samples	C (mg/L)	Time (hr)	Samples	C (mg/L)	Time (hr)	Samples	C (mg/L)
0	3-104708-1	<0.07	0	3-104761-1	<0.07	0	3-104762-1	<0.07
0.25	3-104708-2	0.083	0.25	3-104761-2	0.102	0.25	3-104762-2	0.072
0.5	3-104708-3	0.129	0.5	3-104761-3	0.119	0.5	3-104762-3	no sample
0.75	3-104708-4	0.117	0.75	3-104761-4	0.132	0.75	3-104762-4	0.134
1	3-104708-5	0.087	1	3-104761-5	no sample	1	3-104762-5	0.165

2	3-104708-6	0.233	2	3-104761-6	0.182	2	3-104762-6	0.127
4	3-104708-7	0.244	4	3-104761-7	0.305	4	3-104762-7	0.139
10	3-104708-8	0.211	10	3-104761-8	0.146	10	3-104762-8	0.097
12	3-104708-9	0.141	12	3-104761-9	0.131	12	3-104762-9	0.142
24	3-104708-10	0.114	24	3-104761-10	0.103	24	3-104762-10	0.248
48	3-104708-11	0.075	48	3-104761-11	<0.07	48	3-104762-11	0.099

Time (hr)	**Samples**	**C (mg/L)**	**Time (hr)**	**Samples**	**C (mg/L)**	**Time (hr)**	**Samples**	**C (mg/L)**
0	3-104763-1	<0.07	0	3-104709-1	<0.07	0	3-104931-1	<0.07
0.25	3-104763-2	<0.07	0.25	3-104709-2	0.26	0.25	3-104931-2	0.107
0.5	3-104763-3	<0.07	0.5	3-104709-3	0.168	0.5	3-104931-3	0.147
0.75	3-104763-4	0.095	0.75	3-104709-4	0.348	0.75	3-104931-4	0.226
1	3-104763-5	0.053	1	3-104709-5	0.199	1	3-104931-5	0.156
2	3-104763-6	0.126	2	3-104709-6	0.147	2	3-104931-6	0.144
4	3-104763-7	0.141	4	3-104709-7	0.226	4	3-104931-7	0.567
10	3-104763-8	0.201	10	3-104709-8	0.129	10	3-104931-8	0.284
12	3-104763-9	0.122	12	3-104709-9	0.145	12	3-104931-9	0.163
24	3-104763-10	0.075	24	3-104709-10	<0.07	24	3-104931-10	0.075
48	3-104763-11	<0.07	48	3-104709-11	<0.07	48	3-104931-11	<0.07

(a) Treatment 1, 3mg/kg

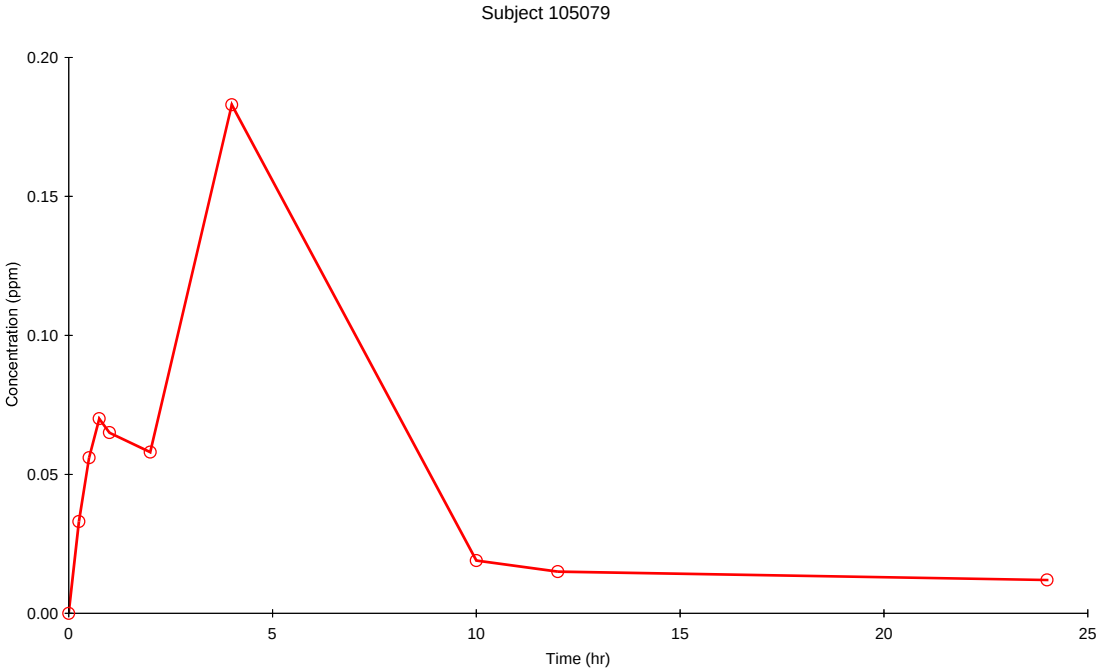

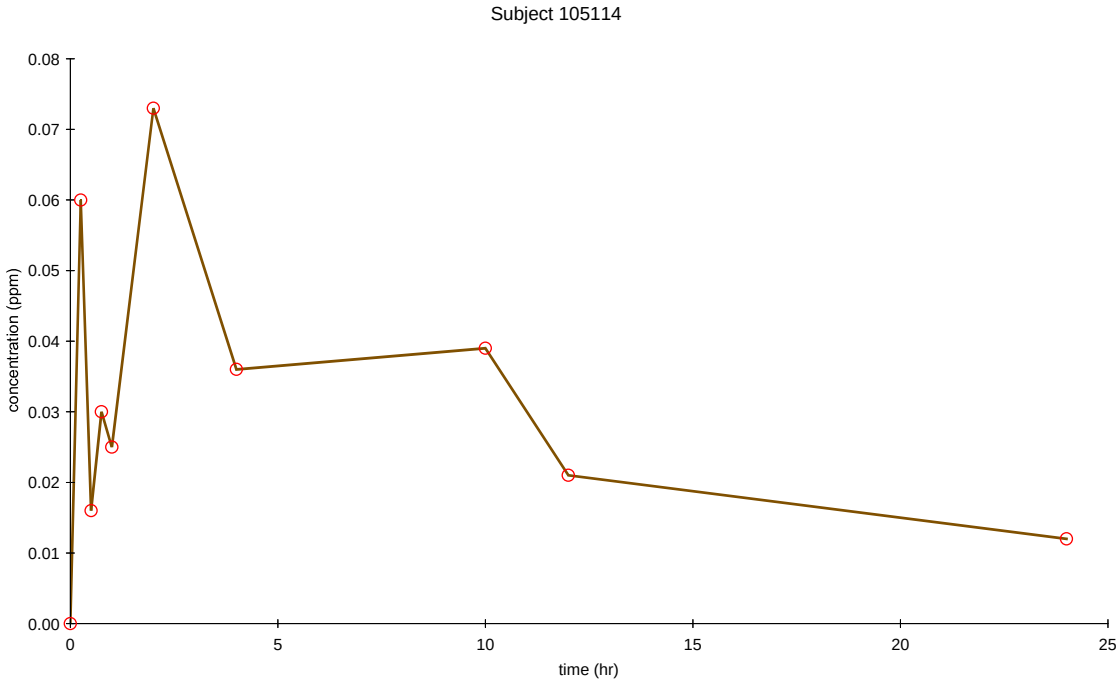

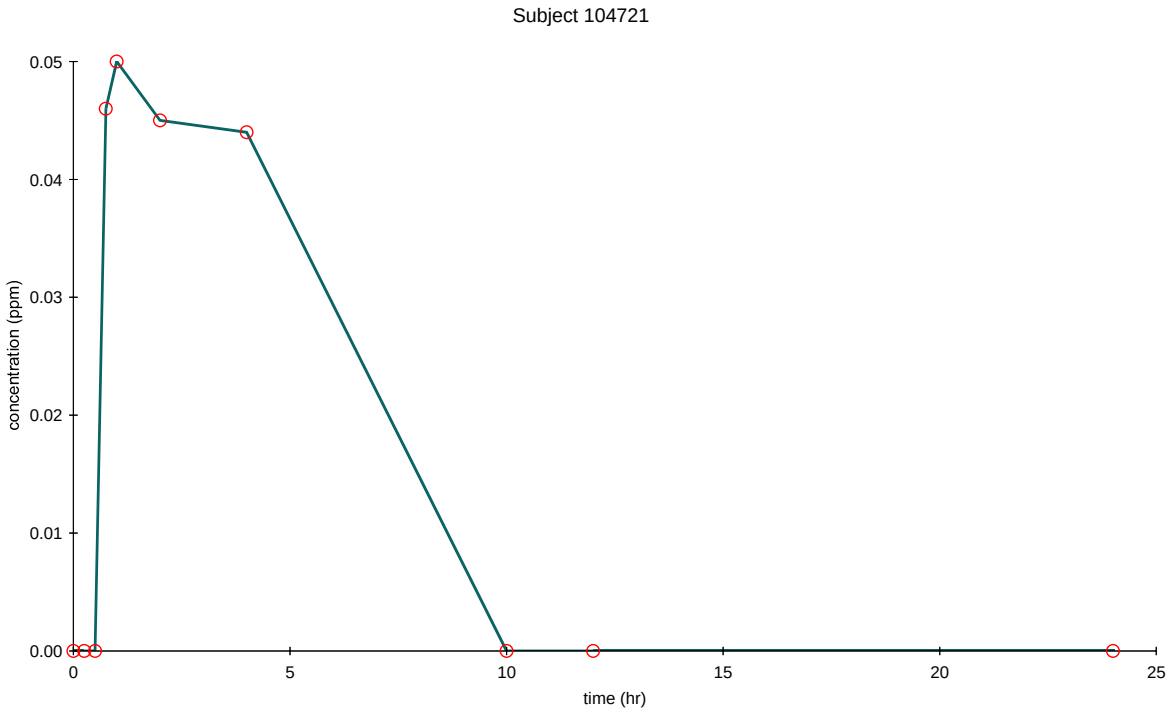
Subject 104721
concentration (ppm)
0.05
0.04
0.03
0.02
0.01
0.00
0
5
10
15
20
25
time (hr)

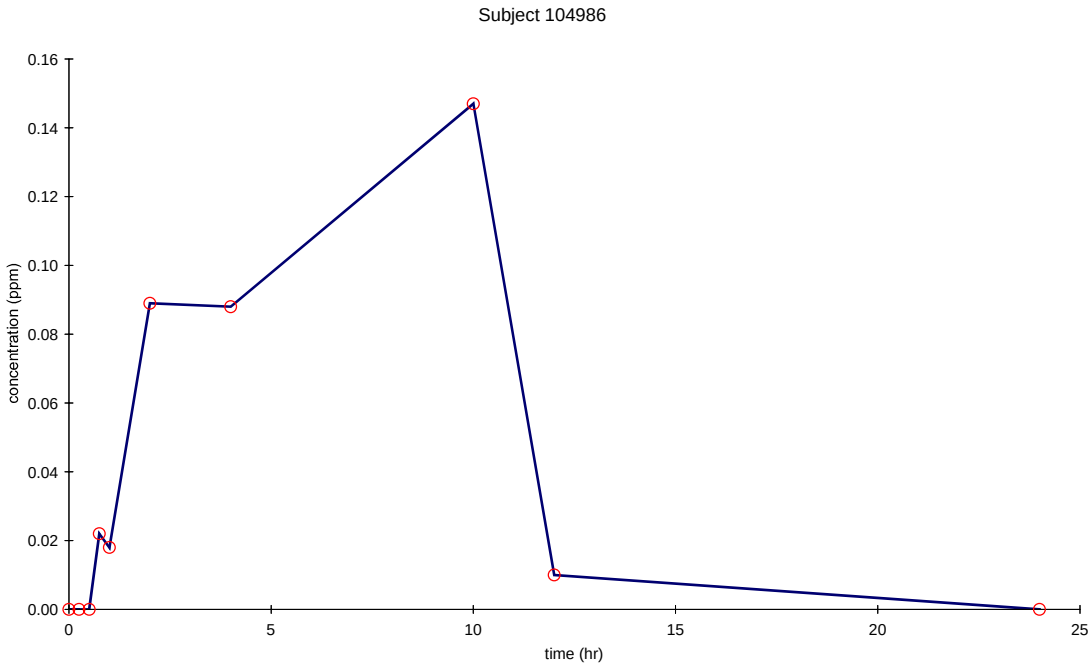
Subject 104986
concentration (ppm)
0.16
0.14
0.12
0.10
0.08
0.06
0.04
0.02
0.00
0
5
10
15
20
25
time (hr)

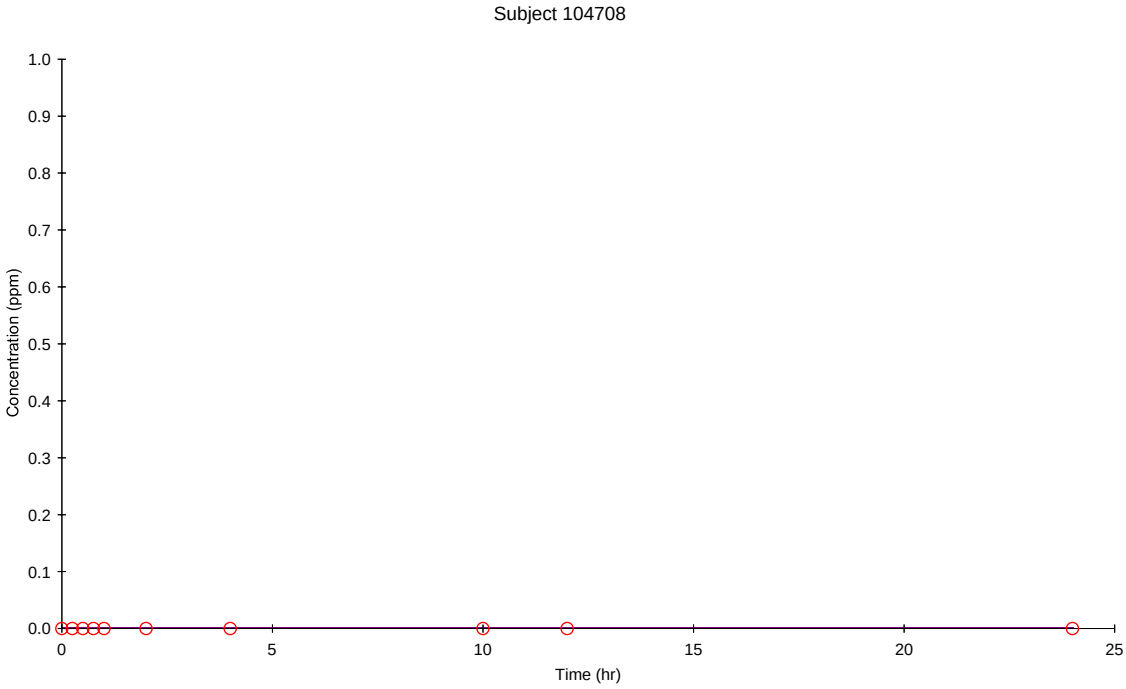
Subject 104708
Concentration (ppm)
1.0
0.9
0.8
0.7
0.6
0.5
0.4
0.3
0.2
0.1
0.0
0
5
10
15
20
25
Time (hr)

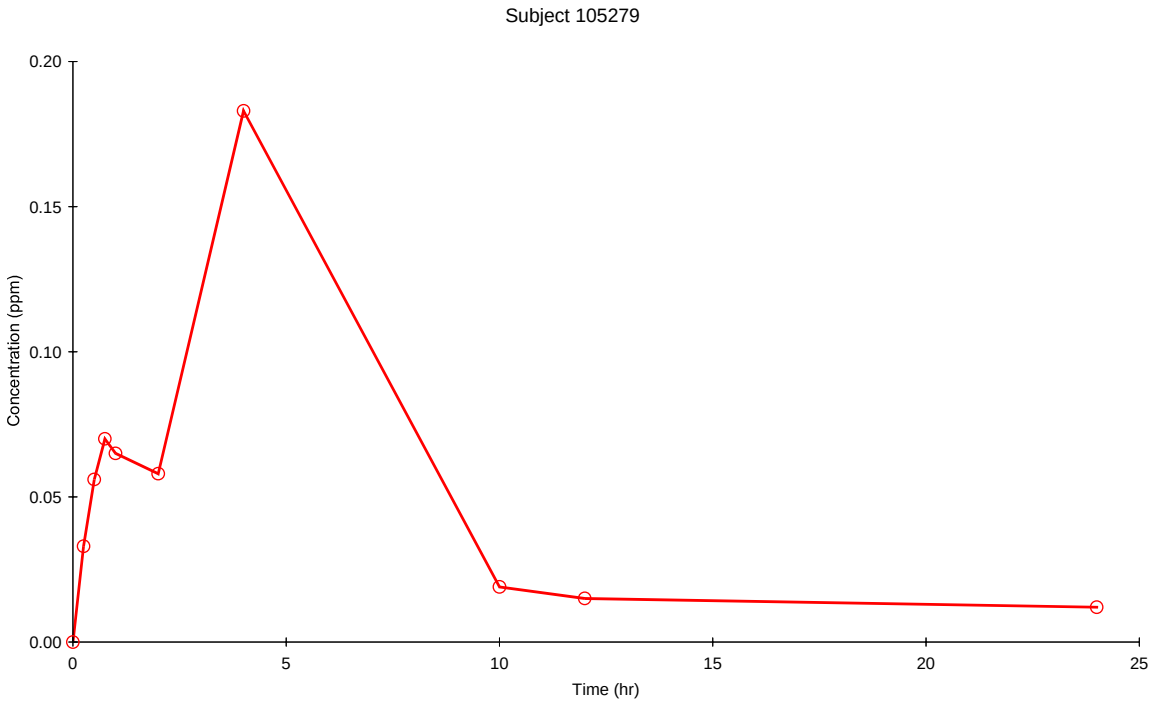
Subject 105279
Concentration (ppm)
0.20
0.15
0.10
0.05
0.00
0
5
10
15
20
25
Time (hr)

Subject 104903

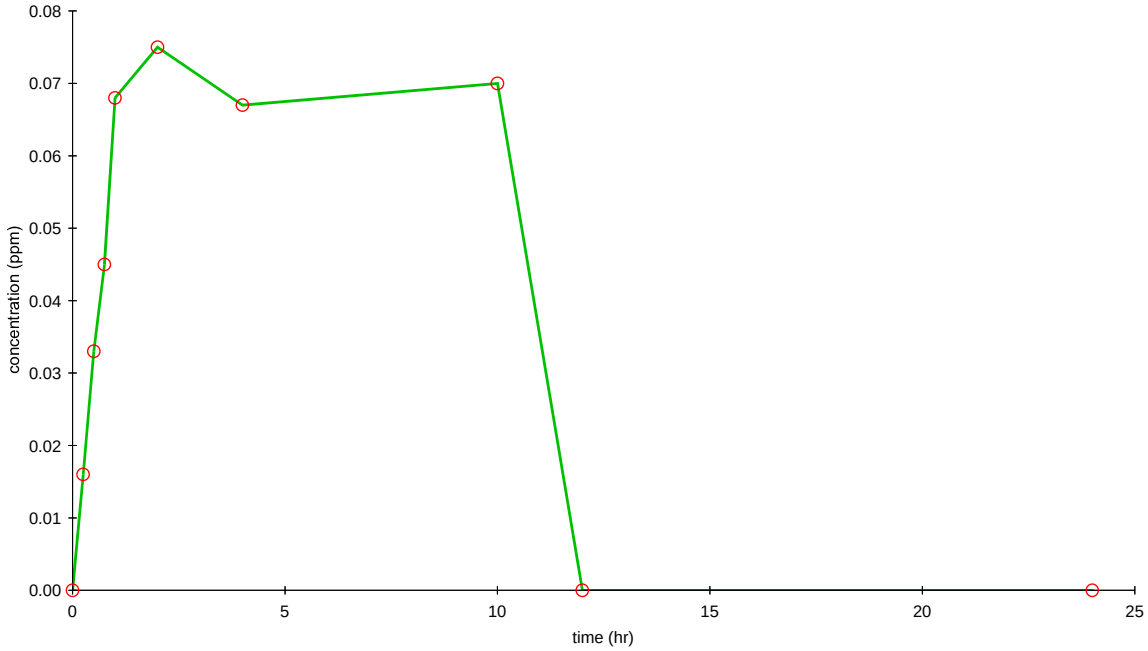

Subject 105040

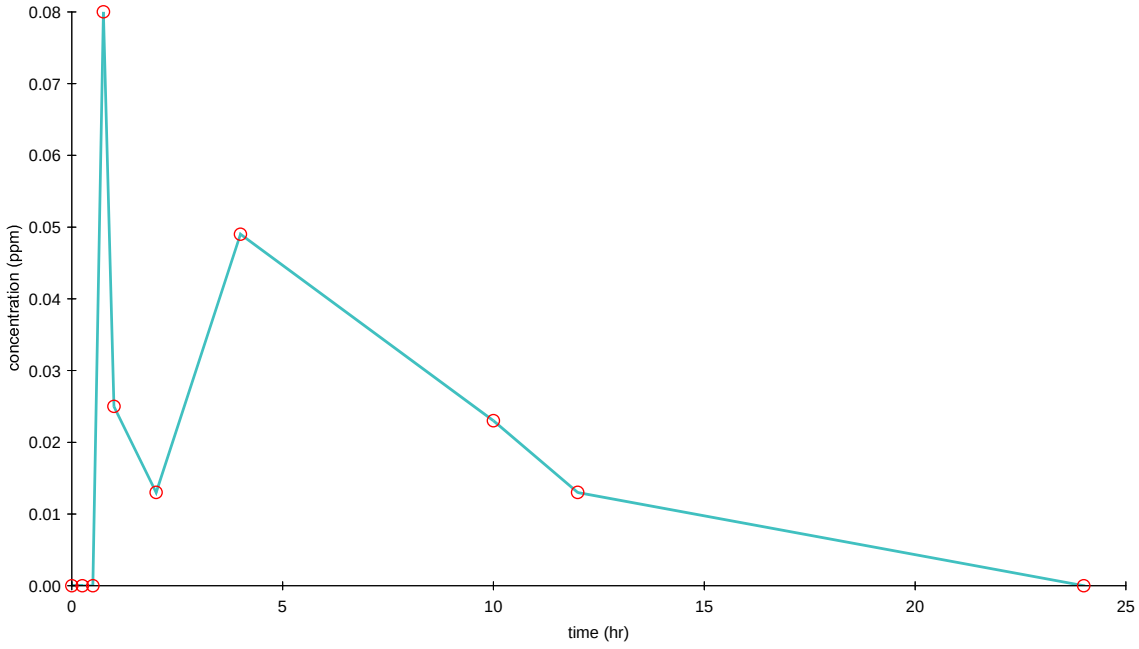

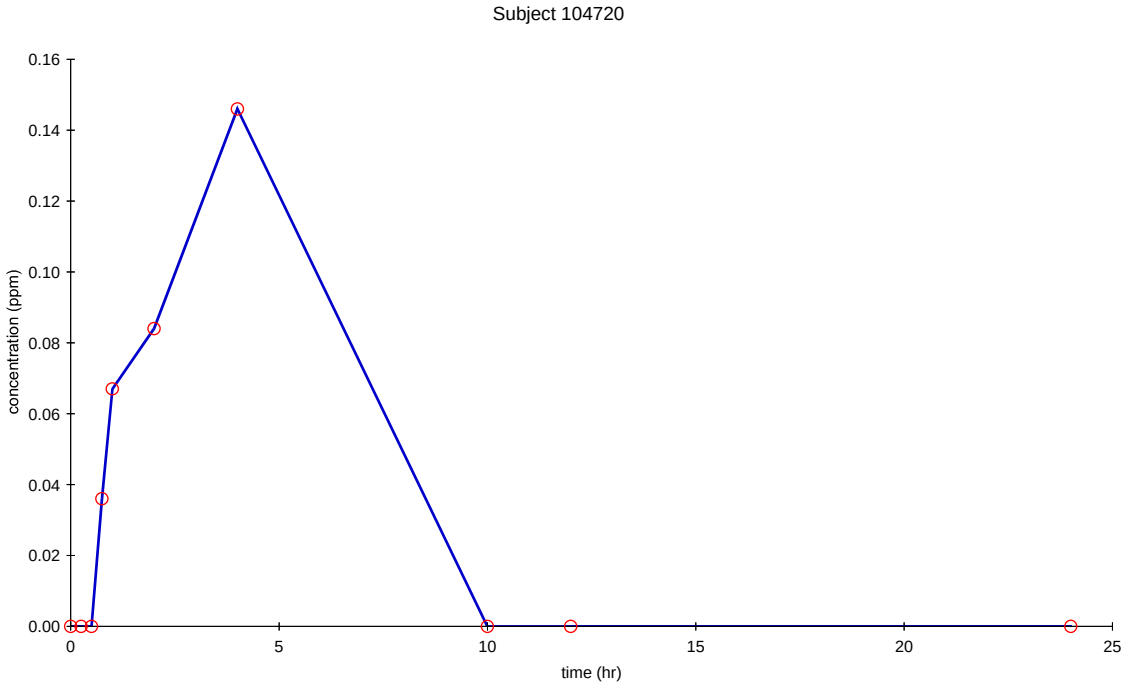

(b) Treatment 2, 7mg/kg

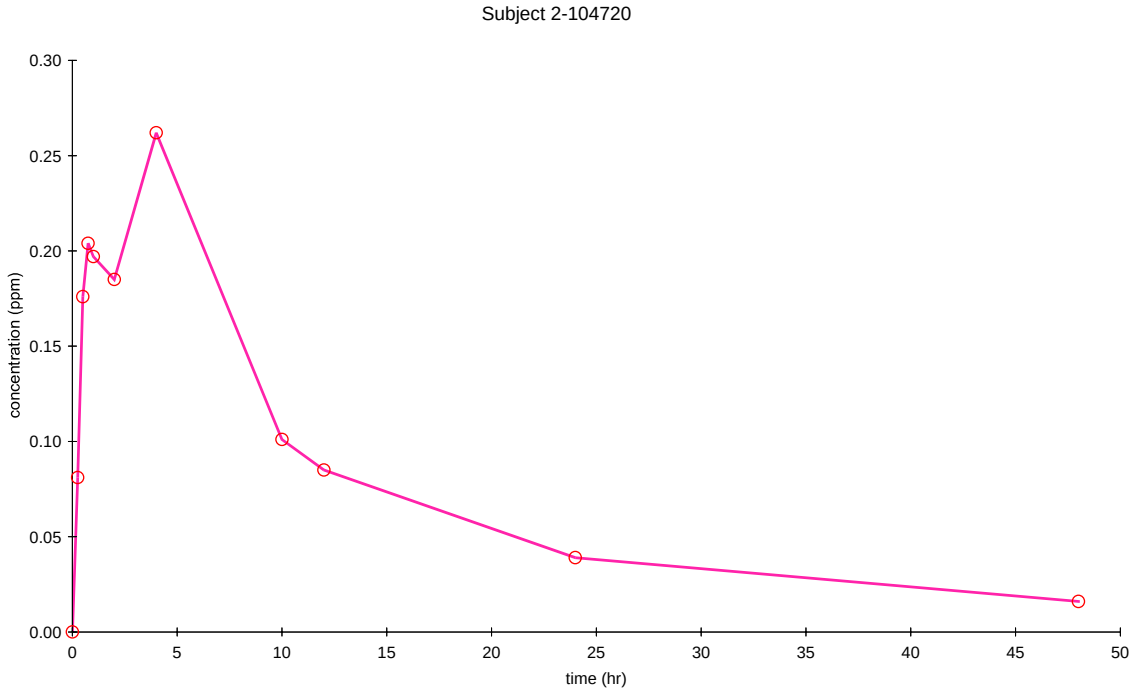

Subject 2-104993

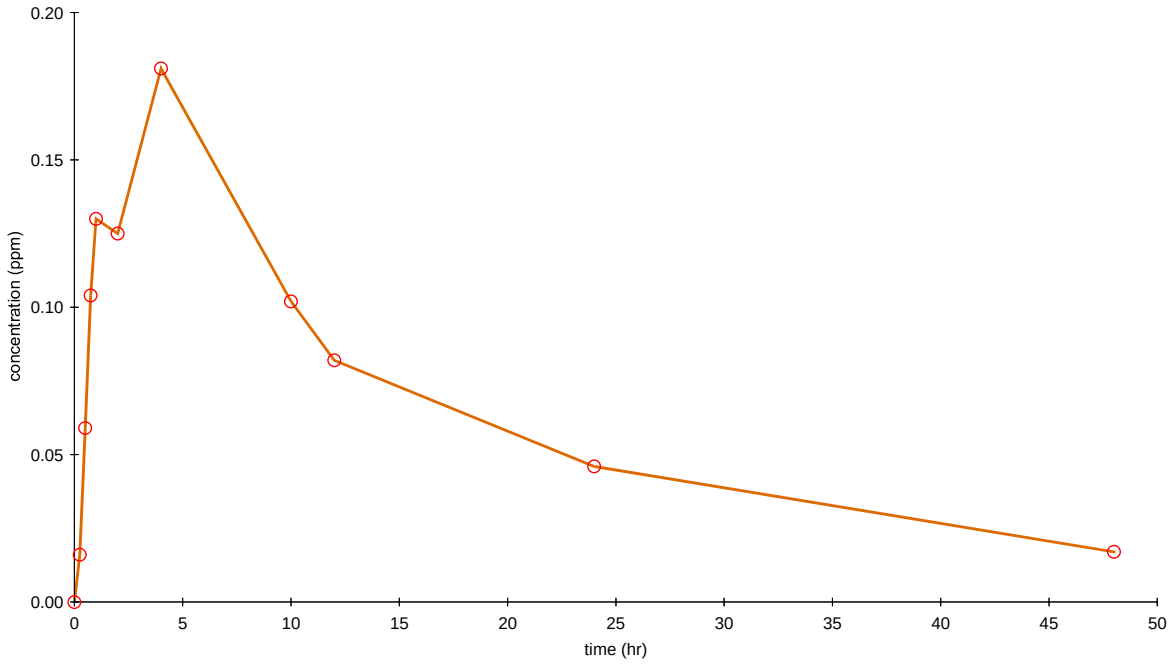

Subject 2-104763

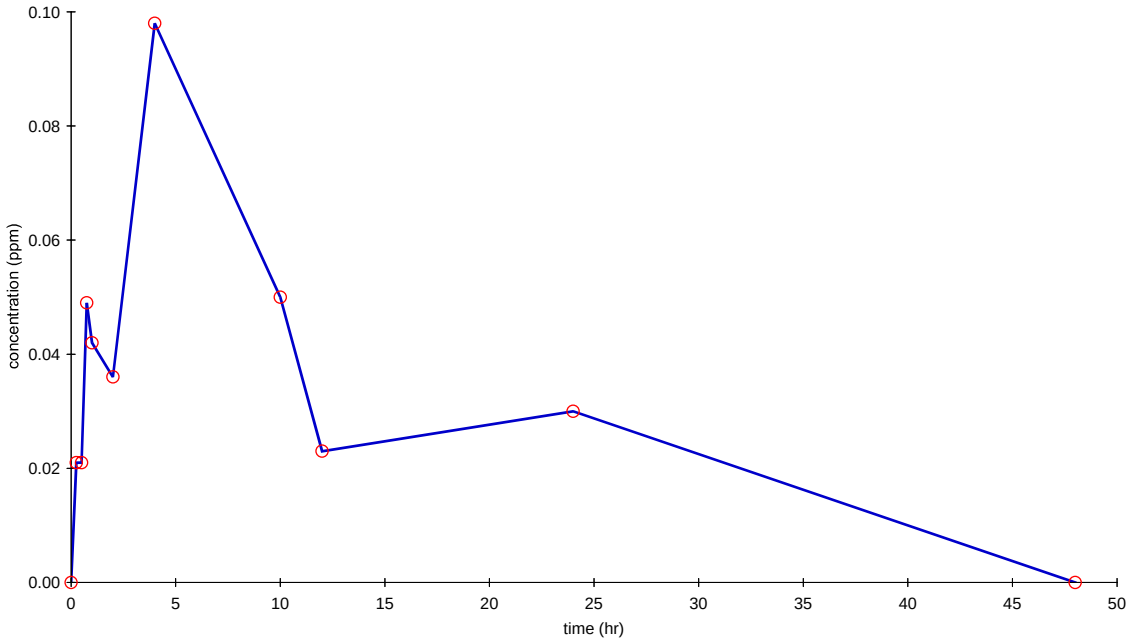

Subject 2-105079

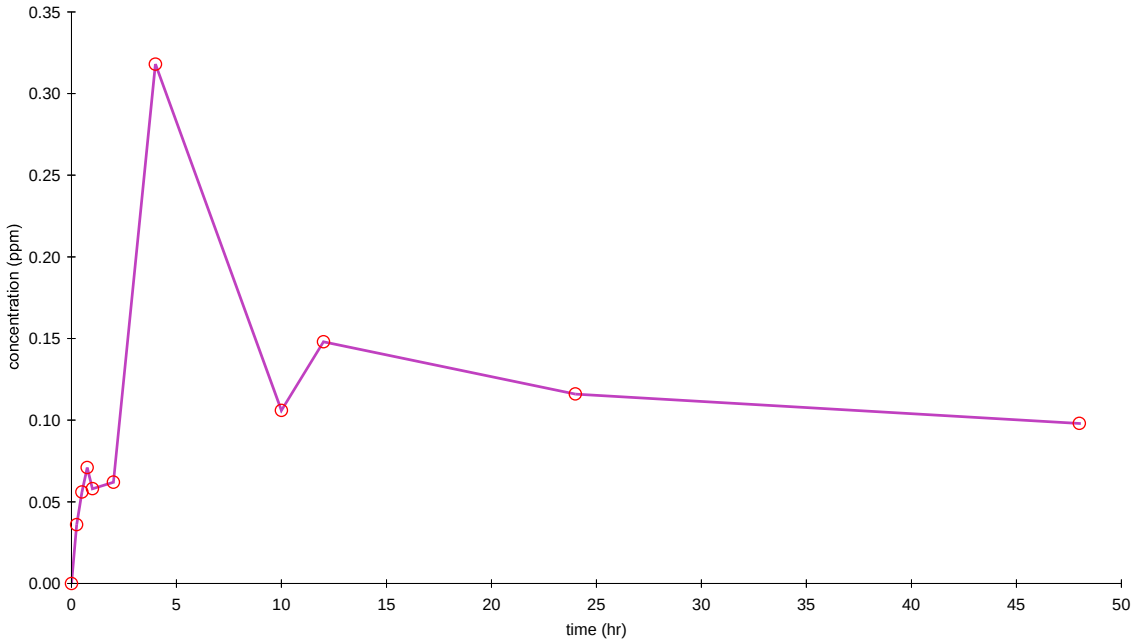

Subject 3-104721

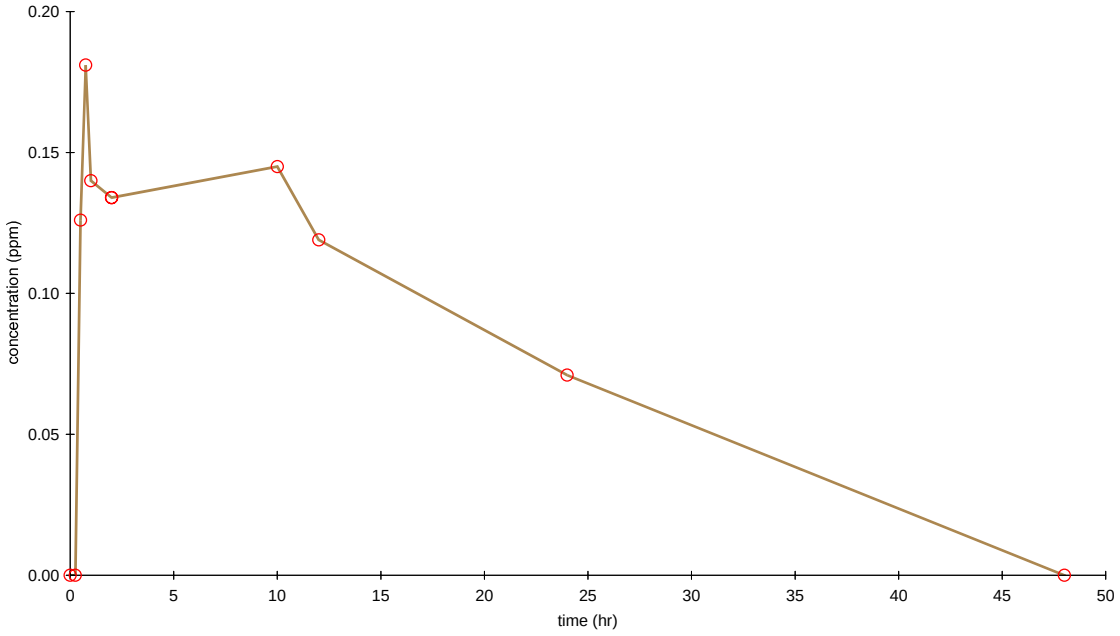

Subject 2-104708

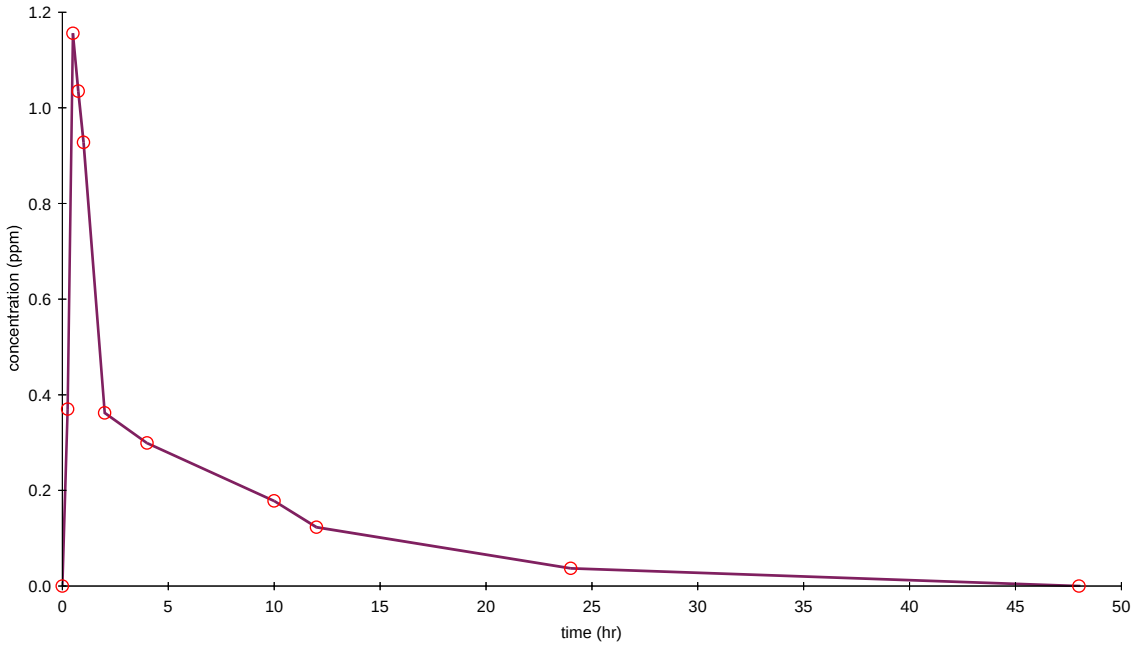

Subject 2-105279

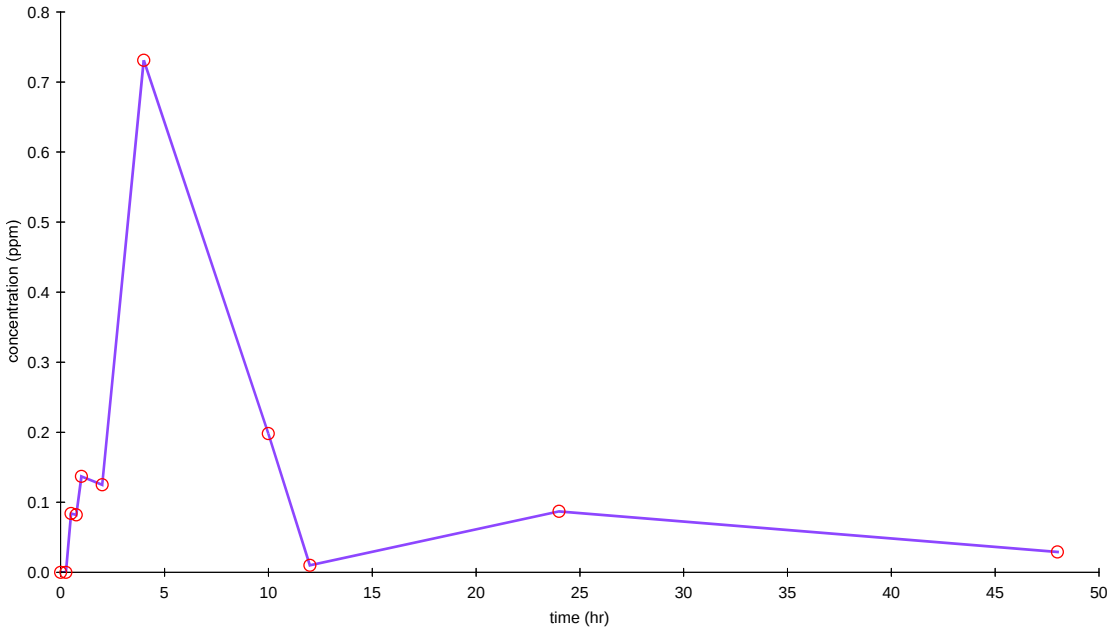

Subject 2-105114

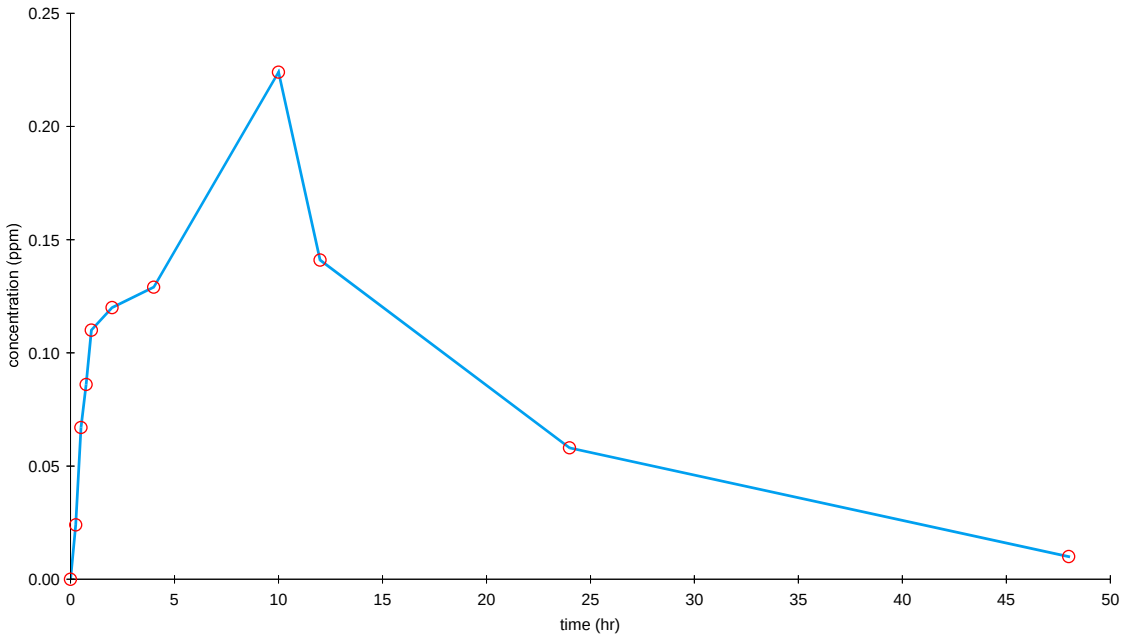

Subject 3-104759

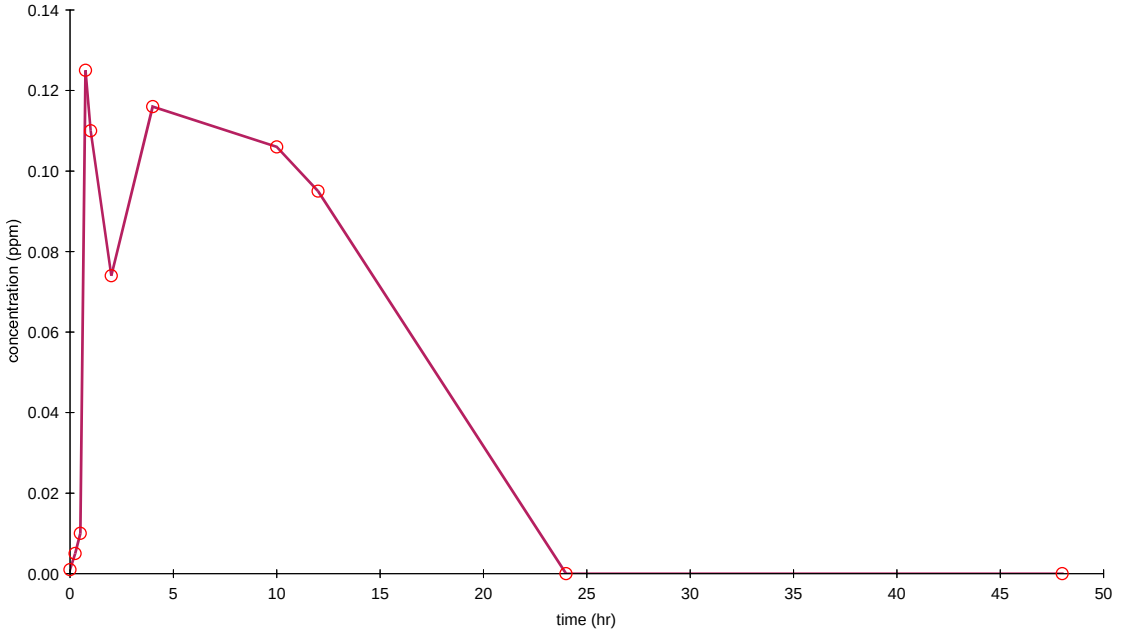

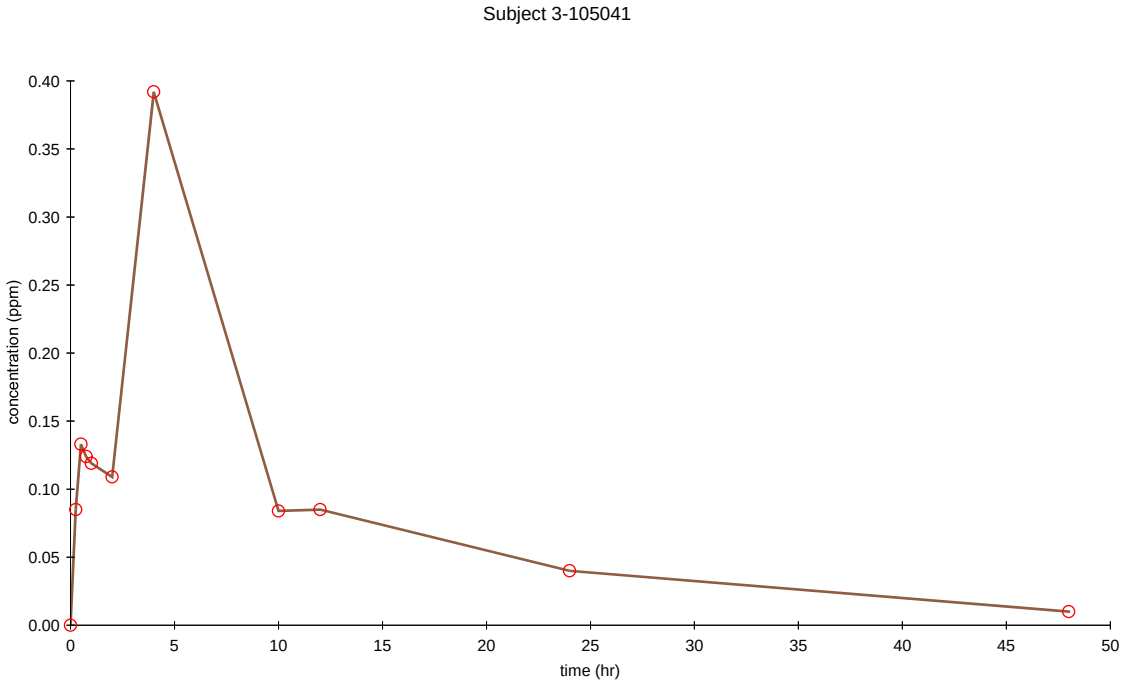

(c) Treatment 3, 15mg/kg

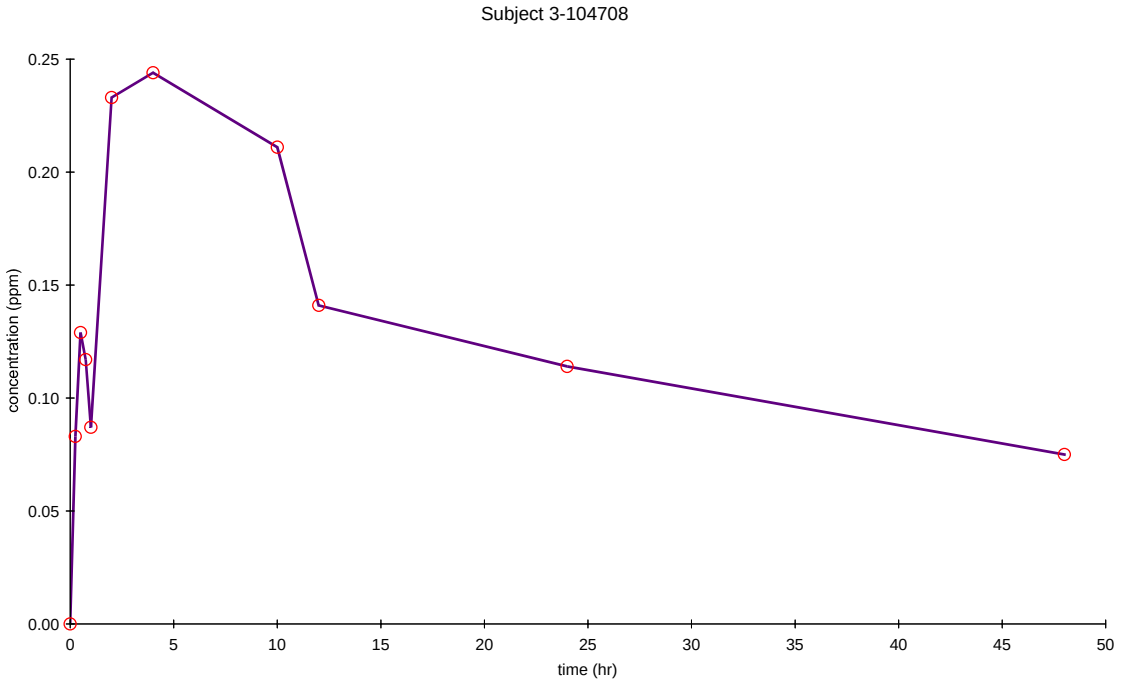

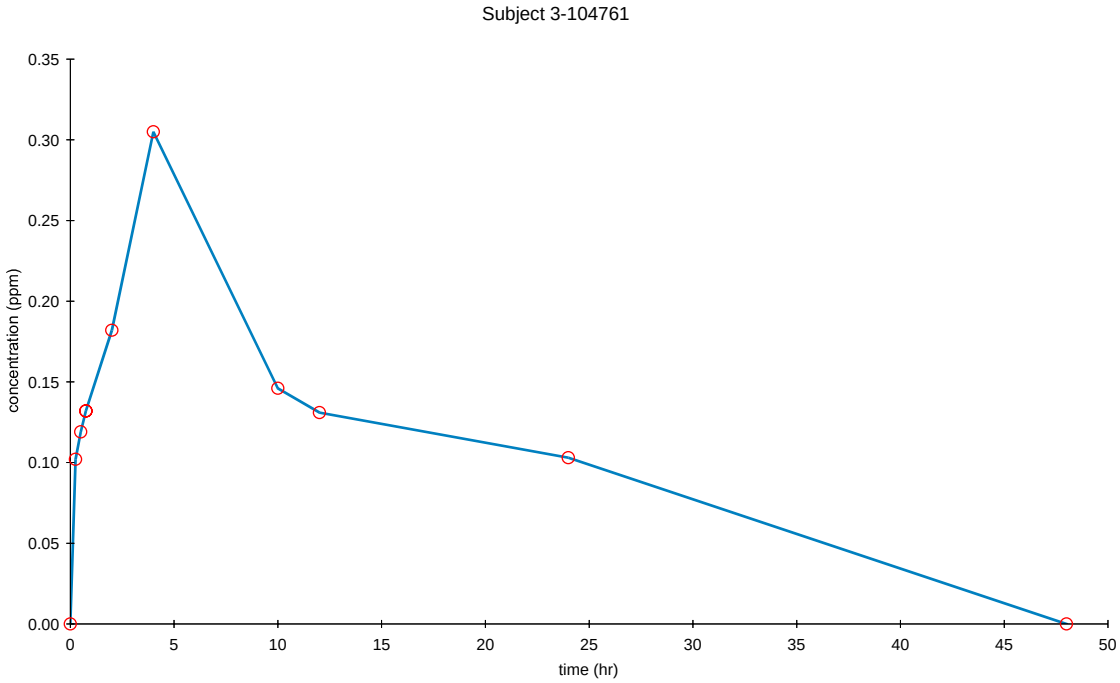
Subject 3-104761
concentration (ppm)
0.35
0.30
0.25
0.20
0.15
0.10
0.05
0.00
0
5
10
15
20
25
30
35
40
45
50
time (hr)

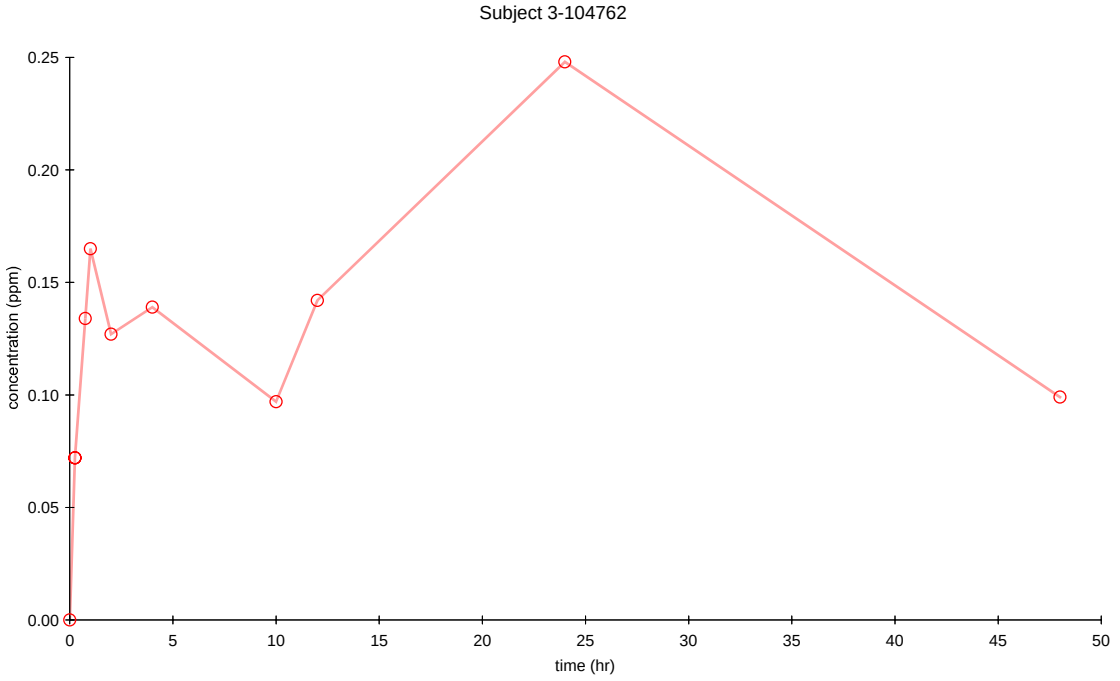
Subject 3-104762
concentration (ppm)
0.25
0.20
0.15
0.10
0.05
0.00
0
5
10
15
20
25
30
35
40
45
50
time (hr)

Subject 3-104709

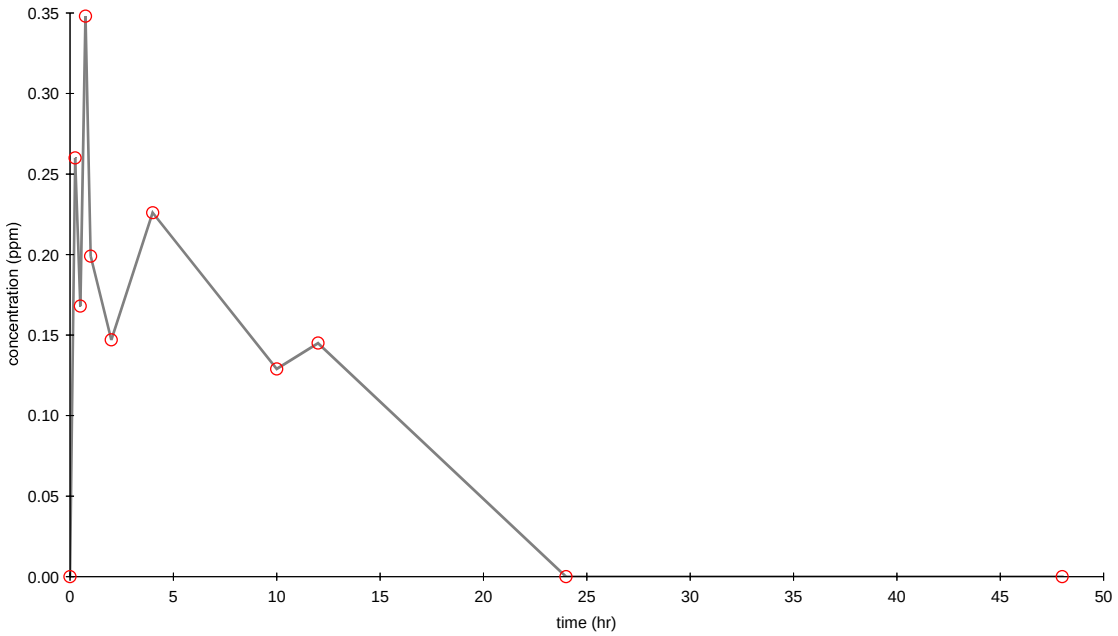

Subject 3-104931

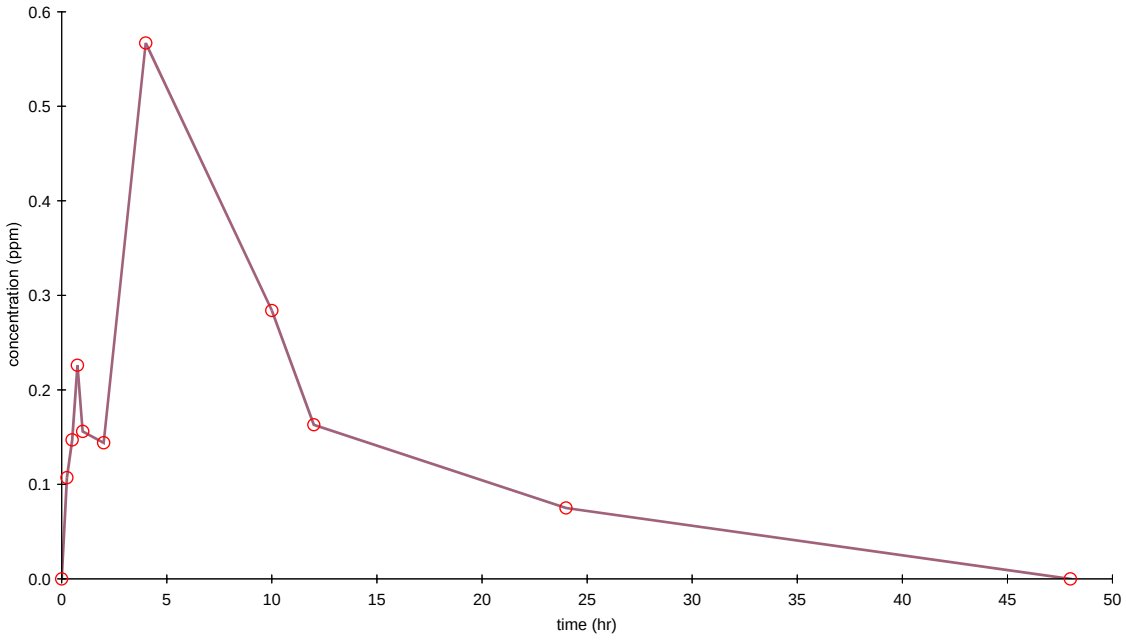

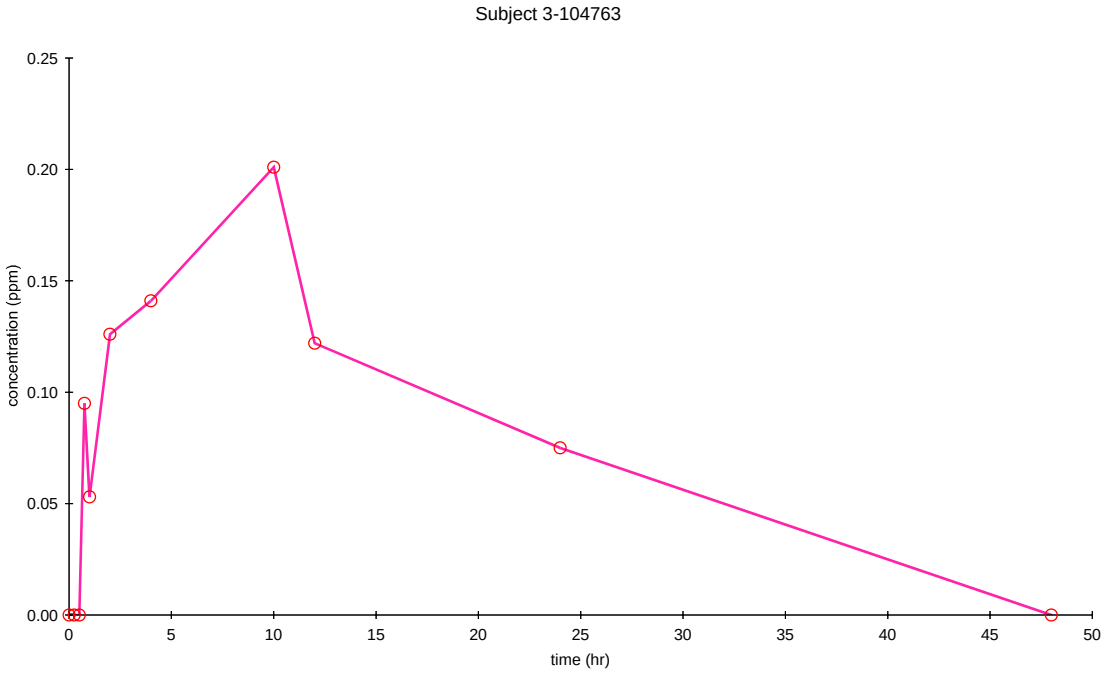

Figure 3.4. The individual plasma concentration time curve of individual subjects: (a) treatment 1, 3mg/kg, (b) treatment 2, 7mg/kg, (c) treatment 3, 15mg/kg.

(a)

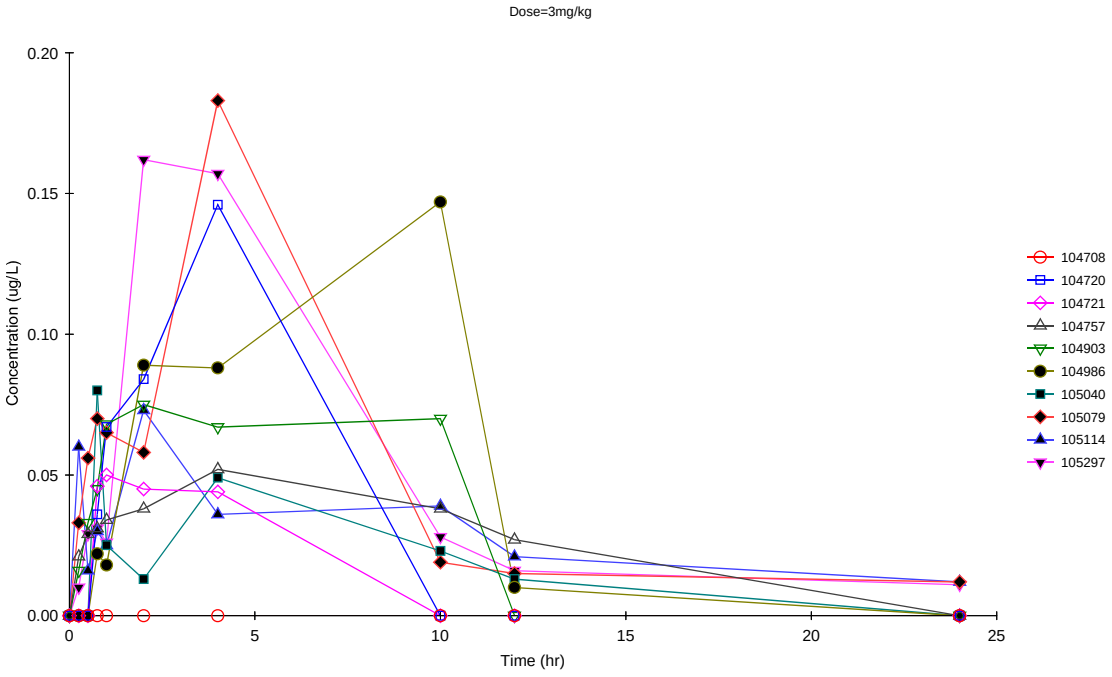

(b)

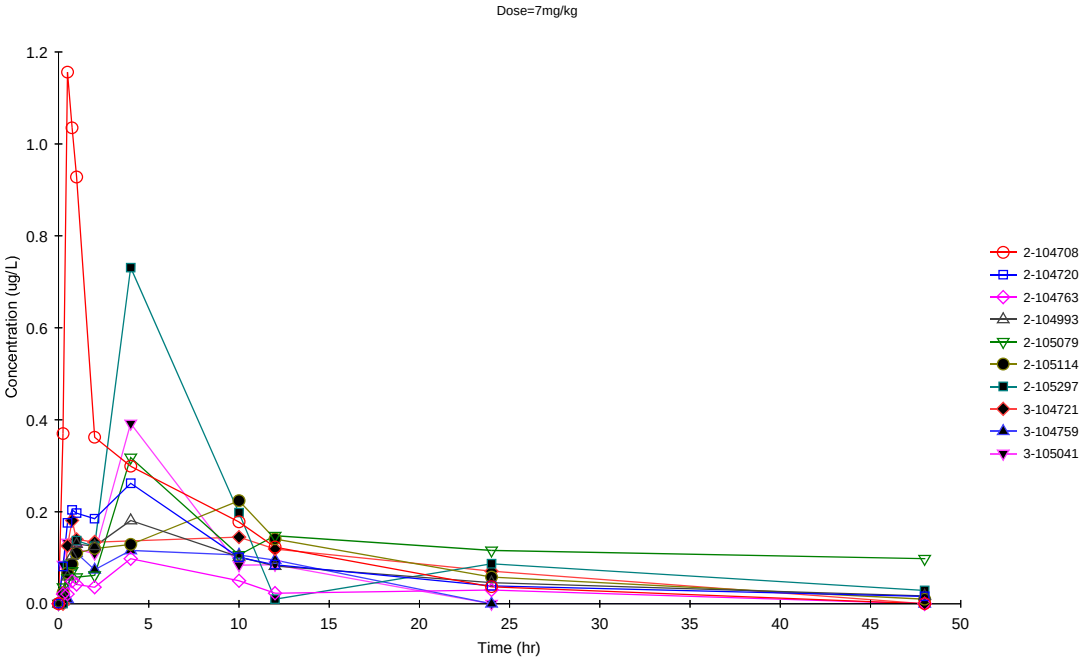

(c)

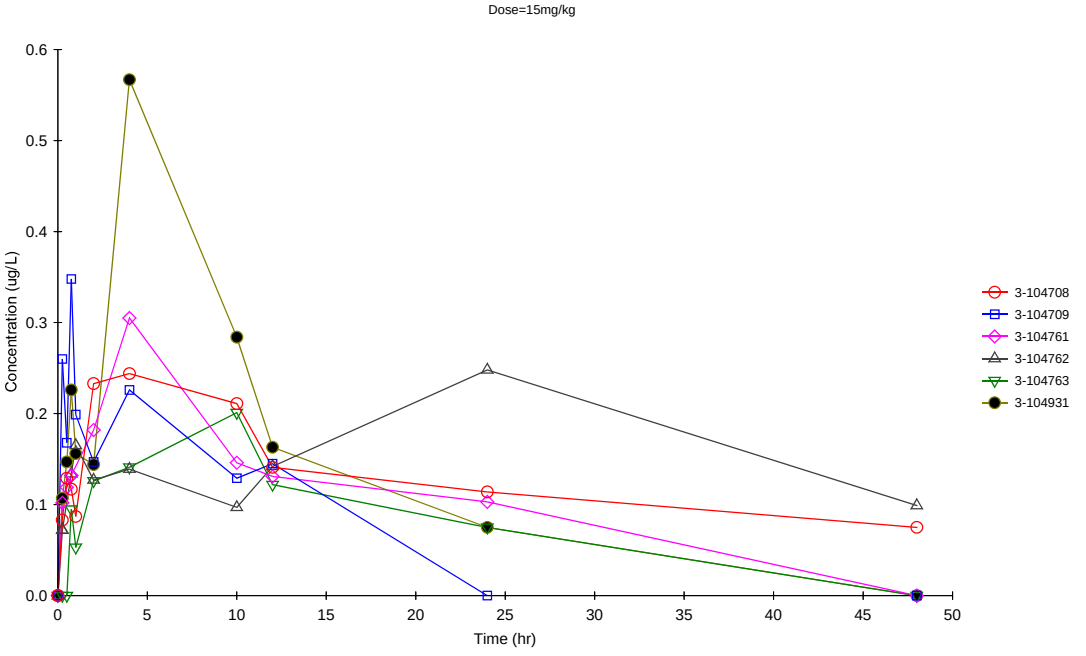

Figure 3.5. Spaghetti-scatter plots of the three dosing regimes (a) 3mg/kg, (b) 7mg/kg, 15mg/kg for Terbinafine given as a single oral dose to penguins

Table 3.4. Mean plasma concentration of three single dosing treatments 3mg/kg, 7mg/kg, 15mg/kg

Treatment	Time (hour)	Mean plasma concentration (mg/L)	Standard deviation
3mg/kg			
	0	0	0.0000
	0.25	0.0156	0.0203
	0.5	0.0181	0.0200
	0.75	0.0434	0.0195
	1	0.0420	0.0205
	2	0.0686	0.0444
	4	0.0913	0.0558
	10	0.0404	0.0453
	12	0.0113	0.0098
	24	0.0039	0.0058
7mg/kg			
	0	0.0001	0.0003
	0.25	0.0719	0.1096
	0.5	0.1938	0.3430
	0.75	0.2084	0.2951
	1	0.2028	0.2596
	2	0.1383	0.0921
	4	0.2788	0.1859
	10	0.1250	0.0554
	12	0.0877	0.0448
	24	0.0492	0.0320
	48	0.0196	0.0291
15mg/kg			
	0	0	0.0000
	0.25	0.1040	0.0856
	0.5	0.1126	0.0657
	0.75	0.1753	0.0957
	1	0.1320	0.0600
	2	0.1598	0.0412
	4	0.2703	0.1586
	10	0.1780	0.0676
	12	0.1407	0.0139
	24	0.1025	0.0816
	48	0.0290	0.0456

The data and spaghetti-scatter plots demonstrate that there was high inter-subject variability among all of the subjects in all dosing regimens, 3mg/kg, 7mg/kg, 15mg/kg.

At the low 3mg/kg dose, Terbinafine concentrations were under the limit of detection in the subject 104608. Subjects 104721 and 10420 had drug concentrations over the minimum limit of detection only from 0.75 hours to 4 hours. The last sampling-time point for the single oral dose of 3mg/kg was 24 hours as concentrations were low. For single oral dosing of 7mg/kg and 15mg/kg, sampling continued to 48 hours post administration. Mean plasma concentration profiles of the three single oral dosing treatments reveal that 3mg/kg has C_{max} under 0.1mg/kg. The C_{max} of 7mg/kg was higher than the C_{max} of 15mg/kg. However, the variability of the plasma concentration time curves for both treatment was very high. Thus, no certain conclusions could be stated concerning the C_{max} from these dosing regimens as to whether they were different.

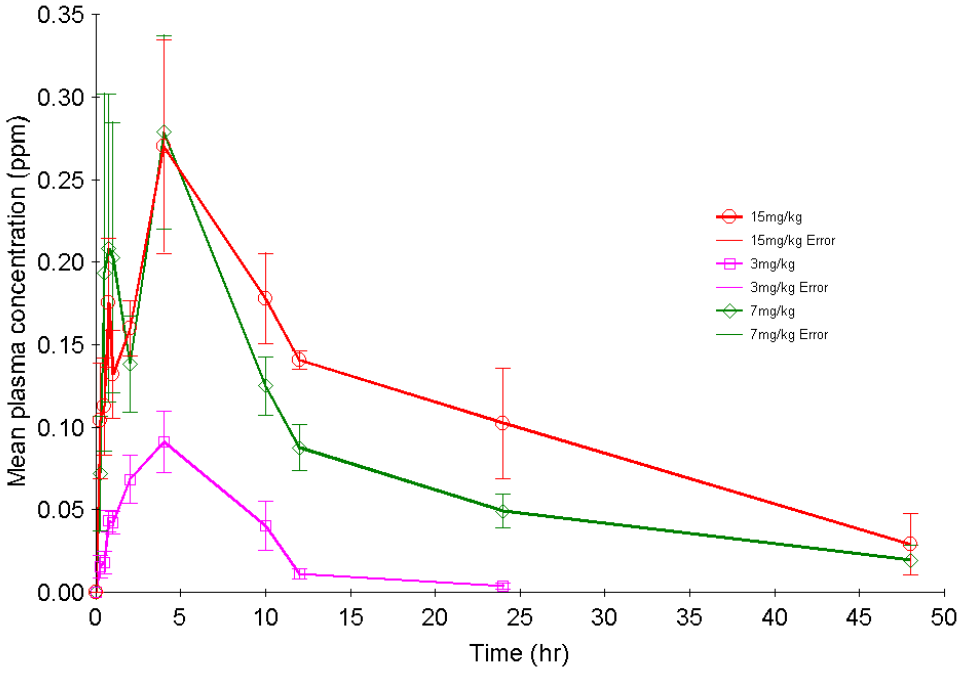

Figure 3.6. Mean Terbinafine plasma concentrations versus time and SE error bars of the three single oral doses given in penguins: 3mg/kg, 7mg/kg, 15mg/kg

Non-compartmental analysis

This is the simplest way to calculate bioavailability is by the non-compartmental pharmacokinetic analysis. Non-compartmental analysis allows the calculation of pharmacokinetic parameters regardless of the number of compartments the model has. There are six non-compartmental pharmacokinetic models in the WinNonlin. They are extra-vascular dosing, IV infusion, and IV bolus dosing for both plasma and urine drug concentration data. The selected model to analyze the Terbinafine penguin data is extra-vascular input for plasma concentrations; the model named 200 in the WinNonlin. Depending on the type of data, the WinNonlin provides non-steady and steady state calculations of the pharmacokinetic parameters. With dosing regimens in the current experiment, the non-steady state is the proper method for pharmacokinetic parameter calculation.

The following parameters will be presented from non-compartmental analysis:

Dosing time: Time of the last administered dose, this is assumed to be zero unless other wise specified.

T_{lag}: T lag is the time prior to the first measurable concentration

T_{max}: Time of maximum observed concentration

C_{max}: Concentration corresponding to T_{max}

T_{last}: Time of last measurable concentration

C_{last}: Concentration corresponding to T_{last}

AUC is the area under the plasma cocnetration time curve

AUC calculation and interpolation formulas

Four methods are available for the calculation of area under the curve, in the non-compartmental-analysis settings tab of the model options dialog. The method chosen applies to all AUC and partial area computations. All methods reduce to the log trapezoidal rule and/or linear trapezoidal rule, but differ with regard to when these rules are applied.

The linear-trapezoidal rule (linear interpolation) is the default method. This method uses the linear trapezoidal rule, given below, and is applied to each pair of consecutive points in the data set that have non-missing values and sums up these areas. If a partial area is selected that has an endpoint that is not in the data set, then the linear interpolation rule, given below, is used to inject a concentration value for that endpoint.

The linear-trapezoidal method with linear/log interpolation is the method 4. As above except when a partial area is selected that has an endpoint that is not in the data set: the linear interpolation rule is used to inject a concentration value for that endpoint if the endpoint is before C_{max}; the logarithmic interpolation is used after C_{max}. If C_{max} is not unique, then the first occurrence of C_{max} is used.

The linear/log-trapezoidal method is method 1, which uses the linear trapezoidal rule up to C_{max} and then the log trapezoidal rule for the remainder of the curve. If the C_{max} is not unique, then the first occurrence of C_{max} is used. Linear interpolation is used up to C_{max} for injecting points for partial areas, and logarithmic interpolation is used after C_{max}.

The linear up/log down method (method 3): the linear trapezoidal rule is used any time that the concentration data is increasing, and the logarithmic trapezoidal rule is used any time that the concentration data is decreasing. The points for partial areas are injected using the linear interpolation rule if the surrounding points show that the concentration is increasing, meanwhile the logarithmic interpolation rule is used if the concentration is decreasing.

The computational formulas for the area under the curve calculations and interpolation follow.

Linear-trapezoidal rule

$$AUC\,|_{t_1}^{t_2} = \delta_t * \frac{C_1 + C_2}{2}$$

$$AUMC\,|_{t_1}^{t_2} = \delta_t * \frac{t_1 * C_1 + t_2 * C_2}{2}$$

Logarithmic-trapezoidal rule

$$AUC\,|_{t_1}^{t_2} = \delta_t * \frac{C_2 - C_2}{\ln\left(\frac{C_2}{C_1}\right)}$$

$$AUMC\,|_{t_1}^{t_2} = \delta_t * \frac{t_2 * C_2 - t_1 * C_1}{\ln\left(\frac{C_2}{C_1}\right)} - \delta_t^{\,2}$$

where δt is $(t_2\text{-}t_1)$.

Linear-interpolation rule (to find C* at time t*)

$$C^* = C_1 + \left|\frac{t^* - t_1}{t_2 - t_1}\right|\left(C_2 - C_1\right)$$

Logarithmic-interpolation rule

$$C^* = \exp\left(\ln(C_1) + \left| \frac{t^* - t_1}{t_2 - t_1} \right| * (\ln(C_2) - \ln(C_1)) \right)$$

AUC_{last}: Area under the curve from time of dosing to the last measurable concentration.

AUC_{all}: Area under the curve from the time of dosing to the last time of the last observation.

$AUMC_{last}$: Area under the moment curve from the time of dosing to the last measurable concentration to the time of last measurable concentration.

MRT_{last}: Mean residence time from the time of dosing to the last measurable concentration. For non–infusion models, $MRT_{last} = AUMC_{last}/AUC_{last}$.

λ_z: Lamda z, first order rate constant associated with the terminal portion of the curve. This is estimated via linear regression of log concentration vs. time.

HL_Lamda _z: Terminal half life =ln(2)/ λ_z

AUC_{INF}: AUC from the time of dosing extrapolated to infinity:

$$AUC_{\inf} = AUC_{last} + \frac{C_{last}}{\lambda_z}$$

AUC_{INF_D}: AUC_{INF} divided by the administered dose.

$AUC_{\_\%Extrap}$: Percentage of AUC that is due to extrapolation from T_{last} to infinity:

$$AUC_{\_\%Extrap} = \frac{AUC_{INF} - AUC_{last}}{AUC_{INF}} * 100$$

$AUMC_{\_\%}$: Percent of AUM_{INF} that is extrapolated:

$$AUMC_{\_\%} = \frac{AUMC_{INF} - AUMC_{last}}{AUMC_{INF}} * 100$$

V_{z_F}: Apparent volume of distribution based on the terminal phase

$$V_{z\_F} = \frac{Dose}{\lambda_z * AUC_{INF}}$$

Cl_F: Apparent total body clearance for extra-vascular administration.

$$Cl_{\_F} = \frac{Dose}{AUC_{INF}}$$

$AUMC_{INF}$: Area under the first moment curve (AUMC) extrapolated to infinity:

$$AUMC_{INF} = AUMC_{last} + \frac{t_{last} * C_{last}}{\lambda_z} + \frac{C_{last}}{\lambda_z^2}$$

MRT_{INF}: Mean residence time (MRT) extrapolated infinity for non-infusion models:

$$MRT_{INF} = \frac{AUMC_{INF}}{AUC_{INF}}$$

MRT_{INF}: Mean residence time (MRT) extrapolated to infinity for infusion models:

$$MRT_{INF} = (AUMC_{INF} / AUMC_{INF})$$

Non-compartmental pharmacokinetic analysis allows users to select lambda range the number of points to fit the elimination phase and the partial area to calculate AUC.

Insert of initial time points

If a pharmacokinetic profile does not contain the dosing time, a value for the time the drug is given, the WinNonlin automatically inserts a value based on the following rules:

For extravascular single dosing, a concentration equal to zero will be applied.

For extravascular, the minimum value observed during the dosing interval will be used.

For IV-bolus data, the C_0 will be extrapolated back to the intercept of plasma concentration curve and the Y axis.

Missing values: If Either X or Y value is missing, the associated record is excluded from Non-compartmental analysis.

Data points preceding the dosing time: If the time value for a data point is earlier than the dosing time, the point then is excluded from NCA computations.

Data deficiencies that will result in missing value for PK parameter:

The number of non-missing value data points is <=1

Multiple observations at the same time point:

The WinNonlin permits one observation at each time point within a profile. If the software detects more than one such point, the NCA analysis is halted, and an error message is issued. No PK output is generated in this instance.

Partial areas

Rules for interpolation and extrapolation

If a starting or ending time occurs within the range of the data but does not coincide with an observed data point, then a linear or logarithmic interpolation is done to estimate the corresponding Y, according to whether the linear trapezoidal rule, the linear/log trapezoidal rule, or the Linear up/Log down trapezoidal rule was selected in the Model Options dialog box.

If a starting or ending time occurs after the last observation (Tlast) and lambda z is estimable, lambda z is used to estimate the corresponding Y:

Y = exp(alpha - Lambda-Z * t)

= exp(alpha - Lambda-Z * tlast) * exp(-Lambda-Z * (t-tlast))

= (predicted concentration at tlast) * exp(-Lambda-Z * (t-tlast))

If a starting or ending time occur after the last data observation and lambda z is not estimable, the partial area will not be calculated.

If both the start and end times for a partial area occurs after the last data observation, then the log trapezoidal rule will be used regardless of the selection made because a logarithmic decline must be assumed in order to obtain the predicted values.

If the start time for a partial area is before the last data observation and the end time is after the last data observation, then the log trapezoidal rule will be used for the area from the last data observation time to the end time for the partial area, regardless of the selection made.

Partial area boundaries

There are limitations regarding partial area boundaries that will evoke an error message from the software: The end time for the partial area must be greater than the start time. Both the start and end time for the partial area must be at or after the dosing time.

Therapeutic windows

For therapeutic windows, one or two boundaries for concentration values can be given, and the program computes the time spent in each window determined by the boundaries and computes the area under the curve contained in each window. To

compute these values for each pair of consecutive data points including the inserted point at dosing time. It is determined if a boundary crossing occurrs in that interval, then the pair of time values from the data set (t_i, t_{i+1}) are called the boundaries y_{lower} and y_{upper}.

If no boundary crossing occurred, the difference t_{i+1}- t_i is added to the appropriate parameter TimeLow, TimeDur, or TimeHgh, depending in which window the concentration values are. The AUC for (t_i, t_{i+1}) is computed following the user's specified AUC calculation method as described above in section 3. Call this AUC*. The parts of this AUC* are added to the appropriate parameters AUCLow, AUCDur, or AUCHgh. For example, if the concentration values for this interval occur above the upper boundary, the rectangle that is under the lower boundary is added to AUCLow, the rectangle that is between the two boundaries is added to AUCDur and the piece that is left is added to AUCHgh. This is equivalent to these formulae:

$AUCLow = AUCLow + y_{lower} * (t_{i+1} - t_i)$

$AUCDur = AUCDur + (y_{upper} - y_{lower}) * (t_{i+1} - t_i)$

$AUCHgh = AUCHgh + AUC* - y_{upper} * (t_{i+1} - t_i)$

Dosing regimen 3mg/kg 7mg/kg, 15mg/kg were fitted with weighting uniform, 1/Y and $1/Y^2$.

The non-compartmental fitted plot (Figure 3.6) showed that for treatment 1, 3mg/kg single dose, the mean plasma concentration time curve does not have a clear elimination phase. There are only two time points that appear to belong the to

elimination phase. Taking time-point samples over 24 hours only may not be long enough to detect the entire elimination phase.

Because curve fitting by WinNonlin needs at least 3 time points the WinNonlin automatically selected the last three points. The curve fitted line may contain a point in the absorption phase. This may cause high elimination rate to be predicted compared to the other treatments.

For treatment 2, the WinNonlin used the last three time points for curve fitting, and for treatment three the WinNonlin used the last five time points for curve fitting.

The mean-plasma concentration time curve also reveals that non-compartmental analysis should be carried out by using a non-lag time model since at the high dose, a lag time for Terbinafine absorption time was not detected at the first time point of sampling for most subjects.

Mean plasma concentrations of all three dosing regimens have T_{max} at 4 hour (Table 3.3). C_{max} was 0.09 mg/L (mg/L), 0.28 mg/L, 0.27 mg/L for single oral Terbinafine treatments one (3mg/kg), two (7mg/kg) and three (15mg/kg), respectively. The elimination rate constant was slightly different when different weighting was used to fit the data and the values are 0.1574, 0.0412, 0.0481 for uniform weighting, 0.1225, 0.0404, 0.048 for 1/Y weighting and 0.0992, 0.0398, 0.0481 for 1/YY weighting respectively for the three treatments 3, 7 and 15mg/kg. AUC values observed from 0 hour to infinity are close in value for all three weighting functions (Table 3.4).

The volume of distribution is calculated by $V_{z\_F} = \frac{Dose}{\lambda_z * AUC_{INF}}$. It means the volume of distribution is inversely proportional to the rate of drug elimination. Since the

λ_z is highest for treatment one (3mg/kg), the volume of distribution value would be expected to be smaller for treatment 1 (3mg/kg). Using the volume of distribution values (V_d) of the high dosing regimen better represent Terbinafine V_d. Presented in the following section, the weighting 1/Y to the data allowed the best fit to the data. Thus, the volume of distribution for 7mg/kg regimen is 4.04 L/kg and 5.22 for 15mg/kg. The values of the volumes of distribution suggest extensive tissue distribution. The clearance was 1.63 L/kg and 2.5 L/kg for these two doses. The mean residence times are around 20-21 hours. AUC is calculated by default method, linear-trapezoidal (linear interpolation). AUC for the three treatment regimens are 0.81, 4.29 and 6 respectively for 3mg/kg, 7mg/kg, and 15mg/kg. No proportionality of Dose to AUC was observed for all three weighting functions.

The mean residence time calculated by the areas from 0 to 24 hours is shorter than the mean-residence time calculated by the areas from 0 to infinity. In other words, the ratio of $AUMC_{0\text{-}t}/AUC_{0\text{-}t\ is}$ smaller than $AUMC_{0\text{-}inf}/AUC_{0\text{-}inf}$. The average time the drug was excreted out of body from 24 hours to infinity is longer than from 0-24 hours.

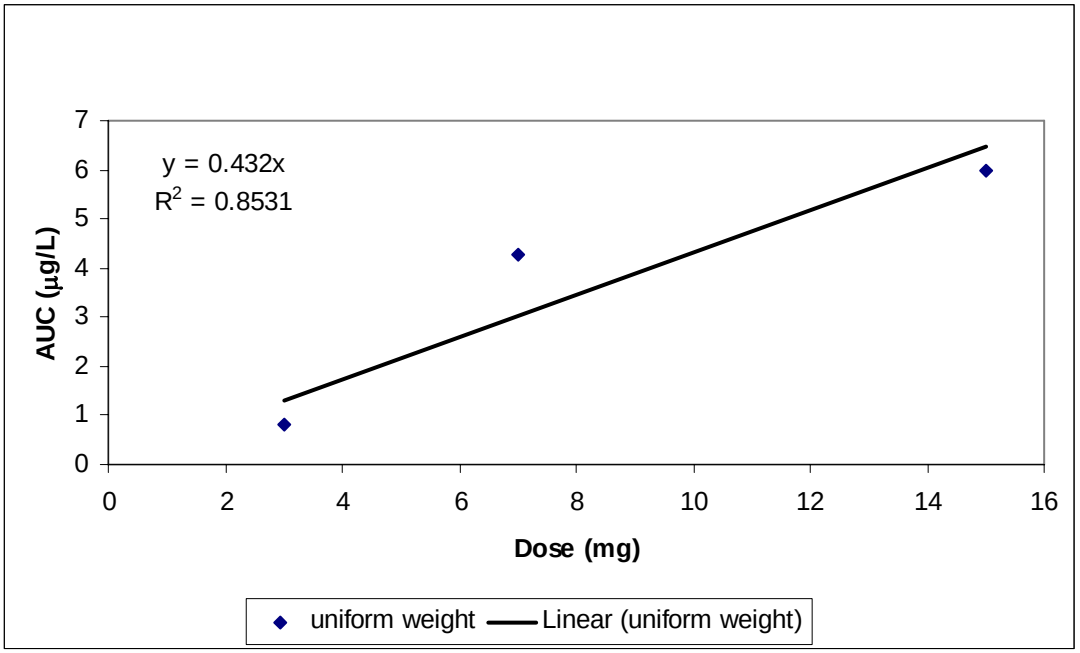
y = 0.432x
R2 = 0.8531
AUC (µg/L)
Dose (mg)
uniform weight
Linear (uniform weight)

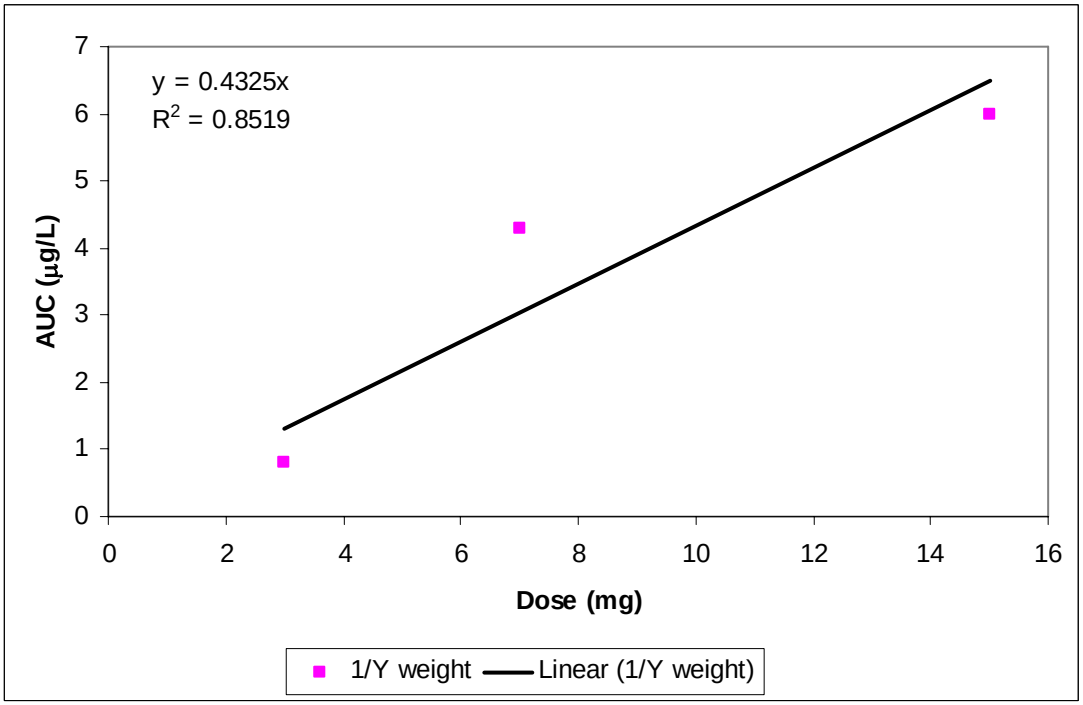
y = 0.4325x
R2 = 0.8519
AUC (µg/L)
Dose (mg)
1/Y weight
Linear (1/Y weight)

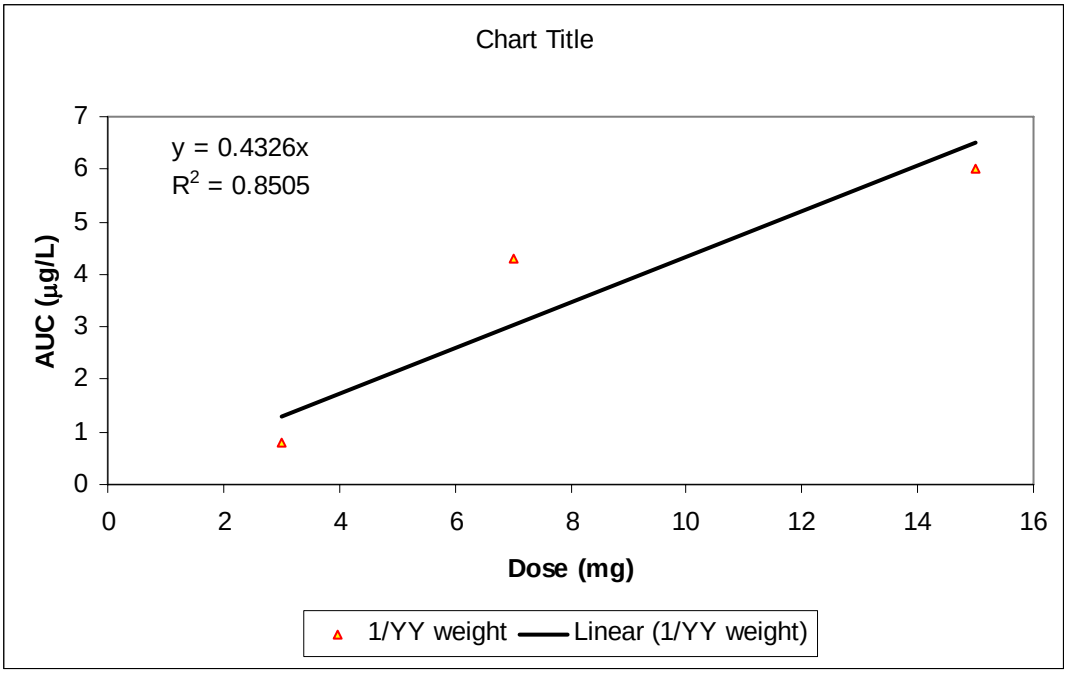

Figure 3.7. Dose and AUC proportional evaluation of AUC calculated using non-compartmental analysis by linear regression. (a) uniform weight, (b) weight 1/Y, (c) weight 1/YY

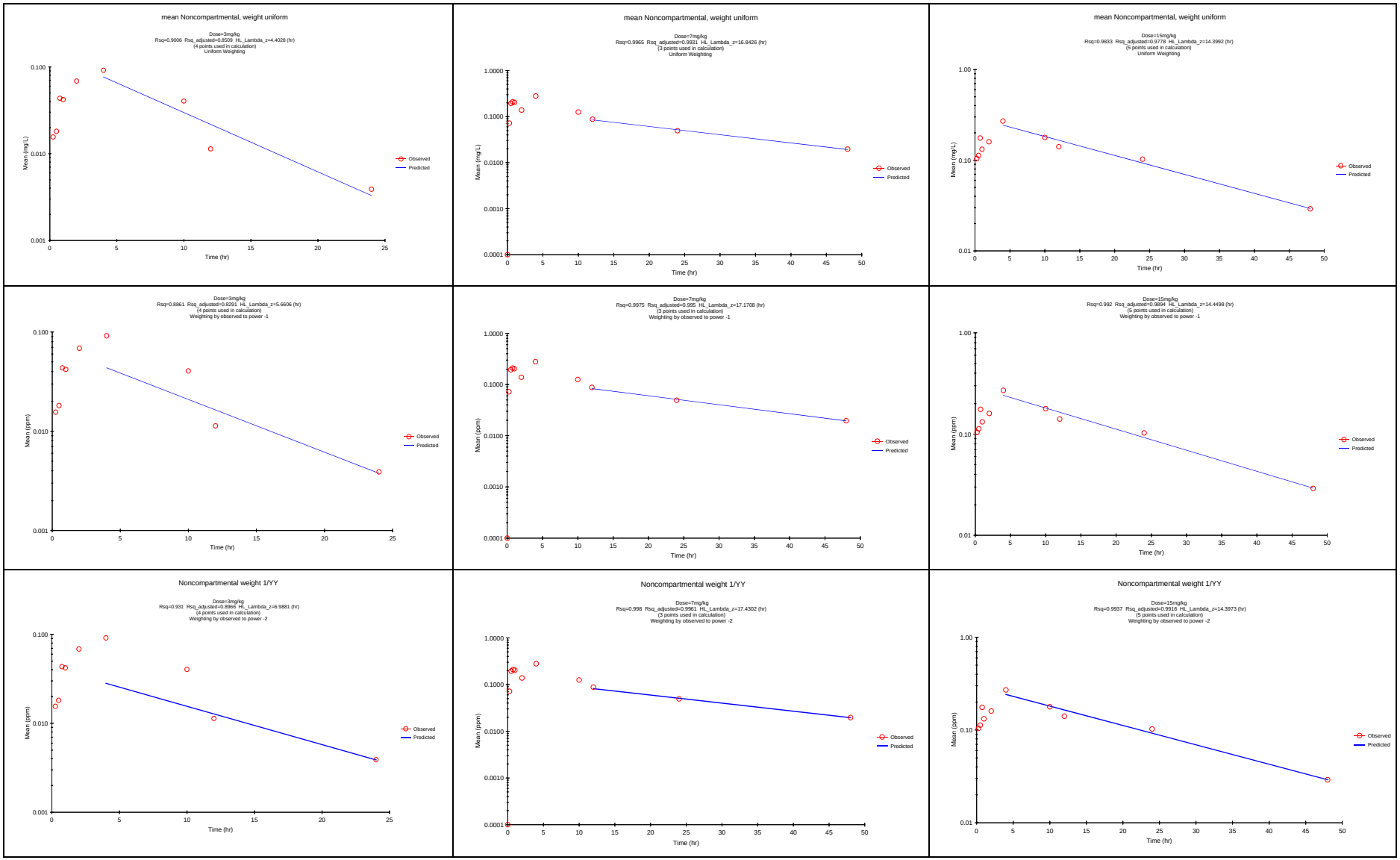

Figure 3.8. Non compartmental analysis of average plasma concentration versus time for the three single oral Terbinafine doses given to penguins (3, 7, and 15mg/kg) with three different weighting functions: uniform, 1/Y and 1/YY

Table 3.5. Pharmacokinetic parameters for Terbinafine in penguins after fitting single-dosing mean-plasma concentration versus time data fitting with uniform weight, 1/Y, 1/YY

Subject	Lambda_z	HL_Lambda_z	Tlag	Tmax	Cmax	Tlast	Clast	AUClast	AUCall	AUCINF_obs	AUCifn_D_ob	AUC_%Ext_obs	Vz_F_obs	Cl_F_obs	AUCinf_pre	AUCinf_Dpre	AUC%Extrapre	Vz_F_pred	Cl_F_pred	AUMClast	AUMC_infob	AUMC_%Ex_ob	AUMCinfpre	AUMC%Expre	MRTlast	MRTinf_obs	MRTinfpred
Dose	1/hr	hr	hr	hr	(mg/L)	hr	(mg/L)	hr*mg/L	hr*g/L	hr*g/L	hr*kg/L	%	L/kg	L/hr/kg	hr*mg/L	hr*kg*/L	%	L/kg	L/hr/kg	hr*hr*mg/L	hr*hr*mg/L	%	hr*hr*mg/L	%	hr	hr	hr
Weight uniform																											
3mg/kg	0.1574	4.40	0	4	0.09	24	0	0.78	0.78	0.81	0.27	3.08	23.7	3.74	0.8	0.27	2.61	23.8	3.75	4.83	5.58	13.4	5.47	11.6	6.21	7	6.84
7mg/kg	0.0412	16.8	0	4	0.28	48	0.02	3.8	3.8	4.28	0.61	11.1	39.8	1.64	4.27	0.61	11	39.8	1.64	50	84.4	40.8	83.8	40.4	13.1	20	19.6
15mg/kg	0.0481	14.4	0	4	0.27	48	0.03	5.39	5.39	5.99	0.40	10.1	5.2	2.5	6	0.40	10.1	51.9	2.5	84.9	126	32.8	127	33	15.7	21	21.1
Weight 1/Y																											
3mg/kg	0.1225	5.66	0	4	0.09	24	0	0.78	0.78	0.81	0.27	3.92	30.3	3.7	0.81	0.27	3.8	30.3	3.71	4.83	5.86	17.4	5.82	17	6.21	7	7.20
7mg/kg	0.0404	17.17	0	4	0.28	48	0.02	3.8	3.8	4.29	0.61	11.3	404	1.63	4.29	0.61	11.3	40.5	1.63	50	85.3	41.4	85.1	41.3	13.1	20	19.9
15mg/kg	0.048	14.4	0	4	0.27	48	0.03	5.39	5.39	6	0.40	10.1	52.2	2.5	6	0.40	10.1	52.1	2.5	84.9	126	32.9	127	33.1	15.7	21	21.1
Weight 1/YY																											
3mg/kg	0.0992	6.99	0	4	0.09	24	0	0.78	0.78	0.82	0.27	4.8	37.0	3.67	0.82	0.27	4.78	37.0	3.67	4.83	6.17	21.7	6.17	21.6	6.21	8	7.55
7mg/kg	0.0398	17.4	0	4	0.28	48	0.02	3.8	3.8	4.3	0.61	11.5	41.0	1.63	4.29	0.61	11.5	41.0	1.63	50	86	41.9	86	41.9	13.1	20	20.0
15mg/kg	0.0481	14.4	0	4	0.27	48	0.03	5.39	5.39	5.99	0.40	10.1	52.0	2.5	6	0.40	10.1	52.0	2.5	84.9	126	32.8	126	32.9	15.7	21	21.1

Table 3.6. Pharmacokinetic parameters for Terbinafine in each individual penguin by non-compartmental analysis, and uniform weighting

Subject	Lambda_z	HL_Lamb da_z	Tlag	Tmax	Cmax	Tlast	Clast	AUClast	AUCall	AUCINF_obs	AUCinf_D_obs	AUC%Ext_obs	Vz_F_obs	Cl_F_obs	AUCinf_pre	AUCinf/Dpre	AUC%Extra_pre	Vz_F_pred	Cl_F_pred	AUMClast	AUMC_infob	AUMC_%Ex_ob	AUMCinf_pred	AUMC%Expre	MRTlast	MRTinf_obs	MRTinfpred
	1/hr	hr	hr	hr	(mg/L)	hr	(mg/L)	hr*mg/L	hr*mg/L	hr*mg/L	hr*kg/L	%	L/kg	L/hr/kg	hr*mg/L	hr*kg*/L	%	L/kg	L/hr/kg	hr*hr*mg/L	hr*hr*mg/L	%	hr*hr*mg/L	%	hr	hr	hr
3mg/kg																											
105079	0.019	37.3	0	4	0.183	24	0.012	1.15	1.152	1.80	0.599	35.9	89.7	1.67	1.80	0.599	35.9	89.7	1.67	6.91	57.1	87.9	57.1	87.9	5.99	31.8	31.8
105114	0.047	14.9	0	2	0.073	24	0.012	0.671	0.671	0.928	0.309	27.73	69.3	3.23	0.928	0.309	27.7	69.3	3.23	5.87	17.6	66.6	17.6	66.6	8.76	18.9	18.9
104721	0.036	19.1	0.5	1	0.05	4	0.044	0.154	0.286	1.37	0.456	88.73	60.5	2.19	1.35	0.451	88.6	61.2	2.22	0.351	38.7	99.1	38.3	99.1	2.28	28.3	28.3
104986	1.344	0.516	0.5	10	0.147	12	0.01	1.1	1.16	1.11	0.369	0.672	20.2	2.71	1.11	0.369	0.672	20.2	2.71	7.69	7.79	1.22	7.78	1.22	6.99	7.03	7.03
104708																											
105297	0.031	22.2	0	2	0.162	24	0.011	1.20	1.195	1.55	0.516	22.77	62.1	1.94	1.55	0.516	22.8	62.1	1.94	7.07	26.8	73.6	26.8	73.6	5.92	17.3	17.3
104757	0.171	4.06	0	4	0.052	12	0.027	0.456	0.618	0.614	0.205	25.76	28.6	4.89	0.614	0.205	25.8	28.6	4.89	2.76	5.58	50.5	5.58	50.5	6.06	9.10	9.10
104903	0.056	12.3	0	2	0.075	10	0.07	0.657	0.727	1.90	0.633	65.41	28.0	1.58	1.50	0.501	56.3	35.4	1.99	3.45	37.9	90.9	26.9	87.2	5.26	19.9	17.9
105040	0.285	2.43	0.5	0.75	0.08	12	0.013	0.356	0.434	0.402	0.134	11.34	26.2	7.47	0.402	0.134	11.3	26.2	7.47	1.93	2.64	26.8	2.64	26.8	5.42	6.56	6.56
104720			5	4	0.146	0.323	0.761																		2.74		
Average	0.249	**2.79**	0.222	3.306	0.108	14	0.038	0.674	0.778	1.21	0.403	34.79	**42.1**	**2.48**	1.16	0.386	33.6	**42.2**	**2.59**	4.10	24.3	62.1	22.8	61.6	**4.65**	**12.7**	**12.5**
SE	0.16	**4.47**	0.088	0.937	0.017	2.708	0.015	0.13	0.109	0.192	0.064	10.21	**28.5**	**1.99**	0.171	0.57	9.77	**29.8**	**0.38**	0.944	6.44	11.3	6.18	11.2	**0.86**	**2.93**	**2.84**

7mg/kg																											
2-104720	0.037	18.7	0	4	0.262	48	0.016	3.46	3.457	3.89	0.555	11.09	48.5	1.80	3.89	0.555	11.1	48.5	1.80	42.2	74.5	43.4	74.5	43.4	12.2	19.16	19.2
2-104993	0.042	16.7	0	4	0.181	48	0.017	3.05	3.052	3.46	0.495	11.84	48.8	2.02	3.46	0.495	11.8	48.8	2.02	44.0	73.6	40.2	73.6	40.2	14.4	21.3	21.3
2-104763	0.388	1.79	0	4	0.098	24	0.03	1.04	1.396	1.11	0.159	6.941	16.2	6.29	1.04	0.148	0.054	17.4	6.75	9.97	12.0	17.1	9.98	0.149	9.62	10.8	9.63
2-105079	0.007	98.7	0	4	0.318	48	0.098	6.17	6.166	20.1	2.874	69.35	49.5	0.348	20.1	2.874[3]	69.4	49.5	0.35	128.6	2783	95.4	2783	95.4	20.9	138.4	138.4
3-104721	0.043	16.1	0.25	0.75	0.181	24	0.071	2.75	3.603	4.40	0.629	37.49	36.9	1.59	4.40	0.629	37.5	36.9	1.59	28.8	107	73.0	106.7	73.0	10.5	24.25	24.3
2-104708	0.1	6.92	0	0.5	1.156	24	0.037	4.75	5.198	5.12	0.732	7.214	13.7	1.37	5.12	0.732	7.21	13.7	1.37	29.6	42.2	29.8	42.2	29.8	6.22	8.23	8.23
2-105297	0.046	15.1	0.25	4	0.731	48	0.029	6.02	6.015	6.65	0.95	9.529	23.0	1.05	6.65	0.95	9.53	23.0	1.05	75.2	120	37.0	119.5	37.0	12.5	17.9	17.9
2-105114	0.073	9.46	0	10	0.224	48	0.01	3.86	3.856	3.99	0.57	3.42	23.9	1.75	3.99	0.57	3.42	23.9	1.75	54.1	62.6	13.5	62.6	13.5	14.0	15.7	15.7
3-104759	0.094	7.42	0	0.75	0.348	12	0.145	2.10	2.974	3.66	0.244	42.45	43.9	4.10	3.25	0.217	35.2	49.4	4.62	11.2	46.4	75.9	37.2	69.9	5.32	12.7	11.4
3-105041	Missing	Missing	0	4	0.392	48	0.01	3.66	3.662	Missing	Missing	Missing	Missing	Missing	Missing	Missing	Missing	Missing	Missing	40.3	Missing	Missing	Missing	Missing			
Average	0.092	**7.52**	0.05	3.6	0.389	37.2	0.046	3.69	3.938	5.82	0.801	22.15	**27.2**	**1.25**	5.77	0.797	20.6	**27.7**	**1.26**	46.4	369	47.2	367.7	44.7	**10.1**	**16.1**	**15.5**
SE	0.038	**4.9**	0.033	0.868	0.101	4.543	0.014	0.512	0.465	1.76	0.257	7.131	**51.7**	**0.59**	1.86	0.272	7.51	**52.9**	**0.69**	11.0	286	8.89	286.7	9.53	**4.4**	**41**	**41.2**
15mg/kg																											
3-104708	0.017	39.7	0	4	0.244	48	0.075	6.25	6.245	10.5	0.703	40.77	81.5	1.42	10.5	0.703	40.8	81.5	1.42	117.4	570	79.4	570.2	79.4	18.8	54.1	54.1
3-104761	0.02	34.6	0	4	0.305	24	0.103	3.79	5.025	8.93	0.595	57.57	83.8	1.68	8.93	0.595	57.6	83.8	1.68	37.2	417	91.1	417.1	91.1	9.83	46.7	46.7
3-104762	0.0383	18.1	0	24	0.248	48	0.099	7.96	7.9609	10.55	0.7032	24.53	37.2	1.42	10.5	0.7	24.5	37.2	1.42	183	375	51.2	375	51.2	23	35.5	35.5
3-104709	0.094	7.42	0	0.75	0.348	12	0.145	2.10	2.974	3.65	0.244	42.45	43.9	4.10	3.25	0.217	35.2	49.4	4.62	11.18	46.4	75.9	37.2	69.9	5.32	12.7	11.4
3-104931	0.115	6.02	0	4	0.567	24	0.075	5.43	6.329	6.08	0.405	10.71	21.4	2.47	5.92	0.395	8.30	22.0	2.53	45.5	66.8	31.8	61.6	26.1	8.39	10.9	10.4
3-104763	0.041	17.1	0.5	10	0.201	24	0.075	2.92	3.818	4.77	0.318	38.8	77.6	3.15	4.77	0.318	38.8	77.6	3.15	31.8	122	73.9	121.8	73.9	10.9	25.6	25.6
Average	0.051	**13.6**	0.083	4.458	0.328	26	0.096	4.05	4.903	7.15	0.477	41.31	**50.6**	**2.1**	7.06	0.470	39.7	**52.3**	**2.13**	46.7	273.2	73.8	270.8	71.9	**9.15**	**22.2**	**21.1**
SE	0.017	**5.4**	0.083	1.229	0.052	4.817	0.011	0.63	0.54	1.11	0.074	7.007	**18.6**	**0.33**	1.16	0.077	7.41	**19.3**	**0.35**	14.9	90.7	8.93	91.8	9.83	**1.64**	**7.21**	**7.25**

Table 3.7. Pharmacokinetic parameters for Terbinafine in each individual penguin by non-compartmental analysis, and weight 1/Y

Subject	Lambda_z	HL_Lambda_z	Tlag	Tmax	Cmax	Tlast	Clast	AUClast	AUCall	AUCINF_obs	AUCifn_D_ob	AUC_%Ext_obs	Vz_F_obs	Cl_F_obs	AUCinf_pre	AUCinf_Dpre	AUC%Extrapre	Vz_F_pred	Cl_F_pred	AUMClast	AUMC_infob	AUMC_%Ex_ob	AUMCinfpre	AUMC%Expre	MRTlast	MRTinf_obs	MRTinfpred
	1/hr	hr	hr	hr	(mg/L)	hr	(mg/L)	hr*mg/L	hr*mg/L	hr*mg/L	hr*mg/L	%	L/kg	L/hr/kg	hr*mg/L	hr*mg/L	%	L/kg	L/hr/kg	hr*hr*mg/L	hr*hr*mg/L	%	hr*hr*mg/L	%	hr	hr	hr
3mg/kg																											
105079	0.019	37.3	0	4	0.183	24	0.012	1.152	1.152	1.80	0.599	35.9	8.974	1.669	1.798	0.599	35.9	8.974	1.669	6.913	57.1	87.89	57.1	87.89	5.999	31.77	31.77
105114	0.047	14.9	0	2	0.073	24	0.012	0.671	0.671	0.928	0.309	27.73	6.933	3.233	0.928	0.309	27.73	6.933	3.233	5.874	17.57	66.56	17.57	66.56	8.759	18.93	18.93
104721	0.037	18.6	0.5	1	0.05	4	0.044	0.154	0.286	1.34	0.446	88.46	6.032	2.244	1.322	0.441	88.33	6.1	2.269	0.351	36.88	99.05	36.42	99.04	2.275	27.58	27.55
104986	1.34	0.516	0.5	10	0.147	12	0.01	1.1	1.16	1.11	0.369	0.672	2.015	2.708	1.108	0.369	0.672	2.015	2.708	7.69	7.785	1.218	7.785	1.218	6.99	7.028	7.028
104708	Missing	Missing	Missing	Missing	Missing	Missing	Missing	Missing	Missing	Missing	Missing	Missing	Missing	Missing	Missing	Missing	Missing	Missing	Missing	Missing	Missing	Missing	Missing	Missing	Missing	Missing	Missing

105297	0.031	22.2	0	2	0.162	24	0.011	1.195	1.20	1.55	0.516	22.77	6.21	1.939	1.547	0.516	22.77	6.21	1.939	7.072	26.81	73.62	26.81	73.62	5.92	17.33	17.33
104757	0.171	4.06	0	4	0.052	12	0.027	0.456	0.618	0.614	0.205	25.76	2.862	4.89	0.614	0.205	25.76	2.862	4.89	2.762	5.583	50.53	5.583	50.53	6.064	9.1	9.1
104903	0.056	12.3	0	2	0.075	10	0.07	0.657	0.727	1.89	0.633	65.41	2.803	1.581	1.503	0.501	56.33	3.538	1.995	3.453	37.87	90.88	26.94	87.18	5.26	19.96	17.92
105040	0.285	2.43	0.5	0.75	0.08	12	0.013	0.356	0.434	0.402	0.134	11.34	2.618	7.468	0.402	0.134	11.34	2.618	7.468	1.93	2.636	26.8	2.636	26.8	5.418	6.563	6.563
104720	Missing	Missing	0.5	4	0.146	4	0.146	0.323	0.761	Missing	Missing	Missing	Missing	Missing	Missing	Missing	Missing	Missing	Missing	0.885	Missing	Missing	Missing	Missing	2.74	Missing	Missing
Average	0.249	2.79	0.222	3.306	0.108	14	0.038	0.674	0.778	1.21	0.4.01	34.75	4.21	2.49	1.153	0.384	33.6	1.22	2.6	4.103	24.03	62.07	22.61	61.61	4.65	12.6	12.5
SE	0.16	4.46	0.088	0.937	0.017	2.708	0.015	0.13	0.109	0.18	0.06	9.602	2.81	0.4	0.171	0.057	9.738	2.98	0.38	1.001	6.764	12.03	6.479	11.87	0.86	2.91	2.83
7mg/kg																											
2-104720	0.037	18.7	0	4	0.262	48	0.016	3.457	3.46	3.89	0.555	11.09	4.85	1.801	3.888	0.555	11.09	4.85	1.801	42.18	74.48	43.37	74.48	43.37	12.2	19.16	19.16
2-104993	0.042	16.7	0	4	0.181	48	0.017	3.052	3.05	3.46	0.495	11.84	4.876	2.022	3.461	0.495	11.84	4.876	2.022	44.01	73.57	40.18	73.57	40.18	14.42	21.25	21.25
2-104763	0.388	1.79	0	4	0.098	24	0.03	1.036	1.39	1.11	0.159	6.941	1.619	6.288	1.037	0.148	0.054	1.739	6.753	9.967	12.02	17.08	9.982	0.149	9.621	10.8	9.63
2-105079	0.007	98.7	0	4	0.318	48	0.098	6.166	6.17	20.1	0.2874	69.35	4.953	0.348	20.11	2.874	69.35	4.953	0.348	128.6	2783	95.38	2783	95.38	20.85	138.4	138.4
3-104721	0.043	16.1	0.25	0.75	0.181	24	0.071	2.751	3.60	4.40	0.629	37.49	3.696	1.591	4.401	0.629	37.49	3.696	1.591	28.81	106.7	73.01	106.7	73.01	10.47	24.25	24.25
2-104708	0.1	6.92	0	0.5	1.156	24	0.037	4.754	5.19	5.12	0.732	7.214	1.365	1.366	5.124	0.732	7.214	1.365	1.366	29.59	42.15	29.8	42.15	29.8	6.224	8.227	8.227
2-105297	0.046	15.1	0.25	4	0.731	48	0.029	6.015	6.02	6.65	0.95	9.529	2.3	1.053	6.648	0.95	9.529	2.3	1.053	75.23	119.5	37.03	119.5	37.03	12.51	17.97	17.97
2-105114	0.073	9.46	0	10	0.224	48	0.01	3.856	3.86	3.99	0.57	3.42	2.394	1.753	3.993	0.57	3.42	2.394	1.753	54.14	62.56	13.46	62.56	13.46	14.04	15.67	15.67
3-104759	0.055	12.7	0	0.75	0.125	12	0.095	1.198	1.77	2.93	0.419	59.15	4.358	2.387	2.932	0.419	59.15	4.358	2.387	7.552	60.02	87.42	60.02	87.42	6.304	20.47	20.47
3-105041	Missing	Missing	0	4	0.392	48	0.01	3.662	3.66	Missing	Missing	Missing	Missing	Missing	Missing	Missing	Missing	Missing	Missing	40.26	Missing	Missing	Missing	Missing	10.99	Missing	Missing
Average	0.088	**7.89**	0.05	3.6	0.367	37.2	0.041	3.595	3.82	5.74	0.82	24	**2.71**	1.22	5.733	0.819	23.24	2.75	1.22	46.03	370.5	48.52	370.3	46.64	10.4	17	16.6
SE	0.039	**5.69**	0.033	0.868	0.105	4.543	0.011	0.55	0.507	1.77	0.253	7.901	**5.16**	0.55	1.868	0.267	8.556	5.13	0.63	11.12	301.8	9.934	301.8	10.82	1.46	3.28	3.3
15mg/kg																											
3-104708	0.017	39.7	0	4	0.244	48	0.075	6.245	6.25	10.54	0.703	40.77	8.154	1.423	10.54	0.703	40.77	8.154	1.423	117.4	570.2	79.4	570.2	79.4	18.8	54.08	54.08
3-104761	0.02	34.6	0	4	0.305	24	0.103	3.789	5.03	8.93	0.595	57.57	8.383	1.68	8.929	0.595	57.57	8.383	1.68	37.24	417.1	91.07	417.1	91.07	9.829	46.71	46.71
3-104762	0.038	18.1	0	24	0.248	48	0.099	7.961	7.96	10.6	0.703	24.53	3.717	1.422	10.55	0.703	24.53	3.717	1.422	182.7	374.5	51.21	374.5	51.21	22.95	35.51	35.51
3-104709	0.094	7.42	0	0.75	0.348	12	0.145	2.104	2.97	3.66	0.244	42.45	4.391	4.104	3.249	0.217	35.24	4.94	4.617	11.18	46.41	75.9	37.18	69.92	5.316	12.69	11.44
3-104931	0.115	6.02	0	4	0.567	24	0.075	5.429	6.33	6.08	0.405	10.71	2.141	2.467	5.92	0.395	8.296	2.199	2.534	45.52	66.79	31.84	61.57	26.06	8.386	10.99	10.4
3-104763	0.041	17.1	0.5	10	0.201	24	0.075	2.918	3.82	4.77	0.318	38.8	7.76	3.146	4.768	0.318	38.8	7.76	3.146	31.77	121.8	73.91	121.8	73.91	10.89	25.55	25.55
Average	0.054	**12.8**	0.083	7.792	0.319	30	0.095	4.741	5.39	7.42	0.495	35.8	**4.5**	**2.02**	7.326	0.488	34.2	4.63	2.05	70.98	266.1	67.22	263.7	65.26	**10**	**21.7**	**20.6**
SE	0.099	**4.46**	0.083	3.466	0.054	6	0.011	0.9	0.745	1.22	0.081	6.604	**1.31**	**0.33**	1.271	0.085	6.772	1.35	0.36	26.8	88.66	8.841	89.83	9.481	**2.36**	**6.62**	**6.69**

Table 3.8. Pharmacokinetic parameters for Terbinafine in each individual penguin by non-compartmental analysis, and weight 1/YY

Subject	Lambda_z	HL_Lambda_z	Tlag	Tmax	Cmax	Tlast	Clast	AUClast	AUCall	AUCINF_obs	AUCifn_D_ob	AUC_%Ext_obs	Vz_F_obs	Cl_F_obs	AUCinf_pre	AUCinf_Dpre	AUC%Extrapre	Vz_F_pred	Cl_F_pred	AUMClast	AUMC_infob	AUMC_%Ex_ob	AUMCinfpre	AUMC%Expre	MRTlast	MRTinf_obs	MRTinfpred
	1/hr	hr	hr	hr	(mg/L)	hr	(mg/L)	hr*mg/L	hr*mg/L	hr*mg/L	hr*kg/L	%	L/kg	L/hr/kg	hr*mg/L	hr*kg*/L	%	L/kg	L/hr/kg	hr*hr*mg/L	hr*hr*mg/L	%	hr*hr*mg/L	%	hr	hr	hr
3mg/kg																											
105079	0.019	37.28	0	4	0.183	24	0.012	1.152	1.152	1.798	0.599	35.9	89.74	1.669	1.798	0.599	35.9	89.74	1.669	6.913	57.1	87.89	57.1	87.89	5.999	31.77	31.77

105114	0.047	14.86	0	2	0.073	24	0.012	0.671	0.671	0.928	0.309	27.73	69.33	3.233	0.928	0.309	27.73	69.33	3.233	5.874	17.57	66.56	17.57	66.56	8.759	18.93	18.93
104721	0.036	19.13	0.5	1	0.05	4	0.044	0.154	0.286	1.369	0.456	88.73	60.5	2.192	1.354	0.451	88.61	61.15	2.216	0.351	38.72	99.09	38.26	99.08	2.275	28.29	28.26
104986	1.344	0.516	0.5	10	0.147	12	0.01	1.1	1.16	1.108	0.369	0.672	20.15	2.708	1.108	0.369	0.672	20.15	2.708	7.69	7.785	1.218	7.785	1.218	6.99	7.028	7.028
104708	Missing	Missing	Missing	Missing	Missing	Missing	Missing	Missing	Missing	Missing	Missing	Missing	Missing	Missing	Missing	Missing	Missing	Missing	Missing	Missing	Missing	Missing	Missing	Missing	Missing	Missing	Missing
105297	0.031	22.2	0	2	0.162	24	0.011	1.195	1.195	1.547	0.516	22.77	62.1	1.939	1.547	0.516	22.77	62.1	1.939	7.072	26.81	73.62	26.81	73.62	5.92	17.33	17.33
104757	0.171	4.057	0	4	0.052	12	0.027	0.456	0.618	0.614	0.205	25.76	28.62	4.89	0.614	0.205	25.76	28.62	4.89	2.762	5.583	50.53	5.583	50.53	6.064	9.1	9.1
104903	0.056	12.29	0	2	0.075	10	0.07	0.657	0.727	1.898	0.633	65.41	28.03	1.581	1.503	0.501	56.33	35.38	1.995	3.453	37.87	90.88	26.94	87.18	5.26	19.96	17.92
105040	0.285	2.43	0.5	0.75	0.08	12	0.013	0.356	0.434	0.402	0.134	11.34	26.18	7.468	0.402	0.134	11.34	26.18	7.468	1.93	2.636	26.8	2.636	26.8	5.418	6.563	6.563
104720	Missing	Missing	0.5	4	0.146	4	0.146	0.323	0.761	Missing	Missing	Missing	Missing	Missing	Missing	Missing	Missing	Missing	Missing	0.885	Missing	Missing	Missing	Missing	2.74	Missing	Missing
Aevrage	0.249	**2.79**	0.222	3.306	0.108	14	0.038	0.674	0.778	1.208	0.403	34.79	**42.1**	**2.48**	1.157	0.386	33.64	**12.2**	**2.59**	4.103	24.26	62.08	22.84	61.61	**4.65**	**12.7**	**12.5**
SE	0.16	**4.47**	0.088	0.937	0.017	2.708	0.015	0.13	0.109	0.192	0.064	10.21	**28.1**	**0.39**	0.171	0.057	9.766	**29.8**	**0.38**	0.944	6.439	11.34	6.178	11.2	**0.86**	**2.93**	**2.84**
7mg/kg																											
2-104720	0.037	18.67	0	4	0.262	48	0.016	3.457	3.457	3.888	0.555	11.09	48.5	1.801	3.888	0.555	11.09	48.5	1.801	42.18	74.48	43.37	74.48	43.37	12.2	19.16	19.16
2-104993	0.042	16.71	0	4	0.181	48	0.017	3.052	3.052	3.461	0.495	11.84	48.76	2.022	3.461	0.495	11.84	4876	2.022	44.01	73.57	40.18	73.57	40.18	14.42	21.25	21.25
2-104763	0.388	1.785	0	4	0.098	24	0.03	1.036	1.396	1.113	0.159	6.941	16.19	6.288	1.037	0.148	0.054	17.39	6.753	9.967	12.02	17.08	9.982	0.149	9.621	10.8	9.63
2-105079	0.007	98.66	0	4	0.318	48	0.098	6.166	6.166	20.11	0.2874	69.35	49.53	0.348	20.11	2.874	69.35	49.53	0.348	128.6	2783	95.38	2783	95.38	20.85	138.4	138.4
3-104721	0.043	16.11	0.25	0.75	0.181	24	0.071	2.751	3.603	4.401	0.629	37.49	36.96	1.591	4.401	0.629	37.49	36.96	1.591	28.81	106.7	73.01	106.7	73.01	10.47	24.25	24.25
2-104708	0.1	6.924	0	0.5	1.156	24	0.037	4.754	5.198	5.124	0.732	7.214	13.65	1.366	5.124	0.732	7.214	13.65	1.366	29.59	42.15	29.8	42.15	29.8	6.224	8.227	8.227
2-105297	0.046	15.14	0.25	4	0.731	48	0.029	6.015	6.015	6.648	0.95	9.529	23.0	1.053	6.648	0.95	9.529	23.0	1.053	75.23	119.5	37.03	119.5	37.03	12.51	17.97	17.97
2-105114	0.073	9.464	0	10	0.224	48	0.01	3.856	3.856	3.993	0.57	3.42	23.94	1.753	3.993	0.57	3.42	23.94	1.753	54.14	62.56	13.46	62.56	13.46	14.04	15.67	15.67
3-104759	0.055	12.65	0	0.75	0.125	12	0.095	1.198	1.768	2.932	0.419	59.15	43.58	2.387	2.932	0.419	59.15	43.58	2.387	7.552	60.02	87.42	60.02	87.42	6.304	20.47	20.47
3-105041	Missing	Missing	0	4	0.392	48	0.01	3.662	3.662	Missing	Missing	Missing	Missing	Missing	Missing	Missing	Missing	Missing	Missing	40.26	Missing	Missing	Missing	Missing	10.99	Missing	Missing
Average	0.088	**7.89**	0.05	3.6	0.367	37.2	0.041	3.595	3.817	5.742	0.82	24	**27.1**	**1.22**	5.733	0.819	23.24	**27.5**	**1.22**	46.03	370.5	48.52	370.3	46.64	**10.4**	**17**	**16.6**
SE	0.04	**5.69**	0.03	0.87	0.1	4.54	0.01	0.55	0.51	1.87	0.27	8.33	**51.6**	**0.55**	1.87	0.27	8.56	**51.3**	**0.55**	11.1	302	9.93	302	10.8	**1.32**	**3.28**	**3.3**
15mg/kg																											
3-104708	0.017	39.73	0	4	0.244	48	0.075	6.245	6.245	10.54	0.703	40.77	81.54	1.423	10.54	0.703	40.77	81.54	1.423	117.4	570.2	79.4	570.2	79.4	18.8	54.08	54.08
3-104761	0.02	34.59	0	4	0.305	24	0.103	3.789	5.025	8.929	5.95	57.57	83.83	1.68	8.929	0.595	57.57	83.83	1.68	37.24	417.1	91.07	417.1	91.07	9.829	46.71	46.71
3-104762	0.038	18.12	0	24	0.248	48	0.099	7.961	7.961	10.55	0703	24.53	37.17	1.422	10.55	0.703	24.53	37.17	1.422	182.7	374.5	51.21	374.5	51.21	22.95	35.51	35.51
3-104709	0.094	7.417	0	0.75	0.348	12	0.145	2.104	2.974	3.655	0.244	42.45	43.91	4.104	3.249	0.217	35.24	49.4	4.617	11.18	46.41	75.9	37.18	69.92	5.316	12.69	11.44
3-104931	0.115	6.015	0	4	0.567	24	0.075	5.429	6.329	6.079	0.405	10.71	21.41	2.467	5.92	0.395	8.296	21.99	2.534	45.52	66.79	31.84	61.57	26.06	8.386	10.99	10.4
3-104763	0.041	17.1	0.5	10	0.201	24	0.075	2.918	3.818	4.768	0.318	38.8	77.6	3.146	4.768	0.318	38.8	77.6	3.146	31.77	121.8	73.91	121.8	73.91	10.89	25.55	25.55
Average	0.054	**12.8**	0.083	7.792	0.319	30	0.095	4.741	5.392	7.421	0.495	35.8	**45.0**	**2.02**	7.326	0.488	34.2	**46.3**	**2.05**	70.98	266.1	67.22	263.7	65.26	**10**	**30.9**	**30.6**
SE	0.017	**4.46**	0.083	3.466	0.054	6	0.011	0.9	0.745	1.222	0.081	6.604	**13.1**	**0.33**	1.271	0.085	6.772	**13.1**	**0.33**	26.8	88.66	8.841	89.83	9.481	**2.36**	**6.62**	**6.69**

Fitting individual

Fitting data of individual penguins by non-compartmental analysis with single-dose oral-Terbinafine regimens shows a high inter-subject variability among all three treatments 1 (3mg/kg), 2 (7mg/kg), and 3 (15mg/kg). Subject 104708 of treatment 1 (3mg/kg) had every measured drug concentration below the limit of detection. According to WinNonlin's rules of calculation, all pharmacokinetic parameters of this subject were considered missing. For subject 3-105041, treatment 2 (7mg/kg), the time points of 10 and 12 hours had plasma concentrations of 0.084 mg/L and 0.085 mg/, respectively. The drug concentration for subject 3-105041 at the previous time point of 4 hours was the C_{max} with the value was 0.392 mg/L, while the drug concentration at the last collected time point, 24 hours, was under the limit of detection <0.07mg/L. The abnormal last three time points caused WinNonlin not be able to determine the elimination-rate constant as well as other secondary pharmacokinetic parameters calculated from the elimination rate constant (half-life, $AUC_{o\text{-}inf}$, the volume of distribution, clearance, $AUMC_{0\text{-}inf,}$ and MRT). However, C_{max}, T_{max}, C_{last}, $AUC_{0\text{-}t}$, $AUMC_{0\text{-}t}$ can be calculated. All the pharmacokinetic parameters values are presented in Table 3.6, 3.7, 3.8 using different weighting values to fit the data. Similarly, for subject 104720 (3mg/kg), there was an abnormal concentration vs the time curve observed. The plasma concentration reaches a C_{max} at 4 hours (0.146). At 10, 12, 24 hours the Terbinafine concentration values were all under the limit of detection. The were not a sufficient number of data points to calculate an elimination half-life. Only C_{max}, T_{max}, C_{last}, $AUC_{0\text{-}t}$, $AUMC_{0\text{-}t}$ are presented in the report. There is no adequate

way to extrapolate or determine other pharmacokinetic parameters of half life, $AUC_{o\text{-}inf}$, the volume of distribution, clearance, $AUMC_{0\text{-}inf,}$ and MRT.

For all of the subjects that contain sufficient plasma-concentration-time points for interpolating the eliminating rate constant (lamda_z), a high variability in values can be seen. The data for subject 104986, a 3mg/kg dose, yielded a high elimination-rate constant since the plasma concentration time curve profile consists of only two points in the elimination phase; one is the C_{max} and another time point at 10 hours is 0.01. The rest of the concentration versus time points were under the detection limit (0.01) mg/L. Using two points, the C_{max} (0.147mg/L) and a very low concentration 0.01mg/L made the elimination-rate constant value high. This value may be higher than the true value due to a lack of data points.

There were fewer outliers observed with the higher dosing treatments, treatment 2 (7mg/kg) and treatment 3 (15mg/kg). Subject 2-104763 had a Terbinafine concentration at 10 hours of 0.023 mg/L and 0.03 mg/L at 12 hours. However, after the C_{max} value at 4 hours, there were three concentration time points total for determining the elimination process. There were no subjects in treatment 3 (15mg/kg oral dose) considered outliers. All fittings of the Terbinafine concentration time data by non-compartmental analysis yielded good results.

The harmonic mean and its standard errors of each pharmacokinetic parameter was calculated and the results are in bold font size in Tables 3.6, 3.7, and 3.8. There is not much difference observed in the pharmacokinetic-parameter values among the three weighting schemes used to fit the data.

Fitting the data to compartmental models

Initial estimates of the pharmacokinetic parameters are required for the iterative estimation in compartmental model analysis. In some instances with compartmental models, the WinNonlin is capable of producing the initial estimates. Fitting the data to simple compartmental models the (one-compartmental open model and two-compartmental open models, or three-compartmental open model) does not require initial estimates of the pharmacokinetic parameters. Fitting the single oral dosing Terbinafine concentration versus time data with or without initial parameter values was performed. The fitted models were run on the WinNonlin for both one-compartmental and two-compartmental models.

For the data put into the models, AIC and SBC criteria were used to evaluate the closeness of fit to the concentration versus time curve. Since the t_{lag} had been investigated in the non-compartmental model, and most of the subjects had a very short lag time or no lag time, the compartmental fitting of the data yielded that the appropriate model to explain the data was a one-compartmental open model without lag time.

One compartment fitting

Since penguins were given Terbinafine by oral, administration, the appropriate model was Model 3

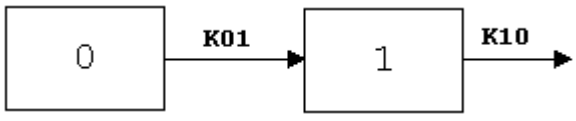


```
C(T)=D*K01/V/(K01-K10)*(EXP(-K10*T)
   -EXP(-K01*T))
```

Figure 3.9. Model 3, one-compartment open model, 1st-order absorption, no lag time, 1st order elimination.

In detail this model expresses of the drug-plasma-concentration profiles, which follow the equation:

$$C_{(t)} = \frac{D * K01}{V * (K01 - K10)} * [\exp(-K01 * T) - \exp(-K01 * T)]$$

Estimated parameters:

(1) V-F

(2) K01=absorption rate

(3) K10 = elimination rate

Constant input:

(1) Does

(2) Doses 1

(3) Time of dose 1

Secondary parameters:

(1) AUC =D/V/K01

(2) K01 half –life

(3) K10 half life

(4) CL_F

(5) T_{max} = time of maximum concentration = $\frac{\ln(K01/K10)}{(K01 - K10)}$

(6) C_{max} = Maximum concentration = $C_{(Tmax)}$

Clearance Primary parameters

(1) V_F

(2) K01

(3) CL_F

Secondary parameters:

(1) V_F

(2) K01 half-life

(3) K10 half-life

(4) K10

(5) T_{max}

(6) C_{max}

The treatment 1(3mg/kg oral dose) sets of plasma concentrations in penguins were pretty low. The drug concentrations at the first time points and the last time points were so low that most of the drug concentrations were lower than the limit detection of the instrumental analysis. This makes the initial estimation of pharmacokinetic parameters difficult because of the importance of the last time points in the curve used to calculate the elimination-rate constant and choose the best model that appropriately fitted the data. Thus, the WinNonlin's ability to select the best model to fit the data starts with treatment 2 (7mg/kg) and treatment 3 (15 mg/kg). Too many subjects in treatment 1 (3mg/kg) had concentrations that were under the limit of detection. Therefore, the curve fitting process may not reflect accurately the best

model fitted to the Terbinafine concentration versus time profiles of the penguins. To reduce error and make selecting best-fitted models to the data more accurately the pharmacokinetic model fitting was mainly performed with higher doses of Terbinafine.

No initial pharmacokinetic parameter estimates fitting

Fitting data to pharmacokinetic models without initial parameter estimates is normally carried out when researchers do experiments where there are no pharmacokinetic data in the test subjects and the last concentration-time points are unstable to calculate the pharmacokinetics parameters by manual-curve striping.

The major pharmacokinetic parameters for Terbinafine in penguins are listed in the following tables. The AIC and SBC criteria was used in order to evaluate the goodness of fit of a model.

Table 3.9. Pharmacokinetic parameters for a one-compartment open model fitted with no initial parameter estimates, and uniform weight

Subject	**V_F** (L/kg)	**K01** (1/hr)	**K10** (1/hr)	**AUC** (mg/L*hour/kg)	**AIC criteria**	**SBC criteria**
7mg/kg						
2-104720	25.5	1.71	0.0904	3.03	-47.7	-46.5
2-104993	42.2	1.17	0.0502	3.31	-59.7	-58.5
2-104763	115.9	1.54	0.375	0.16	-60.8	-59.6
2-105079	23.4	0.37	0.0716	4.17	-29.5	-28.6
3-104721	37.7	1.72	0.0425	4.36	-40.8	-39.9
2-104708	39.3	2.12	0.809	2.20	-9.25	-8.06
2-105297	64.8	0.242	0.243	4.45	-11.7	-10.5
2-105114	22.6	0.309	0.074	4.17	-42.4	-41.5
3-104759	38.9	0.576	0.0831	2.16	-43.8	-42.6
3-105041	96.7	0.269	0.265	2.73	-30.2	-29.0
15mg/kg						
3-104708	57.5	0.879	0.0337	7.73	-45.0	-43.8
3-104761	47.8	0.822	0.0678	4.63	-39.4	-38.5
3-104762	10.1	3.13	0.0015	99.9	-35.3	-34.4

3-104709	6.05	2.53	0.0692	3.58	-32.9	-31.8
3-104931	1.32	0.217	0.213	5.34	-23.4	-22.2
3-104763	4.89	0.245	0.0785	3.91	-49.3	-48.1

Table 3.10. Pharmacokinetic parameters for a one-compartment open model fitted with no initial parameter estimates, and weight 1/Y

Subject	**V_F** (L/kg)	**K01** (1/hr)	**K10** (1/hr)	**AUC** (mg/L*hour/kg)	**AIC criteria**	**SBC criteria**
7mg/kg						
2-104720	28.1	1.98	0.0807	3.09	-51.8	-50.9
2-104993	36.9	0.756	0.0627	3.02	-56.0	-55.1
2-104763	119	1.25	0.0412	1.43	-52.1	-51.5
2-105079	47.7	0.632	0.0091	15.97	-37.8	-36.9
3-104721	43.9	3.84	0.0293	5.45	-37.8	-38.0
2-104708	83.6	4.21	0.199	4.22	-13.9	-13.3
2-105297*	missing	missing	missing	missing	missing	missing
2-105114	25.9	0.392	0.0696	3.89	-53.3	-52.4
3-104759	21.1	0.155	0.155	2.14	-57.1	-56.5
3-105041	42.7	2.51	0.0571	2.87	-40.0	-39.1
15mg/kg						
3-104708	63.8	0.946	0.0273	8.58	-39.6	-38.7
3-104761	62.3	1.38	0.0421	5.71	-33.2	-32.9
3-104762	105.9	3.20	0.0039	35.45	-35.2	-34.6
3-104709	68.3	25.8	0.0429	5.12	-25.7	-25.4
3-104931	29.4	0.432	0.0947	5.38	-21.7	-21.1
3-104763	62.2	0.356	0.0559	4.32	-32.9	-33.0

*The subject 2-105297 has a high variability and the WinNonlin could not determine the best curve to fit and no results come out.

Table 3.11. Pharmacokinetic parameters for a one-compartment open model fitted with no initial parameter estimates, and weight 1/Y

Subject	**V_F** (L/kg)	**K01** (1/hr)	**K10** (1/hr)	**AUC** (mg/L*hour/kg	**AIC criteria**	**SBC criteria**
7mg/kg						
2-104720	28.4	2.14	0.0705	3.50	-22.9	-22.0
2-104993	37.7	0.888	0.0584	3.18	-27.7	-26.8
2-104763	34.3	0.155	0.119	1.70	-14.5	-13.6

2-105079	35.4	0.660	0.0179	11.0	-9.7	-8.83
3-104721	33.3	1.22	0.0540	3.89	-12.8	-12.2
2-104708	71.2	4.24	0.1890	5.20	0.957	1.87
2-105297	14.5	0.467	0.0656	7.38	4.55	5.46
2-105114	22.7	0.377	0.0747	4.13	-22.5	-21.6
3-104759	33.2	0.532	0.1168	1.80	-11.9	-10.9
3-105041	19.2	0.686	0.1042	3.51	-8.08	-7.18
15mg/kg						
3-104708	61.0	1.11	0.0273	8.98	-20.4	-19.5
3-104761	52.8	1.14	0.0603	4.71	-15.8	-15.2
3-104762	97.0	2.45	0.0015	98.1	-13.8	-13.2
3-104709	57.3	13.0	0.0899	2.91	-10.9	-10.0
3-104931	22.5	0.445	0.1200	5.55	-7.57	-6.60
3-104763	34.3	0.155	0.1195	3.65	-14.5	-13.6

Table 3.12. Pharmacokinetic parameters for a one-compartment open model fitted with no initial parameter estimates, and weight 1/YY

Subject	**V_F** (L/kg)	**K01** (1/hr)	**K10** (1/hr)	**AUC** (mg/L*hour)	**AIC criteria**	**SBC criteria**
7mg/kg						
2-104720	34.6	2.55	0.0605	3.34	-64.6	-63.7
2-104993	42.6	0.624	0.0517	3.18	-63.7	-62.8
2-104763	164.8	2.10	0.0239	1.78	-57.7	-57.1
2-105079	71.5	1.37	0.00001	9.83	-47.8	-46.9
3-104721	43.9	3.65	0.0310	5.15	-39.8	-39.9
2-104708	12.3	5.57	0.1200	4.74	-35.9	-35.2
2-105297	17.6	0.44	0.4319	0.923	-47.0	-46.5
2-105114	27.9	0.453	0.0697	3.60	-73.6	-72.7
3-104759	23.7	0.0876	0.0929	3.18	-89.8	-89.1
3-105041	49.6	3.84	0.0544	2.59	-69.8	-68.9
15mg/kg						
3-104708	72.9	1.08	0.0223	9.19	-40.2	-39.3
3-104761	73.6	1.96	0.0308	6.59	-37.3	-37.0
3-104762	110.4	3.26	0.0054	25.08	-40.0	-39.4
3-104709	74.1	25.8	0.0358	5.65	-28.7	-28.4
3-104931	75.7	3.03	0.0348	5.68	-30.0	-29.4
3-104763	65.0	0.351	0.0541	4.26	-34.5	-34.7

Table 3.13. Pharmacokinetic parameters for a one-compartment open model fitted with no initial parameter estimates, and weight 1/YY

Subject	V_F (L/kg)	K01 (1/hr)	K10 (1/hr)	AUC (mg/L*hour)	AIC criteria	SBC criteria
7mg/kg						
2-104720	30.3	2.44	0.0602	3.83	-0.868	0.038
2-104993	40.8	0.98	0.0513	3.34	0.262	1.17
2-104763	97.0	1.13	0.0537	1.34	13.6	14.5
2-105079	33.2	0.565	0.0219	9.60	9.44	10.3
3-104721	46.8	3.27	0.0198	7.57	13.1	13.7
2-104708	85.7	4.26	0.1478	5.52	15.0	15.9
2-105297	99.2	0.231	0.0259	27.1	21.6	22.5
2-105114	22.6	0.416	0.0756	4.10	-3.32	-2.4
3-104759	33.5	0.471	0.1287	1.62	22.7	23.6
3-105041	25.2	1.48	0.0736	3.78	10.3	11.2
15mg/kg						
3-104708	64.8	1.49	0.0241	9.58	-1.90	-0.996
3-104761	59.0	1.34	0.0483	5.26	9.60	10.2
3-104762	95.2	2.20	0.0020	75.1	3.43	4.03
3-104709	58.0	5.34	0.0791	3.27	16.29	17.2
3-104931	26.9	0.626	0.0951	5.87	12.39	13.3
3-104763	78.6	0.518	0.0361	5.28	18.9	19.8

Fitting data to a one-compartment open model using initial estimates of pharmacokinetic parameter values

The initial parameters were manually calculated by excel. The values of the volume of distribution (V_F), absorption-rate constant (K01), and elimination rate constant (K10) were calculated and put into a one-compartment open model of the WinNonlin for obtaining fitted values for the pharmacokinetic parameters.

Table 3.14. Pharmacokinetic parameters for a one-compartment open model fitted with initial parameter estimates, and uniform weight

Subject	V_F (L/kg)	K01 (1/hr)	K10 (1/hr)	AUC (mg/L*hour)	AIC criteria	SBC criteria
7mg/kg						
2-104720	25.8	1.75	0.0885	3.06	-47.7	-46.5

2-104993	33.4	0.792	0.0761	2.75	-59.7	-58.5
2-104763	63.8	0.521	0.0978	1.12	-61.2	-59.9
2-105079	33.6	0.550	0.0230	9.04	-31.7	-30.5
3-104721	37.6	1.715	0.0428	4.34	-40.8	-39.9
2-104708	25.6	1.71	0.0900	3.04	-47.7	-46.5
2-105297*	missing	missing	missing	missing	missing	missing
2-105114	22.0	0.284	0.0771	4.12	-47.2	-46.0
3-104759	42.5	0.720	0.0745	2.21	-45.0	-43.8
3-105041	125	0.349	0.1999	2.81	-30.0	-28.8
15mg/kg						
3-104708	26.8	0.884	0.0335	16.6	-45.0	-43.8
3-104761	47.7	0.817	0.0682	4.61	-39.4	-38.5
3-104762	112	3.12	0.0013	110	-35.3	-34.4
3-104709	60.6	25.5	0.0691	3.58	-32.9	-31.8
3-104931	14.1	0.233	0.1991	5.35	-23.4	-22.2
3-104763	48.2	0.242	0.0801	3.89	-49.3	-48.1

* Data of Subject 2-105297 has high variability and the WinNonlin failed to fit the data of the curve and no output was obtained.

Table 3.15. Pharmacokinetic parameters for a one-compartment open model fitted with initial parameter estimates, and weight 1/Y

Subject	**V_F** (L/kg)	**K01** (1/hr)	**K10** (1/hr)	**AUC** (mg/L*hour)	**AIC criteria**	**SBC criteria**
7mg/kg						
2-104720	28.1	1.983	0.0806	3.09	-51.8	-50.9
2-104993	37.0	0.754	0.0627	3.023	-56.0	-55.1
2-104763	116	1.20	0.0430	1.40	-52.1	-51.5
2-105079	46.8	0.614	0.010	14.86	-37.8	-36.9
3-104721	43.9	3.88	0.0292	5.47	-37.8	-38.0
2-104708	50.9	2.00	0.545	2.52	-12.6	-12.0
2-105297	13.2	0.355	0.358	1.48	-24.5	-23.9
2-105114	26.5	0.408	0.068	3.90	-53.3	-52.4
3-104759	26.6	0.447	0.0670	3.92	-48.5	-48.0
3-105041	42.7	2.51	0.0571	2.87	-40.0	-39.1
15mg/kg						
3-104708	63.8	0.945	0.0275	8.54	-39.6	-38.7
3-104761	62.3	1.37	0.0420	5.73	-33.2	-32.9

3-104762	83.6	0.600	0.0118	15.2	-27.1	-26.5
3-104709	64.6	4.97	0.0505	4.59	-23.7	-23.5
3-104931	29.5	0.4336	0.0942	5.39	-21.7	-21.1
3-104763	63.3	0.3665	0.0541	4.38	-32.9	-33.0

Table 3.16. Pharmacokinetic parameters for a one-compartment open model fitted with initial parameter estimates, and weight 1/Y

Subject	**V_F** (L/kg)	**K01** (1/hr)	**K10** (1/hr)	**AUC** (mg/L*hour)	**AIC criteria**	**SBC criteria**
7mg/kg						
2-104720	28.5	2.13	0.0713	3.45	-22.8	-21.9
2-104993	38.1	0.909	0.0576	3.19	-27.7	-26.8
2-104763	75.3	0.667	0.0702	1.32	-23.7	-22.8
2-105079	34.9	0.568	0.0207	9.67	-9.56	-8.65
3-104721	30.5	1.05	0.0629	3.65	-12.5	-11.9
2-104708	54.2	1.57	0.2250	5.74	6.56	7.47
2-105297	13.9	0.426	0.0965	5.22	5.32	6.22
2-105114	23.2	0.389	0.0740	4.08	-22.5	-21.6
3-104759	23.2	0.401	0.0710	4.25	-20.8	-20.2
3-105041	19.2	0.686	0.1042	3.51	-8.09	-7.18
15mg/kg						
3-104708	60.5	1.10	0.0284	8.71	-20.4	-19.49
3-104761	52.2	1.11	0.0618	4.64	-15.7	-15.1
3-104762	92.6	1.91	0.0038	42.2	-13.3	-12.7
3-104709	53.5	5.00	0.0967	2.90	-10.2	-9.30
3-104931	21.2	0.418	0.127	5.58	-7.60	-6.69
3-104763	34.1	0.154	0.119	3.67	-14.5	-13.6

Table 3.17. Pharmacokinetic parameters for a one-compartment open model fitted with initial parameter estimates, and weight 1/YY

Subject	**V_F** (L/kg)	**K01** (1/hr)	**K10** (1/hr)	**AUC** (mg/L*hour)	**AIC criteria**	**SBC criteria**
7mg/kg						
2-104720	34.9	2.60	0.0601	3.34	-64.6	-63.7
2-104993	42.7	0.626	0.00516	3.182	-63.7	-62.8
2-104763	165	2.10	0.0239	1.78	-57.7	-57.1
2-105079	71.5	1.37	0.00001	9784	-47.9	-46.9

3-104721	44.0	3.67	0.0308	5.162	-39.8	-39.9
2-104708	11.3	2.00	0.130	4.773	-31.9	-31.3
2-105297	18.1	0.457	0.421	0.921	-47.0	-46.5
2-105114	28.3	0.467	0.0691	3.58	-73.6	-72.7
3-104759	27.5	0.467	0.0699	3.64	-67.1	-66.5
3-105041	49.6	3.83	0.0545	2.59	-69.8	-68.9
15mg/kg						
3-104708	73.0	1.08	0.0223	9.21	-40.2	-39.3
3-104761	75.3	2.07	0.0292	6.82	-37.3	-37.0
3-104762	101.9	2.00	0.0079	18.5	-38.1	-37.5
3-104709	70.8	5.00	0.0416	5.09	-26.6	-26.3
3-104931	75.7	3.03	0.0348	5.69	-23.0	-29.4
3-104763	65.5	0.355	0.0535	4.28	-34.5	-34.7

Table 3.18. Pharmacokinetic parameters for a one-compartment open model fitted with initial parameter estimates, and weight 1/ŸŸ

Subject	**V_F** (L/kg)	**K01** (1/hr)	**K10** (1/hr)	**AUC** (mg/L*hour)	**AIC criteria**	**SBC criteria**
7mg/kg						
2-104720	59.4	1.66	0.164	7.17	16.6	17.5
2-104993	38.5	0.917	0.0529	3.43	0.143	1.05
2-104763	64.3	0.572	0.0680	1.60	13.3	14.2
2-105079	35.3	0.588	0.0132	15.1	9.82	10.7
3-104721	42.5	1.87	0.0467	3.53	14.6	15.2
2-104708	59.4	1.66	0.164	7.17	16.6	17.5
2-105297	20.2	0.549	0.0535	6.47	22.6	23.5
2-105114	23.5	0.412	0.0746	3.99	-2.87	-1.96
3-104759	21.6	0.409	0.0768	4.22	-4.27	-3.67
3-105041	25.2	1.48	0.0736	3.78	10.3	11.2
15mg/kg						
3-104708	62.9	1.320	0.0260	9.16	-1.62	-0.713
3-104761	63.4	1.71	0.0463	5.11	9.62	10.2
3-104762	83.7	2.00	0.0052	34.4	3.29	3.88
3-104709	48.2	3.13	0.0981	3.17	17.0	17.9
3-104931	27.7	0.658	0.0959	5.65	12.6	13.5
3-104763	98.1	0.606	0.0309	4.95	20.2	21.1

If the plasma concentrations versus time points have high variability, the WinNonlin may fail to fit the curve, and the errors would be stated in the report and the pharmacokinetic parameters of the subjects which have the error report were named “missing”.

There was not a significant difference in the pharmacokinetic parameters obtained between using initial pharmacokinetic estimates put in the WinNonlin and the WinNonlin’s automatic calculation without the initial estimates. This suggests that the WinNonlin’s creation of initial estimates is close to the manual estimates.

The smallest AIC and SBC values for the data fitted to the model occurring with a weighting of $1/YY$. As the results listed in the above table indicates, among all extravascular-compartmental model fitting to the data, weighting by $1/YY$ gives the best fit to the data.

Two-compartment fitting

A two-compartmental open model was used to fit the data of the penguins Terbinafine plasma concentration time curves. In the WinNonlin, model 11 is a micro model: two compartment open model with first-order input, first-order output, no lag time and micro-constants as primary parameters; model 13 is a two-compartment open model with first-order input, first-order output, no lag time, and macro-constants as primary parameters.

The micro-constant pharmacokinetic parameters or the estimated parameters in model 11 are the volume of distribution of the central compartment (V1_F), absorption-rate costant (K01), elimination-rate constant (K10), transfer-rate constant

from compartment 1 to compartment 2 (K12), transfer-rate constant from compartment 2 to compartment 1 (K21). Whereas, macro-constant pharmacokinetic parameters or the estimated parameters in model 13 are A, B, absorption-rate constant (K01), Alpha, and Beta. These macro-constant pharmacokinetic parameters become secondary parameters in model 11. Conversely, the primary parameters in model 11 were the secondary parameters in model 13.

Because we have an interest in Alpha, Beta, A, B, rather than the micro-constant parameters, model 13 was chosen, the two-compartmental open model with 1st order, macro-constants, no lag time, and 1st-order elimination.

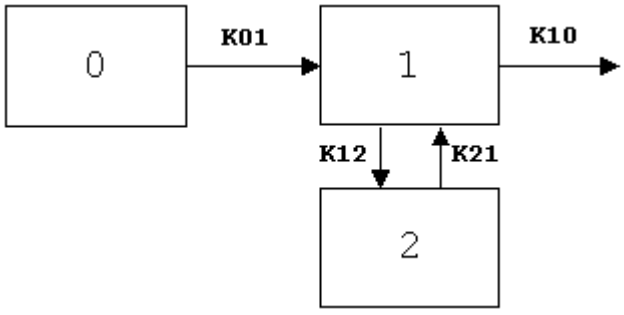

C(T)=A*EXP(-ALPHA*T)+B*EXP(-BETA*T)+ C*EXP(-K01*T)

Figure 3.10. Model 13, two-compartment open model, 1st-order absorption, no lag time, 1st-order elimination.

In detail this model expressed the drug-plasma concentration profile as follow**:**

Estimated parameters:

(1) A

(2) B

(3) K01=absorption rate

(4) ALPHA

(5) BETA

(Note: C = -(A+B)

Constant input:

(1) stripping dose

(2) doses

(3) dose 1

(4) time of dose 1

(Repeat 3-4 for additional dose)

Secondary parameters:

(1) K10

(2) K12

(3) K21

(4) AUC = D/V/K10

(5) K01 half-life

(6) K10 half-life

(7) ALPHA half-life

(8) BETA half-life

(9) V1_F

(10) CL_F

(11) V2_F

(12) CLD2_F

(13) Tmax

(14) C_{max}

Similar to the one-compartmental open model, the weighting of data for fitting to a pharmacokinetic model can be uniform (no weighting), 1/Y, $1/\hat{Y}$, 1/YY, $1/\hat{Y}\hat{Y}$. The AIC and SBC were the criteria used to select the best-fitted model to the data. The data can be fitted with or without initial parameter estimates.

Fitting data with no initial parameter estimates

Table 3.19. Pharmacokinetic parameters for a two-compartment open model fitted using no initial parameter estimates, and uniform weight

Subject	A (mg/L)	B (mg/L)	K01 (1/hr)	Alpha (1/hr)	Beta (1/hr)	AUC (mg/L*hr)	AIC criteria	SBC criteria
7mg/kg								
2-104720	0.0821	0.0031	1.64	0.101	0.00003	361.0	-43.7	-41.7
2-104993	0.0813	0.0262	0.568	0.202	0.0337	3.47	-57.3	-55.3
2-104763	0.2521	0.0096	0.320	0.268	0.0313	1.50	-58.1	-56.2
2-105079	6E-06	9.8E-05	0.377	0.263	0.0614	4.68	-26.5	-24.5
3-104721*	missing	missing	Missing	missing	Missing	missing	missing	missing
2-104708	8.51	0.258	1.80	1.80	0.0597	5.54	-8.87	-6.88
2-105297	12.0	0.0048	0.255	0.233	0.0055	5.21	-7.74	-5.75
2-105114*	missing	missing	missing	missing	Missing	missing	missing	missing
3-104759	0.0699	0.102	0.765	0.0641	0.0672	2.39	-41.6	-39.7
3-105041	14.5	3.98	0.485	0.528	0.300	2.68	-27.6	-25.6
15mg/kg								
3-104708	0.290	0.131	0.581	0.142	0.0115	12.77	-42.7	-40.7
3-104761	0.871	0.213	0.471	0.313	0.0452	5.19	-36.2	-34.7
3-104762*	missing	missing	missing	missing	Missing	missing	missing	missing
3-104709	82.3	0.244	23.7	23.30	0.0674	3.66	-29.1	-27.1
3-104931	4.69	0.369	0.242	0.193	0.19237	5.3280	-19.4	-17.4
3-104763*	missing	missing	missing	missing	missing	missing	missing	missing

For subjects 3-104721, 2-105114, 3-104762, and 3-104763, no successful fitting of the data to the pharmacokinetic model occurred. Error warnings were observed and no output could be seen.

Table 3.20. Pharmacokinetic parameters for a two-compartment open model fitted using no initial parameter estimates, and weight 1/Y

Subject	A	B	K01	Alpha	Beta	AUC	AIC	SBC

	(mg/L)	(mg/L)	(1/hr)	(1/hr)	(1/hr)	(mg/L*hr)	criteria	criteria
7mg/kg								
2-104720	0.269	0.0205	1.69	0.110	0.0068	5.31	-50.2	-48.6
2-104993	1.40	0.0983	0.366	0.296	0.0356	3.40	-54.9	-53.4
2-104763*	missing	missing	Missing	missing	missing	missing	missing	missing
2-105079	0.824	0.117	0.306	0.247	0.0035	33.8	-34.1	-32.5
3-104721*	missing	missing	missing	missing	missing	missing	missing	missing
2-104708	15.5	0.328	1.68	1.50	0.0819	4.93	-15.7	-14.7
2-105297	8.95	0.0137	0.402	0.381	0.0001	138	-20.7	-19.7
2-105114*	missing	missing	missing	missing	missing	missing	missing	missing
3-104759*	missing	missing	missing	missing	missing	missing	missing	missing
3-105041	1.93	0.104	0.398	0.324	0.0468	3.07	-35.6	-34.1
15mg/kg								
3-104708	0.293	0.142	0.550	0.160	0.0132	11.8	-36.6	-35.0
3-104761	0.0267	0.250	1.364	1.34	0.0426	5.67	-29.2	-28.8
3-104762*	missing	missing	missing	missing	missing	missing	missing	missing
3-104709	83.0	0.210	28.8	26.4	0.0373	5.89	-22.4	-22.0
3-104931	3.70	0.0536	0.257	0.204	0.0016	37.1	-17.9	-16.8
3-104763*	missing	missing	missing	missing	missing	missing	missing	missing

For subjects 3-104721, 2-105114, 3-104762, and 3-104763, no successful fitting of the data to the pharmacokinetic model occurred. Error warnings were observed and no output could be seen.

Table 3.21. Pharmacokinetic parameters for a two-compartment open model fitted using no initial parameter estimates, and weight 1/ Y

Subject	A (mg/L)	B (mg/L)	K01 (1/hr)	Alpha (1/hr)	Beta (1/hr)	AUC (mg/L*hr)	AIC criteria	SBC criteria
7mg/kg								
2-104720	0.294	0.0258	1.51	0.119	0.0117	4.45	-22.8	-21.3
2-104993	0.410	0.115	0.505	0.273	0.0395	3.37	-26.7	-25.2
2-104763*	missing	missing	missing	missing	missing	missing	missing	missing
2-105079	0.757	0.125	0.329	0.219	0.0042	30.8	-7.84	-6.3
3-104721*	missing	missing	missing	missing	missing	missing	missing	missing
2-104708	9.99	0.374	1.545	0.0931	0.0931	4.90	-2.56	-1.05
2-105297	2.75	0.0557	0.297	0.206	0.0102	9.36	6.92	8.44
2-105114	0.41	0.115	0.505	0.274	0.0396	3.37	-26.68	-25.2
3-104759*	missing	missing	missing	missing	missing	missing	missing	missing
3-105041	2.13	0.0964	0.379	0.284	0.0449	3.77	-6.11	-4.59
15mg/kg								
3-104708	0.226	0.0754	0.901	0.0754	0.0016	51.3	-16.9	-15.38

3-104761	0.068	0.332	1.036	1.08	0.0643	4.84	-11.9	-10.9
3-104762*	missing	missing	missing	missing	missing	missing	missing	missing
3-104709	82.0	0.276	8.263	8.38	0.0856	3.06	-6.77	-5.78
3-104931	1.04	0.619	0.360	0.232	0.107	5.65	-3.68	-2.17
3-104763*	missing	missing	missing	missing	missing	missing	missing	missing

For subjects 3-104721, 2-105114, 3-104762, and 3-104763, no successful fitting of the data to the pharmacokinetic model occurred. Error warnings were observed and no output could be seen.

Table 3.22. Pharmacokinetic parameters for a two-compartment open model fitted using no initial parameter estimates, and weight 1/YY

Subject	A (mg/L)	B (mg/L)	K01 (1/hr)	Alpha (1/hr)	Beta (1/hr)	AUC (mg/L*hr)	AIC criteria	SBC criteria
7mg/kg								
2-104720	0.239	0.0525	1.63	0.133	0.0252	3.70	-69.8	-68.3
2-104993	1.58	0.0919	0.304	0.256	0.0348	3.32	-61.9	-60.4
2-104763*	missing	missing	missing	missing	missing	missing	missing	missing
2-105079	0.402	0.0978	1.38	1.38	0.00006	1677	-43.8	-42.3
3-104721*	missing	missing	missing	missing	missing	missing	missing	missing
2-104708	11.39	0.405	1.79	1.61	0.0981	4.63	-36.6	-35.6
2-105297	3.88	0.0125	0.675	0.622	0.00004	6.014	-44.9	-43.9
2-105114*	missing	missing	missing	missing	missing	missing	missing	missing
3-104759*	missing	missing	missing	missing	missing	missing	missing	missing
3-105041	0.0012	0.143	3.87	2.57	0.0545	3.662	-65.8	-64.3
15mg/kg								
3-104708	0.189	0.0719	0.805	0.0598	0.0026	30.5	-36.4	-34.9
3-104761	0.0091	0.204	2.02	1.98	0.0299	6.72	-33.3	-32.9
3-104762*	missing	missing	missing	missing	missing	missing	missing	missing
3-104709	83.60	0.193	29.2	26.1	0.0304	6.69	-25.9	-25.5
3-104931	0.00001	0.200	3.08	1.51	0.0347	5.69	-26.0	-25.0
3-104763*	missing	missing	missing	missing	missing	missing	missing	missing

For subjects 3-104721, 2-105114, 3-104762, and 3-104763, no successful fitting of the data to the pharmacokinetic model occurred. Error warnings were observed and no output could be seen.

Table 3.23. Pharmacokinetic parameters for a two-compartment open model fitted using no initial parameter estimates, and weight 1/ Y Y

Subject	A (mg/L)	B (mg/L)	K01 (1/hr)	Alpha (1/hr)	Beta (1/hr)	AUC (mg/L*hr)	AIC criteria	SBC criteria
7mg/kg								
2-104720	0.3019	0.0647	1.2969	0.1661	0.0293	3.7446	-7.0292	-5.52
2-104993	0.2537	0.1079	5.69E-01	0.2134	0.0381	3.3835	1.6533	3.17
2-104763*	missing	missing	missing	missing	missing	missing	missing	missing
2-105079	0.4381	0.1429	0.3655	0.1934	0.0075	19.7717	10.7988	12.3
3-104721*	missing	missing	missing	missing	missing	missing	missing	missing
2-104708	11.3904	0.4046	1.7946	1.6091	0.0981	4.6304	-36.6262	-35.6
2-105297	2.7721	0.0562	0.3019	0.2013	0.0102	9.9088	22.7715	24.3
2-105114*	missing	missing	missing	missing	missing	missing	missing	missing
3-104759	missing	missing	missing	missing	missing	missing	missing	missing
3-105041	1.8142	0.1542	0.4618	0.3524	0.0567	3.6042	10.9334	12.4
15mg/kg								
3-104708	0.2001	0.0550	1.2982	0.0417	0.0023	28.2203	1.8932	3.41
3-104761	0.0859	0.2369	1.3879	0.6979	0.0449	5.1674	13.7364	14.7
3-104762*	missing	missing	missing	missing	missing	missing	missing	missing
3-104709	82.0562	0.2829	7.8437	7.8426	0.0656	4.2769	19.1769	20.7
3-104931*	missing	missing	missing	missing	missing	missing	missing	missing
3-104763*	missing	missing	missing	missing	missing	missing	missing	missing

For subjects 3-104721, 2-105114, 3-104762, and 3-104763, no successful fitting of the data to the pharmacokinetic model occurred. Error warnings were observed and no output could be seen.

Initial parameter estimate

Table 3.24. Pharmacokinetic parameters for a two-compartment open model fitted using initial parameter estimates, and uniform weight

Subject	A (mg/L)	B (mg/L)	K01 (1/hr)	Alpha (1/hr)	Beta (1/hr)	AUC (mg/L*hr)	AIC criteria	SBC criteria
7mg/kg								
2-104720	0.0109	0.287	1.64	0.0006	0.101	22.2	-43.8	-41.8
2-104993	0.0918	0.285	0.567	0.0337	0.202	3.47	-57.3	-55.3
2-104763	0.846	0.0350	0.321	0.268	0.0336	1.46	-58.1	-56.1

2-105079	1.57	0.0944	0.274	0.218	0.00002	6.17	-29.6	-27.6
3-104721	0.0751	0.0751	1.72	0.0435	0.0410	4.39	-36.8	-35.2
2-104708	2.96	0.249	2.25	1.07	0.0576	5.65	-8.45	-6.46
2-105297	12.0	0.0048	0.255	0.233	0.0055	5.21	-7.74	-5.75
2-105114	1E-08	0.443	0.282	1.948	0.0781	4.10	-43.2	-41.2
3-104759	0.0858	0.0854	0.803	0.0710	0.0680	2.25	-41.0	-39.0
3-105041	2.43	0.415	0.835	0.885	0.0999	3.49	-24.2	-22.2
15mg/kg								
3-104708	0.2906	0.131	0.581	0.142	0.0115	12.8	-42.7	-40.7
3-104761	1.2013	0.215	0.452	0.337	0.0463	5.08	-36.2	-34.7
3-104762	0.4615	0.144	2.03	1.73	0.00051	282	-31.4	-29.9
3-104709	82.257	0.244	23.6	23.3	0.0674	3.66	-29.1	-27.1
3-104931	5.4847	0.0133	0.243	0.198	0.0130	6.09	-19.4	-17.4
3-104763	0.0190	0.473	0.239	0.229	0.0808	3.88	-45.3	-43.3

Table 3.25. Pharmacokinetic parameters for a two compartment open model fitted using initial parameter estimates, and weight 1/Y

Subject	A (mg/L)	B (mg/L)	K01 (1/hr)	Alpha (1/hr)	Beta (1/hr)	AUC (mg/L*hr)	AIC criteria	SBC criteria
7mg/kg								
2-104720	0.269	0.0205	1.70	0.110	0.0067	5.32	-50.2	-48.7
2-104993	1.30	0.0990	0.369	0.294	0.0358	3.40	-55.0	-53.4
2-104763	0.924	0.0247	0.366	0.317	0.00013	188	-49.2	-48.2
2-105079	0.408	0.118	0.335	0.227	0.0036	33.0	-34.0	-32.5
3-104721	0.149	0.159	3.205	2.57	0.0285	5.53	-33.9	-34.1
2-104708	0.301	0.142	0.544	0.162	0.0132	11.8	-36.6	-35.0
2-105297	7.15	0.0139	0.405	0.379	0.0002	65.9	-20.7	-19.7
2-105114*	missing	missing	Missing	missing	Missing	missing	missing	missing
3-104759*	missing	missing	Missing	missing	Missing	missing	missing	missing
3-105041	1.925	0.104	0.398	0.324	0.0469	3.07	-35.6	-34.1
15mg/kg								
3-104708	0.301	0.142	0.544	0.162	0.0132	11.8	-36.6	-35.0
3-104761	0.283	0.0920	0.848	0.152	0.0001	822	-29.9	-29.5
3-104762	0.504	0.134	1.78	1.45	0.0026	51.7	-31.5	-30.5
3-104709	0.283	0.194	6.00	2.88	0.0291	6.69	-21.6	-21.2
3-104931	3.37	0.0547	0.260	0.2023	0.0025	25.5	-17.8	-16.8
3-104763	0.300	0.287	0.356	0.356	0.0559	4.32	-28.9	-29.2

For subjects 2-105114, and 3-104759, no successful fitting of the data to the pharmacokinetic model occurred. Error warnings were observed and no output could be seen.

Table 3.26. Pharmacokinetic parameters for a two compartment open model fitted using initial parameter estimates, and weight 1/Y

Subject	A (mg/L)	B (mg/L)	K01 (1/hr)	Alpha (1/hr)	Beta (1/hr)	AUC (mg/L*hr)	AIC criteria	SBC criteria
7mg/kg								
2-104720	0.298	0.0283	1.4800	0.124	0.0137	4.24	-22.8	-21.3
2-104993	0.675	0.113	0.437	0.289	0.0391	3.42	-26.7	-25.1
2-104763	0.303	0.0869	0.478	0.382	0.0597	1.43	-20.3	-18.8
2-105079	0.940	0.0994	0.292	0.207	0.0002	6.17	-7.57	-6.05
3-104721	0.113	0.310	0.808	0.647	0.0747	3.79	-8.40	-7.42
2-104708	2.181	0.331	2.59	1.03	0.0875	4.92	-2.25	-0.739
2-105297	3.38	0.296	0.251	0.201	0.0580	7.28	7.44	8.95
2-105114	0.410	0.115	0.505	0.274	0.0396	3.37	-26.7	-25.2
3-104759	0.117	0.236	0.862	0.0757	1.33	0.106	-8.07	-6.55
3-105041	2.13	0.0963	0.379	0.284	0.0450	3.77	-6.11	-4.59
15mg/kg								
3-104708	0.206	0.0844	0.931	0.0656	0.0053	18.63	-16.9	-15.4
3-104761	0.922	0.303	0.651	0.533	0.0634	4.63	-11.4	-10.4
3-104762	0.654	0.145	1.93	1.72	0.00064	226.5	-9.72	-8.73
3-104709	0.0041	0.277	8.37	0.268	0.0932	2.96	-6.93	-5.42
3-104931	0.527	0.997	0.46	0.513	0.121	5.950	-3.82	-2.31
3-104763	0.446	0.402	0.327	0.373	0.0803	3.610	-10.8	-9.28

Table 3.27. Pharmacokinetic parameters for a two compartment open model fitted using initial parameter estimates, and weight 1/YY

Subject	A (mg/L)	B (mg/L)	K01 (1/hr)	Alpha (1/hr)	Beta (1/hr)	AUC (mg/L*hr)	AIC criteria	SBC criteria
7mg/kg								
2-104720	missing	missing	missing	missing	missing	missing	missing	missing
2-104993	1.37	0.092	0.307	0.253	0.0349	3.29	-61.8	-60.3
2-104763	0.029	0.026	1.51	0.171	0.00017	156	-54.2	-53.2
2-105079	0.066	0.098	1.35	1.33	0.00007	1425	-43.8	-42.3
3-104721	missing	missing	missing	missing	missing	missing	missing	missing
2-104708	0.119	0.159	3.29	2.81	0.0307	5.16	-35.8	-36.0

2-105297	2.62	0.012	0.687	0.609	0.000005	2715	-44.9	-43.9
2-105114*	missing	missing	missing	missing	missing	missing	missing	missing
3-104759*	missing	missing	missing	missing	missing	missing	missing	missing
3-105041	1.93	0.104	0.398	0.324	0.0468	3.07	-35.6	-34.1
15mg/kg								
3-104708	0.184	0.0652	0.858	0.0527	0.0020	35.2	-36.4	-34.9
3-104761	0.620	0.204	2.03	2.03	0.0299	6.73	-33.3	-32.9
3-104762	0.469	0.126	1.65	1.26	0.0033	38.6	-36.8	-35.8
3-104709	0.114	0.185	20.0	2.99	0.0262	7.10	-25.3	-24.9
3-104931	0.374	0.200	3.02	3.00	0.0348	6.33	-26.0	-25.0
3-104763	0.436	0.273	0.342	0.337	0.0541	4.26	-30.5	-30.8

For subjects 3-104 720, 3-104 721, 2-105114, and 3-104759, no successful fitting of the data to the pharmacokinetic model occurred. Error warnings were observed and no output could be seen.

Table 3.28. Pharmacokinetic parameters for a two-compartment open model fitted using initial parameter estimates, and weight 1/YY

Subject	A (mg/L)	B (mg/L)	K01 (1/hr)	Alpha (1/hr)	Beta (1/hr)	AUC (mg/L*hr)	AIC criteria	SBC criteria
7mg/kg								
2-104720	0.303	0.0678	1.31	0.166	0.0304	3.77	-7.2	-5.68
2-104993	0.647	0.110	0.411	0.268	0.0386	3.41	2.3	3.85
2-104763	0.270	0.118	0.587	0.508	0.0671	1.18	16.9	18.4
2-105079	0.465	0.118	0.366	0.212	0.0040	30.0	12.2	13.4
3-104721*	missing	missing	missing	missing	missing	missing	missing	missing
2-104708	0.213	0.206	0.684	0.329	0.0602	3.46	19.9	20.9
2-105297*	missing	missing	missing	missing	missing	missing	missing	missing
2-105114*	missing	missing	missing	missing	missing	missing	missing	missing
3-104759*	missing	missing	missing	missing	missing	missing	missing	missing
3-105041	1.814	0.154	0.462	0.352	0.0567	3.60	10.9	12.5
15mg/kg								
3-104708	3.23	0.294	0.212	0.160	0.0502	9.40	22.3	23.8
3-104761	0.930	0.229	0.722	0.552	0.0460	5.06	14.1	15.1
3-104762	0.515	0.156	1.87	1.563	0.00095	164	7.29	8.28
3-104709	0.110	0.159	11.8	0.0790	0.0520	4.42	19.1	20.6
3-104931	0.507	0.593	0.718	0.654	0.0932	5.60	16.6	18.1

3-104763	0.502	0.271	0.380	0.319	0.0597	4.08	22.5	24.0

Table 3.29. AIC and SBC values for comparison after fitting the data to a one-compartment open model using no initial-parameter estimates, weight 1/YY

Subject	AIC criteria	SBC criteria
7mg/kg		
2-104720	-64.6	-63.7
2-104993	-63.7	-62.8
2-104763	-57.7	-57.1
2-105097	-47.8	-46.9
3-104721	-39.8	-39.9
2-104708	-35.8	-35.2
2-105297	-47.0	-46.5
2-105114	-73.6	-72.7
15mg/kg		
3-104759	-89.8	-89.2
3-105041	-69.8	-68.9
3-104708	-40.2	-39.3
3-104761	-37.3	-37.0
3-104762	-40.0	-39.5
3-104709	-28.7	-28.4
3104931	-30.0	-29.4
3-104763	-34.5	-34.7

Overall, the single oral dosing data of Terbinafine in penguins fitted a one-compartmental open model better except for only one subject. When fitting the data of subjects to a two-compartmental open model with the WinNonlin, more of the subjects did not yield any output. The initial pharmacokinetic parameter estimates guide the WinNonlin to obtain usefull the outcome in fitting the data. Thus, the number of subjects for which the WinNonlin produced useful output when initial kinetic

parameter estimates were provided were higher than the number it provided for subjects that did not have initial kinetic parameter estimates for the computer run.

Table 3.30. Pharmacokinetic parameters for the Terbinafine concentration time data that fitted the model for a one-compartment open model best, weight 1/YY

Subject	V_F	K01	K10	AUC	K01_HL	K10_HL	CL_F	T_{max}	C_{max}
	(L/kg)	(1/hr)	(1.hr)	(mg/L*hr)	(hr)	(hr)	(L/kg)	(hr)	(mg/L)
3mg/kg									
105079	44.1	3.14	0.1098	0.619	4.84	6.31	4.84	1.11	0.0602
105114	52.1	0.771	0.0662	0.869	0.898	10.4	3.45	3.48	0.0457
104721	60.6	4.45	0.0341	1.45	0.156	20.3	2.07	1.10	0.0477
104986	26.7	0.295	0.2953	0.381	2.34	2.35	7.89	3.38	0.0413
104708	missing	missing	missing	missing	missing	missing	missing	missing	missing
105297	56.9	1.00	0.0800	0.658	0.691	8.66	4.56	2.74	0.0423
104757	71.7	2.38	0.0271	1.55	0.291	25.6	1.94	1.90	0.0398
104903	38.4	1.08	0.0103	7.60	0.641	67.50	0.395	4.35	0.0747
105040	43.8	0.204	0.2026	0.338	3.41	3.42	8.88	4.92	0.0253
104720	missing	missing	missing	missing	missing	missing	missing	missing	missing
Average	**45.4**	1.67	0.1032	**0.706**	**0.537**	**6.72**	**1.78**	2.87	**0.0432**
SE	**56.8**	1.51	0.0985	**0.184**	**0.295**	**2.74**	**1.71**	1.42	**0.0054**
7mg/kg									
2-104720	3.56	2.55	0.0605	3.40	0.271	11.5	2.10	1.50	0.1845
2-104993	4.26	0.624	0.0517	3.18	1.11	13.4	2.20	4.35	0.1313
2-104763	16.5	2.10	0.0239	1.78	0.331	28.9	3.94	2.16	0.0403
2-105079	7.15	1.37	0.000001	140662	0.507	996191.7	0.00005	10.6	0.0979
3-104721	4389.8	3.65	0.0310	5.15	0.190	22.4	136	1.32	0.1531
2-104708	7.29	1.08	0.0224	9.19	0.643	31.0	1.63	3.67	0.1894
2-105297	1.76	0.445	0.4320	0.923	1.559	1.60	7.54	2.28	0.1488
2-105114	2.79	0.454	0.0697	3.60	1.56	9.94	1.94	4.88	0.1788
3-104759	2.37	0.088	0.0930	3.18	7.91	7.46	2.20	11.08	0.1055
3-105041	4.96	3.84	0.0545	2.59	0.181	12.7	2.70	1.12	0.1329
Average	**4.14**	1.62	0.0839	**2.82**	**0.428**	**8.27**	**2.50**	4.30	**0.1121**
SE	**9.94**	1.36	0.1252	**0.895**	**0.122**	**6.85**	**2.61**	3.68	**0.0278**
15mg/kg									
3-104708	7.30	1.08	0.0224	9.194	0.643	31.0	1.63	3.67	0.1894
3-104761	7.36	1.96	0.0309	6.597	0.353	22.4	2.27	2.15	0.1908
3-104762	11.0	3.26	0.0054	25.082	0.212	128	0.598	1.96	0.1345
3-104709	7.15	1.37	0.000001	140661.5	0.507	996192	0.00005	10.60	0.0979
3-104931	7.57	3.03	0.0349	5.680	0.229	19.9	2.64	1.49	0.1881
3-104763	16.5	2.10	0.0239	1.776	0.331	29.0	3.94	2.16	0.0403
Average	**8.62**	2.13	0.0196	**5.772**	**0.325**	**35.4**	**3.01**	3.67	**0.1029**
SE	**9.53**	0.873	0.0139	**4.475**	**0.056**	**10.1**	**1.36**	3.47	**0.0447**

For subjects 3-104721, 2-105297, 2-105114, and 3-104759, no successful fitting of the data to the pharmacokinetic model occurred. Error warnings were observed and no output could be seen. Generally, the WinNonlin failed to fit highly variable Terbinafine plasma versus time data to the model.

The AIC and SBC were used to select the best fit of the data to the model. The one-compartmental open model fitted to the data by a weighting of 1/YY gave a better fit to the data than a two-compartmental open model. The one-compartmental open model in the WinNonlin ran well with initial or without initial-kinetic-parameter estimates provided to fit the data.

The final kinetic parameters of the data fit to a one-compartmental open model, weight $1/YY$, are listed in the following table.

The harmonic mean (the bold numbers) for the volume of distribution, AUC, half-life, clearance and the, C_{max} values were calculated. Compared to the non-compartmental analysis of the data, the results with the data weighted by 1/YY in Table 3.8, the harmonic-mean calculation appeared to be a good approach. However, different volumes of distribution, clearance, half-life, and AUC were observed when fitting the mean-plasma concentration versus time profile to the one-compartmental open model, weight 1/YY, the pharmacokinetic parameters obtained are enumerated in Table 3.29.

Figure 3.11 describes the mean-plasma-concentration-time curve with the predicted line fitted to the curve of a one-compartment open model for Terbinafine plasma concentrations in penguins for single oral dosing (3, 7, 15mg/kg). The predicted C_{max} value from the selected best-fitted model appeared to be an

underestimate compared to the true C_{max}. Other pharmacokinetic parameters such as the volume of distribution V_F, $AUC_{0\text{-}inf}$, and clearance are similar to the values presented in the non-compartmental analysis. The calculated harmonic-mean pharmacokinetic parameters and their standard error are presented in bold.

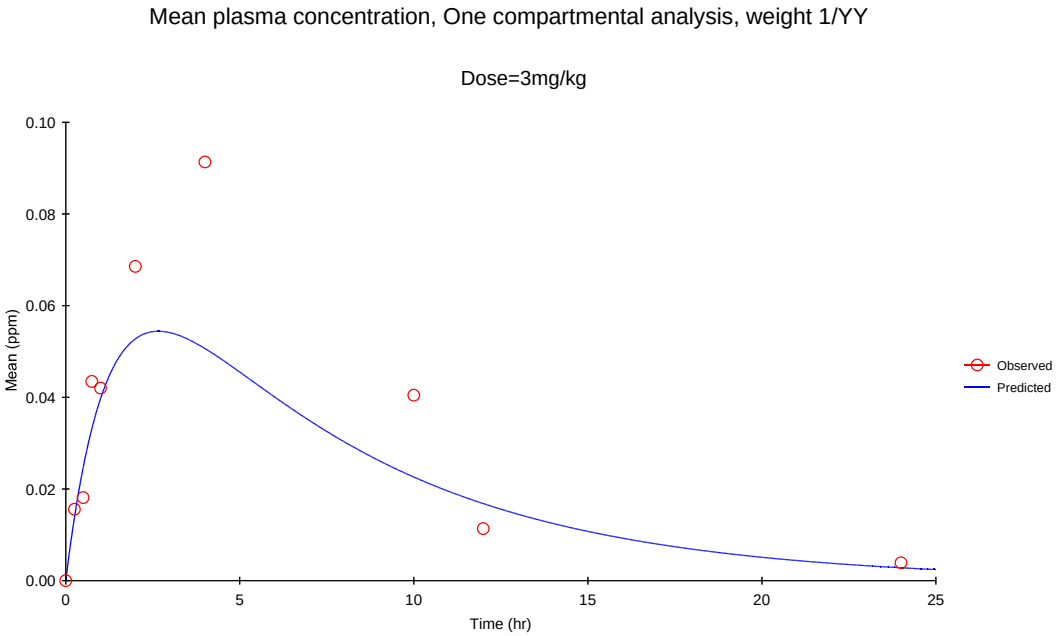

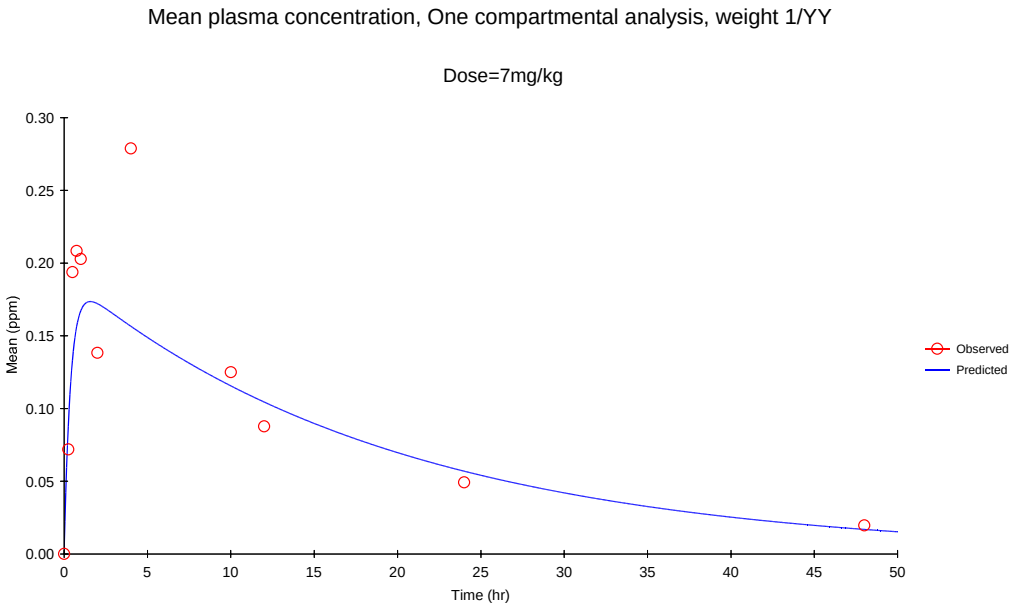

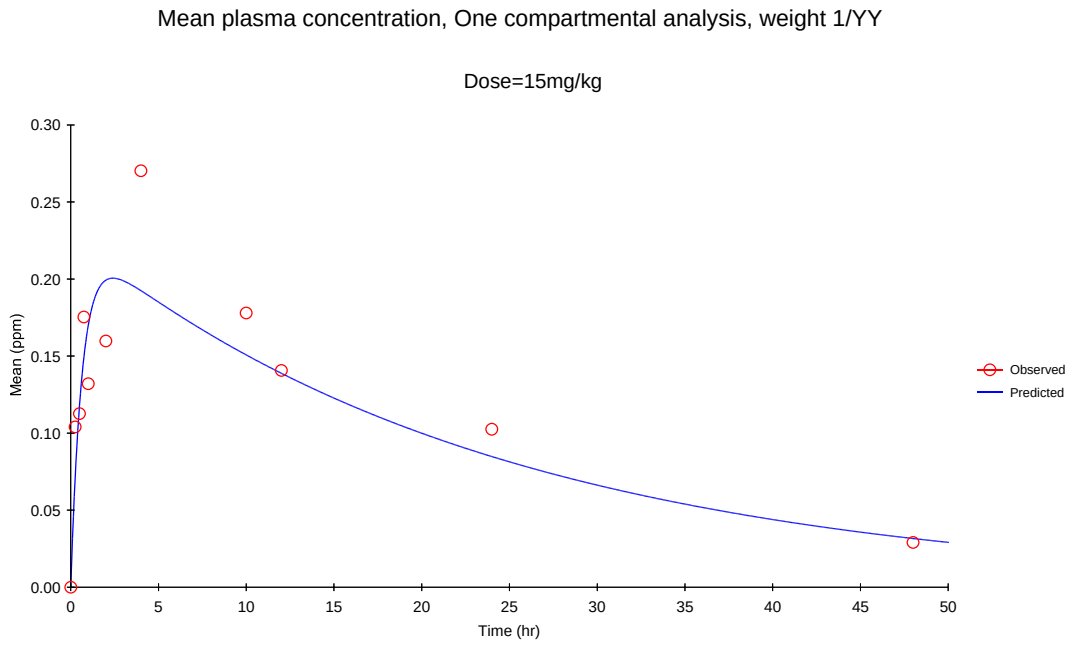

Figure 3.11. Terbinafine-plasma-concentration-time curve in penguins fitted to a one-compartment open model, weight 1/YY

Table 3.31. Pharmacokinetic parameters from best fitted one compartment open model, weight 1/YY, for mean Terbinafine plasma-concentration-time curve

Subject	V_F	K01	K10	$AUC_{0\text{-}inf}$	K01_HL	K10_HL	CL_F	T_{max}	C_{max}
	(L/kg)	(1/hr)	(1/hr)	(mg/L*hr)	(hr)	(hr)	(L/kg)	(hr)	(mg/L)
3mg/kg	37.08	0.762	0.1491	0.543	0.909	4.65	5.53	2.66	0.054
7mg/kg	37.25	2.542	0.0506	3.714	0.273	13.7	1.89	1.57	0.174
15mg/kg	67.76	1.553	0.0411	5.386	0.446	16.9	2.79	2.40	0.201
average	**43.75**	1.619	0.0803		**0.428**	**8.64**	**2.80**	2.21	
SD	**7.28**	0.892	0.0598		**0.158**	**5.58**	**0.864**	0.569	

MULTIPLE DOSING

The multiple dosing of Terbinafine was performed in 10 subjects. To fit the data obtained in penguins to the multiple dosing models found in the WinNonlin, initial parameter estimates were required. Pharmacokinetic parameters from curve fitting Terbinafine-plasma-concentration-time curves of the single-dosing data made

with the WinNonlin with the same dose 15mg/kg were used for the initial parameter estimates.

Table 3.32 Terbinafine plasma concentration versus time in penguins after dosing 15mg/kg/day for four days

Penquins-Aug 2004
Treatment 4
15mg/kg, dosing time at 0, 24, 48,72 hours

Subject	Time (hour)	Concentration (mg/L)	Subject	Time (hour)	Concentration (mg/L)	Subject	Time (hour)	Concentration (mg/L)
5-105297-1	0	0	5-104708-1	0	0	5-104709-1	0	0
5-105297-2	2	0.16	5-104708-2	2	0.215	5-104709-2	2	0.361
5-105297-3	4	0.589	5-104708-3	4	0.202	5-104709-3	4	0.221
5-105297-4	8	0.491	5-104708-4	8	0.115	5-104709-4	8	0.221
5-105297-5	11	0.313	5-104708-5	11	0.044	5-104709-5	11	0.11
5-105297-6	23	0.186	5-104708-6	23	0.044	5-104709-6	23	0.001
5-105297-7	26	0.14	5-104708-7	26	1.4	5-104709-7	26	0.931
5-105297-8	28	0.83	5-104708-8	28	0.728	5-104709-8	28	0.46
5-105297-9	32	0.397	5-104708-9	32	0.214	5-104709-9	32	0.326
5-105297-10	35	0.32	5-104708-10	35	0.145	5-104709-10	35	0.165
5-105297-11	47	0.277	5-104708-11	47	0.075	5-104709-11	47	0.123
5-105297-12	50	2.35	5-104708-12	50	1.52	5-104709-12	50	1.139
5-105297-13	52	1.51	5-104708-13	52	0.518	5-104709-13	52	0.757
5-105297-14	56	0.634	5-104708-14	56	0.23	5-104709-14	56	0.389
5-105297-15	59	0.624	5-104708-15	59	0.187	5-104709-15	59	0.316
5-105297-16	71	0.491	5-104708-16	71	0.118	5-104709-16	71	0.182
5-105297-17	74	2.13	5-104708-17	74	1.28	5-104709-17	74	1.915
5-105297-18	76	1.52	5-104708-18	76	1.26	5-104709-18	76	1.29
5-105297-19	80	0.865	5-104708-19	80	0.625	5-104709-19	80	0.508
5-105297-20	83	0.757	5-104708-20	83	0.311	5-104709-20	83	No sample
5-105297-21	95	0.664	5-104708-21	95	0.268	5-104709-21	95	No sample

Subject	Time (hour)	Concentration (mg/L)	Subject	Time (hour)	Concentration (mg/L)	Subject	Time (hour)	Concentration (mg/L)
5-104720-1	0	0	5-104721-1	0	0	5-104761-1	0	0
5-104720-2	2	0.103	5-104721-2	2	0.774	5-104761-2	2	0.193
5-104720-3	4	0.053	5-104721-3	4	0.409	5-104761-3	4	0.202
5-104720-4	8	0.034	5-104721-4	8	0.332	5-104761-4	8	0.07
5-104720-5	11	0	5-104721-5	11	0.197	5-104761-5	11	0.03
5-104720-6	23	0	5-104721-6	23	0.098	5-104761-6	23	0.01
5-104720-7	26	1.39	5-104721-7	26	1.01	5-104761-7	26	1.09
5-104720-8	28	1.05	5-104721-8	28	0.537	5-104761-8	28	0.551

5-104720-9	32	0.414	5-104721-9	32	0.253	5-104761-9	32	0.197
5-104720-10	35	0.221	5-104721-10	35	0.174	5-104761-10	35	0.121
5-104720-11	47	0.1045	5-104721-11	47	0.189	5-104761-11	47	0.086
5-104720-12	50	2.31	5-104721-12	50	1.71	5-104761-12	50	1.72
5-104720-13	52	0.903	5-104721-13	52	1.53	5-104761-13	52	0.934
5-104720-14	56	0.49	5-104721-14	56	0.5295	5-104761-14	56	0.515
5-104720-15	59	0.351	5-104721-15	59	0.414	5-104761-15	59	0.302
5-104720-16	71	0.207	5-104721-16	71	0.264	5-104761-16	71	0.169
5-104720-17	74	2.61	5-104721-17	74	0.273	5-104761-17	74	2.54
5-104720-18	76	0.928	5-104721-18	76	1.16	5-104761-18	76	1.38
5-104720-19	80	0.439	5-104721-19	80		5-104761-19	80	0.525
5-104720-20	83	0.412	5-104721-20	83	0.479	5-104761-20	83	0.395
5-104720-21	95	0.291	5-104721-21	95	0.365	5-104761-21	95	0.311

Subject	Time (hour)	Concentration (mg/L)	Subject	Time (hour)	Concentration (mg/L)	Subject	Time (hour)	Concentration (mg/L)
5-104986-1	0	0	5-105040-1	0	0	5-105041-1	0	0
5-104986-2	2	0.19	5-105040-2	2	0.167	5-105041-2	2	0.214
5-104986-3	4	0.125	5-105040-3	4	0.23	5-105041-3	4	0.974
5-104986-4	8	0.099	5-105040-4	8	0.333	5-105041-4	8	0.393
5-104986-5	11	0.045	5-105040-5	11	0.129	5-105041-5	11	0.205
5-104986-6	23	0.03	5-105040-6	23	0	5-105041-6	23	0.076
5-104986-7	26	0.93	5-105040-7	26	1.24	5-105041-7	26	0.733
5-104986-8	28	0.471	5-105040-8	28	0.775	5-105041-8	28	0.945
5-104986-9	32	0.16	5-105040-9	32	0.539	5-105041-9	32	0.314
5-104986-10	35	0.097	5-105040-10	35	0.26	5-105041-10	35	0.204
5-104986-11	47	0.059	5-105040-11	47	0.163	5-105041-11	47	0.142
5-104986-12	50	1.98	5-105040-12	50	2.05	5-105041-12	50	1.2
5-104986-13	52	0.846	5-105040-13	52	1.23	5-105041-13	52	1.35
5-104986-14	56	0.301	5-105040-14	56	0.371	5-105041-14	56	0.463
5-104986-15	59	0.213	5-105040-15	59	0.309	5-105041-15	59	0.349
5-104986-16	71	0.184	5-105040-16	71	0.241	5-105041-16	71	0.246
5-104986-17	74	3.56	5-105040-17	74	1.32	5-105041-17	74	2.33
5-104986-18	76	1.73	5-105040-18	76	1.09	5-105041-18	76	1.23
5-104986-19	80	0.508	5-105040-19	80	0.448	5-105041-19	80	0.614
5-104986-20	83	0.524	5-105040-20	83	0.337	5-105041-20	83	0.467
5-104986-21	95	0.376	5-105040-21	95	0.243	5-105041-21	95	0.327

Subject	Time (hour)	Concentration (mg/L)
5-104903-1	0	0
5-104903-2	2	1.45
5-104903-3	4	0.944
5-104903-4	8	0.482
5-104903-5	11	0.355
5-104903-6	23	0.18
5-104903-7	26	2.66

5-104903-8	28	1.22
5-104903-9	32	0.492
5-104903-10	35	0.408
5-104903-11	47	0.384
5-104903-12	50	2.48
5-104903-13	52	1.44
5-104903-14	56	0.678
5-104903-15	59	0.572
5-104903-16	71	0.429
5-104903-17	74	2.92
5-104903-18	76	1.32
5-104903-19	80	0.707
5-104903-20	83	0.696
5-104903-21	95	0.53

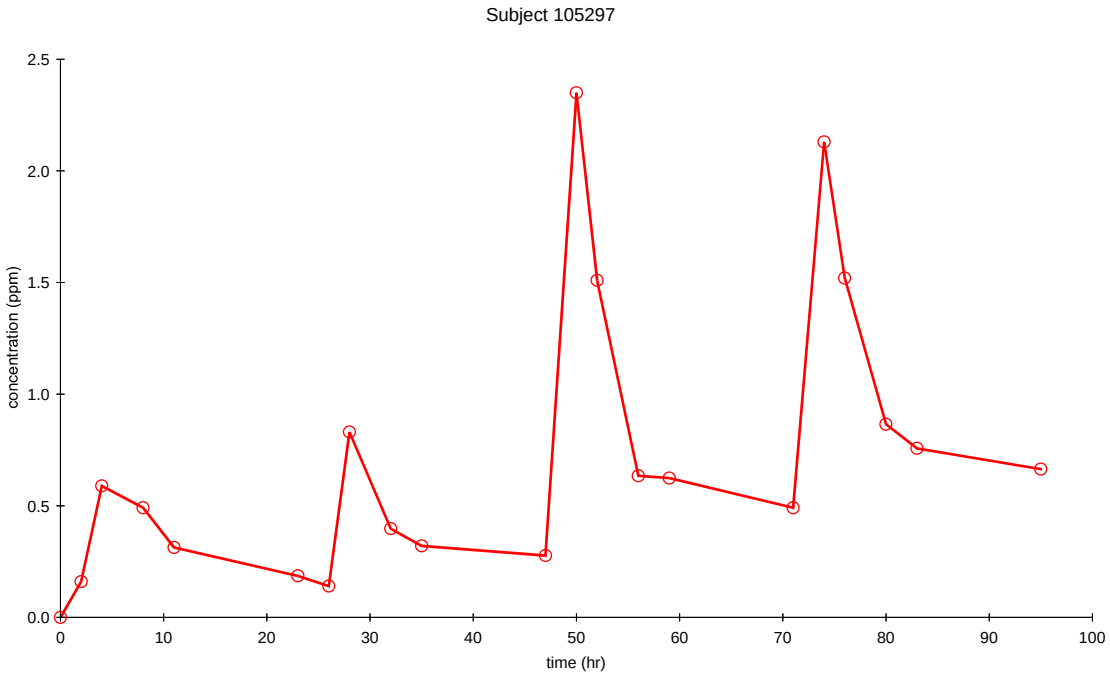

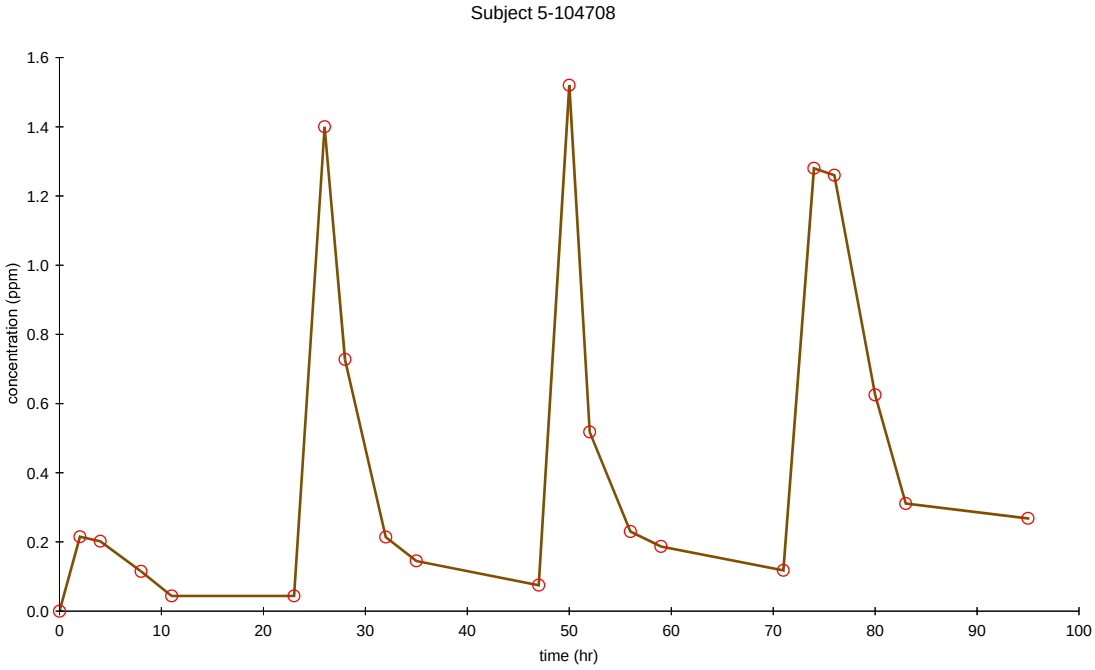
Subject 5-104708
concentration (ppm)
time (hr)
0.0
0.2
0.4
0.6
0.8
1.0
1.2
1.4
1.6
0
10
20
30
40
50
60
70
80
90
100

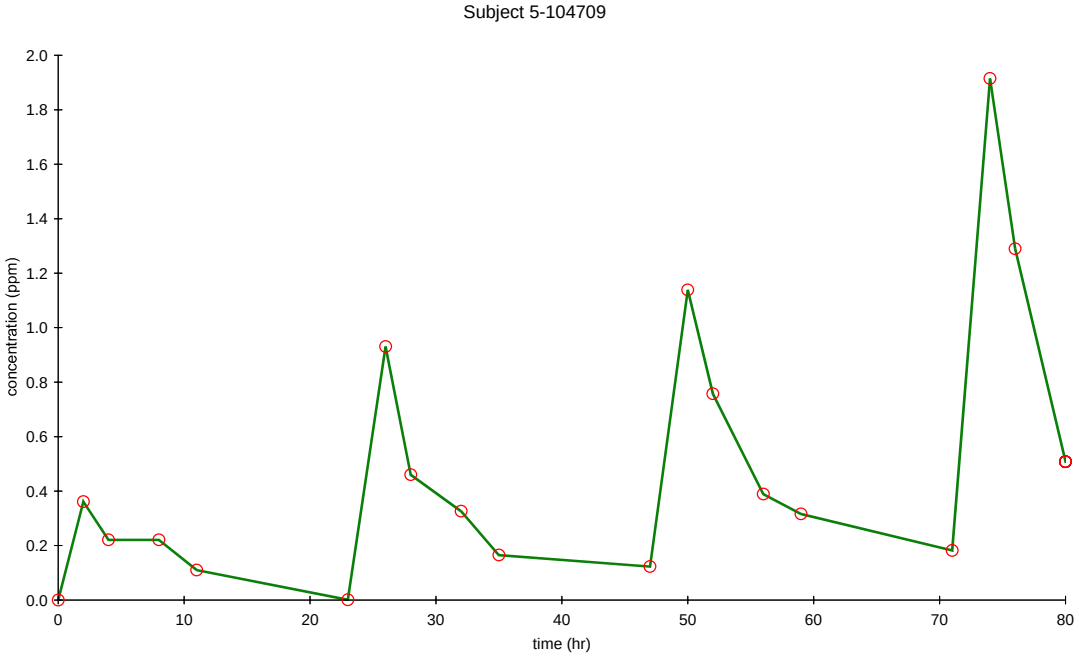
Subject 5-104709
concentration (ppm)
time (hr)
0.0
0.2
0.4
0.6
0.8
1.0
1.2
1.4
1.6
1.8
2.0
0
10
20
30
40
50
60
70
80

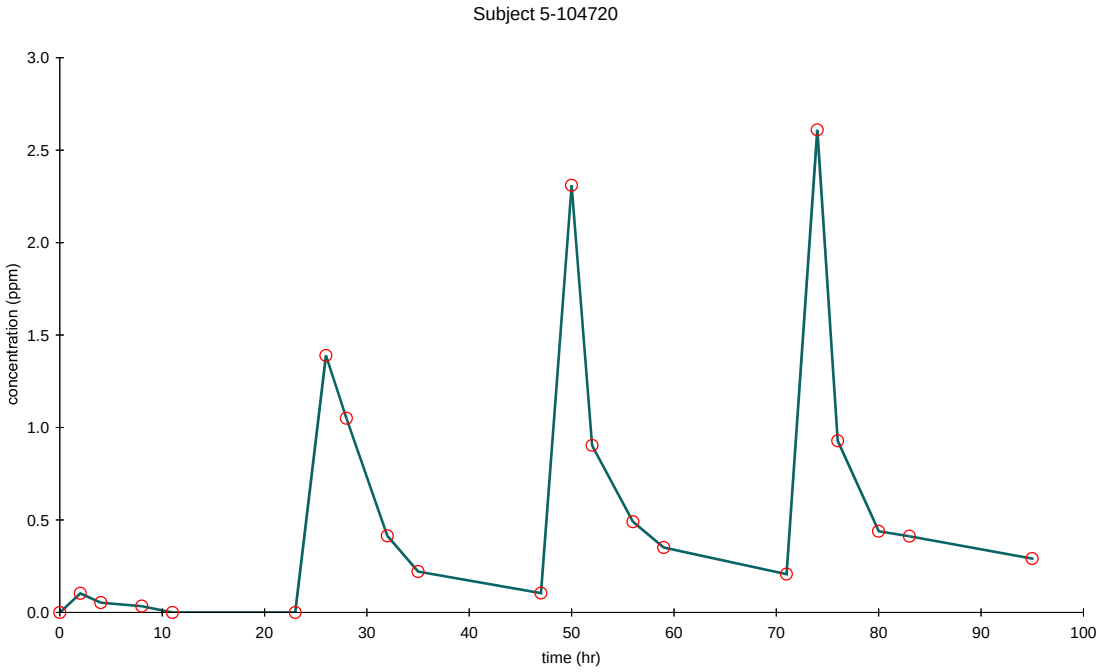
Subject 5-104720
concentration (ppm)
3.0
2.5
2.0
1.5
1.0
0.5
0.0
0
10
20
30
40
50
60
70
80
90
100
time (hr)

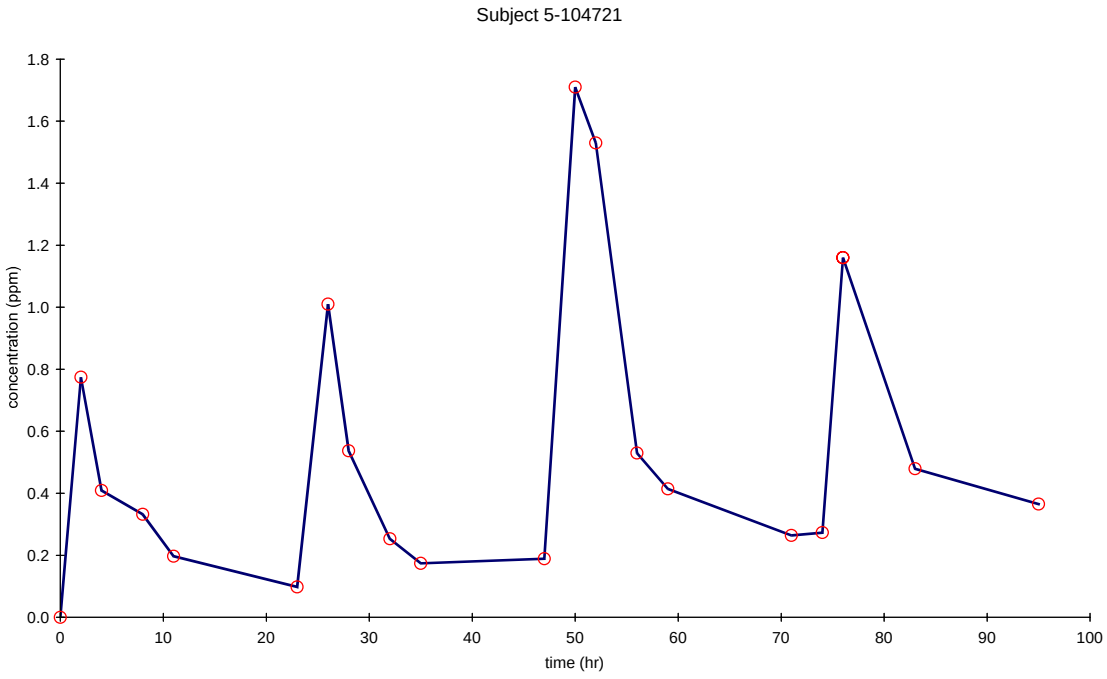
Subject 5-104721
concentration (ppm)
1.8
1.6
1.4
1.2
1.0
0.8
0.6
0.4
0.2
0.0
0
10
20
30
40
50
60
70
80
90
100
time (hr)

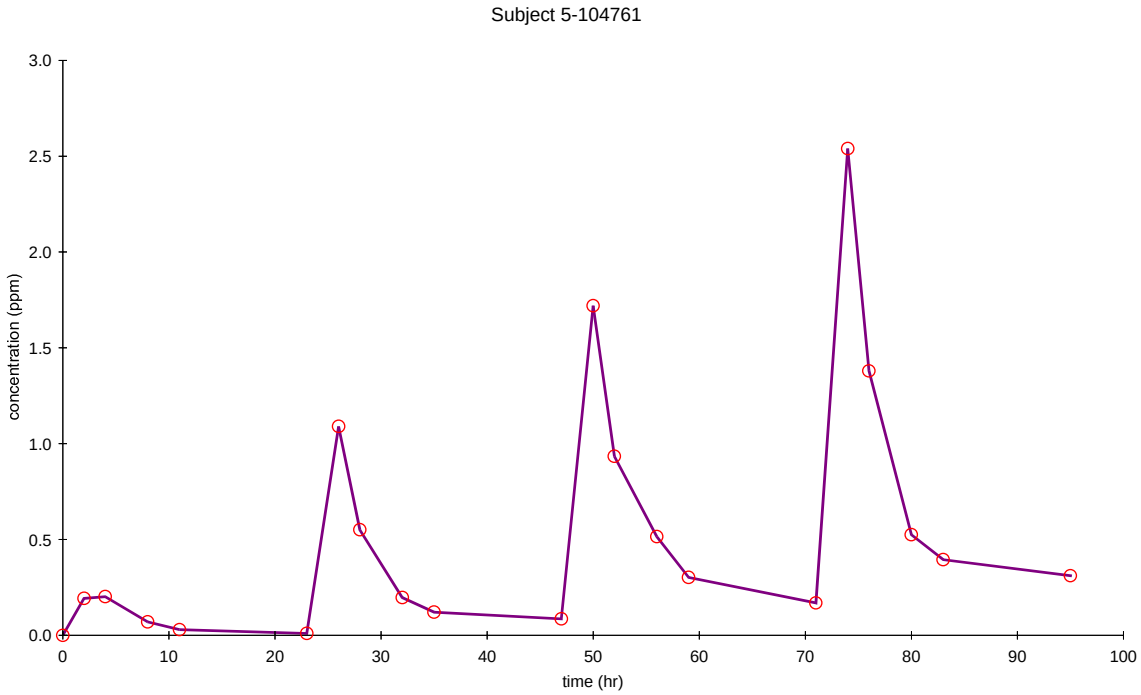
Subject 5-104761
concentration (ppm)
time (hr)
0.0
0.5
1.0
1.5
2.0
2.5
3.0
0
10
20
30
40
50
60
70
80
90
100

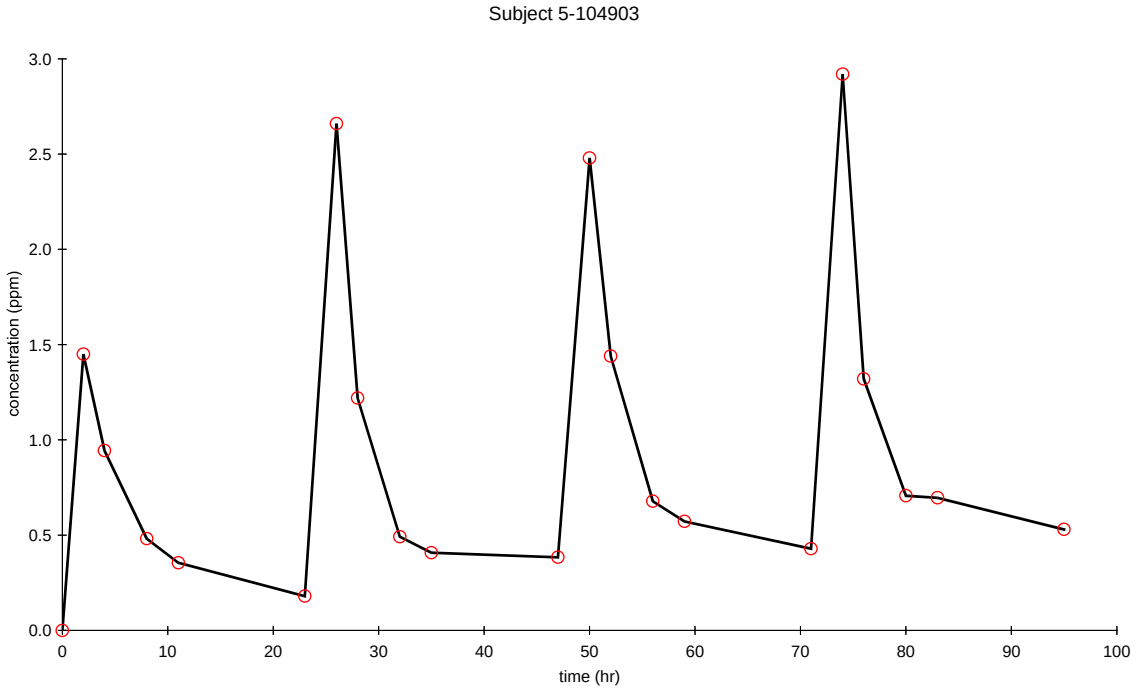
Subject 5-104903
concentration (ppm)
time (hr)
0.0
0.5
1.0
1.5
2.0
2.5
3.0
0
10
20
30
40
50
60
70
80
90
100

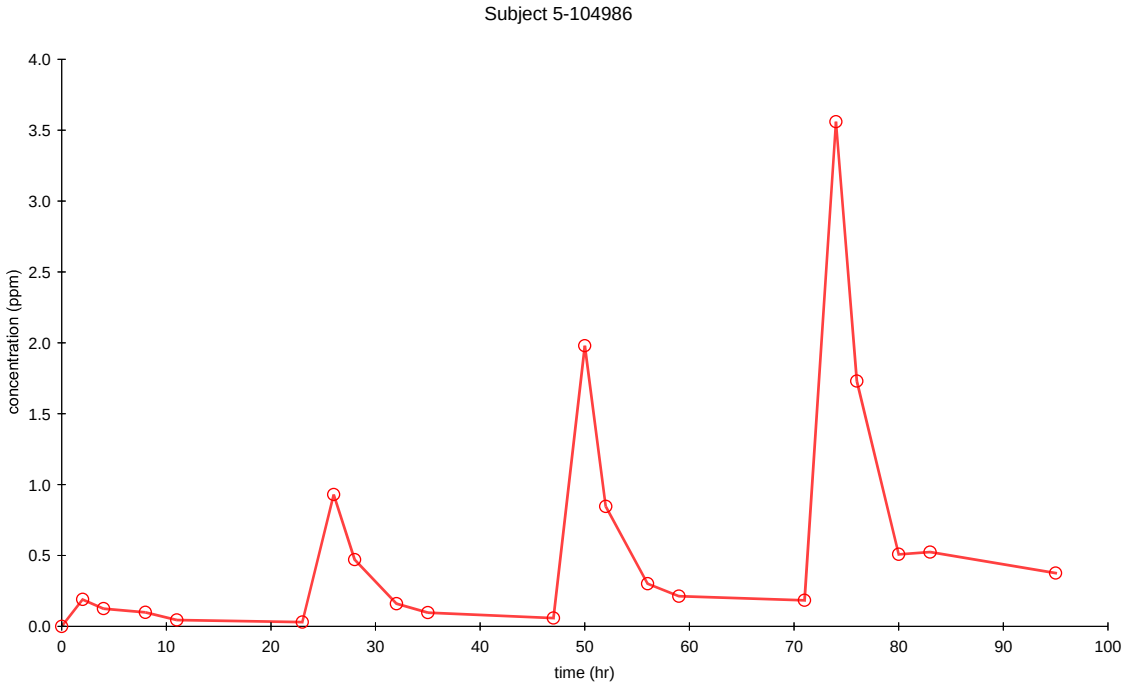
Subject 5-104986
concentration (ppm)
time (hr)
0.0
0.5
1.0
1.5
2.0
2.5
3.0
3.5
4.0
0
10
20
30
40
50
60
70
80
90
100

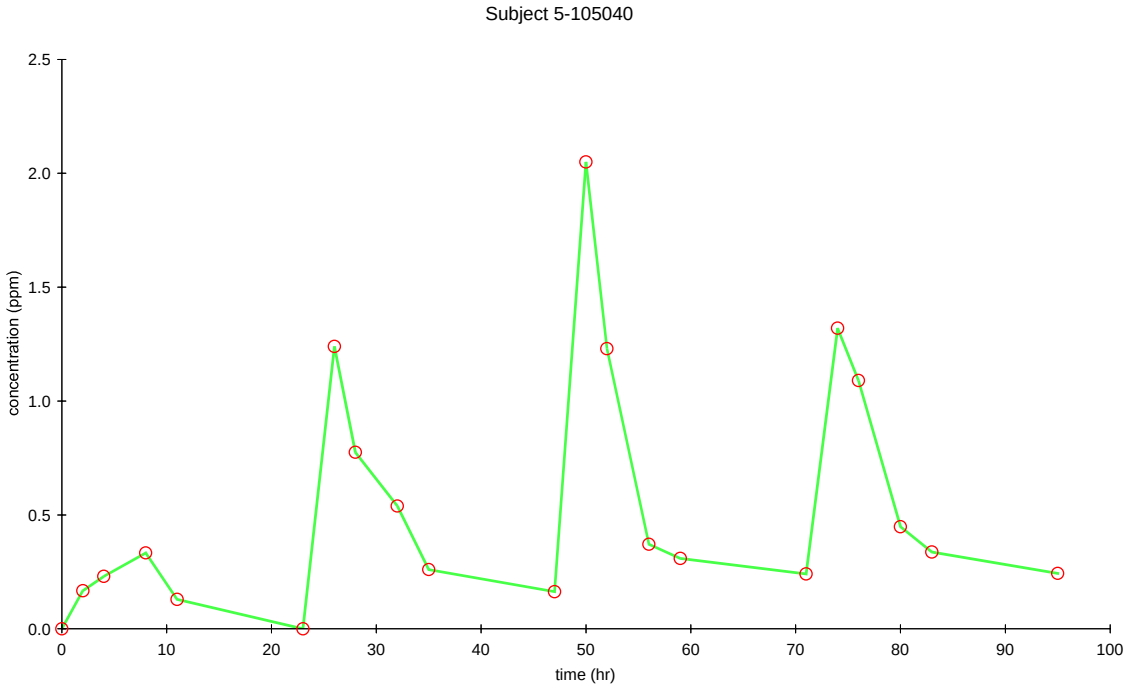
Subject 5-105040
concentration (ppm)
time (hr)
0.0
0.5
1.0
1.5
2.0
2.5
0
10
20
30
40
50
60
70
80
90
100

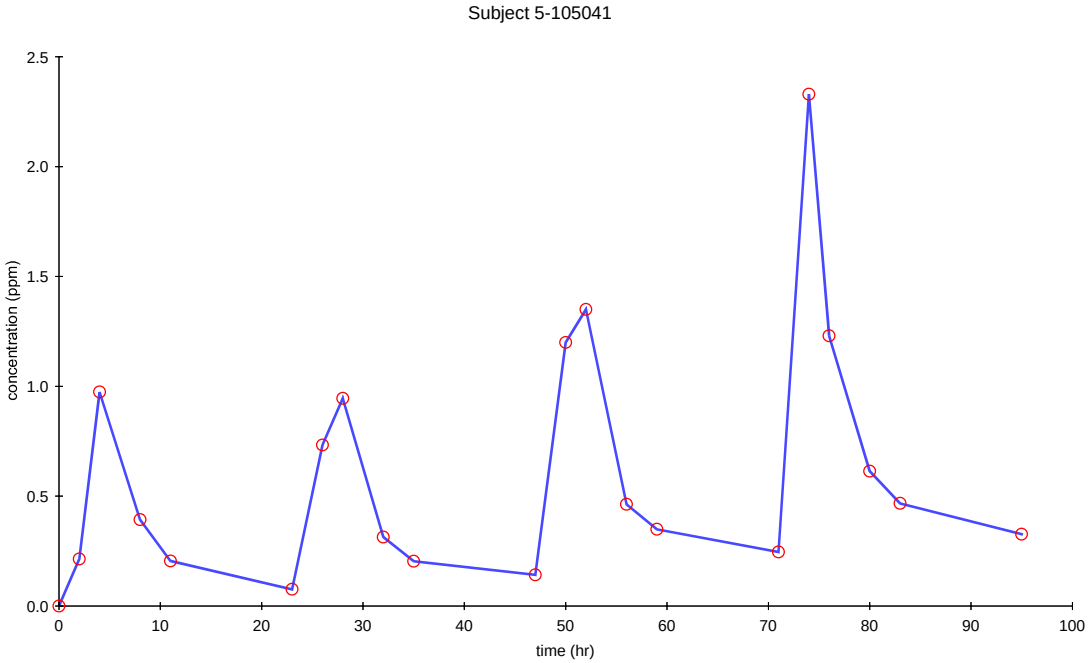

Figure 3.12. The individual penguin Terbinafine plasma-concentration-time curves of treatment 4, multiple dosing 15mg/kg per day for four days

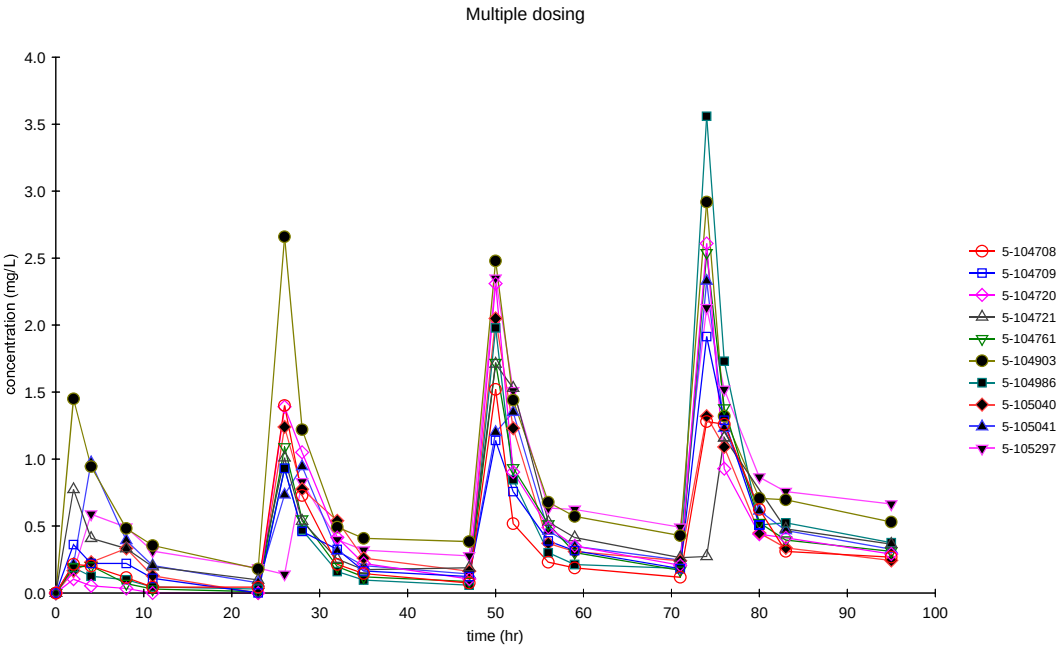

Figure 3.13. Terbinafine plasma concentration time-curves for each penguin presented as spaghetti plots of all subjects for multiple-dosing regimens of 15mg/kg per day for four days

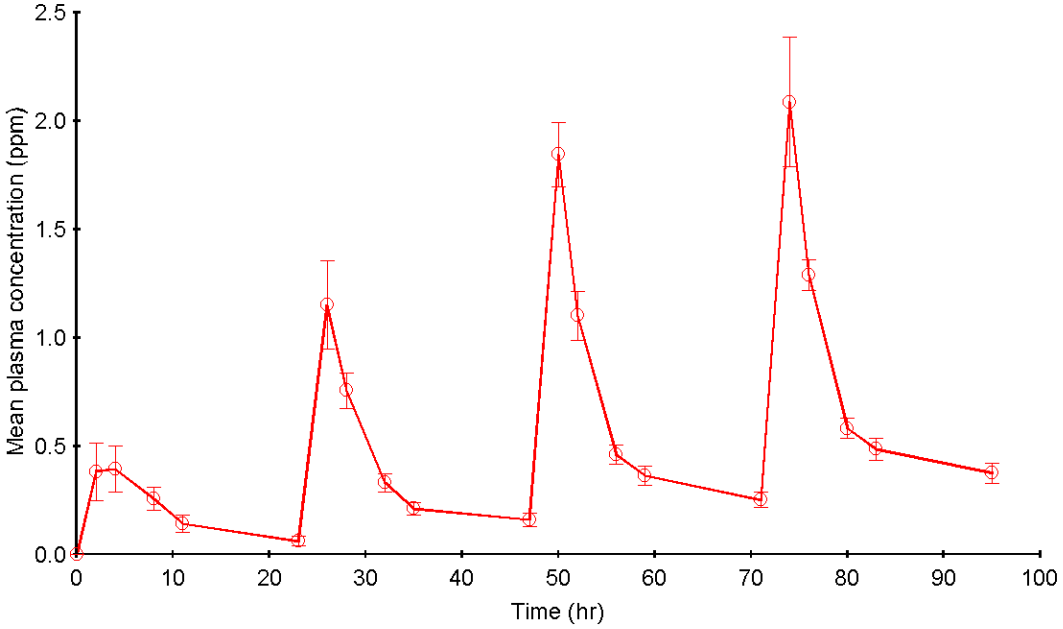

Figure 3.14. The mean Terbinafine plasma-concentration time-curve of multiple dosing of 15mg/kg/day for four days in penguins

Table 3.33. Mean-plasma-concentration-time-curve values of Terbinafine after 15mg//kg/day oral multiple dosing in penguins for four days

Time (hour)	Concentration (mg/L)	Standard deviation
0	0	0.000
2	0.383	0.421
4	0.395	0.333
8	0.257	0.172
11	0.143	0.122
23	0.0625	0.0717
26	1.152	0.643
28	0.757	0.259
32	0.331	0.128
35	0.212	0.0956
47	0.160	0.101
50	1.846	0.470
52	1.102	0.355
56	0.460	0.145
59	0.364	0.140
71	0.253	0.118
74	2.088	0.941
76	1.291	0.223
80	0.582	0.138

83	0.486	0.153
95	0.375	0.137

Non-compartmental analysis for multiple-dosing data

Table 3.34. Pharmacokinetic parameters for Terbinafine in penguins determined by non-compartmental analysis of multiple dosing 15mg/kg/day for four days in penguins

Subject	Lamda_z	Lamda_z _HL	T_{max}	C_{max}	AUClast	AUC_o-inf	V_F	CL_F	MRT_{last}	MRT_{0inf}
	(1.hr)	1/hr	(hr)	(mg/L)	(mg/L*hr)	(mg/L*hr)	(L/kg)	(L/kg)	hr	hr
15mg/kg	0.027	26.072	74	2.081	15.984	30.089	18.751	0.499	8.260	32.802

Multiple dosing requires initial pharmacokinetic estimates. Kinetic parameters needed are volume of distribution (V_F), elimination-rate constant (K10), absorption-rate constant (K01) to run the WinNonlin. The best-fitted model was selected previously and was a one-compartmental open model fitted with data, weighted $1/YY$. The pharmacokinetic parameters for the mean-plasma concentration time-curve are listed in Table 3.30. These pharmacokinetic parameters were used as estimates the initial kinetic values and used to fit the multiple-dose data by the WinNonlin.

Initial pharmacokinetic estimate:

V_F: 43.750 **(**L/kg)

K01: 1.6191 (1/hr)

K10: 0.0803 (1/hr)

Table 3.35. Pharmacokinetic parameters of Terbinafine in penguins after 15mg/kg/day for four days multiple dosing after fitting with unique initial pharmacokinetic parameter estimates

Subject	V_F	K01	K10	AUC	K01_HL	K10_HL	CL_F	T_{max}	C_{max}
	(L/kg)	(1/hr)	(1.hr)	(mg/L*hr)	(hr)	(hr)	(L/kg)	(hr)	(mg/L)
15mg/kg	27.9	5.18	0.0756	7.13	0.134	9.17	2.11	0.828	0.506

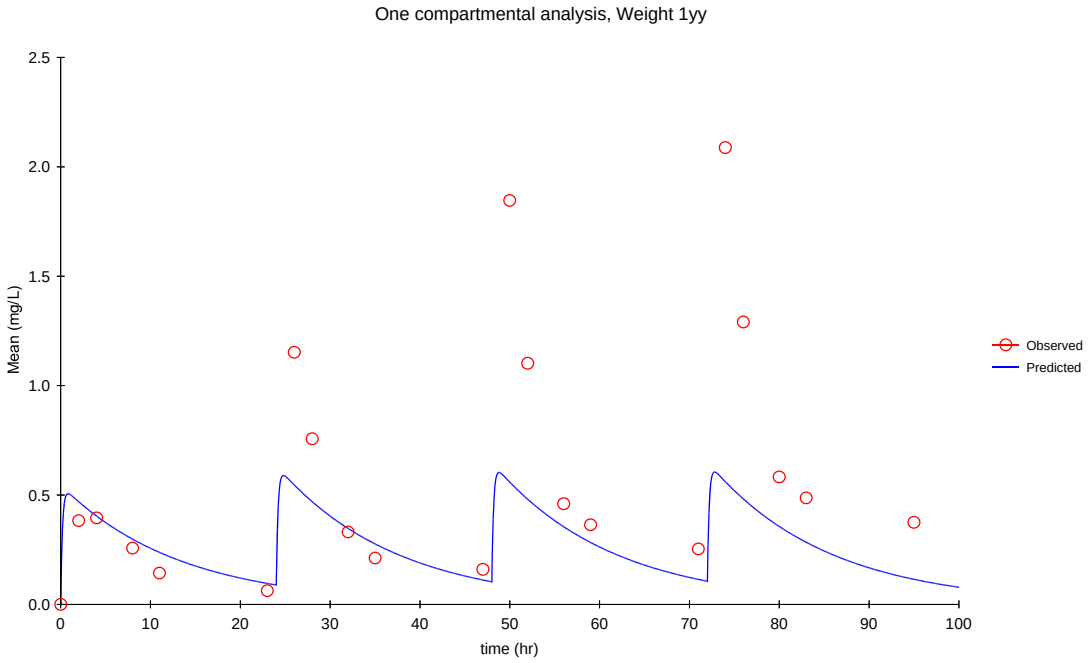

Figure 3.15. One-compartmental analysis with initial pharmacokinetic estimates

An under estimation of the predicted plasma-concentration time-curve was observed when fitting the multiple dose data by the WinNonlin with the initial kinetic-parameter estimates from a single oral dose of 15mg/kg as the plasma concentrations were much higher than the predicted plasma concentration. In addition, previous pharmacokinetic studies in humans revealed that Terbinafine has a strong affinity to adipose tissue[21-24]. Consequently, a deep-tissue distribution compartment causes a long elimination of Terbinafine with a small elimination-rate constant. Penguins have a thick subcutaneous fatty layer. This fatty layer serves as insulation and a valuable energy store [42]. It is suspected that a long elimination phase occurs when administering Terbinafine in penguins. To test if accumulation occurs, convergence

methods such as non-linear regression of fitting the trough and maximum concentrations can be applied.

$$C = C_{ss}(1 - e^{-\beta t})$$

C is the trough concentration, C_{ss} is the drug concentration of the trough or maximum concentration at a steady state. The trough and the maximum concentration profile can be fitted by non-linear regression.

Trough concentration time profile of the mean-plasma concentration time curve is in Table 3.34.

Table 3.36. The mean trough-penguin-Terbinafine concentrations of the multiple-dose study

Time (hour)	Concentration (mg/L)
0	0
23	0.0625
47	0.160
71	0.253
95	0.375

Determining the terminal elimination constant and deep tissue half-life

The acceleration-convergence method is used to calculate the deep-tissue elimination phase.

$$Y_\infty = Y_3 - \frac{(Y_3 - Y_2)^2}{Y_3 - 2Y_2 + Y_1}$$
$$Y_i = Y_\infty - slope(Y_{i+1} - Y_i)$$
$$slope = \frac{Y_\infty - Y_i}{(Y_{i+1} - Y_i)}$$

Performing the fitting to trough plasma concentrations yields a steady state or trough concentration of around 0.4 mg/L. The slope-of-fit of the mean-trough plasma concentration time-curve gives an elimination constant rate of 0.005368 hr^{-1}.

Table 3.37. Deep-tissue elimination constant of mean plasma concentration time curve

Time	C (mg/L)	Ci+1-Ci (mg/L)	C_{inf} (mg/L)	1-e(-beta*t)	Beta (hr^{-1})	half life (hr)
23	0.0625	0.0978		0		
47	0.160	0.0928	0.4	0.232	0.00562	123.4
71	0.253	0.1219	0.4	0.30475	0.00512	135.4
95	0.375			**average**	**0.005368**	**129.4**

The final result yields the terminal-elimination constant and half-life of Terbinafine from the deep tissue elimination phase. The half life is calculated by the harmonian mean method:

$$\frac{1}{t_{1/2average}} = \frac{1}{t_1} + \frac{1}{t_2} + \ldots + \frac{1}{t_n}$$

The half-life of the mean concentration time curve is around 129.4 hours in penguins following a multiple oral dosing.

The AUC value from 0 to t is 15.9837mg/L*hr. If we calculate from 95 hour to infinity, the deep tissue elimination phase, the AUC value from 95 hours to infinity, which includes C/beta = 0.375/0.005368 = 69.85mg/L*hr. The total AUC for each dosing value becomes (15.9837*4+69.85)/4= 33.4462 mg/L*hr. Clearance becomes 15/33.4462 = 0.4484 L/hr. The volume of distribution is 83.54L.

Comparing the values obtained by non-compartmental analysis and fitting the data to the one-compartmental open model above, the pharmacokinetic results revealed a big difference due to the terminal elimination-rate constant changing (Table 3.38).

The manual calculation of the elimination phase of the plasma concentrations of the individual data are listed in Table 3.39.

Table 3.38. Pharmacokinetic parameters of Terbinafine after multiple dosing in penguins accounting for deep tissue elimination phase

Dose	V_F (L/kg)	K01 (1/hr)	K10 (1.hr)	$AUC_{o\text{-}inf}$ (mg/L*hr)	K01_HL (hr)	K10_HL (hr)	CL_F (L/kg)	T_{max} (hr)	C_{max} (mg/L)
15mg/kg	83.5401	5.1813	0.0054	133.1400	0.1338	129.40	0.4484	0.8280	0.5057

Table 3.39. The individual pharmacokinetic parameters of Terbinafine in penguins after manual fitting of the data to one compartment open model

Dose	λz (1/hr)	Lamda_z_HL (hr)	T_{max} (hr)	C_{max} (mg/L)	AUC_{last} (hr*mg/L)	AUC_{inf} (hr*mg/L)	Vz_F (L/kg)	Cl_F (L/hr//kg)
15mg/kg								
5-105297	0.0056	124	74	2.13	59.8	178	60.1	0.336
5-104708	0.0056	124	74	1.28	31.7	126	84.8	0.475
5-104709	0.0054	128	74	1.915	41.0	111	100	0.543
5-104720	0.0112	61.9	76	0.928	41.1	62.8	85.4	0.956
5-104721	0.0066	105	76	1.16	39.6	89.2	102	0.673
5-104761	0.002	346	74	2.54	37.8	193	155	0.311
5-104903	0.0078	88.9	74	2.92	71.9	120	64.0	0.499
5-104986	0.0062	112	74	3.56	40.7	126	76.7	0.476
5-105040	0.0101	68.6	74	1.32	40.0	64.0	92.7	0.937
5-105041	0.0061	114	74	2.33	45.5	99.1	99.3	0.606
Average	0.0066	**104**	74.4	**1.69**	**42.7**	**103**	**86.3**	**0.513**
SE	0.0026	**12.9**	0.843	**0.852**	**0.244**	**2.83**	**12.8**	**7.05**

Dose calculation

The MI95 concentration for Aspergillus niger is 0.4 mg/L and Aspergillus fumigatus is 1.2mg/L. If the volume of distribution at a steady state is 83.54 L/kg, then to calculate the loading dose is 83.54*1.2= 100mg/kg.

$$C_{\min} = \frac{De^{-kt}}{V(1-e^{-kt})}$$

$$D = \frac{C_{\min}V(1-e^{-kt})}{e^{-kt}}$$

$$D = \frac{1.2*83.54*(1-e^{-0.005368*24})}{e^{-0.005368*24}} = 13.8 mg/kg$$

CONCLUSIONS

Terbinafine can be given to penguins by oral administration. A pretty high concentration of Terbinafine in the blood demonstrates good absorption of Terbinafine. The Terbinafine disposition is similar in behavior to that in humans: It follows a two-compartmental open model for extra-vascular dosing: A deep-tissue elimination phase with a small elimination-rate constant (beta 1), and a faster elimination-phase that was not from adipose tissues had a higher elimination rate constant (beta 2). This elimination-rate constant (beta 2) was the average value of the elimination-rate constant of single-dosing treatment 2 and 3 (7 and 15mg/kg) obtained by running a non-compartmental analysis, weight 1/YY (Table 3.8). The absorption-rate constant was obtained as average value shown in Table 3.30.

Table 3.40. The final pharmacokinetic parameters of terbinafine in penguins with 15mg/kg/day multiple dosing

Dose	Beta 1	Beta 2	K10	Beta 1_HL	Beta 2_HL	V_F	CL_F	$AUC_{o\text{-}inf}$
	(hr^{-1})	(hr^{-1})	(hr^{-1})	(hr)	(hr)	(L/kg)	(L/kg)	(mg/L*hr)
15mg/kg	0.00537	0.0440	1.82	129.4	15.8 hr	83.5	0.448	133

There is no evidence that there was a distribution phase after the oral administration of Terbinafine. Also observed was high inter-subject variability in the plasma concentrations and pharmacokinetic parameters for Terbinafine in penguins. It was probably due to conditions that were not easy to control: the effect of oral drug administration, the effect of food on drug absorption, differences in the kinetics of Terbinafine in genders, age effect etc…

Finally, a recommendation of an oral dose of 14mg/kg of Terbinafine is best for the treatment of aspergillosis in penguins.

REFERENCES

1. Database, S.B.G.A.I., ***Penguins***. 2002, Busch Entertainment Corporation.
2. Lynch, W., ***Penguins of the world.*** 1997.
3. Simpson, G.G., ***Penguins: Past and present, Here and there***. 1976: New Haven and Lodon, Yale press.
4. Aimley, D.G., ***the Adélie penguins***. 2002: Columbia University Press.
5. Fichtner, D.G., *Spheniscus demersus*. 1999.
6. Wolfaardt, A., *All about penguins*. 2008, International Penguin Conservation work group.
7. Khan, Z.U., et al., *Aspergillosis in imported penguins.* Sabouraudia, 1977. **15**(1): p. 43-5.
8. Shear, N.H., V.V. Villars, and C. Marsolais, *Terbinafine: an oral and topical antifungal agent.* Clin Dermatol, 1991. **9**(4): p. 487-95.
9. Balfour, J.A. and D. Faulds, *Terbinafine. A review of its pharmacodynamic and pharmacokinetic properties, and therapeutic potential in superficial mycoses.* Drugs, 1992. **43**(2): p. 259-84.
10. Garber, G., *An overview of fungal infections.* Drugs, 2001. **61 Suppl 1**: p. 1-12.
11. Gupta, A.K., R. Baran, and R. Summerbell, *Onychomycosis: strategies to improve efficacy and reduce recurrence.* J Eur Acad Dermatol Venereol, 2002. **16**(6): p. 579-86.
12. Darkes, M.J., L.J. Scott, and K.L. Goa, *Terbinafine: a review of its use in onychomycosis in adults.* Am J Clin Dermatol, 2003. **4**(1): p. 39-65.
13. Abdel-Rahman, S.M. and M.C. Nahata, *Oral Terbinafine: a new antifungal agent.* Ann Pharmacother, 1997. **31**(4): p. 445-56.
14. Schmitt, H.J., et al., *MIC and fungicidal activity of Terbinafine against clinical isolates of Aspergillus spp.* Antimicrob Agents Chemother, 1988. **32**(5): p. ban780-1.
15. Nedelman, J., et al., *The effect of food on the pharmacokinetics of multiple-dose Terbinafine in young and elderly healthy subjects.* Biopharm Drug Dispos, 1997. **18**(2): p. 127-38.
16. Ryder, N.S., *The mechanism of action of Terbinafine.* Clin Exp Dermatol, 1989. **14**(2): p. 98-100.
17. Petranyi, G., J.G. Meingassner, and H. Mieth, *Antifungal activity of the allylamine derivative Terbinafine in vitro.* Antimicrob Agents Chemother, 1987. **31**(9): p. 1365-8.
18. McClellan, K.J., L.R. Wiseman, and A. Markham, *Terbinafine. An update of its use in superficial mycoses.* Drugs, 1999. **58**(1): p. 179-202.
19. Tanuma, H., et al., *Usefulness of 1% Terbinafine HCl (Lamisil) cream for hyperkeratotic-type tinea pedis and its transfer into the horny layer.* Mycoses, 2000. **43**(11-12): p. 417-32.
20. Tan, J.S. and W.S. Joseph, *Common fungal infections of the feet in patients with diabetes mellitus.* Drugs Aging, 2004. **21**(2): p. 101-12.

21. Humbert, H., et al., *Pharmacokinetics of Terbinafine and five known metabolites in children, after oral administration.* Biopharm Drug Dispos, 1998. **19**(7): p. 417-23.
22. Debruyne, D. and A. Coquerel, *Pharmacokinetics of antifungal agents in onychomycoses.* Clin Pharmacokinet, 2001. **40**(6): p. 441-72.
23. Meinhof, W., *Kinetics and spectrum of activity of oral antifungals: the therapeutic implications.* J Am Acad Dermatol, 1993. **29**(1): p. S37-41.
24. Alberti, I., et al., *Assessment and prediction of the cutaneous bioavailability of topical Terbinafine, in vivo, in man.* Pharm Res, 2001. **18**(10): p. 1472-5.
25. Almeida, S., et al., *Comparative bioavailability of two formulations of Terbinafine. Data from a cross-over, randomised, open-label bioequivalence study in healthy volunteers.* Arzneimittelforschung, 2004. **54**(11): p. 757-62.
26. Wahllander, A. and G. Paumgartner, *Effect of ketoconazole and Terbinafine on the pharmacokinetics of caffeine in healthy volunteers.* Eur J Clin Pharmacol, 1989. **37**(3): p. 279-83.
27. Abdel-Rahman, S.M., et al., *Potent inhibition of cytochrome P-450 2D6-mediated dextromethorphan O-demethylation by Terbinafine.* Drug Metab Dispos, 1999. **27**(7): p. 770-5.
28. Trepanier, E.F., A.N. Nafziger, and G.W. Amsden, *Effect of Terbinafine on theophylline pharmacokinetics in healthy volunteers.* Antimicrob Agents Chemother, 1998. **42**(3): p. 695-7.
29. Hosseini-Yeganeh, M. and A.J. McLachlan, *Tissue distribution of Terbinafine in rats.* J Pharm Sci, 2001. **90**(11): p. 1817-28.
30. Van Der Kuy, P.H., et al., *Pharmacokinetic interaction between nortriptyline and Terbinafine.* Ann Pharmacother, 2002. **36**(11): p. 1712-4.
31. Kovarik, J.M., et al., *Multiple-dose pharmacokinetics and distribution in tissue of Terbinafine and metabolites.* Antimicrob Agents Chemother, 1995. **39**(12): p. 2738-41.
32. Nedelman, J.R., et al., *Pharmacokinetics and pharmacodynamics of multiple-dose Terbinafine.* J Clin Pharmacol, 1996. **36**(5): p. 452-61.
33. Kevin D. Sanborn, R.M., *Physician's desk reference*. 2007, Montvale, New Jersey: Thomson.
34. Corporation, P., *WinNonlin reference book.* 2003. **version 4.0**: p. 68-71.
35. Karolczak, M., *[Diagnosis and treatment of spermatic cord torsion in children].* Pediatr Pol, 1984. **59**(10): p. 853-6.
36. Dennis D. Wackerly, W.M.I., Richard L. Scheaffer, ***Mathematical Statistics with Applications***. six ed. 2002: Wadsworth Group, Duxury.
37. Lam, F.C., C.T. Hung, and D.G. Perrier, *Estimation of variance for harmonic mean half-lives.* J Pharm Sci, 1985. **74**(2): p. 229-31.
38. Schaaf, L.J., F.C. Lam, and D.G. Perrier, *Comparison of harmonic mean versus arithmetic mean clearance values.* J Pharm Sci, 1986. **75**(4): p. 427-9.
39. Burnham, K.P., D. R. Anderson, *Model Selection and Multimodel Inference: A Practical-Theoretic Approach*. second ed. 2002: Springer-Verlag.
40. Fred Ramsey, *The Statistical Sleuth: A Course in Methods of Data Analysis*. 2 ed. 2001, New York: Duxbury Press.

41. Wagner, J.G. and J.W. Ayres, *Bioavailability assessment: methods to estimate total area (AUC O to infinity) and total amount excreted (A infinity e) and importance of blood and urine sampling scheme with application to digoxin.* J Pharmacokinet Biopharm, 1977. **5**(5): p. 533-57.
42. Rubin, J., *Lonely Planet Antarctica*. 3 ed. 2005: Lonely Planet Publications.

BIBLIOGRAPHY

1. *Handbook of Pharmaceutical Excopients*. Hydropropyl Methylcellulose, ed. A.H. Kibbe. 2000. 252-255.

2. A. Cavallo, M.H., *Stability of melatonin in aqueous solution.* Journal of Pineal Research, 1995. **18**(2): p. 90-92.

3. Abdel-Rahman, S.M., et al., *Potent inhibition of cytochrome P-450 2D6-mediated dextromethorphan O-demethylation by terbinafine.* Drug Metab Dispos, 1999. **27**(7): p. 770-5.

4. Abdel-Rahman, S.M. and M.C. Nahata, *Oral terbinafine: a new antifungal agent.* Ann Pharmacother, 1997. **31**(4): p. 445-56.

5. Agency, E.P., *Clean Air Act*. 1970.

6. Aimley, D.G., ***the Adélie penguins***. 2002: Columbia University Press.

7. Alan K. Fritz, D.P.B., James E. Peterson, George B. Park, Jerome Adelson, *Relative Bioavailability and Pharmacokinetics: A Combination of Pentazocine and Acetaminophen.* Journal of Pharmaceutical Sciences, 1984. **73**(3): p. 326-331.

8. Alberti, I., et al., *Assessment and prediction of the cutaneous bioavailability of topical terbinafine, in vivo, in man.* Pharm Res, 2001. **18**(10): p. 1472-5.

9. Albery, W.J. and J. Hadgraft, *Percutaneous absorption: theoretical description.* J Pharm Pharmacol, 1979. **31**(3): p. 129-39.

10. Almeida, S., et al., *Comparative bioavailability of two formulations of terbinafine. Data from a cross-over, randomised, open-label bioequivalence study in healthy volunteers.* Arzneimittelforschung, 2004. **54**(11): p. 757-62.

11. Anita Cavallo, W.A.R., *Pharmacokinetics of Melatonin in Human Sexual Maturation.* Journal of Clinical Endocrinology and Metabolism, 1996. **81**(5): p. 1882-1886.

12. Aronoff DM, O.J., Boutaud O, *New insights into the mechanism of action of acetaminophen: Its clinical pharmacologic characteristics reflect its inhibition of the two prostaglandin H2 synthases. Clinical Pharmacology Therapy*, 2006. **79**(1): p. 9-19.

13. Ayres, e.a., *Compactable Self-sealing Drug Delivery Agents*, U.S. Patent, Editor. 1998, Oregon State University: USA.

14. B.J. Anderson, N.H.G.H., *Rectal Acetaminophen Pharmacokinetics.* Anesthesiology, 1998.

15. Balfour, J.A. and D. Faulds, *Terbinafine. A review of its pharmacodynamic and pharmacokinetic properties, and therapeutic potential in superficial mycoses.* Drugs, 1992. **43**(2): p. 259-84.

16. Bamba, F.L. and J. Wepierre, *Role of the appendageal pathway in the percutaneous absorption of pyridostigmine bromide in various vehicles.* Eur J Drug Metab Pharmacokinet, 1993. **18**(4): p. 339-48.

17. Barry, B.W., *Penetration enhancer classification*. Percutaneous Penetration Enhancers, ed. H.I.M. Eric Wane Smith. Vol. 1. 2006: Taylor and Francis Group. 14.

18. Binh T. Ly, A.B.S., Richard F. Clark, *Effect of Whole Bowel Irrigation on the Pharmacokinetics of an Acetaminophen Formulation and Progression of Radiopaque Markers through the Gastrointestinal Tract.* Toxicology/Original Research, 2004. **43**(2): p. 189-195.

19. Bledsoe, R.K., et al., *Crystal structure of the glucocorticoid receptor ligand binding domain reveals a novel mode of receptor dimerization and coactivator recognition.* Cell, 2002. **110**(1): p. 93-105.

20. Borne, R.F., *Nonsteroidal Anti-inflammatory Drugs*. *Principles of Medicinal Chemistry*, Fourth Edition. 1995. 544-545.

21. Bouwstra, J.A., et al., *The role of ceramide composition in the lipid organisation of the skin barrier.* Biochim Biophys Acta, 1999. **1419**(2): p. 127-36.

22. Bowe, K.E., *Recent advances in sugar-based excipients.* Pharmaceutical Sciences Technology, 1998. **1**(4): p. 166-173.

23. Brinkmann, I. and C.C. Muller-Goymann, *Role of isopropyl myristate, isopropyl alcohol and a combination of both in hydrocortisone permeation across the human stratum corneum.* Skin Pharmacol Appl Skin Physiol, 2003. **16**(6): p. 393-404.

24. Brown, D., *Orally Disintegrating Tablets – Taste Over Speed.* Drug Delivery Technology, 2001. **3**(6): p. 58-61.

25. Burnham, K.P., D. R. Anderson, *Model Selection and Multimodel Inference: A Practical-Theoretic Approach*. second ed. 2002: Springer-Verlag.

26. Caniato R, F.R., Piovan A, Puricelli L, Borsarini A, Cappelletti E, *Melatonin in plants.* Advanced Experimetal medical biology, 2003. **527**: p. 593-597.

27. Chandrahas G, S., James W. Ayres, *Multiple-Dose Acetaminophen Pharmacokinetics.* 1991. **80**(9): p. 855-860.

28. Chang X. X., T.R., *The prediction of variability occurring in fluidized bed coating equipment. I. The measurement of particle circulation rates in a bottom-spray fluidized bed coater.* Pharmaceutical development and technology, 2000. **5**(3): p. 311-322.

29. Corporation, P., *WinNonlin reference book.* 2003. **version 4.0**: p. 68-71.

30. Darkes, M.J., L.J. Scott, and K.L. Goa, *Terbinafine: a review of its use in onychomycosis in adults.* Am J Clin Dermatol, 2003. **4**(1): p. 39-65.

31. Database, S.B.G.A.I., ***Penguins***. 2002, Busch Entertainment Corporation.

32. David T. Lowenthal, S.Ø., John C. Van Stone, *Pharmacokinetics.* Journal of Pharmacology and Experiment Therapeutics, 1976. **196**(3): p. 570-578.

33. Debruyne, D. and A. Coquerel, *Pharmacokinetics of antifungal agents in onychomycoses.* Clin Pharmacokinet, 2001. **40**(6): p. 441-72.

34. Dennis D. Wackerly, W.M.I., Richard L. Scheaffer, ***Mathematical Statistics with Applications***. six ed. 2002: Wadsworth Group, Duxury.

35. E.J Middleton, E.N., and A.B. Morrison, English Journal of Medicine, 1966.

36. E.Rinaki, G.V., P. Macheras, *The power law can describe the entire drug release.* Internnational Journal of Pharmaceutics, 2003. **255**: p. 199-207.

37. Ebling F.J. G., R.V.A., *Physiology, biochemistry, and molecular biology of the skin*. Hormones and hair growth, ed. R.V.A. Ebling F.J. G. Vol. 1. 1991, New York: Oxford University Press. 660-698.

38. Ed L. Hamilton, E.M.L., *Advanced Orally Disintegrating Tablets Bring Significant Benefits to Patients & Product Life Cycles.* Drug Delivery Technology, 2005. **5**(1): p. 34-37.

39. Edward M. Rudnic, M.K.K., *Tablet Dosage forms*, in *Mordern Pharmaceutics*. 1996. p. 33-390.

40. Elias, P.M., et al., *Percutaneous transport in relation to stratum corneum structure and lipid composition.* J Invest Dermatol, 1981. **76**(4): p. 297-301.

41. Elias, P.M. and D.S. Friend, *The permeability barrier in mammalian epidermis.* J Cell Biol, 1975. **65**(1): p. 180-91.

42. Eriksen, S., in *In the Thepry and Practice of Industrial Pharmacy*, H.A.L. L.

Lachman, J.L. Kanig, Editor. 1970. p. 408.

43. Fichtner, D.G., *Spheniscus demersus*. 1999.

44. Food & Drug Administration, C.-O.o.P.S., *The Biopharmaceutics Classification System (BCS) Guidance.* 2007.

45. Food and Drug Administration, C.F.D.E.a.R., *Guidance for Industry: Orally Disintegrating Tablets*. 2007.

46. Fred Ramsey, *The Statistical Sleuth: A Course in Methods of Data Analysis*. 2 ed. 2001, New York: Duxbury Press.

47. Fu Y, Y.S., Jeong SH, Kimura S, Park K, *Orally fast disintegrating tablets: developments, technologies, taste-masking and clinical studies.* 2004. **21**(6): p. 433-476.

48. Garber, G., *An overview of fungal infections.* Drugs, 2001. **61 Suppl 1**: p. 1-12.

49. Gerhard Levy, N.N.K., David M. Soda, *Pharmacokinetics of Acetaminophen in Human Neonate: Formation of Avetaminophen Glucuronide and Sulfate in Relation to Plasma Bilirubin Concentration and D-Glucaric Acid Excretion.* Pediatrics, 1975. **55**(6).

50. Graham GG, S.K., *Mechanism of action of paracetamol. American journal of therapeutics*, 2005. **12**(1): p. 46-55.

51. Grimbaldeston, M.A., et al., *Effect and potential immunoregulatory roles of mast cells in IgE-associated acquired immune responses.* Curr Opin Immunol, 2006. **18**(6): p. 751-60.

52. Gupta, A.K., R. Baran, and R. Summerbell, *Onychomycosis: strategies to improve efficacy and reduce recurrence.* J Eur Acad Dermatol Venereol, 2002. **16**(6): p. 579-86.

53. Harmon, T.M., *Orally Disintegrating Tablets: A Valluable Life Cycle Management Strategy.* Pharmaceutical Commerce, 2007. **3**.

54. Hixson A. W., C.J.H., *Dependence of Reaction Velocity upon Surface and Agitation.* Industrial and Engineering Chemistry, 1931. **23**(9): p. 923-931.

55. Högestätt ED, J.B., Ermund A, *et al*, *Conversion of acetaminophen to the bioactive N-acylphenolamine AM404 via fatty acid amide hydrolase-dependent arachidonic acid conjugation in the nervous system.* The Journal of biological chemistry, 2005. **280**(36): p. 31405-12.

56. Holt, P.G. and P.D. Sly, *Th2 cytokines in the asthma late-phase response.*

Lancet, 2007. **370**(9596): p. 1396-8.

57. Hosseini-Yeganeh, M. and A.J. McLachlan, *Tissue distribution of terbinafine in rats.* J Pharm Sci, 2001. **90**(11): p. 1817-28.

58. Huang, A.L., et al., *The cells and logic for mammalian sour taste detection.* Nature, 2006. **442**(7105): p. 934-8.

59. Hueber, F., J. Wepierre, and H. Schaefer, *Role of transepidermal and transfollicular routes in percutaneous absorption of hydrocortisone and testosterone: in vivo study in the hairless rat.* Skin Pharmacol, 1992. **5**(2): p. 99-107.

60. Humbert, H., et al., *Pharmacokinetics of terbinafine and five known metabolites in children, after oral administration.* Biopharm Drug Dispos, 1998. **19**(7): p. 417-23.

61. Igor Loniewski, M.S., Andrzej Pawlik, Jerzy Wójcicki, Marek Drozdzik, *Lack of Effect of Physical exercise on.* Acta Plonia Pharmaceutica-Drug Research, 2001. **58**(2): p. 141-144.

62. Inc., T.U.S.P.C., in *The United States Pharmacopeia 28-The National Formulary NF-23*. 2005.

63. J Goole, D., F. Vanderbist, K. Amighi, *New Levodopa Sustained release Floating minitablets coated with Insoluble acrylic polymer.* European Journal of Pharmaceutics and Biopharmaceutics, 2008. **68**: p. 310-318.

64. Janeway, C., Paul Travers, Mark Walport, Mark Shlomchik, *Immunobiology*. 2001, New York and London: Garland Science.

65. Janne RØmsing, D.Ø., Thomas Senderovitz, Mominika Drozdziewicz, Jesper Sonne, Grete Ravn, *Pharmacokinetics of oral diclofenac and acetaminophen in children after surgery.* Paediatric Anaesthesia, 2001. **11**: p. 205-213.

66. John T. Slattery, J.M.W., Thomas F. Kalhorn, Sidney D. Nelson, *Dose-dependent pharmacokinetics of acetaminophen: Evience of glutathione depletion in humans.* Clinical Pharmacology, 1987. **41**(4): p. 413-418.

67. Joseph M. Scavone, G.T.B., David J. Greenblatt, *Lack of Effect of Influenze Vaccine on the Pharmacokinetics of Antipyrine, Alprozolam, Paracetamol (Acetaminophen) and Lorazepam.* Clinical Pharmacokinetics, 1989. **16**: p. 180-185.

68. Karolczak, M., *[Diagnosis and treatment of spermatic cord torsion in children].* Pediatr Pol, 1984. **59**(10): p. 853-6.

69. Kenneth A. Walters, M.S.R., *Dermatological and Transdermal Formulation*. Skin transport, ed. S.E.C. Michael Roberts, Mark A. Pellet. Vol. 4. 2002.

70. Kenneth S. Albert, A.J.S., John G. Wagner, *Pharmacokinetics of Orally Administered Acetaminophen in Man.* Journal of Pharmacokinetics and Biopharmaceutics, 1974. **2**(5): p. 381-393.

71. Kevin D. Sanborn, R.M., *Physician's desk reference*. 2007, Montvale, New Jersey: Thomson.

72. Khan, Z.U., et al., *Aspergillosis in imported penguins.* Sabouraudia, 1977. **15**(1): p. 43-5.

73. Köfalvi A., *Chapter 9: Alternative interacting sites and novel receptors for cannabinoid ligands.* 'Cannabinoids and the Brain, 2008: p. 131-160.

74. Korsmeyer R. W., G.R., Doelker E., Buri P., Peppas, *Mechanism of solute from porous hydrophilic polymers.* Internnational Journal of Pharmaceutics, 1983. **12**: p. 25-35.

75. Kovarik, J.M., et al., *Multiple-dose pharmacokinetics and distribution in tissue of terbinafine and metabolites.* Antimicrob Agents Chemother, 1995. **39**(12): p. 2738-41.

76. Lam, F.C., C.T. Hung, and D.G. Perrier, *Estimation of variance for harmonic mean half-lives.* J Pharm Sci, 1985. **74**(2): p. 229-31.

77. Lane E.A., M.H.B., *Pharmacokinetics of Melatonin in Man: First pass Hepatic Metabolism.* Journal of Clinical Endocrinology and Metabolism, 1985. **61**(6): p. 1214-1216.

78. Lynch, W., ***Penguins of the world.*** 1997.

79. M. Hossain, J.W.A., *Variables that influence coat integrity in laboratory spray coater.* Pharmaceutical Technology, 1990. **14**(10): p. 72-82.

80. Maria Antonietta casadei, G.P., Rossella Calabrese, Patrizia Paolicelli, Gaetano Giammona, *Biodegradable and pH-Sensitive Hydrogels for Potential Colon-Specific Drug Devilvery: Characteriazation and In Vitro Release Studies.* Biomacromolecules, 2008. **9**: p. 43-49.

81. Markus R.P., F.Z.S., Fernandes P.A., Cecon E., *The immune-pineal axis: a shuttle between endocrine and paracrine melatonin sources.* Neuroimmunomodulation, 2007. **14**(3-4): p. 126-133.

82. Martha M. Rumore, R.G.B., *Influence of Age-Dependent Pharmacokinetics*

and Metabolism on Acetaminophen Hepatotoxicity. American Pharmaceutical Association, 1982. **81**(3): p. 1982.

83. Martin, *Physical Pharmacy and Pharmaceutical Sciences*. 5 ed. transport pathway, ed. P.J. Sinko. Vol. 12. 2006: Lippincott Williams & Wilkins. 319-327.

84. Martin, A., *Martin's Physical Pharmacy and Pharmaceutical Sciences: Physical Chemical and Biopharmaceutical Principles in the Pharmaceutical Sciences*. Diffusion, ed. P.J. Sinko. 2006. 301-335.

85. Mattek corp., *Epiderm™ skin model.* http://www.mattek.com/pages/products/epiderm.

86. McClellan, K.J., L.R. Wiseman, and A. Markham, *Terbinafine. An update of its use in superficial mycoses.* Drugs, 1999. **58**(1): p. 179-202.

87. Meinhof, W., *Kinetics and spectrum of activity of oral antifungals: the therapeutic implications.* J Am Acad Dermatol, 1993. **29**(1): p. S37-41.

88. Mesut Ciper, R.B., *Modified conventional hard gelatin capsules as fast disintegrating dosage form in the oral cavity.* European Journal of Pharmaceutics and Biopharmaceutics, 2006. **62**: p. 178-184.

89. Mizumoto, T., et al., *Formulation design of a novel fast-disintegrating tablet.* Int J Pharm, 2005. **306**(1-2): p. 83-90.

90. Muller, H. and R. Hilger, *Curative and palliative aspects of regional chemotherapy in combination with surgery.* Support Care Cancer, 2003. **11**(1): p. 1-10.

91. Na Zhao, L.L.A., *The Influence of Granulation on Super Disintegrant Performance.* Pharmaceutical Development and Technology, 2006. **11**(1): p. 47-53.

92. Nedelman, J., et al., *The effect of food on the pharmacokinetics of multiple-dose terbinafine in young and elderly healthy subjects.* Biopharm Drug Dispos, 1997. **18**(2): p. 127-38.

93. Nedelman, J.R., et al., *Pharmacokinetics and pharmacodynamics of multiple-dose terbinafine.* J Clin Pharmacol, 1996. **36**(5): p. 452-61.

94. Patrik K. Birmingham, M.J.T., Thomas K. Henthorn, Dennis M. Fisher, Maura C. Berkelhamer, Fredrick A. Smith, Kaaren B. Fanta, R. N., Charles J. Cote, *Twenty-four-Hour Pharmacokinetics of Rectal Acetaminophen in Children.* Anesthesiology, 1997. **87**: p. 244-252.

95. Peppas N. A., S.J.J., *A simple equation for the descriptionof solute release: III Couple of diffusion and relaxation.* Internnational Journal of Pharmaceutics, 1989. **57**: p. 169-172.

96. Per Borgquist, A.K., Lennart Picylell, anette Larsson, Anders Axelsson, *A model for the drug release from a polymer matrix tablet-effects of swelling and dissolution.* Journal of Controlled Release, 2006. **113**: p. 216-225.

97. Petranyi, G., J.G. Meingassner, and H. Mieth, *Antifungal activity of the allylamine derivative terbinafine in vitro.* Antimicrob Agents Chemother, 1987. **31**(9): p. 1365-8.

98. Pike, A.C., et al., *Structure of the ligand-binding domain of oestrogen receptor beta in the presence of a partial agonist and a full antagonist.* Embo J, 1999. **18**(17): p. 4608-18.

99. Pontes G.N., C.E.C., Carneiro Sampaio M.M., Markus R.P., *Pineal melatonin and the innate immune response: the TNF-alpha increase after cesarean section suppresses nocturnal melatonin production.* Journal of pineal research, 2007. **43**(4): p. 365-371.

100. products, M., *Nylon membrane and net filter-specification*. 2007.

101. R. Don Brown, J.T.W., Gregory L. Kearns, Calerie F. Eichler, Virginia A. Johnson, and Karl M. Bertrand, *Single-Dose Pharmacokinetics of Ibuprofen and acetaminophen in febrile children.* Journal of Clinical Pharmacology, 1992. **32**: p. 231-241.

102. R. K. Chang, C.H.H., J. R. Robinson, *A Review of Aqueous Coating techniques and Preliminary data on release from a Theophylline product.* Pharmaceutical Technology, 1987. **11**(3): p. 56-58.

103. Radoja, N., et al., *Novel mechanism of steroid action in skin through glucocorticoid receptor monomers.* Mol Cell Biol, 2000. **20**(12): p. 4328-39.

104. Ralph F. Shangraw, W.D.W., *Effect of Vehicle Dielectric Properties on Rectal Absorption of Acetaminophen.* Journal of Pharmaceutical Sciences, 1971. **60**(4): p. 600-602.

105. Ramsey F. L., S.D.W., *The Statistical Sleuth: Acourse in Methods od Data Analysis*. 2002.

106. Richard A. van Lingen, H.T.D., Coby M.E. Quak, Albert Okken, Dick Tibboel, *Multiple-dose pharmacokinetics of rectally administered acetaminophen in term infants.* Clinical Pharmacology & Therapeutics, 1999. **66**(5): p. 509-515.

107. Richard H. Guy, J.H., *Transdermal drug delivery*. Feasibility assessment in topical and transdermal delivery: mathematical models and In vitro studies, ed. J. Hadgraft. Vol. 1. 2003, New York: Marcel Dekker.

108. Robert G. Peterson, B.H.R., *Pharmacokinetics of Acetaminophen.* Padiatrics, 2001. **62**(5): p. Suppl: 877-879.

109. Roberts, D., *Signals and Perception: The Fundamentals of the Human Senses*. 2002: Palgrave Macmillan.

110. Roberts, L.J.I.M., J.D, *Analgesic-antipyretic and Antiinflammatory Agents and Drugs Employed in the Treatment of Gout.* The Pharmacological Basis of Therapeutics, 2001: p. 687-731.

111. Robinson, G.M.J.a.J.R., *Sustained- and Controlled-Release Drug Delivery*, in *Morden Pharmaceutics*, G.S.B. Christopher, Editor. 1996, Marcel Dekker. p. 575-609.

112. Roger H. Rumble, M.S.R., Michael J. Denton, *Effects of Posture and Sleep on the Pharmacokinetics of Paracetamol (Acetaminophen) and Its Metabolites.* Clinical Pharmacokinetics, 1991. **20**(2): p. 167-173.

113. Rubin, J., *Lonely Planet Antarctica*. 3 ed. 2005: Lonely Planet Publications.

114. Ryder, N.S., *The mechanism of action of terbinafine.* Clin Exp Dermatol, 1989. **14**(2): p. 98-100.

115. S. Indiran Pather, R.K., John Siebert, *Quick-Dissolving Intraoral Tablets*. Srug Delivery to the Oral Cavity: Molecules to Market, ed. W.R.P. Tapash K. Ghosh. 2005.

116. Sanborn, K.D., *Physician's Desk Reference*. 2007: Thomson. 1870-1872.

117. Sato, K., K. Sugibayashi, and Y. Morimoto, *Species differences in percutaneous absorption of nicorandil.* J Pharm Sci, 1991. **80**(2): p. 104-7.

118. Schaaf, L.J., F.C. Lam, and D.G. Perrier, *Comparison of harmonic mean versus arithmetic mean clearance values.* J Pharm Sci, 1986. **75**(4): p. 427-9.

119. Schafer-Korting, M., et al., *Glucocorticoids for human skin: new aspects of the mechanism of action.* Skin Pharmacol Physiol, 2005. **18**(3): p. 103-14.

120. Scheuplein, R.J., *Mechanism of percutaneous adsorption. I. Routes of penetration and the influence of solubility.* J Invest Dermatol, 1965. **45**(5): p. 334-46.

121. Schmitt, H.J., et al., *MIC and fungicidal activity of terbinafine against clinical*

isolates of Aspergillus spp. Antimicrob Agents Chemother, 1988. **32**(5): p. 780-1.

122. Scott R. C., W.M., Dugard P.H., *A comparison of the in vitro permeability properties of human and some laboratory animal skins.* International Journal of Cosmetics Sciences, 1986. **8**: p. 189-194.

123. Shahin, V., et al., *Glucocorticoids remodel nuclear envelope structure and permeability.* J Cell Sci, 2005. **118**(Pt 13): p. 2881-9.

124. Shear, N.H., V.V. Villars, and C. Marsolais, *Terbinafine: an oral and topical antifungal agent.* Clin Dermatol, 1991. **9**(4): p. 487-95.

125. Shigeo Shinoda, T.A., Yukio Aoyama, Sachiko Tomioka, Yoshiaki Matsumoto, Yoko Oche, *Pharmacokinetics/Pharmacodynamics of Acetaminophen Analgesia in Japanese Patients with Chronic Pain.* Biological & pharmaceutical bulletin, 2007. **30**(1): p. 157-161.

126. Simpson, G.G., ***Penguins: Past and present, Here and there***. 1976: New Haven and Lodon, Yale press.

127. Srikonda V. Sastry, J.N., *Process develpment ans Scale-Up of Oral Fast-Dissolving Tablets*. Drug Delivery to the Oral Cavity: Molecules to Market, ed. W.R.P. Tapash K. Ghosh. 2005. 311-336.

128. Sweeney, T.M. and D.T. Downing, *The role of lipids in the epidermal barrier to water diffusion.* J Invest Dermatol, 1970. **55**(2): p. 135-40.

129. Tan, J.S. and W.S. Joseph, *Common fungal infections of the feet in patients with diabetes mellitus.* Drugs Aging, 2004. **21**(2): p. 101-12.

130. Tanuma, H., et al., *Usefulness of 1% terbinafine HCl (Lamisil) cream for hyperkeratotic-type tinea pedis and its transfer into the horny layer.* Mycoses, 2000. **43**(11-12): p. 417-32.

131. Trepanier, E.F., A.N. Nafziger, and G.W. Amsden, *Effect of terbinafine on theophylline pharmacokinetics in healthy volunteers.* Antimicrob Agents Chemother, 1998. **42**(3): p. 695-7.

132. Van Der Kuy, P.H., et al., *Pharmacokinetic interaction between nortriptyline and terbinafine.* Ann Pharmacother, 2002. **36**(11): p. 1712-4.

133. Van Hal, D.A., et al., *Structure of fully hydrated human stratum corneum: a freeze-fracture electron microscopy study.* J Invest Dermatol, 1996. **106**(1): p. 89-95.

134. Vecchio C, F.F., Sangalli ME, Zema L, Gazzaniga A, *Rotary tangential spray*

technique for aqueous film coating of indobufen pellets. Drug development and industrial pharmacy, 1998. **24**(3): p. 269-274.

135. Vijayalakshmi P, D.V., Narendra C, Srinagesh S, *Development of extended zero-order release gliclazide tablets by central composite design.* Drug development and industrial pharmacy, 2008. **34**(1): p. 33-45.

136. Wagner, J.G., *Pharmacokinetics for the Pharmaceutical Scientist*. Noncompartmental and System Analysis. 1993: Technomic. 96-99.

137. Wagner, J.G. and J.W. Ayres, *Bioavailability assessment: methods to estimate total area (AUC O to infinity) and total amount excreted (A infinity e) and importance of blood and urine sampling scheme with application to digoxin.* J Pharmacokinet Biopharm, 1977. **5**(5): p. 533-57.

138. Wahllander, A. and G. Paumgartner, *Effect of ketoconazole and terbinafine on the pharmacokinetics of caffeine in healthy volunteers.* Eur J Clin Pharmacol, 1989. **37**(3): p. 279-83.

139. Walters K. A., H.J., *Pharmaceutical Skin Penetration Enhancement*. Water-The most natural penetration enhancer, ed. W.M. Roberts M.S. 1993, New York: marcel Dekker. 1-30.

140. Walters, K.A., *Dermatological and Transdermal Formulations*. The structure and Function of Skin, ed. M.S.R. Kenneth A. Walters. Vol. 1. 2002, New York, Basel: Marcel Dekker, Inc.

141. Wester R.C., N.P.K., *Relevance of animal models for percutanous absorption.* International Journal of Pharmaceutics, 1980. **7**: p. 99-110.

142. William R. Pfister, T.K.G., *Orally Disintegrating Tablets: Products, Technology and Development Issues.* Pharmaceutical Technology, 2005. **29**(10): p. 136-150.

143. Winston H. Lee, W.G.K., George E. Granville, *The Effect of Obesity on Acetaminophen Pharmacokinetics in Man.* Journal of Clinical Pharmacology, 1981. **21**: p. 284-287.

144. Wolfaardt, A., *All about penguins*. 2008, International Penguin Conservation work group.

145. Y. Gonnissen, J.P.R., C. Vervaet, *Effect of maltodextrin and superdisintegrants in directly compressible powder mixtures prepared via co-spray drying.* European Journal of Pharmaceutics and Biopharmaceutics, 2008. **68**: p. 277-282.

146. Ying Liu, J.B.S., Roger L. Schnaare, Edwin T. Sugita, *A multi-mechanistic*

Drug Release Approach in a Bead Dosage and In Vivo Predictions. Pharmaceutical Development and Technology, 2003. **8**(4): p. 419-430.

147. Ying Liu, J.B.S., Roger L. Schnaare, *A Multimechanistic Drug Release Approach in a Bead Dosage Form and In Vitro Predictions.* Pharmaceutical Development and Technology, 2003. **8**(2): p. 163-173.

148. Yuh-Fun Maa, C.I., Mahmoud Ameri, Robert Rigney, Lendon G. Payne, Dexiang Chen, *Spray-Coating for Biopharmaceutical Powder Formulations: Beyond the Conventional Scale and Its Application.* Pharmaceutical Research, 2004. **21**(3): p. 515-523.